CORA Cork Open Research Archive
Cartlann Taighde Oscailte Chorcaí

Title	Axis of placental ageing in adverse pregnancy outcomes
Authors	Manna, Samprikta
Publication date	2023
Original Citation	Manna, S. 2023. Axis of placental ageing in adverse pregnancy outcomes. PhD Thesis, University College Cork.
Type of publication	Doctoral thesis
Rights	© 2023, Samprikta Manna. - https://creativecommons.org/licenses/by-nc-nd/4.0/
Download date	2026-10-29 09:07:26
Item downloaded from	https://hdl.handle.net/10468/15387

UCC
University College Cork, Ireland
Coláiste na hOllscoile Corcaigh

Ollscoil na hÉireann, Corcaigh

National University of Ireland, Cork



Axis of Placental Ageing in Adverse Pregnancy Outcomes

Thesis presented by

Samprikta Manna

for the degree of

Doctor of Philosophy

University College Cork

College of Medicine and Health

Department of Obstetrics and Gynaecology

Head of Department: Professor John Higgins

Supervisors: Dr Fergus McCarthy and Dr Cathal McCarthy

2023

Contents

Declaration 9

Author Contribution 9

Publications and Presentation 10

Conference presentations 11

List of Tables 12

List of Figures 13

List of Abbreviations 17

Acknowledgement 24

Thesis Abstract 27

Chapter 1: Introduction 30

1.1 Cell Cycle and Ageing 31

1.2 Physiology of Redox Signalling 33

1.2.1 Reactive Species 33

1.2.2 Sources of Reactive Species 34

1.2.3 Antioxidant Cellular Systems 35

1.2.4 Free Radical Theory of Ageing 37

1.3 Cellular Senescence 38

1.3.1 Causes of Cellular Senescence 38

1.3.2 Senescence Associated Secretory Phenotypes (SASP) 42

1.3.3 Pathological consequences of cellular senescence 43

1.4 Pre-eclampsia..... 44

1.4.1 Epidemiology of PE..... 45

1.4.2 Risk Factors of PE 45

1.4.3 Pathophysiology of PE..... 47

1.4.4 Histological characteristics of PE..... 50

1.4.5 Maternal Outcomes of Pre-eclampsia..... 51

1.4.6 Fetal Outcomes of PE 52

1.4.7 Management of PE..... 54

1.5 Intrauterine Growth Restriction (IUGR) 57

1.5.1 Definition and Epidemiology 57

1.5.2 Diagnosis of IUGR..... 58

1.5.3 Pathophysiology of IUGR..... 61

1.5.4 Maternal factors of IUGR..... 62

1.5.5 Fetal Health Outcomes of IUGR..... 67

1.5.6 Management of IUGR..... 68

1.6 Placental Ageing in Adverse Pregnancy Outcomes 69

1.6.1 Healthy Placental Ageing..... 69

1.6.2 Evidence of changes in Cellular Senescence in PE & IUGR 71

1.6.3 Evidence of Mitochondrial Dysfunction in PE & IUGR 72

1.6.4 Markers of premature senescence in pregnancy complication 76

1.7 Placental Proteomics and Use of Computational Biology 79

1.8 Summary 82

1.9 Thesis Hypothesis, Aims & Objectives 84

Chapter 2: Heterogenous Differences in Cellular Senescent Phenotypes in Pre-Eclampsia and IUGR following Quantitative Assessment of Multiple Biomarkers of Senescence 86

Abstract 87

2.1 Introduction 88

2.2 Materials and Methods 91

2.2.1 Study Design 91

2.2.2 Sample Collection 92

2.2.3 Placental DNA Extraction and Absolute Telomere Length Quantification 92

2.2.4 Absolute Quantification of Placental mtDNA 93

2.2.5 Isolation of RNA and Real-Time PCR Analysis of Senescence Associated Genes 93

2.2.6 Protein Isolation and Western Blot 95

2.2.7 Senescence Associated Secretory Phenotypes (SASP) Analysis 96

2.2.8 Statistical Analysis 96

2.3 Results 97

2.3.1 Study Demographics 97

2.3.2 Differences in Senescence Associated Gene Expression between PE and IUGR 99

2.3.3 Absolute Telomere Length in placental tissue:..... 102

2.3.4 Placental Expression of Cyclin-Dependent Kinase Inhibitor 105

2.3.5 Expression of nuclear intermediate filament protein Lamin B1 in placental tissue in Pre-eclampsia and IUGR 109

2.3.6 Absolute Quantification for mitochondrial DNA 109

2.4.7 Senescence Associated Secretory Phenotypes in Maternal Plasma Reveal Different Cytokine Profiles in PE and IUGR 112

2.4 Discussion 115

2.5 Conclusion..... 123

Chapter 3: A proteomic profile of the healthy human placenta 124

Abstract 125

3.1 Introduction 127

3.2 Materials and Methods..... 129

3.2.1 Patient Recruitment and Sample Collection..... 129

3.2.2 Protein Extraction and Quantification..... 130

3.2.3 Protein Solubilisation and Desalination..... 130

3.2.4 Mass Spectrometry (MS) sample preparation..... 132

3.2.5 Mass Spectrometry 133

3.2.6 Bioinformatics and Data pre-processing 133

3.2.7 Statistical analysis..... 134

3.2.8 Pathway analysis 134

3.3 Results..... 136

3.3.1 Study Demographics 136

3.3.2 Proteome Profile shows variation across Placental Regions and Sample sites 139

3.3.3 Placental proteome varies with sub-anatomical region 141

3.3.4 Functional analysis of placental proteome..... 143

3.3.5 Placenta specific functional analysis..... 146

3.3.6 Differing Mitochondrial profile across Placental sub-anatomical regions 148

3.3.7 Variation in Senescence status across Placental sub-anatomical regions 152

3.4 Discussion 156

3.5 Conclusion..... 161

Chapter 4: Characterisation of placental proteomic profile in Pre-eclampsia and IUGR.....162

Abstract 163

4.1 Introduction 165

4.2 Material and Methods: 168

4.2.1 Study Design 168

4.2.2 Protein Extraction and Sample preparation 169

4.2.3 Mass Spectrometry 170

4.2.4 Bioinformatics and Statistical Analysis 170

4.2.5 Functional Analysis 171

4.2.6 Regulatory module identification 171

4.3 Results 173

4.3.1 Study Demographics 173

4.3.2 Proteome Profile of healthy, PE and IUGR placenta 175

4.3.3 Functional analysis of protein profiles from healthy, PE and IUGR placenta 176

4.3.4 Differentially expressed protein differences between healthy, PE, and IUGR 179

4.3.5 Functional Analyses of DEP between healthy, PE, and IUGR 181

4.2.6 Regulatory Motifs of dysregulated Proteins in PE and IUGR and healthy placentas 185

4.4 Discussion 190

4.5 Conclusion 198

Chapter 5: General Discussion 199

5.1 Overview and Interpretations of key findings 200

5.2 Strengths and Limitations 208

5.3 Future Research 210

6.0 Conclusion 215

7.0 Bibliography 216

8.0 Appendix: Published Manuscript 288

Declaration

This is to certify that the work I am submitting is my own and has not been submitted for another degree, either at University College Cork or elsewhere. All external references and sources are clearly acknowledged and identified within the contents. I have read and understood the regulations of University College Cork concerning plagiarism and intellectual property.

Author Contribution

All of the work described herein was performed independently by the author, with the following exceptions:

Chapter 3 & Chapter 4

Dr Caitriona Scaife in Conway Institute for Biomolecular and Biomedical Research (University of Dublin), assisted with LC-MS analysis.

Julia Scheel in University of Rostock assisted with data analysis, pathway analysis and placenta specific NaviCenta disease mapping.

Publications and Presentation

- **Manna, S.**, McCarthy, C., & McCarthy, F. P. (2019). Placental Ageing in Adverse Pregnancy Outcomes: Telomere Shortening, Cell Senescence, and Mitochondrial Dysfunction. Oxidative medicine and cellular longevity, 2019, 3095383. https://doi.org/10.1155/2019/3095383
- **Manna, S.**, Ruano, C. S. M., Hegenbarth, J. C., Vaiman, D., Gupta, S., McCarthy, F. P., Méhats, C., McCarthy, C., Apicella, C., & Scheel, J. (2022). Computational Models on Pathological Redox Signalling Driven by Pregnancy: A Review. Antioxidants (Basel, Switzerland), 11(3), 585. https://doi.org/10.3390/antiox11030585
- **Manna, S.**, Scheel, J., Noone, A., McElwain, C. J., Scaife, C., Gupta, S., English, J., McCarthy, C., & McCarthy, F. P. (2023). A proteomic profile of the healthy human placenta. Clinical proteomics, 20(1), 1. https://doi.org/10.1186/s12014-022-09388-4
- **Manna, S**., Mc Elwain, C. J., Maher, G. M., Giralt Martín, M., Musumeci, A., McCarthy, F. P., & McCarthy, C. (2023). Heterogenous Differences in Cellular Senescent Phenotypes in Pre-Eclampsia and IUGR following Quantitative Assessment of Multiple Biomarkers of Senescence. International Journal of Molecular Sciences, 24(4), 3101. https://doi.org/10.3390/ijms24043101

Conference presentations

Oral presentations

- *"Investigation of premature cellular senescence in Pre-eclampsia and Intrauterine Growth restriction"*, 23rd International Conference on Oxidative Stress Reduction, Redox Homeostasis & Antioxidants (Paris Redox 2021), October 13-15, 2021.
- *"Identification of senescence associated pathways in placental anatomical sub-regions using a Proteomics approach"*, International Federation of Placenta Associations (IFPA) 2021 Meeting, Aug 30 - Sep 02, 2021.
- *"Axis of Placental Ageing in Adverse Pregnancy Outcomes: Telomeres and Mitochondria",* iPLACENTA Conference, Dundee, 13-15 May 2022.
- "Investigation of premature cellular senescence in Pre-eclampsia and Intrauterine Growth restriction", iPLACENTA Symposium, Novel perspectives in maternal and fetal health (5-6 May 2021)

  Poster presentations:

- *"Investigation of premature cellular senescence in Pre-eclampsia and Intrauterine Growth Restriction",* Irish Association of Pharmacology Annual Meeting, Limerick, 5th Nov 2021
- *"Characterization of placental anatomical sub-regions through a multi-omics approach",* New Horizons in Medical Research conference, Cork, December 2020

- *"Investigation of premature cellular senescence in Pre-eclampsia and Intrauterine Growth restriction",* 68th Annual Meeting of the Society for Reproductive Investigation (SRI) July 6 – 9, 2021 in Boston, MA, USA

List of Tables

- **Table 1.1** Risk factors associated with Pre-eclampsia.
- **Table 1.2** Senescence markers associated with placental ageing in adverse pregnancy outcomes. Adapted from Manna et al.
- **Table 2.1** Tata Binding Protein (TBP) Sybr green sequence.
- **Table 2.2** Patient characteristics in study cohort. Data are represented as mean ± SD.
- **Table 2.3** Crude and adjusted association between placental absolute telomere length (aTL) in kbp for pre-eclampsia and pre-eclampsia associated with IUGR, compared with controls.
- **Table 2.4** The Crude and adjusted association between placental absolute telomere length (aTL) in kbp for IUGR placentas compared with controls.
- **Table 3.1** Patient demographics and clinical parameters of recruited women.
- **Table 3.2** Summary of differentially expressed proteins (HGNC identifier) between maternal, middle, and fetal sub-anatomical regions.
- **Table 3.3** NaviCenta differential phenotype prediction based on DEP (Benjamini – Hochberg FDR correction) p-value including adj. Pval < 0.01

between maternal, middle, and fetal sub-anatomical regions and the proteins leading to each phenotype prediction.

- **Table 4.1** Patient demographics in study cohort. Data are represented as Mean ± SD.
- **Table 4.2** DEPs between PE, IUGR, and healthy placentas. The comparisons include PE vs normal, IUGR vs normal, and IUGR vs PE. DEP are defined as adj p < 0.05 and log2FC > 0.5 and < - 0.5.
- **Table 4.3** NaviCenta differential phenotype prediction based on DEP including ad. P value < 0.05 between conditions.

List of Figures

- **Figure 1.1** Cell Cycle Progression characterised by Interphase and Mitosis. Image adapted from Maes et al 2017.
- **Figure 1.2a.** Features of Cellular Senescence. Adapted from Di Micco et al., 2021.
- **Figure 1.2b.** Synopsis of Cellular Senescence markers. Adapted from Wan et al., 2021.
- **Figure 1.3** Clinical Management of onset of Hypertension in pregnancy. Image created by Amaral et al 2017.
- **Figure 1.4** Diagnosis of IUGR. Image adapted from Suhag et al 2013.
- **Figure 1.5** Contribution of cellular senescence and mitochondrial dysfunction to placental ageing. Image adapted from Manna et al 2019 [1]

- **Figure 1.6** Biomarkers of Pre-eclampsia, where the genetic factor remains constant whereas the proteome and metabolome are dynamic. This is depicted by the double arrow. Image created by Carty et al 2008.
- **Figure 2.1** Senescence-associated gene expression in placental tissue in pre-eclampsia and IUGR.
- **Figure 2.2** Absolute telomere length in pre-eclampsia. aTL in placental tissue was not significantly altered in pre-eclampsia or pre-eclampsia associated with IUGR compared with controls.
- **Figure 2.3.** Absolute telomere length in IUGR. ATL in placental tissue showed no significant changes in IUGR compared with controls.
- **Figure 2.4** Representative images of p16 protein expression as measured by Western blotting in placental tissue from pre-eclampsia only (n=5) and pre-eclampsia associated with IUGR (n=5) (A) and IUGR (n=5) (B) matched by age. Densitometric analysis was used to quantify expression of p16 in PE.
- **Figure 2.5** Representative images of p21 protein expression as measured by Western blotting in placental tissue from pre-eclampsia only (n=5) and pre-eclampsia associated with IUGR (n=5) (A) and IUGR(n=5) (B) matched by age.
- **Figure 2.6** Representative images of Lamin-B1 protein expression as measured by Western blotting in placental tissue from pre-eclampsia only (n=5) and pre-eclampsia associated with IUGR (n=5) (A) and IUGR(n=5) (B) matched by age.
- **Figure 2.7** Absolute quantification of mitochondrial DNA (*mtDNA*) copy numbers as measured by RTqPCR in placental tissue from pre-eclampsia

only (n=5) and pre-eclampsia associated with IUGR (n=5) and IUGR (n=5) matched by age and BMI.

- **Figure 2.8** Senescence-associated secretory phenotypes (SASP) in pre-eclampsia with or without intrauterine growth restriction.
- **Figure 2.9** Senescence-associated secretory phenotypes (SASP) evident in intrauterine growth restriction IUGR.
- **Figure 2.10** Graphical summarization from results from Chapter 2.
- **Figure 3.1** Histopathological classification of sub-anatomical region sectioning.
- **Figure 3.2** Venn diagram of identified proteins in the maternal, middle, and fetal regions.
- **Figure 3.3** The top four proteins FHL1, ANXA4, HBG2, CBR1 show the strongest interaction between protein content in sub-anatomic regions and sample sites.
- **Figure 3.4** ClueGO functional analysis of differentially expressed proteins (DEP) between maternal, middle, and fetal sub-anatomical regions.
- **Figure 3.5** Mitochondria associated DEPs and their functional analysis.
- **Figure 3.6** Senescence associated DEPs and their functional analysis.
- **Figure 4.1** Venn diagram of proteins identified in placental tissue from normal, PE, and IUGR pregnancies.
- **Figure 4.2** GO biological function analysis of placental proteins identified in PE, IUGR.

- **Figure 4.3** Clustered heatmap of normalized LFQ intensities of DEPs between PE, IUGR, and healthy placentas.
- **Figure 4.4** DEGs analysis and GO biological function annotation in PE, IUGR and healthy placentas.
- **Figure 4.5** Overrepresented GO terms, overlapping with NaviCenta phenotype prediction results including DEPs falling into these terms.
- **Figure 4.6** Interaction networks of dysregulated Proteins including TFs and miRNAs regulating their genes.
- **Figure 4.7** RNA triplexes involved in the core regulatory network including DEPs and miRNAs.

List of Abbreviations

AFV - Amniotic fluid volume

AKI - Acute kidney injury

APEX-1 - Apurinic/apyrimidinic endodeoxyribonuclease 1

ART - Artificial Reproductive Technology

aTL - Absolute Telomere Length

ATM - Ataxia telangiectasia-mutated

ATR - Ataxia telangiectasia and Rad3

BAX - Bcl-2-associated X protein

BMI - Body Mass Index

BP - Blood Pressure

BPD - Bronchopulmonary Dysplasia

BPP - Biophysical profile

CCNB-1 - Cyclin B1

CDK - Cyclin Dependant kinase

CDKN2A - Cyclin-dependent kinase inhibitor 2A

CHEK-1 - Checkpoint kinase-1

CKD - Chronic kidney disease

CKMT1A - Creatine kinase mitochondrial 1A

COL14A1 - Collagen type XIV alpha 1 chain

CPR - Creatinine Protein Ratio

DBP - Diastolic BP

DDA - Data dependent analysis

DDR - DNA Damage Repair

DDX17 - DEAD-Box Helicase 17

DEP - Differentially Expressed Protein

DHA - Docosahexaenoic acid

DIC - Disseminated intravascular coagulation

DNA - Deoxyribonucleic acid

EC - Endothelial cell

ECM - Extracellular matrix

ED - Endothelial dysfunction

ESKD - End-stage kidney disease

ETC - Electron Transport Chain

EVT - Extravillous cytotrophoblast

FA - Formic Acid

FAS - Fetal Alcohol Syndrome

FBLN1 - Fibulin 1

FGR - Fetal Growth Restriction

FN1 - Fibronectin 1

GLB-1 - Lysosomal-β-galactosidase 1

GOI - Gene of Interest

Grx - Glutaredoxins

GSH - Glutathione

GSSG - Glutathione disulphide

H_2O_2 - Hydrogen Peroxide

HELLP - Hemolysis, elevated liver enzymes, and low platelets

HIF-1α - Hypoxia-inducible factor

HNRNPA1 - Heterogeneous nuclear ribonucleoprotein A1

HP - Haptoglobin

HPLC - High-performance Liquid Chromatography

hTERT - Human Telomerase Reverse Transcriptase

HUVEC - Human umbilical vein endothelial cells

IAA - Indole-3-acetic acid

ICC - Individualised customised centile

ID-1 - Inhibitor of DNA binding 1

IDH - Isocitrate dehydrogenases

IFN-γ - Interferon-γ

IGF - Insulin like growth factor

IGFBP - IGF binding proteins

IGHA1 - Immunoglobulin heavy constant alpha 1

IGHG4 - Immunoglobulin Heavy Constant Gamma 4 protein

IL - Interleukin

IUGR - Intrauterine Growth restriction

IV - Intravenously

LC - Liquid Chromatography

LFQ - Label free quantification

LMP - Last menstrual period

lncRNA - Long noncoding RNAs

MAP - Mean arterial blood pressure

MAPK - Mitogen-activated protein kinase

MCP - Monocyte chemoattractant protein

MCP-1 Monocyte chemoattractant protein-1

MIP-1α - Macrophage Inflammatory Protein-1 Alpha

miRNA - MicroRNAs

MMP - Matrix metalloproteinases

mROS - Mitochondrial ROS

MS - Mass Spectrometry

mtDNA - Mitochondrial DNA

NADH - Nicotinamide adenine dinucleotide + hydrogen

NADPH - Nicotinamide adenine dinucleotide phosphate

NHBPEP - National High Blood Pressure Education Program

NK - Natural Killer

NO - Nitric Oxide

NOS - Nitric oxide synthase

PCNA - Proliferating cell nuclear antigen

PE- Pre-eclampsia

PLGF - Placental growth factor

PMSC - Placental mesenchymal stromal cells

pRB - Retinoblastoma protein

PSAP -Prosaposin

PTEN - Phosphatase and tensin homolog

QC - Quality Control

ROS - Reactive Oxygen Species

RS - Reactive Species

SAPK/JNK - Stress-Activated Protein Kinase/Jun N-Terminal Kinase

SASP - Senescence Associated Secretory Phenotypes

SA-β-Gal - Senescence Associated β-Galactosidase

SBP - Systolic BP

sFIt1 - Soluble fms-like tyrosine kinase 1

SGA - Small for Gestational Age

SOD - Superoxide Dismutase

SUA - Single umbilical artery

TBP - TATA Binding Protein

TBX-2 - T-Box Transcription Factor 2

TCA - Tricarboxylic Acid

TEAB - Tetraethylammonium bicarbonate

TF - Transcription factors

TFA - Trifluoroacetic acid

TNF-α - Tumour necrosis factor-alpha

TrxR - Thioredoxin Reductase

UPR - Unfolded Protein Response

VEGF - Vascular endothelial growth factor

VLBW - Very low-birth weight

w/w - weight/weight

α-KG - alpha-ketoglutarate

Acknowledgement

Firstly, I would like to thank my supervisors Dr Fergus McCarthy and Dr Cathal McCarthy who brought me on to this project in 2018. When I first started working in this project, I had very little lab and research experience, but you definitely saw something in me. Over the next few years, I learnt from the best, you both were patient, understanding and extremely supportive. I will always be tremendously grateful to you for providing me this opportunity to be your PhD student. I also appreciate that you trusted me to mentor masters, Erasmus, and medical students, which added to my portfolio and honestly was one of the highlights of my PhD. It was very tough to keep recruiting during COVID-19 pandemic, but we could keep up with sample collection and lab work with your support by getting appropriate approvals from the hospital and university.

Dr Cathal McCarthy, without you I wouldn't have made it through the first day. You helped me build the sample collection protocol and set up the "placenta room". You made sure I always made the deadlines, and you were present with me every step of the way. I honestly cannot thank you enough, this PhD won't have come to fruition without you.

Dr Fergus McCarthy, I would like to thank you for getting me set up in the hospital. It is not easy for a non-clinical person to walk around the hospital, talk to patients, midwives, and obstetricians and to collect the placentas within minutes of delivery, but you made it possible. I am grateful for all the assistance with admin and other issues. I owe this PhD to my supervisors.

This acknowledgement wouldn't be complete without mentioning Colm and Andrea. You both were my left and right arm during my PhD. Sample collection comes with waiting long hours, early mornings, late nights, frustration and even surviving a pandemic. A special mention to Marta and Nikoleta who helped me with sample collection and lab work. I've met some amazing people from all over the world thanks to this PhD, only so many got me a special placenta cake for my birthday!

I also have to mention the Coolest Office group: Aenne, Tamara, Aude Claire, Caroline, Stacy, Laura O'B, Laura Lin, Louise, and Joye. Thank you for listening to me, being with me through tears and happiness. I will never forget the surprise office Diwali party that Tamara and Aenne organised because I couldn't go home. It will always be a day to remember.

A major part of my thesis and publications was the functional analysis and placental specific disease mapping with NaviCenta which was done in conjunction with Julia Scheel. I am truly grateful to Julia for always prioritising me and making sure we got the papers published. Julia, your commitment, and discipline is commendable, you are a true friend and my favourite colleague.

I would also like to thank Dr Jane English for all her help and support with the proteomic experiments. Your expertise and novel ideas really made a difference to my PhD and gave me proper direction and guidance. I also appreciate all the help I received from Aisling Noone and Caitriona Scaife with proteomic sample preparation and running them on mass spectrometer.

During my PhD I was part of the Infant Centre and iPlacenta research groups. I would like to thank Colin Murdoch and Mirren for their input and efforts to keep this research group going. I would also like to thank everyone in Department of Obstetrics and Gynaecology, CUMH and Infant Centre who have helped me with various crucial things over the years.

Lastly, I wouldn't be here without my family and friends. My parents and my brother, Ivan, have been so patient and supportive over the years with all the decisions I have made. My parents made it possible for me to travel across the world and pursue my dreams. I would also like to mention all my friends who have constantly lent me listening ears and always believed that I could finish this PhD. Mike, Sharon, Alba, Jay, Chetna thank you for being my personal cheerleaders.

Finally, I would like to thank the numerous women who provided their precious samples and medical data to make this research a possibility.

I express my gratitude to everyone who made this path easier to walk and for making this journey extraordinary.

Thesis Abstract

Background: Pre-eclampsia (PE), an adverse pregnancy outcome affects 2-5% pregnancies worldwide and significantly adversely impacts both maternal and fetal outcomes. Intrauterine growth restriction (IUGR) is defined as the inability of the fetus to reach normal growth potential within the uterus as a result of various genetic, environmental, or placental factors. Premature ageing of the placenta in pregnancy outcomes such as PE and IUGR is associated with the persistent presence of oxidative stress and placental insufficiency reducing its functional capacity. Placental proteomics has been instrumental in improving our understanding of molecular mechanisms involved in the pathophysiology of placental insufficiency as well as identifying biomarkers to predict and diagnose pregnancy outcomes. In this study, we investigated cellular senescence phenotypes of PE and IUGR pregnancies by simultaneously measuring several biomarkers of senescence, as well as the proteomic signature of the placenta in healthy and adverse pregnancy outcomes PE and IUGR.

Method: Maternal plasma and placental samples were collected at term (>37 weeks) and preterm (<37 weeks) gestation from nulliparous women undergoing prelabour elective Caesarean section with PE without intrauterine growth restriction (PE; n=5), PE associated with intrauterine growth restriction (n=8), intrauterine growth restriction (IUGR <10th centile) (n=6) and age-matched controls (n=20) from Cork University Maternity Hospital, Cork, Ireland. To assess cellular senescence absolute telomere length (aTL) and senescence associated genes in the placentas was performed by RTqPCR. Cyclin-dependent kinase inhibitors (p21 and

p16) expression were determined by Western blotting. Senescence Associated Secretory Phenotype (SASP) were evaluated in maternal plasma by multiplex ELISA assay. Proteomic analysis of placental samples dissected into 3 sub-anatomical regions (maternal, middle, fetal) taken from 3 nulliparous healthy placentas was performed by mass-spectrometry and pathway analysis was conducted. Based on the differentially expressed proteins (DEPs), a placenta specific disease map using NaviCenta focusing on functional analysis to include the placenta specific context for healthy (n=4) compared to PE affected (n=4) and IUGR affected (n=4) placentas.

Results: Placental expression of senescence associated genes CHEK1, PCNA, PTEN, CDKN2A, CCNB-1 was significantly upregulated in PE, while TBX-2, PCNA, ATM and CCNB-1 expression were significantly decreased in IUGR compared to controls. Moreover, placental p16 protein expression was significantly decreased in PE only when compared to controls placentas. We also observed that IL-6 was significantly increased in maternal circulation in PE when compared to controls; while IFN-γ was significantly increased in maternal circulation in women affected with IUGR when compared to controls. Proteomic profiling of healthy placentas divided into three sub-anatomical regions identified 1081, 1086, and 1101 proteins in maternal, middle, and fetal sub-anatomical regions respectively. Depending on sample site location and sub-anatomical regions, 374 differentially expressed proteins (DEP) were identified. When we investigated the proteomic variations between PE and IUGR placentas when compared to controls we observed 314, 391, and 378 proteins in healthy control, PE, and IUGR placenta, respectively. We performed functional analysis by combining ClusterCompare and NaviCenta to analyse a placenta-centric context, and observed regulatory elements predominantly

involved in the immune regulation, complement cascade and antioxidant activities in PE and IUGR compared to control placentas.

Conclusion: This thesis provides evidence of premature senescence in IUGR, while in PE, evidence of activated cell cycle checkpoint regulators is suggestive of cellular repair and proliferation rather than progression to cellular senescence. The heterogeneity within senescence molecular markers of these phenotypes highlights the complexity and disparity between pathophysiological insults unique to each obstetric complication. Proteomic profiling of sub-anatomical placental regions highlighted the variabilities between regions particularly providing evidence of senescence in these regions. Placental proteomic mapping of healthy placentas compared to adverse pregnancy outcomes PE and IUGR revealed the importance of complement system, inflammatory response, and antioxidant activity in placental function in PE placentas. The identification of novel targets such as transcription factor activity and synergistic miRNAs elements within the core regulatory network, might enlighten future placental research within adverse pregnancy outcomes.

Chapter 1: Introduction

Excerpts from this chapter appear in the following publications:

Manna S, McCarthy C, McCarthy FP. Placental Ageing in Adverse Pregnancy Outcomes: Telomere Shortening, Cell Senescence, and Mitochondrial Dysfunction. *Oxid Med Cell Longev*. 2019;2019:3095383. Published 2019 May 22. doi:10.1155/2019/3095383

Manna S, Ruano CSM, Hegenbarth J-C, Vaiman D, Gupta S, McCarthy FP, Méhats C, McCarthy C, Apicella C, Scheel J. Computational Models on Pathological Redox Signalling Driven by Pregnancy: A Review. Antioxidants. 2022; 11(3):585. https://doi.org/10.3390/antiox11030585

1.1 Cell Cycle and Ageing

Ageing is an inevitable process experienced by all cells, tissues, organs, and organisms. This unidirectional process is characterised as either replicative senescence, which is the process of a cell running its course of life by reaching the Hayflick limit or cellular senescence as a result of external or internal stressors. Both senescence phenotypes are characterised by decline in functionality, mitochondrial dysfunction, altered metabolism and signalling.

Cell cycle is a process by which cells divide and replicate through interphase, mitosis and nuclear division [2]. The interphase is categorized as G1, S and G2 phase, while Mitosis or M-phase represents nuclear division [3, 4]. G1 phase is also known as the first gap phase where the cell increases in size, duplicates its intracellular organelles, and generates the molecular building blocks necessary for later stages. In the G1 phase, the cell also establishes the required mechanisms for DNA synthesis to progress through the G1 checkpoint. S phase is where DNA synthesis occurs with the duplication of microtubule-organizing centrosomes which help separate DNA strands during M phase [4].

During the G2 phase or the second gap phase the cell continues to grow and synthesize proteins and organelles. In this phase microtubules begin to reorganize forming a spindle and the G2 checkpoint ensures that the cell is ready to proceed to M phase where mitosis occurs. Mitosis is categorised into 4 stages, namely prophase, metaphase, anaphase, and telophase. During the M phase cell growth is halted and cellular energy is focused on the orderly division into two daughter cells, complete with individual cytoplasm and DNA. G0 is a fifth phase which is a non-

proliferating or quiescent phase where cells have withdrawn from active cell cycle.

The different cell cycle stages are shown in Figure 1.1.

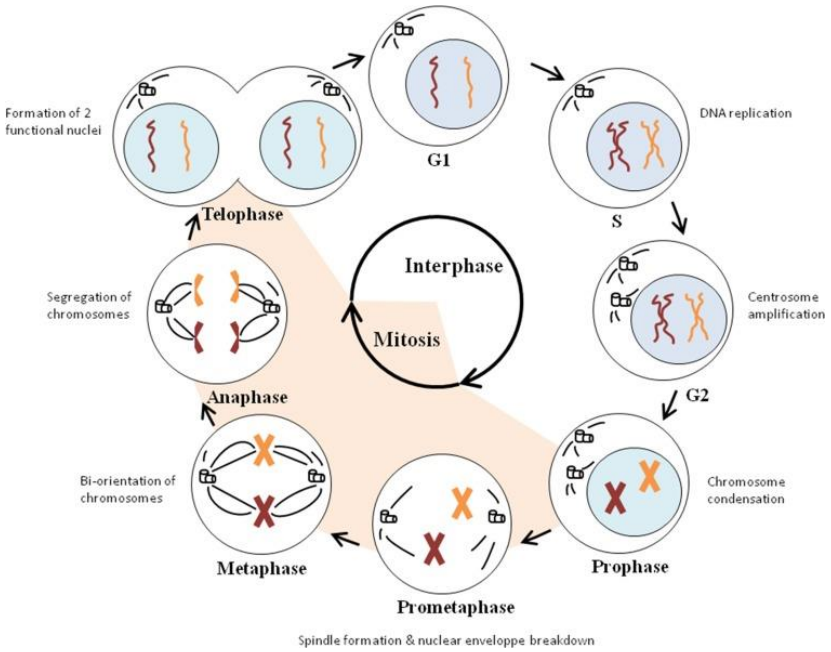


Figure 1.1 Cell Cycle Progression characterised by Interphase and Mitosis. Image adapted from Maes et al 2017 [3].

The number of times a cell divides is limited, as described by German biologist August Weismann in 1881, who stated that "death takes place because a worn-out tissue cannot forever renew itself, and because a capacity for increase by means of cell division is not everlasting but finite" [5]. However, it was only in 1961, when Hayflick and colleagues observed that normal/non-cancerous cells have a finite capacity to replicate, whereas cancer cells, possessed indefinite replicating capacity, making them immortal [5]. This process of finite replicative capacity of normal (healthy) cells was coined by the term Hayflick's limit or Hayflick's theory of ageing [5]. Hayflick's limit was molecularly characterised by telomere shortening and a reduction in telomerase enzyme activity resulting in the damage induced mechanism of ageing [6], loss of proteostasis or proteome homeostasis through misfolded aggregates of damaged polypeptides [7] and mitochondrial dysfunction [8].

Moreover, the hallmarks of ageing can be summarized as: (a) causes of age-related damage; (b) responses to the age-associated damage; and (c) consequences of responses such as apoptosis and oxidative stress on the cellular aging phenotype [9]. However, due to deleterious inter-cellular and intra-cellular events, cellular ageing can be accelerated either inducing programmed cell death or cellular senescence [10]. These events are discussed in detail in the following sections.

1.2 Physiology of Redox Signalling

1.2.1 Reactive Species

Reactive oxygen species (ROS) can be defined as chemically unstable molecules containing oxygen atoms through which cellular and extracellular reactions are more reactive. As a by-product of aerobic metabolism, reactive oxygen species

include both radical (with unpaired electrons) and non-radical forms. Types of ROS include superoxide anion ($O2^{-}$), hydrogen peroxide (H_2O_2), and hydroxyl radicals ($^{\cdot}OH$) [11]. ROS are involved in signal transduction acting as signalling molecules regulating essential biological and physiologic functions [12]. Impaired ROS production and elevated oxidative stress induce cellular dysfunction by damaging lipids, proteins, and DNA and are often described as pathogenic mediators in a myriad of clinical disorders [13].

1.2.2 Sources of Reactive Species

Mitochondrial electron transport chain (ETC) accounts for a majority of ROS produced with faulty electron transport and leaky protons, originating from the oxidation of NADH and $FADH_2$, at complex I (NADH dehydrogenase) and complex III (coenzyme Q and cytochrome c oxidoreductase) respectively [15]. The second most abundant source of ROS is the seven forms of the enzyme complex Nicotinamide adenine dinucleotide phosphate (NADPH) oxidase, which produces ROS in the cytoplasm in response to a variety of external and internal stimuli. ROS production also occurs in peroxisomes, lysosomes, Golgi, and endoplasmic reticulum membranes, mediated in part by xanthine oxidases during purine degradation, and by cytochrome P450 enzymes involved in biosynthesis of fatty acids and clearance of xenobiotics [16].

Another type of reactive species is Reactive Nitrogen Species (RNS) such as nitric oxide ($NO\cdot$) produced from L-arginine by three main enzymatic isoforms of nitric oxide synthase (NOS). The three enzymatic isoforms of NOS are: endothelial NOS (eNOS) involved in vasodilation and vascular regulation; neuronal NOS (nNOS)

associated with intracellular signalling (synaptic plasticity in the central nervous system (CNS), central regulation of blood pressure, smooth muscle relaxation, and vasodilatation via peripheral nitrergic nerves); and inducible NOS (iNOS) which has a variety of functions such as immune regulation, pathogen killing and inhibition of T cell activity [17-19]. RNS act as potent second messengers through glycolytic metabolism by inhibiting mitochondrial respiration via Cytochrome C oxidase and increases in AMPK phosphorylation [20]. Additionally, nitric oxide (NO•−) interacts with superoxide (O2•−) to form peroxynitrite molecule (ONOO•−) a highly reactive molecule which targets and nitrosylates non-enzymatic antioxidant glutathione [21, 22].

1.2.3 Antioxidant Cellular Systems

The term antioxidant originated in early 20th century to refer to molecules preventing consumption of oxygen, especially preventing corrosion of metal. Biologically, antioxidant molecules donate an electron, while themselves remaining stable, to scavenge free radicals and hence reduce cellular oxidative damage [23]. The mechanism of action of antioxidants is either through a chain-breaking mechanism or by removal of reactive species (RS) [24]. The chain breaking antioxidant action is where the primary antioxidant donates an electron to the RS [25, 26]. The removal of RS can be obtained through quenching the chain-initiating catalyst, electron donation, metal ion chelation, co-antioxidants, or by regulation of gene expression [24, 26].

Antioxidants are classified as either intrinsic or extrinsic depending on their source. Extrinsic antioxidants such as Vitamin C, E, A, flavonoids, carotenoids etc cannot be

synthesized in the human body through enzymatic reactions and are absorbed through diet [27]. Intrinsic antioxidant enzymes are produced by the human body, and these include:

a) Superoxide Dismutase (SOD): SODs are the first line of defence against ROS. SOD enzymes accelerate the reaction of the superoxide anion (O2•−) with itself to form hydrogen peroxide (H_2O_2) and oxygen. There are three classes of SODs based on the catalytic metal they react with: Cu/Zn SOD, Mn SOD/Fe SOD, and Ni SOD [28].

b) Catalase (Cat) converts H_2O_2 to water and oxygen, by reduction of the iron atom at the centre of the heme group in the active site [29].

c) Thioredoxin and Thioredoxin Reductase: Thioredoxin Reductase (TrxR) is a ubiquitous enzyme with a described physiological role of reducing NADPH to thioredoxin. There are two variants of TrxR: High molecular weight TrxR (H-TrxR) and Low molecular weight TrxR (L-TrxR) [30].

d) Glutathione (GSH), glutathione (GSSG) and glutaredoxins (Grx): Glutathione is present in almost every cell in the body and acts as a detoxification agent. Glutathione (GSH) acts as a hydrogen donor in the reduction reaction to form water and oxidised glutathione (GSSG) from hydrogen peroxide (H_2O_2). The roles of GSH as the major reducing agent for disulphides and glutathione disulphide (GSSG) as the major thiol-modifying agent are mediated either non-enzymatically or by glutaredoxins (Grx) which play key role in cellular redox homeostasis [31, 32].

1.2.4 Free Radical Theory of Ageing

Over the decades many theories of ageing have been proposed including the 'wear and tear theory of ageing', the 'antagonistic pleiotropy theory of ageing' and the 'disposable soma theory of ageing' [33]. The antagonistic pleiotropy theory of ageing refers to reduction of general fitness seen in the aged population which loosely suggests evolutionary mechanism by elimination through natural selection [34]. The wear and tear theory of ageing proposed in 1882 by German biologist, Dr August Wiesmann suggests that ageing results from wear and tear of cells and tissues due to various factors such as oxidative stress, toxins and other environmental stressors [35]. The disposable soma theory states that ageing is a result of constant damage and counteracted repairs which disbalances energy metabolism [36].

The free radical theory or oxidative stress theory of ageing states that physiological ageing can be triggered by formation of free radicals in the form of Reactive Oxygen Species (ROS). The pumping of electrons across the inner mitochondrial membrane during the mitochondrial electron transport chain (ETC), may cause leaching of electrons leading to generation of free radicals such as ROS which increase oxidative stress (OS) within the cell [33]. The chronological events caused by the imbalance of ROS activity and antioxidant enzyme activity alters physiological redox signalling resulting in premature senescence. [37, 38]. Irreversible and reversible changes occurring within the cells as a result of increased accumulation of ROS and subsequent oxidative damage disrupt molecular functions and result in cellular senescence [39].

Increases in oxidative stress are often counteracted by the release of mitochondrial antioxidants, such as intrinsic antioxidants, including glutathione, superoxide dismutase, thioredoxin reductase etc. However, in the persistent presence of ROS, the threshold is reached resulting in excessive OS [33]. Under conditions of excessive OS, oxidation of macromolecules (lipids, proteins, and DNA) occurs [40]. The exact mechanisms of Free Radical theory of ageing is not fully understood, however, the fate of a cell experiencing increased OS can be either one of: apoptosis, autophagy, necrosis, or senescence.

1.3 Cellular Senescence

Cellular senescence can be defined as a cell-cycle arrest stage which may be instigated by intrinsic or extrinsic stresses on cells which were previously replication component cells [41]. Physiologic senescence act as tumour suppressors that inhibits the progression of malignant or tumour cells from proliferating and becoming carcinogenic [42]. All cells continuously experience stress and stimuli from exogenous and endogenous sources and respond to them by either completely recovering or undergoing cell death. In some cases, active proliferative cells enter permanent cell cycle arrest as a response to external or internal stressors, a process known as cellular senescence. To understand the complex phenomenon that leads to cellular senescence, its causes and consequences must firstly be identified.

1.3.1 Causes of Cellular Senescence

Telomere Dependant Senescence: Telomeres are present at the end of DNA strands in the form of nucleotide repeats (TTAGGG). DNA damage as a result of deleterious stimuli arresting cell division, and promoting cell death, act as precursors for

activation of altered signalling cascades including the DNA damage response signalling pathways such as Ataxia telangiectasia-mutated (ATM) and Ataxia telangiectasia and Rad3-related (ATR) pathways [43]. The presence of proteins like shelterin protect against the cellular recognition of accumulated DNA damage within telomeres [43]. As the proliferative capacity of cells are limited, there is a reduction in telomere length with each replication cycle ultimately leading to the cessation of cellular growth and eventual cell death [44]. Telomerase is an enzyme (RNA-protein complex) which preserves telomere length by replenishing lost nucleotide chains in somatic cells [45]. Telomerase activity is usually downregulated in healthy cells to protect them from neoplastic changes [46, 47].

Telomere Independent Senescence: Cellular senescence is evident even in absence of telomere shortening. This occurs in conjunction with DNA Damage Response (DDR) signalling as a result of elevated oxidative stress. [48, 49]. In the case of excessive OS, accumulation of double stranded DNA breaks leads to an immediate halt of the cell cycle and induction of cellular senescence, irrespective of telomere length or telomerase activity. In states of milder OS, accumulation of single stranded breaks at telomere ends maybe repaired, allowing cells to replicate, hence telomere shortening might still be evident [50, 51].

DNA Damage Response (DDR): DDR can be defined as the actions of checkpoints which determine cell cycle progression and engage in the process of DNA repair. DNA damage in cells has two possible outcomes: cells will continue to proliferate if DNA can be effectively repaired; or if DNA is beyond repair, the cells undergo permanent cell cycle arrest followed by apoptosis or cellular death [52]. An alternative

to apoptosis as a result to DNA damage is the initiation of cellular senescence where the cell shifts towards a senile form, accompanied by hallmarks of senescence [53]. Figure 1.2 a and Figure 1.2 b shows the various molecular features of cellular senescence.

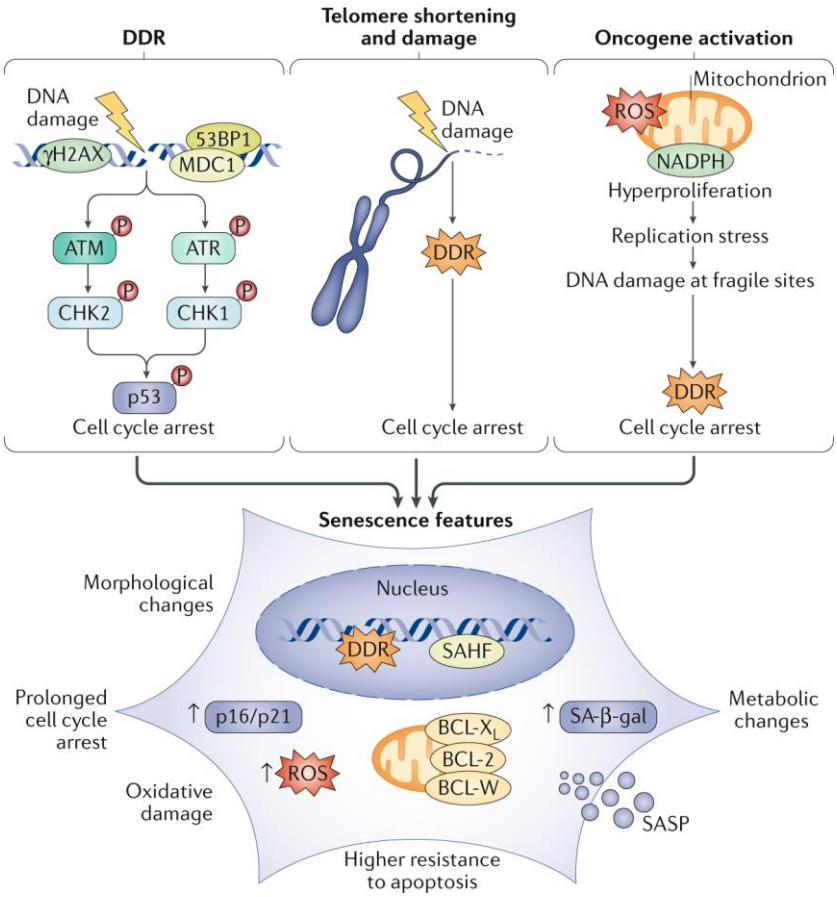


Figure 1.2a. Features of Cellular Senescence. Adapted from Di Micco et al., 2021 [54].

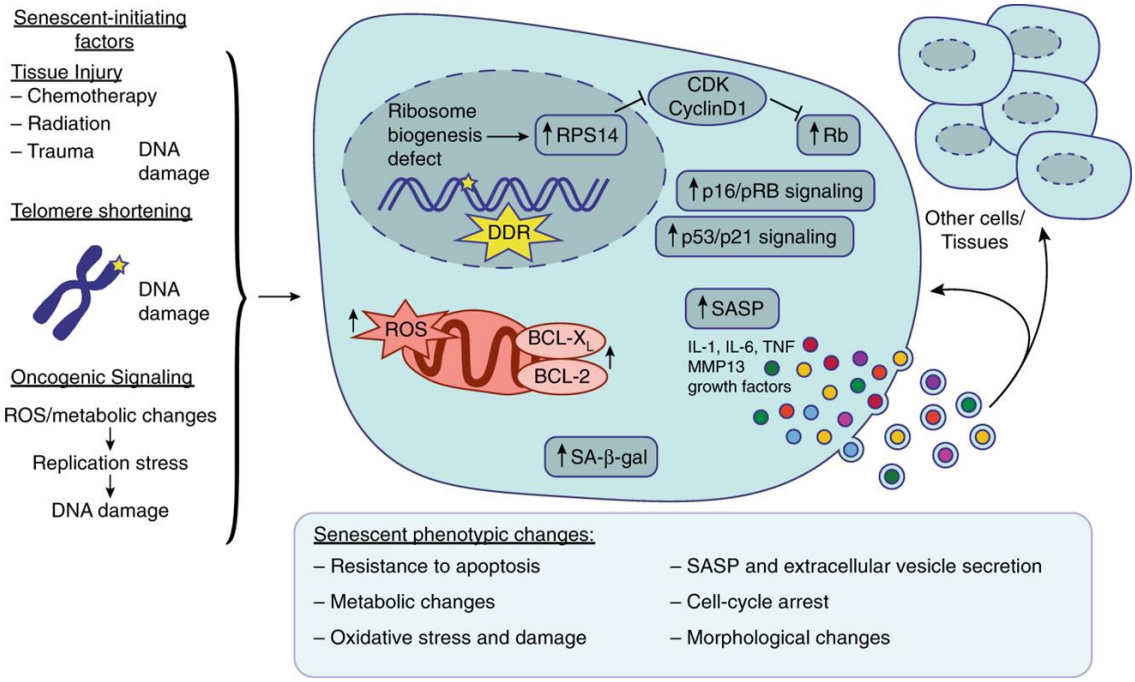


Figure 1.2 b. Synopsis of Cellular Senescence markers**.** Adapted from Wan et al., 2021 [553].

The most relevant pathways regulating cellular senescence are P16Ink4a/Rb (retinoblastoma protein) and p53/P21Cip1/P19Arf pathways, which work either in conjunction or independently to determine cellular fate [55]. Cyclin Dependant kinase (CDK) 4 or it's inhibitor Ink4 form part of the p16/pRB family which is responsible for halting cell cycle progression [55]. Dephosphorylated RB binds to the to the promoter region of E2F, forming the RB-E2F complex inhibiting cell cycle progression and initiating cellular senescence [56]. External stressors promote senescence through the p16/pRB pathway independent of telomere length [57]. p53 is a tumour suppressor protein which is activated by various post-translational modifications including phosphorylation, methylation, acetylation, sumolytion and ubiquitination [57]. Activation of the Ataxia Telangiectasia Mutated (ATM) kinase

family as a result of DNA damage, is responsible for p53 activation and progression of cells towards senescence by triggering multiple anti-proliferative proteins [56].

1.3.2 Senescence Associated Secretory Phenotypes (SASP)

SASP can be defined as cytokines, chemokines, proteases, lipids, and growth factors secreted by senescent cells. This secretome is dependent on the senescent stimuli, and is involved in removing dead and decaying cellular debris [58]. However, accumulation of SASP secretomes may have both beneficial and deleterious effects on the surrounding cellular environment. The recruitment of immune cells can remove mutated and pre-malignant cells and promote the repair of damaged tissues. However, the persistent generation of the pro-inflammatory factors (TNF α, IL-6, IL-8, monocyte chemoattractant protein (MCP-1) by these immune cells, may induce senescence in surrounding non-senile cells due to cytotoxicity [59].

1.3.3 Pathological consequences of cellular senescence

There are a myriad of diseases that have been associated with senescence, which contribute to pathological transformations both intracellularly and within the cellular environment driving disease progression [60]. Impaired senescence Associated β-Galactosidase (SA-β-Gal) activity, cyclin dependant kinase (CDK) activity has been reported in brain aneurysms, Alzheimer's disease, Parkinson's disease, cystic fibrosis, osteoarthritis, intestinal bowel disease (IBS) and glaucoma, [60]. There are three main attributes by which senescent cells can have major pathological impacts within tissues. They are listed as:

Impairment of tissue regeneration: In response to potential harmful stimuli, cells lose their proliferative capacity and as a result of accumulated DNA damage enter senescence [61]. DNA damage leads to alterations in cellular signalling cascades including the p16/pRB, p53/p21 pathways, restricting the cellular potential for repair and further proliferation [62].

Cellular dysfunction: An undesirable consequence of senescent gene expression and altered signalling, is impaired cell function. These changes result in the accumulation of dysfunctional tissue, compromising organ functionality and promoting disease progression [63].

Impact on the microenvironment: The microenvironment created by senescent cells can negatively impact their neighbouring cells by secretion of soluble factors including cytokines and proteases. Senescent cell secreted proteases such as matrix metalloproteinases (MMPs) can degranulate and degrade the extracellular matrix

(ECM) disrupting the physiological and functional integrity of surrounding cells, further contributing to disease progression [64, 65].

1.4 Pre-eclampsia

The International Society for the Study of Hypertension in Pregnancy (ISSHP) defines Pre-eclampsia (PE) as de-novo hypertension (≥140/90 mm Hg) after 20 weeks of gestation in the presence of either proteinuria and/or evidence of maternal acute kidney injury (AKI), liver dysfunction, neurological features, haemolysis or thrombocytopenia, or fetal growth restriction [66]. More specifically, elevated blood pressure is associated with either Proteinuria ≥300 mg per 24-h urine collection (or extrapolated from timed collection), or, protein/creatinine ratio of ≥0.3 mg/dl, or dipstick reading of 2+ [67]. In the absence of proteinuria, PE can be diagnosed if presenting with thrombocytopenia with a platelet count <100,000/mm^3, impaired kidney functioning with serum creatinine concentration >1.1 mg/dl or a doubling of serum creatinine concentration in the absence of other renal disease, impaired liver function with double concentration of liver transaminases compared to normal levels, severe persistent epigastric pain, pulmonary oedema diagnosed by chest x-ray, neurological symptoms with newly onset headache or visual disturbance, and fetal growth restriction with an estimated fetal weight <10th percentile [67].

A serious complication of pregnancy known as the HELLP syndrome is defined as haemolysis, elevated liver enzymes and low platelet count, occurs in 10-20% of severe PE cases [68]. Obstetric haemorrhage and disseminated intravascular coagulation (DIC), a leading cause of maternal mortality, has been associated with

HELLP syndrome [69].DIC is an acquired syndrome characterized by the intravascular activation of coagulation with a loss of localization arising from different causes. It can originate from and cause damage to the microvasculature, which if sufficiently severe, can result in organ dysfunction[69, 70].

1.4.1 Epidemiology of PE

Globally, PE complicates 3-8% of all pregnancies and is one of the main causes of over 500,000 fetal and neonatal deaths as well as over 70,000 maternal deaths worldwide annually [66]. Additionally, PE is responsible for 12-25% of infants born with fetal growth restriction and small for gestational age as well as 15-20% of all preterm births [71]. In Ireland, PE is reported in 2-3% of all pregnancies and around 5-7% of nulliparous pregnancies, with the average cost of PE complicated pregnancy reported at €5243 per case compared with €2452 per case for an uncomplicated pregnancy. Moreover, the national care cost of PE in 2017 was reported between €6.5 and €9.1 million per annum based on the 5% - 7% prevalence rate, with antepartum care and peripartum care accumulating to between €1.5–€2 million per annum [72].

1.4.2 Risk Factors of PE

There are numerous risk factors for PE, as detailed in Table 1.1.

The major risk factors include women with pre-existing hypertension, chronic kidney disease, Type 1 diabetes mellitus and PE in previous pregnancy, multiple pregnancies and greater interval between pregnancies [73]. Moreover, advancing maternal age and higher body mass index (BMI) have been shown to be predisposing factors in PE [74]. Other risk factors include previous miscarriage,

infertility, and even fetal sex with preponderance of male infants among mothers with PE [75, 76].

Table 1.1 Risk factors associated with PE [84].

Risk Factors	Relative Risk (RR)	95% Confidence Interval (CI)
Previous PE	8.4	7.13.7-9.9
Chronic Hypertension	5.1	4.0-6.5
Pregestational Diabetes Mellitus	3.7	3.1-4.3
Multiple gestation	2.9	2.6-3.1
Pre-pregnancy Body Mass Index >30	2.8	2.6-3.1
Antiphospholipid Syndrome	2.8	1.8-4.3
Systemic Lupus Erythematosus (SLE)	2.5	1.0-6.3
History of stillbirth	2.4	1.7-3.4
Pre-pregnancy Body Mass Index >25	2.1	2.0-2.2
Nulliparity	2.1	1.9-2.4
Prior Placental Abruption	2.0	1.4-2.7
Assisted Reproductive Technology (ART)	1.8	1.6-2.1
Chronic Kidney Disease (CKD)	1.8	1.6-2.1
Advanced maternal age >35 years	1.2	1.1-1.3

1.4.3 Pathophysiology of PE

PE is a complex heterogenous condition, whose pathophysiology even after decades of research, is not completely understood. PE can be characterised as early onset or severe, comprising less than 20% of all cases, or late onset or mild, comprising the remaining 80% [1, 43]. Severe PE can be defined as early onset of PE at gestational age <37 weeks with systolic blood pressure (SBP) in >160 mmHg; diastolic blood pressure (DBP) >100 mmHg and proteinuria in >2 g/l [77]. Several hypotheses have been proposed to fully elucidate the underlying pathological mechanisms [78, 79]. The placental origin of PE hypothesis describes inefficient trophoblast invasion and remodelling of maternal spiral arteries, causing "placental syndrome," subsequently resulting in PE and fetal growth restriction [80].Substantial work in this area by Professor Chris Redman initially proposed a two-stage model of PE which was later modified to six stages [1, 80, 81]. A more recent cardiovascular origin of PE hypothesis proposed by Professor Basky Thilaganathan implicated abnormal maternal cardiovascular function as instigating abnormal placentation associated with PE and also proposed that the placental origin of PE only holds true in the case of early onset of the disease [79, 82]. These models are discussed in detail in the following paragraphs.

Classical Two-Stage Model of PE: Proposed by Redman in 1991, the original theory postulated that PE has two stages: Stage 1 comprising of poor placentation and Stage 2 as the clinical manifestations of PE presented as hypertension and proteinuria. However the clinical symptoms or Stage 2 is manifested when Stage 1 assimilates with maternal factors such as genetic, behavioural or environmental

factors [83]. Redman stated that PE has a placental or trophoblastic origin rather than haemodynamic, renal, or even vascular origin, even though these systems are affected. Moreover, Redman stated that placenta is the dysfunctional tissue as neither the fetus nor uterus is required for development of PE [84, 85].

Revised Six-Stage Model of PE: Redman recently reclassified the two-stage model into a more complex six-stage model. In this revised model of disease pathophysiology, stages 1 and 2 could be described as an early phenomenon such as preconception intolerance of the mother towards paternal semen or short duration between the initiation of coital activity to conception interval , leading to poor placentation and impacting the fetal growth[1]. Stage 3 begins at 8 weeks of pregnancy where in uncomplicated pregnancies, trophoblastic plugs sealing the maternal spiral arteries recede and the establishment of uteroplacental circulation begins [1, 80]. However, in PE, there is premature opening of trophoblastic plugs with the resultant influx of arterial blood increasing oxidative stress within the placenta leading to defective placentation [1, 80]. Stage 4 of Redman's model of PE is characterised by a reduction in placental growth factors leading to impaired vascular remodelling of maternal spiral arteries. In Stages 5 and 6 increased placental and endothelial damage is evident which results in the clinical symptoms of PE [1, 80].

Cardiovascular Model of PE: Late-onset PE can be attributed to an underlying maternal cardiovascular dysfunction which fails to meet the haemodynamic and metabolic needs of pregnancy. This also results in adverse postpartum cardiovascular outcomes in over 50% of women, possibly due to the fact that both

PE and cardiovascular diseases share similar genetic and environmental risk factors [79]. During the first two trimesters of a healthy pregnancy, cardiac output increases by over 50% and plateaus thereafter, however, in PE there is elevated cardiac output even after 20 weeks of pregnancy which results in high vascular resistance leading to impaired left ventricular remodelling and isolated left ventricular diastolic dysfunction with concentric left ventricular hypertrophy [86]. Atherosis of maternal arteries as a result of incomplete spiral artery remodelling and placental ischemia contribute to fetal growth restriction [87].

Role of Endothelium: The endothelium is the single layer of active cells lining the inner lumen of blood vessels and is in constant contact with blood flow. The endothelium plays an important role by forming a physiological selective barrier and maintaining vascular homeostasis through balanced vasoconstriction and vasodilation [92]. Moreover, endothelial cells modulate vascular tone, maintain blood fluidity, regulate inflammation and neovascularization [93]. Endothelial dysfunction can be defined as a reduction of NO induced vasodilation and an increase in endothelial-derived vasoconstrictors [94]. This imbalance between endothelial vasodilation and vasoconstriction leads to a specific endothelial activation characterized by a proinflammatory, proliferative, and procoagulant milieu stage.

Placental invasion of maternal spiral arteries establishes the fetoplacental circulation ensuring constant perfusion to the placenta and the developing fetus. Failure to effectively establish this continuous blood supply causes uteroplacental ischaemia [96]. Altered haemodynamic and decreased vascular flow leads to persistent hypoxic-oxygenated state, resulting in elevated oxidative stress within

the placental tissue [1, 97-99]. Equally, defective placentation results in a decrease in production of both angiogenic vascular endothelial growth factor (VEGF) and placental growth factor (PLGF) but an increase in the release of the deleterious placental soluble fms-like tyrosine kinase 1 (sFIt1) into the maternal circulation causing generalized endothelial dysfunction [1, 100]. VEGF regulates the proliferation of vascular endothelial cells (EC) which establishes placental angiogenesis through promotion of blood vessels formation and permeability [101]. Moreover, placental sFlt1 causes endothelial dysfunction by binding to VEGF and PLGF [102]. Circulating sFlt1 is abundant in PE which is attributed to vascular resistance and an increase in arterial blood pressure [1, 103]. Proteinuria in PE can also be associated with increased sFlt1, precipitating glomerular endotheliosis [1, 104].

1.4.4 Histological characteristics of PE

Placental development begins with a decidual reaction evoked by the blastocyst in the maternal endometrium, resulting in the formation of the basal plate. Trophoblasts differentiate into two types: invasive extravillous cytotrophoblast (EVT) or villous cytotrophoblast which later fuse to form the multinucleated syncytiotrophoblasts [1]. Extravillous cytotrophoblasts are responsible for establishment of uteroplacental circulation and regulation of the maternal innate immune system [1, 88, 89]. In an uncomplicated pregnancy, extravillous cytotrophoblasts (EVT) invade maternal spiral arteries, veins, and lymphatic vessels of the endometrium during the first trimester [1, 90, 91].

Despite the heterogeneity of PE, there are consistent histopathological changes evident in placental tissue in PE. These include increased syncytial knots, infarcts

and necrotic spots, thickening of trophoblastic membrane, obliterative enlarged endothelial cells in the fetal capillaries, reduced vascularity of the villi, and atherosis of the spiral arteries [105]. Syncytial knots are formed as a result of cytotrophoblast fusion, and chromatic shrinkage aggregating into knots at the terminal villi [106]. They are usually abundant in mature healthy placenta (>40 weeks of gestation) [106]. In pathological conditions such as PE and IUGR, syncytial knot formation is increased, in part due to placental hypoxia and excessive OS [107]. In addition to syncytial knots, villous and vascular placental lesions are evident in PE, these lesions are consistent with reduced perfusion and subsequent hypoxia in the maternal uteroplacental circulation [108]. Numerous studies have established a significantly higher incidence of infarcts and thrombotic, hyalinised areas due to reduced vascularization and decreased villous vascularity in placental tissue in PE compared to healthy controls [109-111].

1.4.5 Maternal Outcomes of Pre-eclampsia

Cardiovascular and Cerebrovascular: PE has been linked to hypertension, and adverse events associated with cardiovascular and cerebrovascular diseases beyond pregnancy [112]. A Danish cohort study of > 700,000 women with median follow-up of 14.6 years, reported that women experiencing severe PE had a 6-fold (range: 5.45 to 6.77) risk of hypertension, 1.7-fold (range: 1.22 to 2.40) risk of ischemic heart disease, 1.9-fold (range: 1.35 to 2.70) risk of thromboembolism and a 4-fold (range: 3.04 to 4.46) risk of diabetes mellitus type 2 [113, 114]. Moreover, multiple studies have shown that women who had PE are more likely to experience ischemic stroke, haemorrhagic stroke, venous thromboembolism after multivariable adjustment,

and these women have increased morbidity and mortality specifically associated with stroke [115-118].

Renal: End-stage kidney disease (ESKD) is also a recognised maternal outcome of PE, which is directly proportional to timing and severity of the disease and number of pre-eclamptic pregnancies experienced [119]. The risk of microalbuminuria is 4 times higher in women with mild/moderate PE and eight times higher in severe PE [120-122], while the need for dialysis or renal transplant is significantly increased in women with PE [118, 119].

Neurological: There are also significant changes in the maternal cerebrovascular circulation during pregnancy including maintaining brain homeostasis, protecting against Blood-Brain-Barrier (BBB) permeability [123]. Pathological changes observed in PE potentially increase the risk of seizures and haemorrhage [123]. An acute cerebral complication of PE, known as eclampsia is characterised by tonic-clonic seizures either during pregnancy or in the postpartum period [124]. Eclampsia has been attributed to high maternal mortality rates in LMIC countries [125].There also has been a correlation identified between impaired cerebral autoregulation, leading to acute neurovascular complications in women with PE earlier in life [126].

1.4.6 Fetal Outcomes of PE

Uteroplacental dysfunction in PE results in fetal growth restriction defined as an estimated fetal weight <10th percentile for gestational age [127] which results in a number of poor fetal outcomes. PE may account for up to 30% of preterm births. Pre-term birth as a result of early delivery to alleviate maternal PE symptoms have been associated with long term health consequences, affecting cardiovascular,

neurological, behavioural and kidney diseases later in adolescence [128]. There is an increased risk of fetal death both preterm and at term [129]. Severe PE has been associated with a significantly increased risk of stillbirth with a rate of 21 fetal demises per 1000 births, whereas mild PE has been associated with 9 stillbirths every 1000 births [130]. Clinically, the decision of prolonging the pregnancy and risking a stillbirth remains an obstetric challenge in pregnancies less than 37 weeks of gestation [131].

Bronchopulmonary dysplasia (BPD) is the most common fetal complication of PE associated with preterm birth before 30 weeks of gestation and amongst very low-birth weight (VLBW) infants [134, 135].

Neonatal thrombocytopenia is defined as a platelet count < 150,000/µL [136], the degree of severity of thrombocytopenia can be further subcategorized as: mild thrombocytopenia—platelet count 100,000 to 150,000/µL; moderate thrombocytopenia—platelet count 50,000 to 99,000/µL; severe thrombocytopenia—platelet count < 50,000/µL [136]. Certain cerebrovascular events such as brain haemorrhage in neonates include neonatal thrombocytopenia [136]. Moreover, cerebrovascular disorders in infants and children born from a pre-eclamptic pregnancy include pathologies such as motor dysfunction, higher risk of stroke at any age [139], epilepsy, infantile spasms and cerebral palsy [140, 141].

Altered neurodevelopment in the form neuropsychiatric disorders such as increased autism spectrum disorder (ASD) and attention deficit hyperactivity disorder (ADHD) have been associated to children born to PE mothers [142]. The exact mechanism for impaired neurodevelopmental in offspring and PE is not fully

understood, however, a few theories such as redox imbalance and maternal immune activation and upregulation of cytokines in maternal circulation, might lead to childhood disorders such as ASD [141, 143].

1.4.7 Management of PE

According to ISSHP, blood pressure >160/110 mmHg should be treated and monitored with acceptable agents including Nifedipine or Labetalol. Moreover, blood pressures consistently at or above 140/90 mmHg should be treated, aiming for a target diastolic blood pressure of 85 mmHg and systolic blood pressure of 110–140 mmHg to reduce the likelihood of developing severe maternal hypertension and other complications such as HELLP syndrome [66].

Labetalol (a beta-blocker) and/or Nifedipine (a vasodilator) are considered the first-line therapies for the management of high blood pressure in PE. Low-dose aspirin (81 mg/day) is recommended as a prophylaxis for women at high risk for PE, starting at 12 weeks and lasting up to 28 weeks of gestation or until delivery [146]. Hydralazine can also be administered intravenously (IV) in hypertensive emergency [147]. Unfortunately, the only definitive treatment of PE and HELLP syndrome is delivery of the placenta. Magnesium sulphate is administrated either intravenously or intramuscularly to prevent seizures in women at risk of eclampsia [148, 149]. Figure 1.3 shows the clinical management for hypertension in pregnancy.

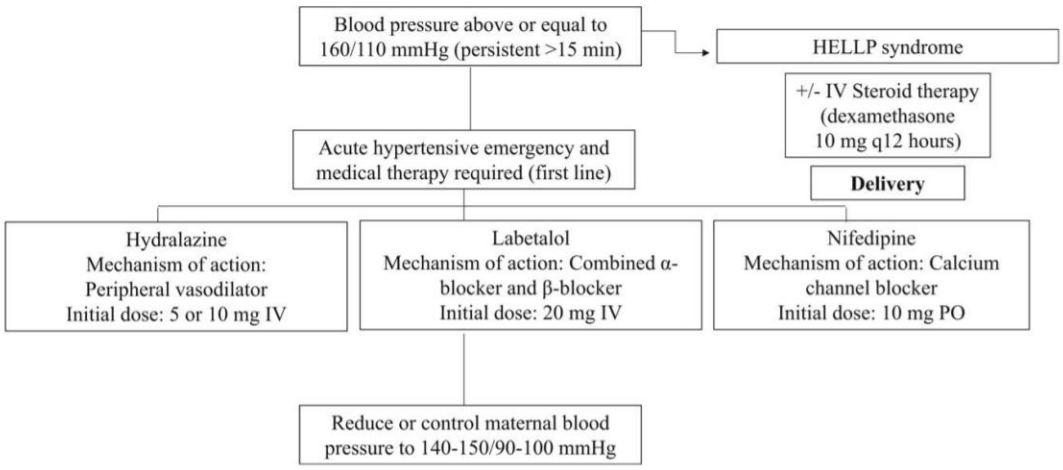


Figure 1.3 Clinical Management of onset of Hypertension in pregnancy. Image created by Amaral et al 2017 (138). (Abbreviations: PE: pre-eclampsia, HELLP: hemolysis, elevated liver enzymes, and low platelet count, IV: intravenous, PO: oral)

Therapeutic Intervention targeting OS: Several therapeutic agents in the form of micronutrients, have been clinically evaluated as possible antioxidant therapies for PE in part due to their ability to reduce ROS production, scavenge existing ROS, regulate NO synthesis, or release and modify antioxidant enzymes targeting free radicals. There have been extensive studies analysing Vitamin C, D & E, through down regulation of NADPH and upregulation eNOS and immune modulation, yet these were unsuccessful in large clinical trials [150, 151]. Lifestyle interventions of modifiable risk factors including regular exercise, weight loss, dietary changes, reducing toxic substances such as tobacco, alcohol and pollutants can help reduce OS and increase physiological antioxidant defence [152]. Melatonin (5-methoxy-N-acetyltryptamine) is primarily produced by the pineal gland to maintain circadian rhythm and has been also shown to improve maternal endothelial function through

acting on endothelial melatonin receptors and reducing circulating levels of sFlt1, sEng, and activin A in PE [153, 154]. Mitochondrial targeted antioxidants have been investigated in preclinical models of PE as a potential therapies including MitoQ [155], MitoTempo, [156] and Ergothioneine [157] have been shown to reduce hypertension and ameliorate the effects of ischemia-induced oxidative damage.

1.5 Intrauterine Growth Restriction (IUGR)

1.5.1 Definition and Epidemiology

Intrauterine growth restriction can be defined as the pathologic inhibition of intrauterine fetal growth and the failure of the fetus to achieve its growth potential [158]. Globally, IUGR is prevalent in 7-15% of pregnancies in high income countries, and 30% of pregnancies in low and moderate income countries [159]. Small for Gestational Age (SGA) can be defined as birth weight less than two standard deviations below the mean or less than the 10th percentile of a population-specific birth weight for specific gestational age [160]. While the terms IUGR and small for gestational age (SGA) have been used interchangeably in the literature, there are specific differences. IUGR indicates neonates born with clinical features of malnutrition and a compromise in in utero growth irrespective of their birth weight percentile [161]. IUGR can be further classified into two types: asymmetrical (type I) and symmetrical (type II). Type II or symmetrical IUGR can be characterized by a proportionate reduction in all auxological parameters, including weight, length, and cranial and abdominal circumference. Whereas Type I or asymmetrical IUGR is characterized by a greater reduction in body weight, when compared to length [159].

Type I or asymmetrical IUGR is most common type accounting for 70-80% of all IUGR cases, it occurs late in the third trimester, where fetal weight gain is normal until the third trimester and restricted thereafter due to placental insufficiency. Reduced abdominal circumference with biparietal diameter, head circumference and femur length are common ultrasound parameters [159, 162, 163]. In asymmetrical IUGR, only weight will be less than 10 centiles and the rest will be as per gestation

age, thus results in “brain sparing,” which can be defined as a process whereby brain growth is less affected than body growth due to the redistribution of cardiac output [163].

Type II or Symmetrical IUGR accounts for 20-30% of all IUGR cases and begins in early pregnancy and is usually associated with genetic disorders or infections intrinsic to the fetus. Ultrasound parameters of Type II IUGR show proportional decrease in biparietal diameter, head circumference, abdominal circumference, and femoral length [164]. Symmetrical IUGR is also associated with poor fetal prognosis and high morbidity and mortality when compared to asymmetrical IUGR [159, 164].

Infants born with symmetrical IUGR are underdeveloped postnatally because of less cell numbers at birth and usually remain small throughout their lives. On the other hand, those with asymmetrical IUGR have good prognosis and have good postnatal growth because of normal cell numbers [159, 164].

1.5.2 Diagnosis of IUGR

The diagnosis of IUGR is based on accurate early dating of pregnancy, assessment of risk factors and the use of ultrasound for fetal growth estimation. In order to exclude other diagnoses such as PE, additional tests such as urine protein assessment, Creatinine Protein Ratio (CPR) are performed. The diagnosis chart of IUGR is shown on Figure 1.4. Accurate dating can be established with an algorithm for determining the estimated date of delivery as follows: before 13 6/7 weeks gestation, if last menstrual period (LMP) and ultrasound day differ by 7 days, or, between 14 and 19 6/7 weeks of gestation, if LMP and ultrasound-based dating differ by 10 days, preference is given to ultrasound-based date [165].

Once accurate dating has been established, other risk factors are assessed such as maternal systemic disorders affecting poor fetal growth outcomes, such as hypertension, renal diseases, long-standing pregestational diabetes with vasculopathy, and other systemic disease. Recording maternal alcohol use, tobacco or use of illicit drugs can also be useful for diagnosis and prognosis of IUGR. Lastly, monitoring maternal nutrition and weight gain, as well as appropriate antenatal care and measurement of the symphysis-fundal height (SFH) height provides a helpful measure to assess fetal growth during pregnancy and can help early detection of IUGR [166].

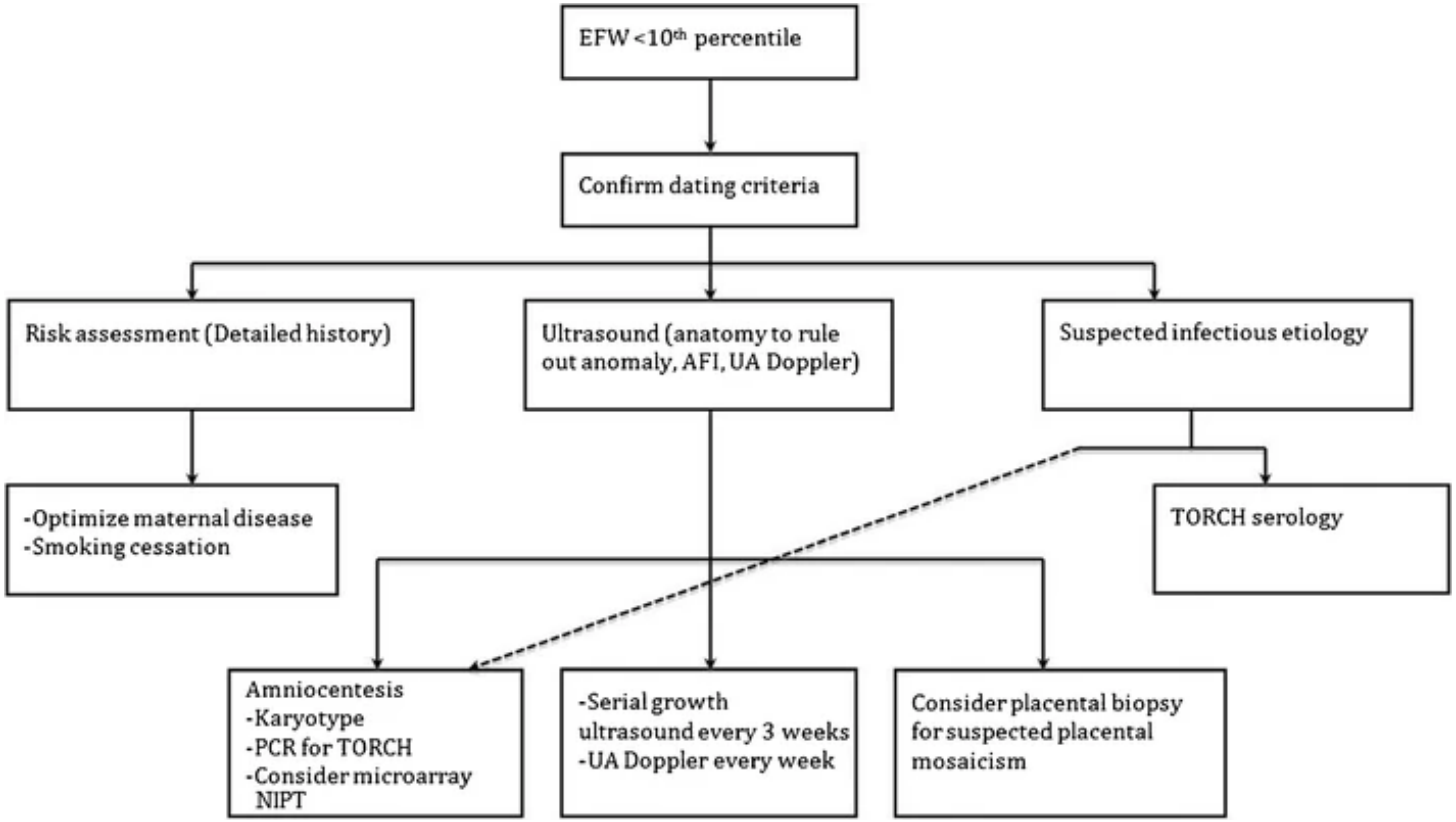


Figure 1.4 Diagnosis of IUGR. Image adapted from Suhag et al 2013 [166]. Abbreviations: EFW = estimated fetal weight; UA = umbilical artery; AFI = amniotic fluid index; TORCH = toxoplasmosis, other (syphilis), rubella, cytomegalovirus, herpes; PCR = polymerase chain reaction; NIPT = non-invasive prenatal testing.

1.5.3 Pathophysiology of IUGR

There are multiple causes of IUGR categorized as maternal, fetal, and placental. The fetal factors involved in the pathogenesis of IUGR include multiple pregnancies, genetic abnormalities, intrauterine infections, and metabolic disorders [167-172]. Genetic mutations in genes responsible for insulin like growth factor (IGF) production, especially mutations in the IGF-1 receptor are responsible for pre- and post-natal growth restriction [169]. Insulin like growth factor I & II mediated by IGF binding proteins (IGFBP) stimulate fetal cell proliferation and differentiation along with synthesis of protein and glycogen which are essential for fetal growth [169].

Intra-uterine infections including placentitis, vascular endothelial lesions, fetal viremia with inhibition of cell multiplication, angiopathy obliterans, chromosomal ruptures and cytolysis account for 5-10% of IUGR cases [173]. These infections are usually caused by rubella virus, cytomegalovirus, varicella zoster virus, and Toxoplasma gondii [173]. IUGR is evident in 15-30% of all multiple pregnancies, usually the growth rates falling after 28-30 weeks of pregnancy, after which growth rate falls by 15-20% [174]. Lastly, metabolic disorders such as the agenesis of the pancreas, congenital absence of the islets of Langerhans, congenital lipodystrophy, galactosemia, generalized gangliosidosis type I, hypophosphatasia, I-cell disease, Leprechaunism, fetal phenylketonuria, and transient neonatal diabetes mellitus may result in IUGR [159, 160, 173].

Given the critical role of the placenta in supporting fetal growth and development, structural disturbances in the utero-placental unit equally contribute to the

development of IUGR [175-182]. Placental weight has been directly linked to fetal birthweight. Placental weight relates to functional tissue mass of placenta and is crucial for the exchange between mother and fetus [183]. IUGR placentas exhibit lesser villous surface area and lower fetal capillary surface area, reducing the capacity for oxygen and nutrition transfer between mother and fetus [175-182]. Reduction in terminal villi number is indicative of malfunctioning vascularization and inadequate trophoblast invasion of spiral arteries which can also result in reduced fetal growth [175-182].

Terminal villi of IUGR placentas are smaller in diameter with an increase in syncytial nuclei, reduced cytotrophoblastic nuclei, thickened basal lamina, and increased stromal deposition of collagen and laminins when compared to healthy placental tissue [184, 185]. Increased rates of apoptosis in syncytiotrophoblasts is more prevalent than cytotrophoblast in IUGR placental tissues [186].Other notable lesions observed are increases in syncytial knots, villous fibrosis, villous oedema and extensive deposition of peri-villous fibrin [187]. Cord complications such as velamentous cord insertion, single umbilical artery (SUA), true umbilical cord knot can lead to IUGR. Placental infections including placental malaria (PM) is a major cause of fetal growth restriction, especially in the developing world [175-182].

1.5.4 Maternal factors of IUGR

Maternal clinical diseases including hypertensive pregnancy diseases such as PE increase the incidence of growth restriction by 2-3-fold as a result of reduced uteroplacental perfusion [159, 160]. Other maternal diseases such as insulin-dependent diabetes mellitus with vasculopathy, congenital cyanotic heart diseases, restrictive

pneumopathies, severe renal diseases, autoimmune diseases, antiphospholipid antibody syndrome, hereditary or acquired thrombophilia, hyperhomocysteinemia, and severe anaemia are also commonly associated with IUGR [159, 160, 167, 189].

Maternal Diet: Maternal nutrition during gestation is crucial for embryonic development and fetal growth. As shown by various animal models and human studies, malnourished mothers alter the fetal growth trajectory modifying placental weight, surface area and nutrient transfer capacity depending on the severity of the nutritional challenge and on the time of deprivation [190, 191]. Fetal growth stages are dependent on appropriate maternal nutrient transfer hence a balanced diet is essential to avoid fetal complications. Vegetarian and vegan maternal diets which lack micro- and macro-nutrients such as proteins, vitamin B12, vitamin D, calcium, Docosahexaenoic acid (DHA), and iron increase the risk of low birthweight, fetal neurological disabilities, malformations, and overall fetal growth. However, supplementation with these improves pregnancy outcomes similar to those reported in the omnivorous population [192].

Smoking, Alcohol and Opioid dependence: Maternal smoking during pregnancy results in fetal exposure to carbon monoxide reducing the ability of fetal haemoglobin to transport oxygen. Nicotine equally induces the release of maternal catecholamines which reduces placental perfusion. There is a direct correlation between the number of cigarettes consumed and the degree of IUGR. The use of alcohol in pregnancy has increased considerably in the last number of decades. Fetal exposure to alcohol during pregnancy results in Fetal Alcohol Syndrome (FAS) which has been associated with growth restriction, facial malformations, and

impairment of the fetal central nervous system. FAS is more prevalent in the western part of the world with the highest estimated alcohol use during pregnancy in Ireland (60.4%), Belarus (46.6%), Denmark (45.8%), UK (41.3%), and Russia (36.5%) [193]. FAS has been linked to various fetal morphological features such as craniofacial dysmorphology, neurological deficits and even behavioural disorders such as ADHD [193, 194].

Opioid dependence has been frequently reported with IUGR and preterm birth [195]. The placenta fetus plays a major role in production of essential hormones and filtration of metabolic waste products to facilitate optimal development of the baby [196]. Highly lipid soluble opioids such as morphine, pethidine, fentanyl, and hydromorphone can cross the placental barrier reaching the fetus during pregnancy [197]. In addition, as a result of cocaine and amphetamine use, placental function is compromised due to the reduction of uterotonic agents such as placental serotonin and norepinephrine transporters across the placenta. This restriction subsequently increases the risk of IUGR and preterm birth as a result of high levels of these monoamines in the intervillous space, with resultant vasoconstriction and uterine contraction [198].

Pollutants/Environmental Factors: Multiple publications have provided evidence that maternal exposure to environmental pollution may impact fetal outcomes [199-202]. Environmental pollutants can be classified as indoor or outdoor pollutants. Outdoor pollutants include ozone (O3), particulate matter (PM10 and PM2.5), carbon monoxide (CO), nitrogen dioxide (NO_2), and sulphur dioxide (SO_2) measuring less than 10 and 2.5 micrometres [203]. Household Air Pollution (HAP) has been

associated with adverse pregnancy outcomes such as IUGR, preterm birth and stillbirth especially in low-income countries which disproportionately suffer from the consequences of HAP, as households predominantly utilize biomass (wood) and kerosene for cooking since cleaner burning fuels such as propane are expensive [204]. Endocrine-disrupting chemicals (EDCs) are exogenous substances which mimic or interfere with the endocrine system, thus altering key biological processes such as organ development, reproduction, immunity, metabolism and behaviour, in part by disrupting normal placental development and have been associated with onset of severe pregnancy outcomes such as PE and IUGR [191].

Epigenetic programming: Epigenetic information responds to internal and external (environmental) stimulus and events create a memory of cell identity that serves to maintain cell identity after differentiation, propagation of essential features of chromosomal architecture, and dosage compensation [205]. Epigenetic modification affects DNA directly through methylation or indirectly through histone modification controlling control transcription, replication, recombination, and repair [205]. Epigenetic mechanisms are essential for healthy placental cell differentiation, and fetal development. Placental methylation has garnered significant interest in recent years, however the roles of placental epigenome in mediating environmental exposure and pregnancy outcomes remain enigmatic [206]. Numerous placental specific imprinting genes such as DNA methyltransferase, cyclin-dependent kinase inhibitor 1C, insulin-like growth factor (IGF) 2 have been associated with pregnancy outcomes such as Silver-Russell syndrome, characterized by IUGR [207, 208].

Social-economic factors: There has been an established link between socio-economic disadvantage and low birthweight, usually co-existing within ethnic and racial groups [209]. It has also been shown that socioeconomic disadvantage remains one of the dominant determinants of IUGR, even in developed countries with universal insurance [210].

1.5.5 Fetal Health Outcomes of IUGR

Neurodevelopment: There are inter-utero neuropathological consequences for the developing brain, usually as a direct result of the severity of placental insufficiency and inversely to gestational age at delivery [211]. Alterations in cytokine levels and neurotrophic growth factors are evident in IUGR as a result of placental insufficiency, affecting the release of neuroprotective metabolites and hormones such as allopregnanolone [212]. Additionally, the essential amino acid tryptophan which is converted to kynurenine via indoleamine 2,3-dioxygenase (IDO), acts a neuroprotectant in late pregnancy. The molecular effects of tryptophan in IUGR have not been fully understood, however there is a link between low levels of tryptophan and impaired brain development of growth restricted fetuses [213, 214]. Moreover, the lack of cerebral blood flow redistribution in IUGR fetuses, results in lack of uniformity of brain perfusion which severely impacts fetal brain development including in the basal ganglia and frontal lobe which may lead to neurobehavioral disabilities [215-217].

Brain injury as a consequence of IUGR has been commonly reported. MRI imaging has shown injury to both grey and white matter in IUGR, with grey matter injury accounting for approximately 28% compared to non-growth restricted newborns [218]. Excitotoxicity, oxidative stress, necrotic and apoptotic degeneration and neuroinflammation as a result of hypoxia, activate a cascade of cellular and biochemical events and potential cell death of immature neurons and neuroglia [219, 220].

In preclinical models of IUGR, total body weight and brain weight are reduced. In addition, there were obvious cellular and structural disturbances including a reduction in hippocampus and cerebellum volume, cortical thickness, delayed neuronal migration to the cortex, retardation of dendritic and axonal outgrowth and reduced number of neurons in IUGR pups when compared to controls [221-223].

Lung Development: Prematurely born neonates with low birth weight are at an increased risk for developing neonatal respiratory distress and Bronchopulmonary Dysplasia (BPD) when compared with premature infants with a normal birth weight [224]. In preclinical *in vivo* models of IUGR, pups exhibited fewer but larger alveoli and developed emphysema [228]. IUGR is also associated with atypical elastin production, derangement of the normal alveolar architecture of the lung, along with dysregulated cell growth and differentiation. Altered IGF-1, PPAR-γ and p53 activity are in part responsible for increased thickness and cellularity of the pulmonary parenchyma [229-232].

Cardiovascular Development: A number of studies have shown myocardial alterations induced by IUGR, affecting cardiac development with significantly reduced number of cardiomyocytes at the time of birth [233, 234]. Alterations in myocardial structure and decreased cardiac function can also be detected in IUGR affected neonates later in childhood [235, 236].

1.5.6 Management of IUGR

Early diagnosis of IUGR can reduce the chances of adverse fetal outcomes such as preterm birth and stillbirth. The current management and interventions used in the treatment of IUGR are described in the following sections.

Ultrasound Surveillance: Ultrasound surveillance is essential for diagnosis and monitoring of fetal growth during pregnancy. Additionally, serial ultrasound measurements can provide continual assessment of fetal growth trajectory, however a time interval between measurements has not been clinically determined [237]. Ultrasound can also help in the diagnosis and management of symmetric growth restriction and associated genetic or congenital malformations [238]. The use of ultrasound also assesses Amniotic fluid volume (AFV) to determine oligohydramnios, which has been associated with growth restriction. In conjunction with doppler studies or as a part of biophysical profile (BPP), it can provide more clinically relevant information on fetal well-being and growth [239]. Additionally doppler ultrasound and umbilical doppler velocimetry can detect impaired utero-placental and feto-placental circulation, which helps elucidate the cause of fetal growth restriction [240].

Corticosteroids: Antenatal corticosteroids are often administered to mothers at risk of premature birth for the prevention of respiratory distress syndrome (RDS). Administration of prenatal corticosteroids can also improve survival and recovery of alveolar cells in the lung, prevents necrotizing enterocolitis and intraventricular haemorrhage, with lower adverse effects seen with single dose administration [241].

1.6 Placental Ageing in Adverse Pregnancy Outcomes

1.6.1 Healthy Placental Ageing

The placenta ages gradually as the pregnancy progresses, exhibiting physiological and morphological senescence and a verge of decline at term (>37 weeks). Placental cells have an invasive capacity, similar to that of cancer cells, promoting

growth of the organ mediated in part by angiogenesis. Trophoblasts are also capable of maintaining telomere length and express elevated Human Telomerase Reverse Transcriptase (hTERT) levels throughout the pregnancy [242, 243]. Morphologically, placental villi change form and appearance between first and third trimesters, which is indicative of villous maturation leading to placental ageing.

Physiologically, upregulation of hypoxia-inducible factor (HIF-1α) in the placenta is associated with a hypoxic state, which is responsible for modelling of villous architecture. The hypoxic state is altered at the end of first trimester, when trophoblastic plugs are dissolved and oxygenated blood flow is restored to the placenta [244-246]. In healthy placentas, the villous trophoblast experiences considerable thinning, with evidence of syncytial senescence, hence decreasing functional capacity at term [247]. The syncytiotrophoblasts are the outermost layer of the villous trophoblast. This layer is in constant contact with maternal blood, exhibiting a rapid ageing morphology and releasing syncytial debris in the form of knots or nuclear aggregates which can be detected in maternal circulation with increasing gestational age [1, 248, 249]. During PE, syncytiotrophoblasts experience accelerated ageing with upregulation of the apoptotic cascade, necrotic breakdown with release of necrotic debris, and increase in syncytial aggregates [1, 105, 250]. Even though, morphological, and pathological changes have been associated with term placenta over >37 weeks, very little is understood about healthy and diseased placental ageing.

1.6.2 Evidence of changes in Cellular Senescence in PE & IUGR

Telomere length remains constant throughout healthy pregnancy, but in certain complications including PE and IUGR, telomere length has been shown to be significantly reduced in some publications [1, 251, 252]. However, more recent research have also reported no change in telomere length in PE compared to controls [253]. Changes in telomere length may be associated with increased oxidative stress, leading to DNA damage and activation of damage response (DDR) through the p53 pathway with subsequent promotion of trophoblast senescence [1, 254, 255]. In 2010, Biron-Shental et al. were the first to provide evidence of cellular senescence in PE and IUGR. They demonstrated that in PE and IUGR pregnancies, trophoblast telomere length was significantly shorter with reduced expression of hTERTs and increased frequency of telomere aggregates when compared to uncomplicated pregnancies [1, 252]. These placental alterations were not present at 37-41 weeks' gestation, indicating premature ageing of the placenta in these pregnancy complications [1, 256].

The presence of senescence markers such as p21, p16, p53, and Rb proteins towards term supports the ageing hypothesis of the normal placenta [1, 257]. A recent study by Nuzzo et al. described changes in the trophoblast cell cycle including upregulated cyclin D1 (cell cycle regulator) and PARP1 (DNA repair gene) expression with reduction in JunB (senescence suppressor gene) expression in placental mesenchymal stromal cells (PMSC) isolated from preeclamptic placental tissue when compared to the normal placental tissue [1, 258]. Additionally, Sharp et al. found an imbalance between p53 (senescence-inducing and proapoptotic gene) and

MDM2 (p53 suppressor) signalling in the syncytiotrophoblasts but not in cytotrophoblasts in placental tissue from women with early-onset PE [1, 259]. Finally, Gao et al. reported an increase in p53 signalling and cell cycle arrest with additional activation of proapoptotic BAX and caspase proteins in human umbilical vein endothelial cells (HUVEC) from women with PE when compared to women with uncomplicated pregnancies [1, 260].

Activation of DDR pathways, mtDNA mutations, and endogenous stress like ROS accumulation and disrupted redox signalling can cause epigenetic modifications. The link between epigenetics, ageing, and age-related disorders has been demonstrated in several studies [1, 261, 262]. Epigenetic changes have been demonstrated within placental tissue including DNA methylation patterns on imprinted regions in H19/IGF2 genes, and methylation of histone proteins within the human growth hormone in placental chromatin [1, 263]. In a recent study by Eddy et al., histone modifications were evident in the BeWo placental cell line following exposure to hypoxic conditions with marked hypomethylation of cytosine, an epigenetic change usually evident in age-related pathologies [1, 264].

1.6.3 Evidence of Mitochondrial Dysfunction in PE & IUGR

The placenta is a highly metabolic organ, requiring robust mitochondrial activity. During normal mitochondrial function, continuous changes within the extravillous trophoblast and vascular remodelling lead to increased ATP production through oxidative phosphorylation [1, 265, 266]. Accumulation of ROS such as superoxide, nitric oxide, and peroxynitrite results in physiologic oxidative stress during early pregnancy [1, 265]. ROS can be generated from a number of sources including

mitochondria (mROS), NADPH oxidases, xanthine oxidase, or p450 enzymes [1, 267, 268]. Increase in ROS production with subsequent alterations in redox signalling has direct links to both mitochondrial and cellular ageing.

Protein nitration and lipid peroxidation have been shown to be significantly higher in placental tissue from women with PE compared with uncomplicated pregnancy [1, 270, 271]. Lipid peroxidation can be either enzymatic, catalysed by lipoxygenase enzymes, or nonenzymatic in the presence of free radicals [1, 272]. Nonenzymatic lipid peroxidation is increased with ageing, and its by-products are highly expressed in age-related diseases such as atherosclerosis [1, 273]. In 1998, Wang and Walsh described that placental lipid peroxidation was significantly higher in PE [1, 270]. They established that elevated lipid peroxidation levels are a result of increased mitochondrial mass, in regions of poor vascular flow, which are unable to meet energy requirements in PE [1, 270].

Extravillous trophoblast activity such as migration and invasion are impacted by the expression of two nitric oxide subtypes eNOS (endothelial nitric oxide synthase) and iNOS (inducible nitric oxide synthase) [1, 274]. Nitration of proteins may either have redundant or exhibit loss/gain of function effects. In PE, increases in peroxynitrite generation may alter vascular reactivity and uteroplacental circulation [1, 257, 275]. Upregulation of NOS activity and peroxynitrite accumulation in placental tissue in PE may also result in the depression of mitochondrial activity by inhibiting the electron transport chain and nitration of mitochondrial proteins and antioxidants such as mitochondrial superoxide dismutase, in addition to activation of apoptosis [1, 276] as shown in Figure 1.5. Placental ageing is often associated with mitochondrial

dysfunction as a direct consequence of loss of mitochondrial dynamics and increased mitochondrial damage [1, 276, 277]. Mitochondria undergo continuous fission and fusion to maintain mitochondrial dynamics, failure of which may lead to accumulation of mitochondrial debris and deteriorating mitochondrial function [1, 276, 277]. It is believed that mitochondrial dynamics are altered in PE with altered expression of mitochondrial autophagy regulator genes like OPA1, SIRT3, and MNF2/1, but limited research has been conducted to fully understand the signalling process [1, 278, 279].

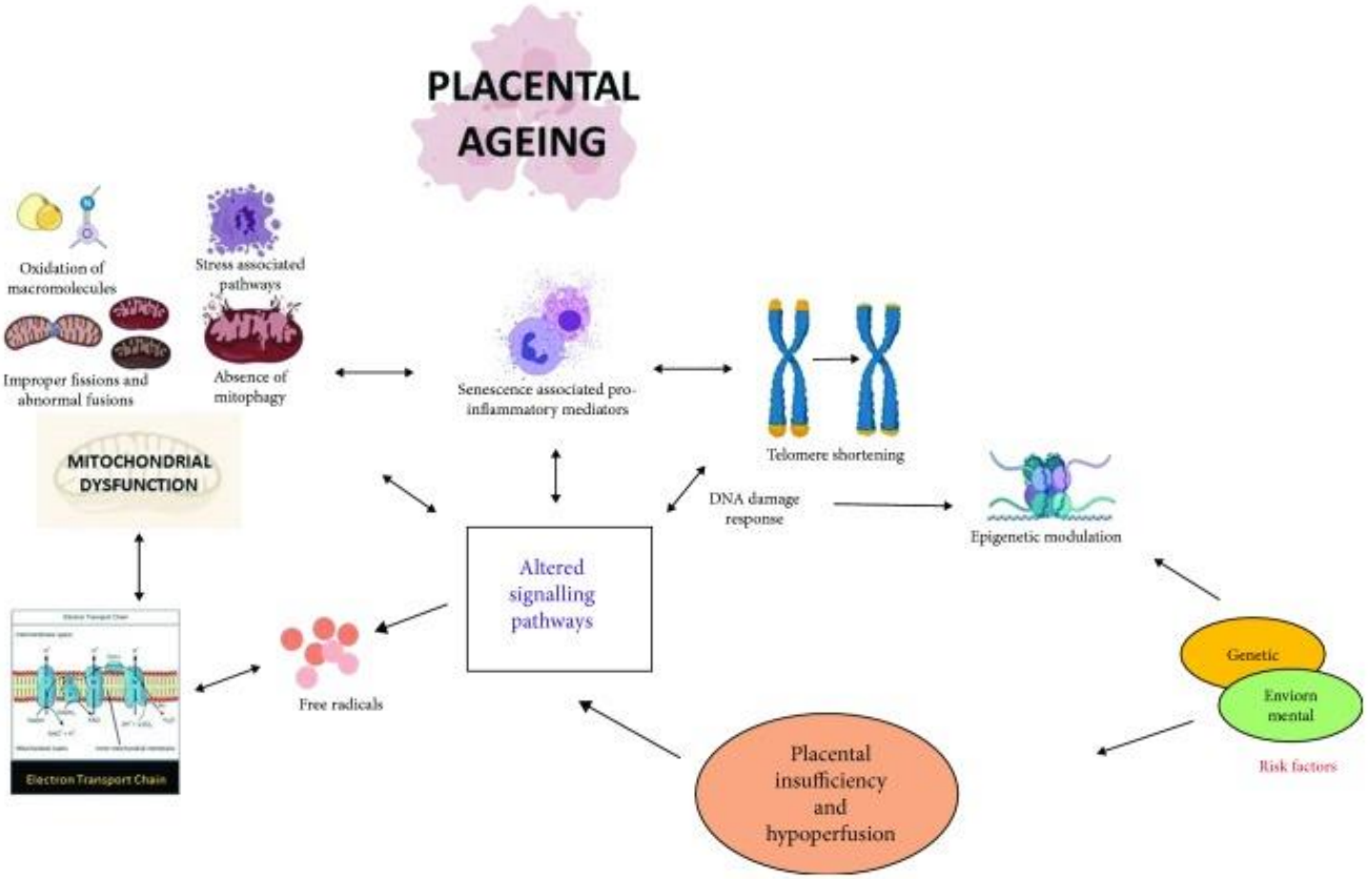


Figure 1.5 Contribution of cellular senescence and mitochondrial dysfunction to placental ageing. Image adapted from Manna et al 2019 [1].

Antioxidants are endogenously produced to neutralise ROS by converting them to more stable oxygen and hydrogen peroxide, which is further broken down to form water. Antioxidants are also considered as anti-aging agents and can be classified into subtypes: enzymatic such as superoxide dismutase (SODs), catalases, and peroxidases or nonenzymatic such as vitamins (A, C, and E), bilirubin, and uric acid [1, 280, 281]. In PE and IUGR, placental antioxidant activity is attenuated when compared to uncomplicated pregnancies [1, 99, 280].

1.6.4 Markers of premature senescence in pregnancy complication

A major obstetric challenge has been to establish biomarkers for detection of pregnancy complications such as PE and IUGR in maternal body fluids. Qiu et al. were the first to report elevated mtDNA levels in the maternal peripheral blood in PE indicating elevated oxidative stress and mitochondrial dysfunction [1, 282]. A recent case-control study by Williamson et al, reported elevated mtDNA copy numbers in maternal plasma at 15-20 weeks' gestation in PE cases compared to those in uncomplicated pregnancy controls [156, 280, 283]. Furthermore, this study also demonstrated a significant reduction in the antioxidant mitochondrial superoxide dismutase activity at 15 weeks' gestation in women who later developed PE, thus proposing mitochondrial dysfunction as an early pathophysiological event in PE [1, 156]. Similar work by Marschalek et al. also identified increased mtDNA copy numbers in maternal serum in early-onset PE [1, 284].

Apart from mitochondrial dysfunction, inflammation and inflammatory mediators are evident in premature ageing of the placenta. Certain ageing-associated inflammatory markers such as Senescence-Associated Secretory Phenotypes

(SASPs) are elevated in PE [1, 285]. Kupferminc et al. showed that TNF-α is significantly elevated in amniotic fluid and maternal plasma in severe PE [1, 286]. sST2 (soluble ST2) is a member of the interleukin-1 family, expressed abundantly in endothelial cells, and usually associated with age-related disorders such as cardiac diseases [1, 287]. A recent longitudinal study by Romero et al. reported significant elevation of sST2 levels in maternal plasma in risk patients almost 6 weeks prior to development of PE [1, 288].

MicroRNAs (miRNA) and long noncoding RNAs (lncRNA) are noncoding RNAs that have the potential for gene regulation [1, 289]. Placental miRNA are solely found within the placenta and are involved in cell differentiation, placental growth, embryonic and regulation of nutritional requirements [290]. miRNAs are available in bodily fluids and are now being regularly investigated as both biomarkers and perspective therapeutics. In the uterus, miRNAs are controlled by steroidal hormones, and they are responsible for efficient placentation [1, 291]. miRNA maybe abnormally expressed in placental diseases such as PE and IUGR as a result of maternal-fetal hypoxia, angiogenesis, immunity, and inflammation through different cellular pathways and modes of action [290]. miRNA and lncRNA are powerful tools for early detection of pregnancy outcomes such as PE and IUGR. Table 1.2 summarises the various senescence markers associated with placental ageing in adverse pregnancy outcomes such as PE and IUGR.

Table 1.2 Senescence markers associated with placental ageing in adverse pregnancy outcomes. Adapted from Manna et al [1].

Maternal plasma/serum/amniotic fluid	(1) Mitochondrial dysfunction (2) Inflammatory markers (IL33/ST2 signalling pathway)	↑ mtDNA copy numbers ↑ sST2 level ↑ TNF- α
Trophoblast Cell Lines	(1) Cell cycle regulators (2) miRNA/lncRNA (3) DNA damage response (4) Senescence regulators (5) Epigenetic changes	↑ Cyclin D1 ↑ Mir-376 ↑ PARP1 ↑ p53 ↓ JunB ↓ MDM2 ↑Hypomethylation of cytosine
Placental Tissue	(1) DNA damage response (2) Cell cycle regulators (3) Mitochondrial dysfunction	↑ p53 ↓ hTERT ↑ Telomere aggregates ↑ BAX ↑Lipid peroxidation ↑ NOS activity ↑ Peroxynitrite synthesis

1.7 Placental Proteomics and Use of Computational Biology

Proteomics can be defined as the identification and quantification of all proteins expressed in a complex biological system, characterising functionality in both health and disease [292]. Within a eukaryotic cell type, a proteome can vary significantly whereas the genomes remain relatively static [292]. There is limited possibility of adequately identifying and quantifying all proteins and their isoforms, referred as a proteome [293]. This can make proteomic research challenging, when comparing the proteome variability between healthy and diseased state. Though still in its infancy, proteomic research has been used in obstetric complications, using various biological samples such as plasma, serum, amniotic fluid, urine, placental tissue, and trophoblast cell lines [294]. Proteomic analysis has also been used for biomarker discovery and as prediction tool in early and late onset PE. However, major limitations remain such as identifying lowly abundant proteins and integration of proteomic data sets with genomics, metabolomics and lipidomic data. Prediction models in early onset or preterm PE or <34 weeks of gestation have combined, assessment of maternal risk factors such as Doppler velocimetry of the uterine arteries, with circulating maternal protein expression of PIGF, PAPP-A, PP-13, pregnancy associated plasma protein A, and inhibitin-A [201, 295, 296].

Discovery proteomics approaches have also been used for identification of novel biomarkers in PE and IUGR [297]. As shown in Figure 1.6, biomarkers of PE can be categorised as: placental perfusion and vascular dysfunction, renal dysfunction, Fetoplacental unit and endothelial dysfunction and OS. These markers in

combination with clinical information, increase the possibility of predicting and diagnosing PE early in pregnancy[298].

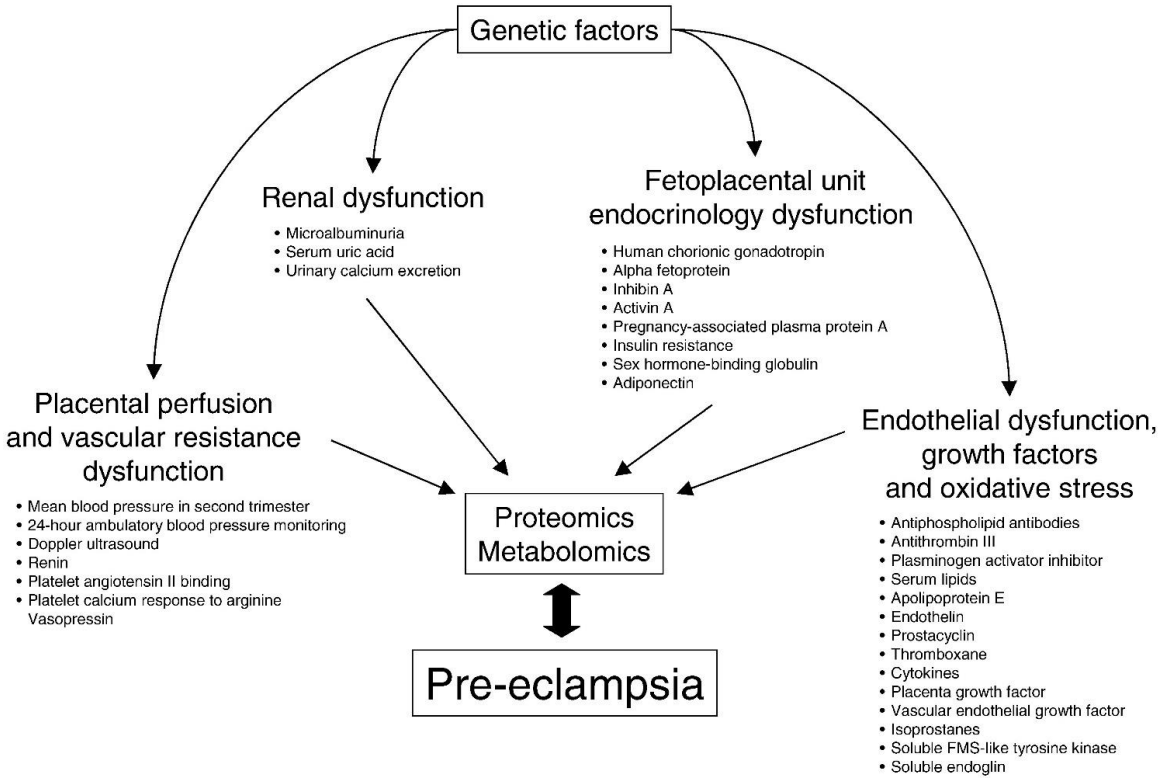


Figure 1.6 Biomarkers of PE, where the genetic factor remains constant whereas the proteome and metabolome are dynamic. This is depicted by the double arrow. Image created by Carty et al 2008 [298].

However, despite substantial research, predicting PE & IUGR remains challenging, especially in early stages of the disease. Some of the obstacles faced by researchers are firstly, the heterogeneity and complexity of the disease physiology with multifactorial involvement [299]. Secondly, *in-vitro* placental models and preclinical animal models fail to mimic early disease placental pathophysiology of PE [300]. Finally, the molecular signature of PE and biomarker discovery is often targeted at the later stage of the disease, and due to the invasive nature of the placenta in the early stages of PE very little information can be obtained non-invasively [301, 302]. One method to circumvent some of these obstacles is to employ a systems biology approach.

Systems biology can be defined as the computational modelling of molecular systems providing an integrative interpretation of large datasets pertaining to proteomics, genomics and metabolomics [303]. Computational modelling in the form of *in-silico* experiments was developed to study the logically controlled *in-vitro* extension of pharmacological and physiological processes [304]. The complex interaction and data integration of hundreds of in-silico experiments which are validated through laboratory experiments can be modelled computationally [304]. This can be used to test hypothesis, interpret results for both *in-vitro* and *in-vivo* models and provide new insights into disease pathogenesis [305].

There are two types of models: static and dynamic models. Dynamic models emphasize the interaction of components such as genes and proteins with each other and their reaction to stimuli using ordinary differential equations (ODE) [306]. Static models provide information of interactions between components such as

protein-protein [306]. Functional biological systems contain an amount of uncertainty, which can be modelled using Stochastic simulation such as Monte Carlo, Markov chain, Random walk, with repeated runs to simulate the variations mimicking random, uncertain reaction, until a definitive result is reached [305, 307]. Systems Biology approaches also consists of static large-scale biological network modelling consisting of omics data integration, visualization, and topological analysis; and dynamic quantitative models, which focuses on characterization of molecular processes and visualization of cells [305].

1.8 Summary

The placenta plays a crucial part in regulation of a healthy pregnancy. Remodelling of the uterine vessels by invasion of trophoblasts resulting in successful placentation is essential for development of the fetus. The optimal functional capacity can be defined as the ability of the placenta to provides oxygen, glucose and nutrients to the fetus and also filtering out harmful waste and carbon dioxide, thus enabling the exchange of oxygen and nutrients between mother and fetus.

As the fetus grows, there is an increase in the demand for oxygen and nutrients, which is met by radical alteration of maternal spiral arteries from low-flow high-resistance vessels to high-flow low-resistance after first trimester of pregnancy, resulting in placental hypoperfusion. Abnormal placentation and inability of the placenta to obtain optimal capacity can lead to adverse pregnancy outcomes including PE (PE), intrauterine growth restriction (IUGR), preterm birth and stillbirth.

The exact pathophysiology of placental insufficiency due to impaired trophoblast invasion and vascular remodelling is unclear. Reduced blood supply as a consequence of placental ischemia may result in oxidative stress (OS). OS is associated with increased production of reactive oxygen species (ROS) and free radicals which inflict oxidative damage on protein, lipids, and nucleic acids. Moreover, the loss of balance between pro and antioxidants results in aberrant ROS production and further deteriorates placental function.

Elevated OS, deficient antioxidant defence and accumulation of OS by-products have also been associated with inducing premature cellular senescence. The placenta ages gradually as the pregnancy progresses, however prolonged pregnancy (>42 weeks) is associated with “true ageing” of the placenta evidenced by declining morphology, physiology, and functional capacity, which have been linked to stillbirth. In adverse pregnancy outcomes such PE and IUGR, premature placental ageing has been associated with increased oxidative stress contributing to both cellular senescence and mitochondrial dysfunction. Optimising maternal health during pregnancy, is essential for improving long term outcomes for both mother and baby. Although the least studied organ of the body, the placenta is the key to understanding and potentially preventing future adverse pregnancy outcomes and reducing future maternal and fetal morbidity.

In this introduction chapter, the role of accelerated placental ageing in the pathogenesis of adverse pregnancy outcomes: PE and IUGR is provided. Additionally, the role of computational biology in the assessment of oxidative stress and identification of potential placental ageing biomarkers are explored.

1.9 Thesis Hypothesis, Aims & Objectives

Hypothesis

A review of the current literature suggests a link exists between oxidative stress, mitochondrial dysfunction, and premature cellular senescence. Characterising this interconnected network and its role in the pathophysiology of PE and IUGR has yet to be fully explored. In this section, we reviewed the current literature for premature placental ageing in adverse pregnancy outcomes. We hypothesised that Oxidative Stress plays a key role in cellular senescence and mitochondrial dysfunction of the placenta, precipitating premature ageing of the organ. We also summarised the current knowledge of placental ageing in the aetiology of adverse pregnancy outcomes and discussed the hallmarks of ageing which could be potential markers for preeclampsia and fetal growth restriction. This thesis will allow us to identify features of placental senescence, which are shared and unique to each adverse pregnancy outcome. These differential features will be further investigated by adopting a proteomic approach of placental tissue from both PE and IUGR pregnancies.

Aims

A. Investigate evidence of cellular senescence in placental tissue obtained from PE & IUGR complicated pregnancies when compared to controls.
B. Characterise the protein signature of sub anatomical regions of the placenta using a proteomic approach.
C. Identify the placental proteomic profile in PE & IUGR

Objectives

In order to achieve these aims the following objectives were identified:

- To evaluate the molecular signatures of cellular senescence in PE, PE associated with IUGR and IUGR phenotypes compared to control pregnancies (Chapter 2).
- To understand the protein composition of a normal healthy placenta (Chapter 3).
- To characterise compositional differences related to placental ageing between the maternal and fetal sub anatomical regions (Chapter 3).
- To map the dynamic and functional pathways and interaction networks of differentially expressed proteins in PE & IUGR compared to controls (Chapter 4).

Chapter 2:

Heterogenous Differences in Cellular Senescent Phenotypes in Pre-Eclampsia and IUGR following Quantitative Assessment of Multiple Biomarkers of Senescence

---

The text of this chapter has been adapted from the following publication:

Manna S, Elwain CJM, Maher GM, Giralt Martín M, Musumeci A, McCarthy FP, McCarthy C. Heterogenous Differences in Cellular Senescent Phenotypes in Pre-Eclampsia and IUGR following Quantitative Assessment of Multiple Biomarkers of Senescence. International Journal of Molecular Sciences. 2023; 24(4):3101. https://doi.org/10.3390/ijms24043101

Abstract

Background: Premature ageing of the placenta in pregnancy outcomes is associated with the persistent presence of oxidative stress and placental insufficiency reducing its functional capacity. In this study, we investigated cellular senescence phenotypes of PE and IUGR pregnancies by simultaneously measuring several biomarkers of senescence.

Methods: Maternal plasma and placental samples were collected at term (> 37 weeks) and preterm (<37 weeks) gestation from nulliparous women undergoing pre-labour elective caesarean section with PE without intrauterine growth restriction (PE; n = 5), PE associated with intrauterine growth restriction (n = 8), intrauterine growth restriction (IUGR < 10th centile; n = 6), and age-matched controls (n = 20). Placental absolute telomere length and senescence gene analysis was performed by RTqPCR. The expression of cyclin-dependent kinase inhibitors (p21 and p16) was determined by Western blot. Senescence-associated secretory phenotypes (SASPs) were evaluated in maternal plasma by multiplex ELISA assay.

Results: Placental expression of senescence-associated genes showed significant increases in CHEK1, PCNA, PTEN, CDKN2A, and CCNB-1 expression ($p < 0.05$) in PE, while TBX-2, PCNA, ATM, and CCNB-1 expression ($p < 0.05$) were significantly decreased in IUGR compared with controls. Placental p16 protein expression was significantly decreased in PE only compared with controls ($p = 0.028$). IL-6 was significantly increased in PE (0.54 pg/mL ± 0.271 vs. 0.3 pg/mL ± 0.102; $p = 0.017$) while IFN-γ was significantly increased in IUGR (4.6 pg/mL ± 2.2 vs. 2.17 pg/mL ± 0.8; $p = 0.002$) compared with controls. No significance was observed in placental

Lamin-B1 level between cases and controls. Similarly, there were no significant variations observed in mitochondrial copy numbers for any subgroups compared to controls.

Conclusion: These results provide evidence of premature senescence in IUGR pregnancies, and while cell cycle checkpoint regulators are activated in PE, the cellular phenotype is one of cell repair and subsequent proliferation rather than progression to senescence. The heterogeneity of these cellular phenotypes highlights the complexity of characterising cellular senescence and may equally be indicative of the differing pathophysiological insults unique to each obstetric complication.

2.1 Introduction

Pre-eclampsia (PE) is a gestational hypertensive disorder which affects 3–5% of pregnancies worldwide and clinically manifests as maternal de-novo hypertension and associated maternal organ dysfunction including uteroplacental dysfunction [66]. Intrauterine growth restriction (IUGR) can be defined as a rate of fetal growth, which is below the normal growth potential, i.e., between the 10th and 90th percentile as per the gestational age [159, 172]. IUGR affects 13.7 million babies born yearly with low birth weight [159]. PE is associated with impaired spiral artery modelling and poor placental perfusion resulting in aberrant redox signalling and an induction of oxidative stress [308]. Additionally, systemic inflammation and endothelial dysfunction are pathogenic mediators of PE which account for a myriad of maternal multi-organ damage and poor long-term maternal cardiovascular outcomes [308].

Senescence can be defined as a cellular defensive mechanism triggered in response to multiple external or internal stressors resulting in irreversible cell cycle arrest [309]. In conditions of exaggerated oxidative stress, persistent impairment of redox balance and subsequent DNA damage result in the initiation of a premature senescence phenotype [310]. Additionally, telomere shortening can trigger cellular senescence, but senescence is equally evident independent of telomere shortening [311, 312]. Premature cellular senescence can be classified by activation of a DNA damage response pathway and its associated signalling kinases which culminate in the stimulation of cell cycle inhibitors, such as p16INK4a, p21/p53, and p27, a reduction in cellular proliferation, and loss of Lamin-B activity, a marker of the altered enlarged and flattened morphology of senescent cells [313]. Moreover, the accumulation of mitochondrial DNA (mtDNA), as a result of ROS inducing damage and strand breaks, has been associated with premature onset of ageing in both *in vivo* and *in vitro* models, with higher susceptibility to mtDNA mutagenesis [314, 315]. Activation of a senescence-associated secretory phenotype (SASP) incorporating a core set of cytokines, enzymes and growth factors, such as IL-6, IL-8, IL-13, IGFBPs, and MMPs, results in accumulated senile cells creating a pro-inflammatory microenvironment that indicates establishment of senescence [316]. The phenotypes of premature cellular senescence are highly heterogeneous and often differ depending on the initial stressor [1]. Senescence-specific gene expression has been extensively studied. Genes such as PTEN and CDKN2A regulate cellular senescence by acting through the p16/p19^{Arf} pathway, whereas CHEK-1, PCNA, and CCNB-1 are modulated by DNA damage response and halt cell cycle progression [317-319]. Additionally, there is no single universal biomarker that specifically identifies

senescence, hence a combination of multiple markers when simultaneously present are used to confirm senescence [320].

The placenta along with maternal decidua normally exhibits progressive senescence closer to term parturition [321]. A recent review by Cox and Redman, which explored evidence of placental ageing through cellular senescence accompanied by morphological changes including modulation of pro-inflammatory phenotypes, highlighted excessive oxidative stress as a driver of premature placental ageing in adverse pregnancy conditions including PE [322]. This stress-induced senescence is proposed to result from poor placental perfusion, resulting in increased ROS generation that subsequently engages biochemical pathways which disrupt cell cycle progression in addition to accelerating the activation of pro-inflammatory cytokines and chemokines, which form part of the senescence-associated secretory phenotype (SASP) [1, 322].

In adverse pregnancy outcomes, such as PE and IUGR, impaired placentation and the subsequent burden of placental oxidative stress may trigger a premature senescence phenotype leading to early parturition and pre-term delivery of the fetus [1]. Syncytiotrophoblasts show features characteristic of senescent cells, including the biomarker senescence-associated β-galactosidase (SA-β-gal), together with increased expression of the cyclin kinases inhibitors p16 and p21, and p53 [323].

To date, the association between altered telomere length and placental pathogenesis of both PE and IUGR has been somewhat contradictory, with some publications reporting no significant difference in placental telomere length between PE and healthy uncomplicated pregnancies [324, 325]. Contrarily, IUGR has consistently been reported to have lower placental telomerase activity and shorter

telomere length when compared with healthy uncomplicated pregnancies [243, 252, 255, 256]. In this study, we examined multiple biomarkers of senescence in PE and IUGR and investigated if premature senescence phenotypes were congruent across both placental pathologies.

2.2 Materials and Methods

2.2.1 Study Design

Participants were recruited as part of the COMRADES study, a non-interventional cohort study of nulliparous singleton pregnancies with the aim of characterizing placental premature senescence in PE and intrauterine growth restriction (IUGR). Patients were recruited from Cork University Maternity Hospital, Ireland, between 2019 and 2021. The COMRADES study was conducted according to the guidelines laid down in the Declaration of Helsinki, and all the procedures were approved by the Clinical Research Ethics Committee of the Cork Teaching (ECM4 (ff) 04/12/18), and all women provided written informed consent. After receiving consent from participants, samples were collected from nulliparous, singleton pregnancies undergoing pre-labour caesarean section. PE was defined according to the ISSHP 2018 guidelines: BP ≥ 140 mm Hg systolic or ≥90 mm Hg diastolic measured on at least 2 occasions at least 4 h, associated with proteinuria (>300 mg protein on 24-h collection, urine protein creatinine > 30 mg/mmol or +3 dipstick) [1]. PE participants were subdivided into two groups: associated with growth restriction (n = 8) and no growth restriction (n = 5). IUGR was defined according to RCOG as estimated fetal weight less than 10th centile for gestational age [166]. IUGR-recruited pregnancies were classified as <10th centile (n = 6). Matched selected controls (n = 20) were

collected from healthy pregnant women who had uncomplicated pregnancies, which were defined as pregnancies not affected by PE or IUGR and delivered at >37 weeks. All control placentas were term gestation (38 ± 0.7 weeks), however the mean gestation age for PE (36 ± 1.9 weeks), PE associated with IUGR (34.6 ± 2.7 weeks) and IUGR (32.43 ± 13.1 weeks) pregnancies were matched as closely as possible. Controls were matched with the PE and IUGR cases for maternal age. Clinical characteristics such as age, body mass index (BMI), mean arterial blood pressure, gestational age, fetal weight, and fetal sex were collected from all participants.

2.2.2 Sample Collection

Maternal fasting blood was collected on the day of elective C-section and plasma extracted in EDTA vacutainers (BD, Ireland) by centrifugation at 2400× *g* for 10 min at 4 °C. Placental tissue was sectioned within 20 min of delivery, with 5 tissue sections (2–4 cm diameter each) taken from identified regions across the placenta. All samples were snap frozen in liquid nitrogen and stored at −80 °C [326].

2.2.3 Placental DNA Extraction and Absolute Telomere Length Quantification

Genomic DNA was extracted from 10 mg of placental tissue using the DNeasy Blood and Tissue kit (Qiagen, Dublin, Ireland) in accordance with the manufacturer's instructions. Absolute quantification of telomere was determined using the ScienCell qPCR Kit (#8918). The telomere primer set recognizes and amplifies telomere sequences, while the single copy reference (SCR) primer set recognizes and amplifies a 100 bp-long region on human chromosome 17 and serves as a reference for data normalisation. All reactions with genomic DNA sample (5 µg/µL)

were performed in duplicate, and template controls were included in each run. Reference genomic DNA was used as an internal control. Comparative ΔΔCq (Quantification Cycle Value) method was used with manufacturer made standard curve for quantification using Cq (Quantification Cycle) values of telomere qPCR (TEL) and single copy reference qPCR (SCR) obtained for the genomic DNA samples as per the manufacturer's instructions.

2.2.4 Absolute Quantification of Placental mtDNA

Mitochondrial DNA (mtDNA) extraction was completed following the methodology described by Williamson et al. (2018) [283]. Real-time PCR was used for mtDNA assessment using the StepOne Plus Detection system (Applied Biosciences, Waltham, MA, USA) with Taqman probes for mtDNA, hMitoF5, hMitoR5 [283, 327]. A standard curve was used to determine the absolute quantification of mtDNA and represented as copies/mL [327, 328].

2.2.5 Isolation of RNA and Real-Time PCR Analysis of Senescence Associated Genes

Placental tissue was mechanically homogenised in Trizol Reagent (Invitrogen™ Thermo Fisher Scientific, Dublin, Ireland) using the TissueLyser II (Qiagen, Manchester, UK) and RNA was isolated and subsequently purified using the Qiagen RNeasy® Plus Mini (#74134) clean-up protocol according to manufacturer's instructions. cDNA synthesis was performed using the Superscript IV Double-Stranded cDNA Synthesis Kit (Invitrogen™ Thermo Fisher Scientific, Ireland). Initial assessment for senescence-associated genes were performed using the RT2 Profiler PCR Array Gene Expression for senescence-associated genes in 96-well plates (Cat

no. PAHS-050Z, Qiagen, Ireland). Samples from each group were pooled into and loaded onto each 96-well plate. In total, there were 4 groups: PE, PE associated with IUGR, IUGR, and controls, and 4 plates were run-on Real-Time qPCR on the Applied Biosciences StepOne Plus Detection System. The qPCR Assays used in PCR Arrays enables 96 genes in a 96-well plate to be simultaneously analysed using the RT^2 SYBR Green qPCR Array System protocol. Relative quantification was performed using data analysis web portal (GeneGlobe, Germantown, MD, USA, https://geneglobe.qiagen.com/us/ (accessed on 20 January 2023)) to calculate the fold change using $2^{-\Delta\Delta CT}$ formula, where ΔCT is calculated between gene of interest (GOI) and an average of reference genes (HKG), followed by ΔΔCT calculations.

Five HKG genes, namely ACTB, B2M, GAPDH, RPLP0, and HPRT1 were included in each PCR plate as internal controls. Eleven genes were selected for validation based on the significant differences between groups when compared with controls, obtained from the RT2 profiler PCR Array: CHEK1, CCNB1, PCNA, PTEN, CDKN2A, ATM, TBX2, GLB1, ID1, IGFBP5, and SOD2. Taqman probes were used for genes of interest (Applied Biosciences, Westmeath, Ireland). The Tata box protein (TBP) gene was used as an internal control with SYBR green primers (Table 2.1). TBP has been shown to be most stable in placental tissue, ensuring sensitivity and specificity of gene expression profile [329]. Real-time PCR was performed on the Applied Biosciences StepOne Plus Detection System. Standard relative PCR quantification was performed to validate fold changes using $2^{-\Delta\Delta CT}$ formula based on relative change between GOI and the internal standard.

Table 2.1 Tata Binding Protein (TBP) Sybr green sequence

TBP Forward Sequence	TGTATCCACAGTGAATCTTGGTTG
TBP Reverse Sequence	GGTTCGTGGCTCTCTTATCCTC

2.2.6 Protein Isolation and Western Blot

Placental tissue (50 mg) was homogenized using TissueLyser II (Qiagen, Hilden, Germany) and protein was isolated using tetraethylammonium bicarbonate buffer (Sigma-Aldrich, Co., Wicklow, Ireland) supplemented with a phosphatase inhibitor (PhosSTOP™, Roche, Dublin, Ireland) and protease inhibitor (Roche, Ireland). Four study groups were investigated, PE, PE associated with IUGR, and IUGR cases were age-matched with controls. We separated 35 µg of protein by SDS-PAGE on a 10% TRIS polyacrylamide-glycine gel (Bio-Rad Laboratories, Kildare, Ireland) and transferred it to a methanol-activated PVDF membrane (Amersham™ Hybond® Sigma-Aldrich, Ireland). Membranes were blocked in 5% BSA for 1h at room temperature and incubated overnight at 4°C with primary antibodies; anti-p21 (1:1000 Abcam; ab109520, Cambridge, UK), anti-Lamin B1 (1:1000 Cell Signaling; E6M5T, Cork, Ireland), anti-p16 (1:500 Abcam; ab108349, UK), or anti-GAPDH (1:3000 Cell Signaling #2118, Brennan and company, Ireland), and anti- β-Tubulin (1:2000 Cell Signaling, #2146, Brenan and company, Dublin, Ireland), secondary anti-rabbit IgG, HRP-linked antibody (1:2000 Cell Signaling Technology, #7074 Brenan and company, Ireland). GAPDH and β-Tubulin were selected as internal reference control proteins for western blots because of their stability and expression within placental cells [330-332]. After overnight incubation membranes

were washed and incubated at room temperature for 1h with anti-HRP secondary antibody, membranes were washed in TBS-T and developed using Pierce™ ECL Western Blotting Substrate, Thermo Fischer Scientific, Biosciences, *Dublin*, Ireland) and LICOR Odyssey image analyzer. Densitometry was performed using LICOR Image Studio Lite Version 5.2. After the protein of interest was developed, membranes were stripped of residual primary and secondary antibodies using a Western Blot Stripping Buffer (Thermo Fischer, Ireland) for 30 min with gentle shaking and re-probed with a suitable internal reference control protein.

2.2.7 Senescence Associated Secretory Phenotypes (SASP) Analysis

Maternal plasma samples were analysed for SASP using the Human U-Plex kit IL-6, IL-8, IL-13, IL-1α, IFN-γ, MCP-1, and MIP-1α (MesoScale Discovery, Rockville, MD, USA; K15067L) and the Human MMP3 Ultra-sensitive kit (MesoScale Discovery, USA; K15034CL). All samples were prepared using the manufacturer's instructions and plates analysed on the Meso QuickPlex SQ 120 platform. Results were generated as calculated concentration means on the Mesoscale (MSD) Discovery Workbench 4.0 assay analysis software. The MSD analysis software determines individual cytokine concentrations from electro chemiluminescent signals via backfitting to the calibration curve.

2.2.8 Statistical Analysis

All data are expressed as mean ± SD, or fold change relative to control. Analysis was performed using GraphPad Prism 8.3. Comparisons of data between cases and controls were performed using a one-way ANOVA. The two-tailed Wilcoxon matched-pairs signed rank test was used for statistical analysis of western blot

experiments with p values < 0.05 were considered as statistically significant. Linear regression analysis, comparing absolute telomere length in cases and controls, was done using STATA 14.2. One-way Anova was used to determine statistical significance for various clinical characteristics collected from participants as shown in Table 2.2.

2.3 Results

2.3.1 Study Demographics

Thirty-nine participants delivered by pre-labour caesarean section were recruited in the Cork University Maternity Hospital between 2019 and 2021. These were grouped as: PE (n = 5), PE associated with intrauterine growth restriction (n = 8), IUGR (<10th centile) (n = 6), and maternal age-matched controls (n = 20) as shown in Table 2.2. There were no significant differences in maternal age, maternal BMI, or gestational age for all groups when compared with controls. While there was no significant difference in maternal mean arterial blood pressure (MAP) during the first trimester (~11 weeks) across study groups, MAP at 20–24 weeks was significantly elevated in both PE (96.4 ± 6.8 vs. 83.2 ± 8.4; p = 0.04) and PE associated with IUGR (97.2 ± 12.7 vs. 83.2 ± 8.4; p = 0.027) compared with controls. Fetal birthweight in PE associated with IUGR (1926 g ± 527.7 g vs. 3218 g ± 359.6 g, p < 0.0001) and IUGR (2585 g ± 401.8 g vs. 3218 g ± 359.6 g, p = 0.035) were significantly reduced when compared with controls. Similarly, fetal individualised customised centile (ICC) was significantly reduced in PE associated with IUGR (2.1 ± 2.5, p = 0.0001) and IUGR (8.11 ± 1.9, p = 0.0034) pregnancies compared with controls.

Table 2.2 Patient characteristics in study cohort. Data are represented as mean ± SD. Mean arterial pressure has been calculated as MAP = [Systolic BP + (2 × Diastolic BP)]/3.

	Pre-Eclampsia	**Pre-Eclampsia Associated with IUGR**	**IUGR (<10th Centile)**	**Term Controls**
	(n = 5)	**(n = 8)**	**(n = 6)**	**(n = 20)**
		Maternal		
Mean Age (years ± SD)	38.6 ± 5.2	33.35 ± 3.1	33.67 ± 3.1	33.7 ± 4.40
Mean BMI (kg/m^2 ± SD)	29.9 ± 9.6	27.7 ± 3.7	25.31 ± 3.5	24.4 ± 5.4
Mean Arterial Blood Pressure (mmHg) ± SD (10–12 weeks)	92 ± 10.4	77.08 ± 32.4	84.61 ± 5.2	86.3 ± 8.9
Mean Arterial Blood Pressure (mmHG) ± SD (20–24 weeks)	96.4 ± 6.8 *	97.2 ± 12.7 *	83.1 ± 7.2	83.2 ± 8.4
		Fetal		
Mean Gestational Age at delivery (weeks ± SD)	36 ± 1.9	34.6 ± 2.7	32.43 ± 13.1	38 ± 0.7
Mean birth weight (grams ± SD)	2878 ± 788.5	1926 ± 572.7 *	2585 ± 401.8 *	3218 ± 359.6
Fetal Sex (M = Male; F = Female)	F = 3 M = 2	F = 3 M = 5	F = 4 M = 2	F = 10 M = 10
Fetal Individualised Customised Centile (±SD)	46.8 ± 39.3	2.15 ± 2.5 *	8.11 ± 1.9 *	40.4 ± 21.9

* Statistically significant compared with controls with $p < 0.05$.

2.3.2 Differences in Senescence Associated Gene Expression between PE and IUGR

Initially, using a Human Cellular Senescence Profiler Array with subsequent real-time PCR validation, multiple senescence-associated genes including cell cycle regulatory and DNA damage response (DDR) genes CHEK-1, CCNB-1, CDKN2A, ATM, GLB-1, ID-1, IGFBP-5, PCNA, PTEN, SOD-2, and TBX2 were examined in placental tissue samples. Of the panel of senescent-associated genes examined, there was a significant increase in placental expression of checkpoint kinase 1 (CHEK-1) (4.9-fold ± 0.94, p = 0.008; Figure 2.1A), Cyclin B (CCNB-1) (3-fold ± 1.4, p = 0.036; Figure 2.1B), proliferating cell nuclear antigen (PCNA) (6.9-fold ± 1.3, p = 0.013; Figure 2.1C), cyclin kinase CDKN2A (3.5-fold ± 0.9, p = 0.007; Figure 2.1D), and phosphatase-tensin homolog PTEN (12.8-fold ± 1, p = 0,003; Figure 2.1E) in pre-eclampsia. The expression of transcription factor TBX2 (0.3-fold ± 0.9, p = 0.016; Figure 2.1F), ataxia kinase ATM (0.7 ± 1.26, p = 0.02; Figure 2.1G), cyclin B CCNB-1 (0.3-fold ± 1.7, p = 0.028; Figure 2.1B), and DNA repair gene PCNA (0.2-fold ± 0.9, p = 0.046; Figure 2.1C) were significantly decreased in the IUGR subgroup, when compared with controls. There was no significant difference amongst the other senescence-associated genes between study groups (Figure 2.1 h-k).

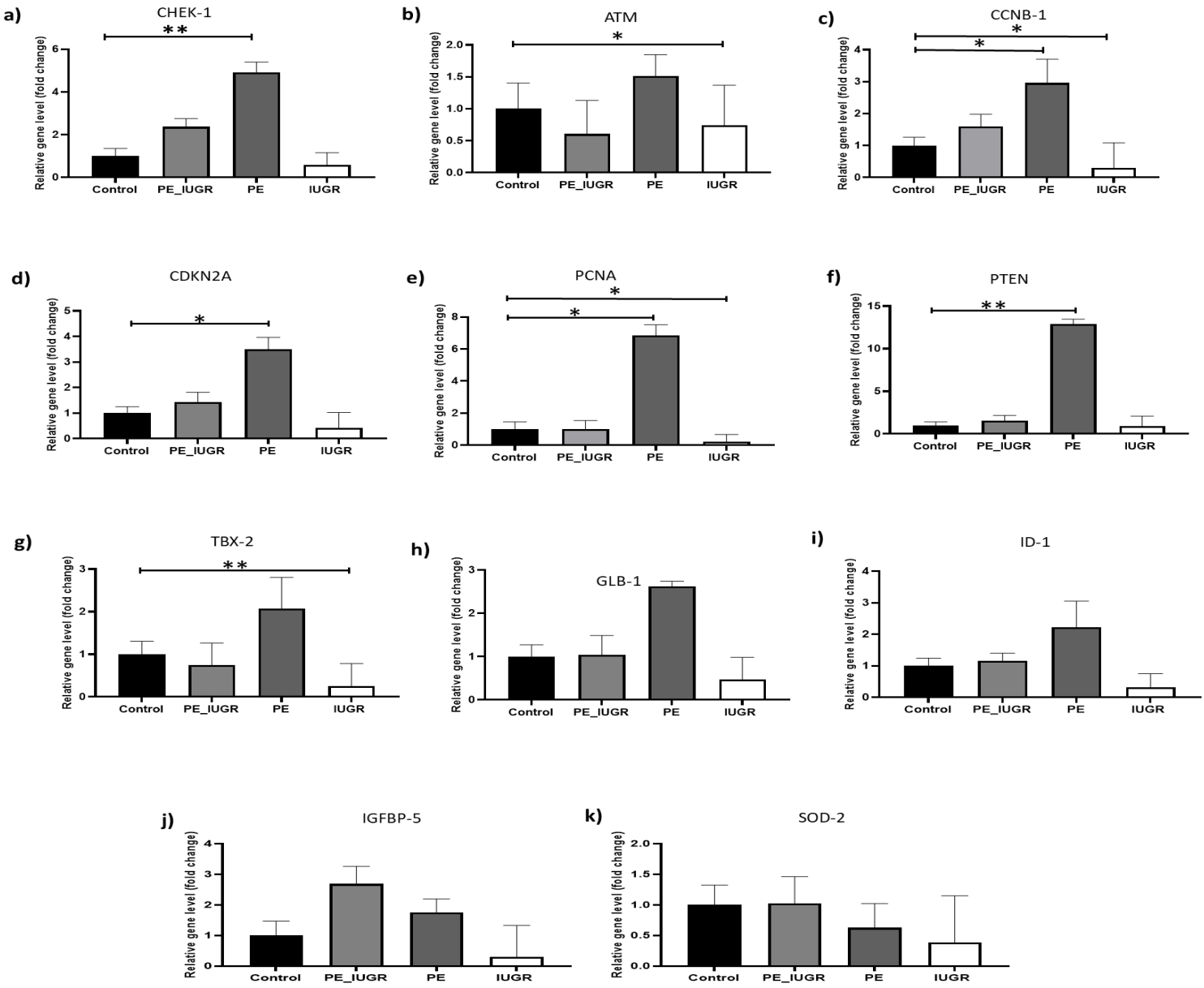

a)
CHEK-1
**
Relative gene level (fold change)
Control
PE_IUGR
PE
IUGR
b)
ATM
*
c)
CCNB-1
*
*
d)
CDKN2A
*
e)
PCNA
*
*
f)
PTEN
**
g)
TBX-2
**
h)
GLB-1
i)
ID-1
j)
IGFBP-5
k)
SOD-2

Figure 2.1 Senescence-associated gene expression in placental tissue in pre-eclampsia and IUGR. (A) CHEK-1 expression in PE only was significantly elevated (p = 0.006); (B) ATM was significantly decreased in IUGR (p = 0.02); (C) CCNB-1 was significantly elevated in PE only (p = 0.028), whereas it was significantly reduced in IUGR (p = 0.036); (D) CDKN2A was significantly elevated in PE only (p = 0.012); (E) PCNA was significantly elevated in PE only (p = 0.014), whereas it was significantly decreased in IUGR (p = 0.04); (F) PTEN was significantly elevated in PE only (p = 0.005); (G) TBX-2 was significantly reduced in IUGR only (p = 0.005). No significant changes were observed for (h) GLB-1, (i) ID-1, IGFBP-5, (j) and SOD-2 (k) when compared to controls. All measurements were relative gene expression compared with controls. Data are mean fold change compared with controls at level 1 ± SD, $p < 0.05$; p-value < 0.05, (*) and p-value < 0.01, (**).

2.3.3 Absolute Telomere Length in placental tissue:

While placental absolute telomere length (aTL) was longer in PE (9.05 kbp ± 5.7 vs. 5.9 kbp ± 4.5) and PE associated with IUGR (6.84 kbp ± 3.2 vs. 5.9 kbp ± 4.5) compared with controls, this increase was not statistically significant (Figure 2.2). Adjusting for the variables maternal age, maternal BMI, gestational age, fetal individualized customized centile (ICC), and fetal sex, PE had a 4.88 kbp (95% CI: −0.391, 10.15) longer telomere length; additionally, PE associated with IUGR had a 1.65 kbp (95% CI: −3.53, 6.88) increase in telomere length compared with controls (Table 2.3).

When absolute telomere length was examined in IUGR (4.96 kbp ± 3.5 vs. 5.9 kbp ± 4.5), there was no significant difference compared with controls (Figure 2.3). Adjusting for the variables maternal age, maternal BMI, gestational age, fetal individualized customized centile (ICC), and fetal sex, placental aTL was shorter in IUGR compared with controls but this reduction in aTL was not statistically significant (−1.5 kbp 95% CI: −6.852, 3.807) (Table 2.4).

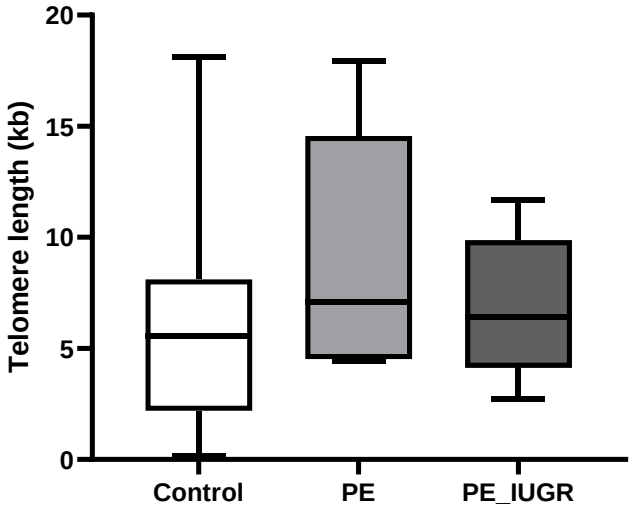


Figure 2.2 Absolute telomere length in pre-eclampsia. aTL in placental tissue was not significantly altered in PE or PE associated with IUGR compared with controls. Data are represented as mean aTL ± SD, $p < 0.05$.

Exposure Groups	Crude Estimate (95% CI)	Adjusted Estimate [a] (95% CI)
Pre-eclampsia only (N = 5)	3.191 (−1.288, 7.671)	4.882 (−0.391, 10.155)
Pre-eclampsia with IUGR (N = 8)	0.986 (−2.761, 4.734)	1.675 (−3.527, 6.878)

Table 2.3 Crude and adjusted association between placental absolute telomere length (aTL) in kbp for PE and PE associated with IUGR, compared with controls. [a] Adjusted for maternal age, BMI, gestational age, ICC, and fetal sex. Abbreviations: 95% CI = 95% confidence interval, BMI = body mass index, ICC = individualised customised centile, aTL = absolute telomere length.

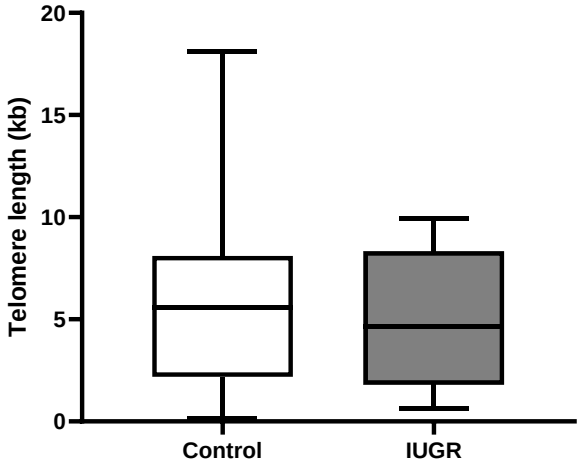


Figure 2.3. Absolute telomere length in IUGR. ATL in placental tissue showed no significant changes in IUGR compared with controls. Data are represented as mean aTL ± SD, $p < 0.05$.

Exposure Groups	Crude Estimate (95% CI)	Adjusted Estimate [a] (95% CI)
IUGR < 10th centile (N = 6)	−0.895 (−5.214, 3.423)	−1.522 (−6.852, 3.807)

Table 2.4 The Crude and adjusted association between placental absolute telomere length (aTL) in kbp for IUGR placentas compared with controls. [a] Adjusted for maternal age, BMI, gestational age, ICC, and fetal sex. Abbreviations: 95% CI = 95% confidence interval, BMI = body mass index, ICC = individualised customised centile, aTL = absolute telomere length.

2.3.4 Placental Expression of Cyclin-Dependent Kinase Inhibitor

Cell cycle arrest resulting from upregulation of cyclin-dependent kinase inhibitors, p21 and p16, is a classical feature of senescence. To elucidate the role of p16 in regulating cellular senescence, protein expression was measured in all study groups (Figure 2.4 A and Figure 2.4B). p16 protein expression was significantly decreased in PE placentas when compared with controls (p = 0.031) (Figure 2.4C), while this reduction in p16 expression was not evident in placental tissue from PE associated with IUGR compared with controls (Figure 2.4D). Additionally, when compared to controls, there was no significant difference in p16 protein expression observed in IUGR subgroup (Figure 2.4E).

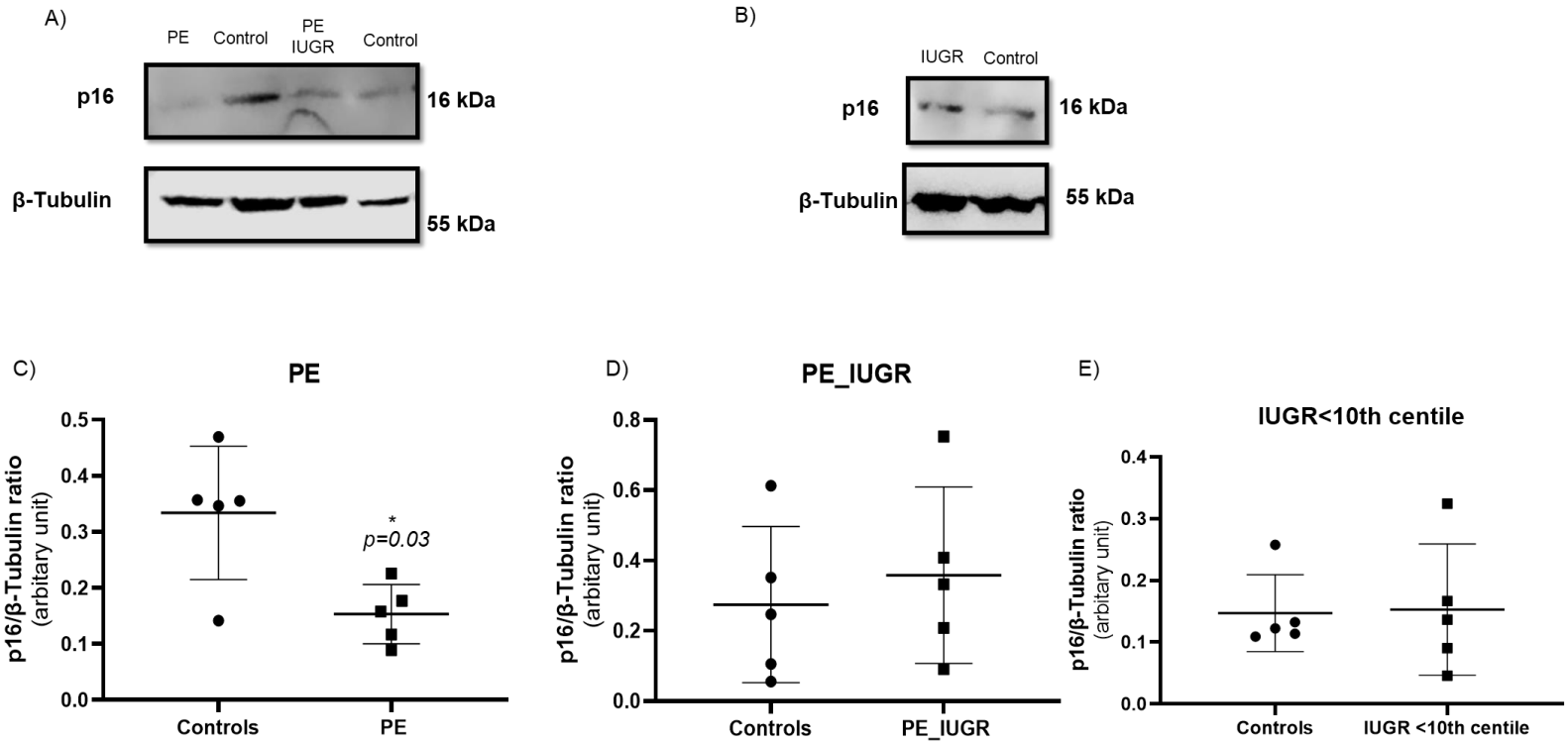


Figure 2.4 Representative images of p16 protein expression as measured by Western blotting in placental tissue from PE only (n=5) and PE associated with IUGR (n=5) (A) and IUGR(n=5) (B) matched by age. Densitometric analysis was used to quantify expression of p16 in PE only (C), PE associated with IUGR (D) and IUGR (E) with expression normalised to β-Tubulin. Statistical analysis with Wilcoxon matched-pairs signed rank test with two-tailed test, * $p < 0.05$ vs. control placenta. p-value < 0.05 (*).

Furthermore, protein expression of p21, was measured in all study groups (Figure 2.5 A and Figure 2.5B). There was no significant difference in p21 protein expression in PE (Figure 2.5C) and PE associated with IUGR (Figure 2.5D) when compared with controls. Similarly, there was no significant difference in p21 protein expression in IUGR (Figure 2.5E) when compared with controls.

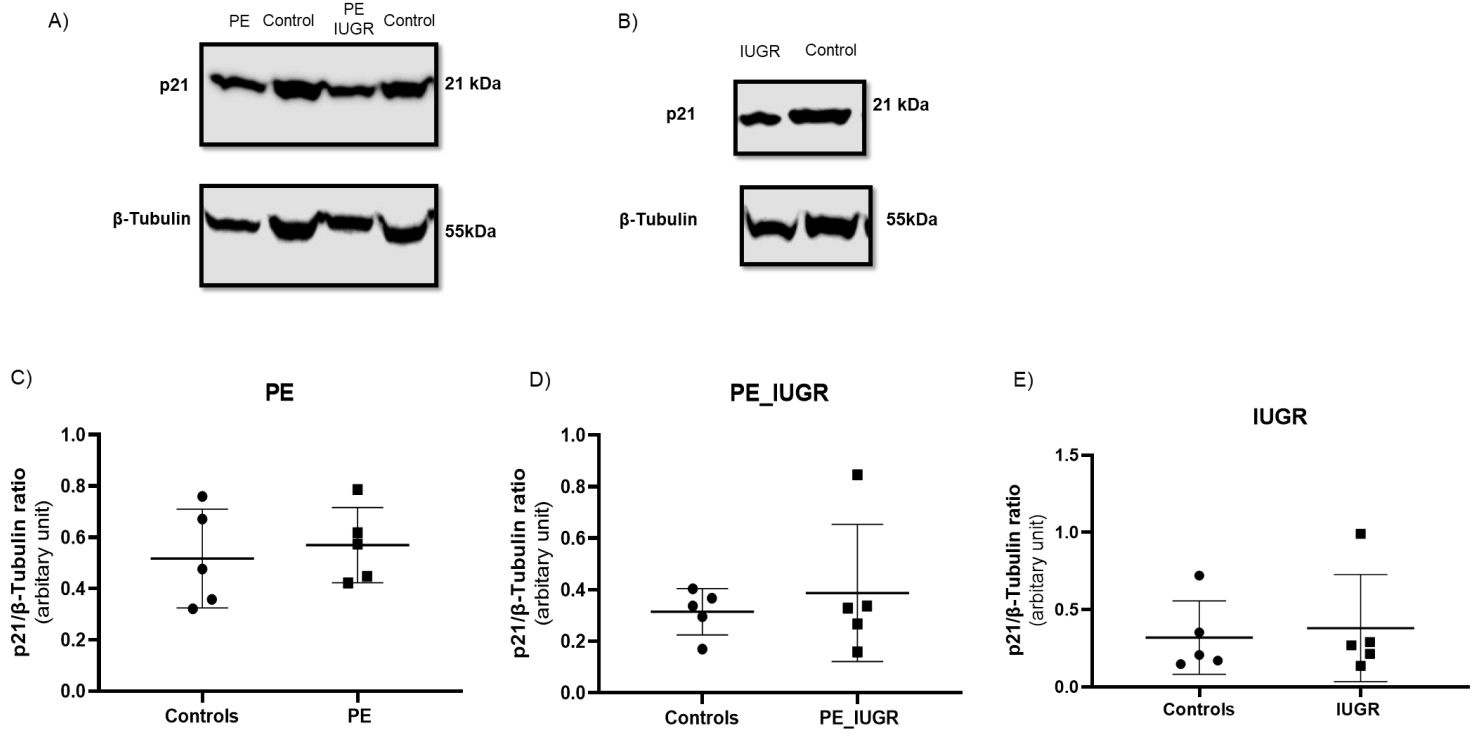


Figure 2.5 Representative images of p21 protein expression as measured by Western blotting in placental tissue from PE only (n=5) and PE associated with IUGR (n=5) (A) and IUGR(n=5) (B) matched by age. Densitometric analysis was used to quantify expression of p21 in PE only (C), PE associated with IUGR (D) and IUGR (E) with expression normalised to β-Tubulin. Statistical analysis with Wilcoxon matched-pairs signed rank test with two-tailed test.

2.3.5 Expression of nuclear intermediate filament protein Lamin B1 in placental tissue in Pre-eclampsia and IUGR

A reduction in Lamin B1 protein expression has been detected in senescent cells and is induced by various triggers including cell replication and oncogene activation. Lamin B1 has roles in DNA replication and cell cycle progression in addition to maintaining nuclear envelope integrity. Expression of Lamin B1 was not significantly different in PE groups (Figure 2.6A) or IUGR (Figure 2.6B), respectively, when compared with controls.

2.3.6 Absolute Quantification for mitochondrial DNA

We compared absolute mtDNA copy numbers in placental tissue for PE subgroups and IUGR, comparing them to controls (Figure 2.7). mtDNA copy numbers when compared to controls with PE (3211713 ± 2780530 v 634312 ± 1230023; P=0.058); PE IUGR (2089319 ± 2534706 v 634312 ± 1230023; P=0.19) and IUGR (1056158 ± 2144337 v 634312 ± 1230023; P=0.9). Even though both PE subgroups showed increases in placental mtDNA copy numbers, these increases did not reach statistical significance compared with controls.

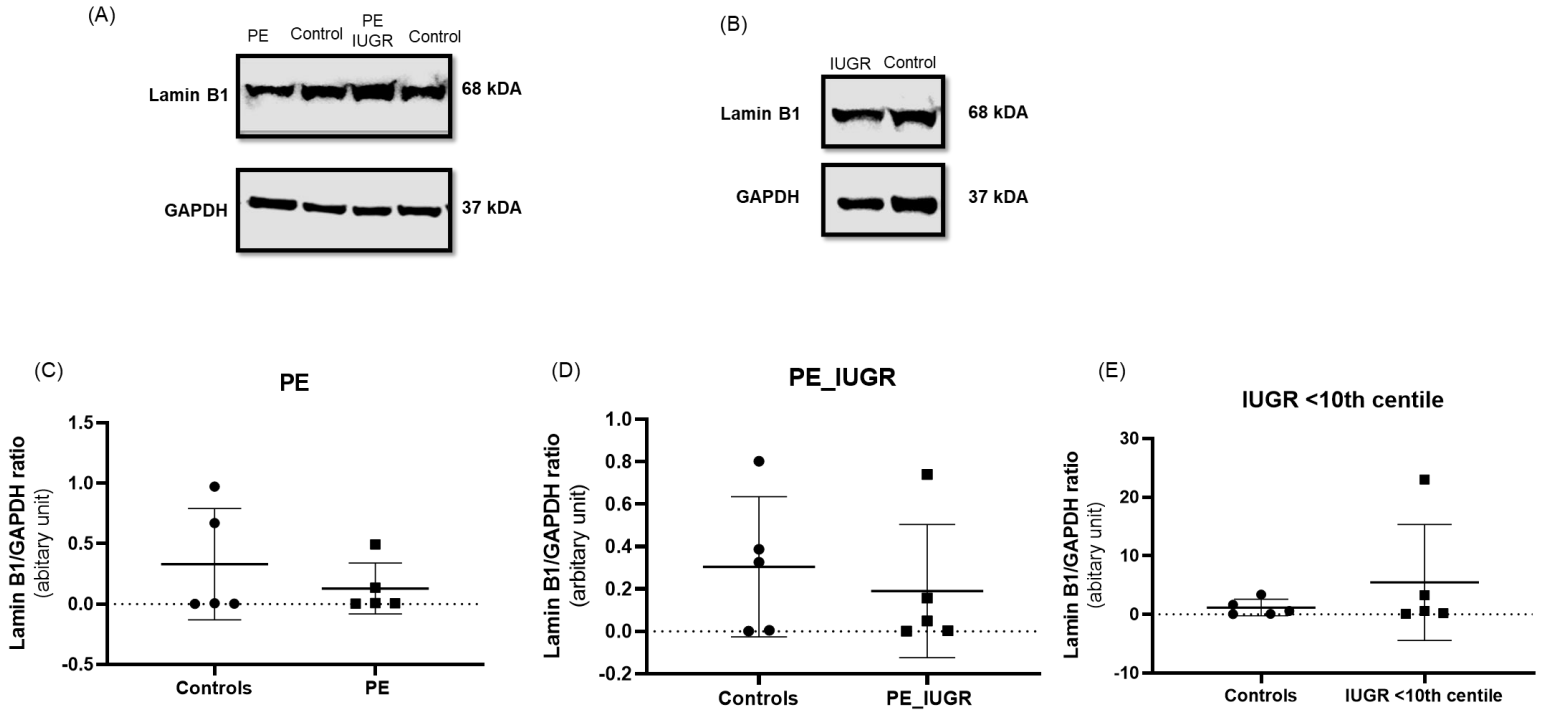


Figure 2.6 Representative images of Lamin-B1 protein expression as measured by Western blotting in placental tissue from PE only (n=5) and PE associated with IUGR (n=5) (A) and IUGR(n=5) (B) matched by age. Densitometric analysis was used to quantify expression of Lamin-B1 in PE only (C), PE associated with IUGR (D) and IUGR (E) with expression normalised to GAPDH. Statistical analysis with Wilcoxon matched-pairs signed rank test with two-tailed test.

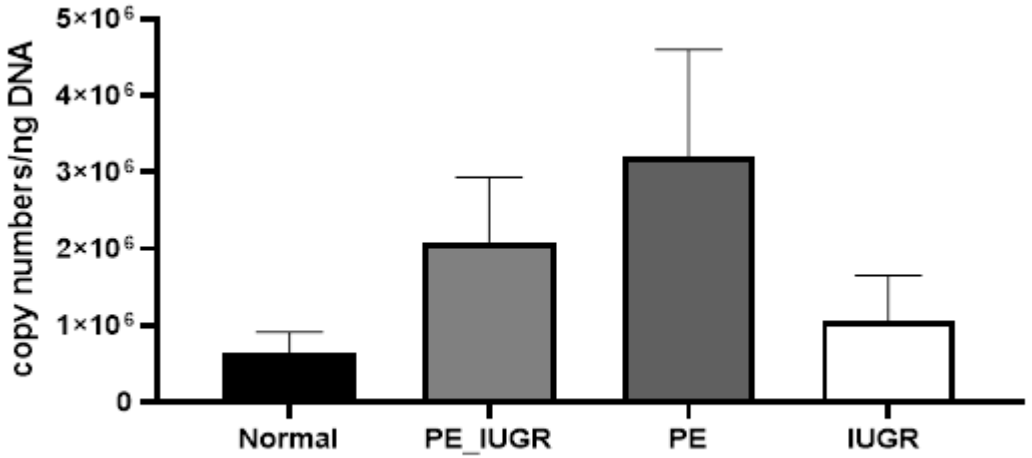


Figure 2.7 Absolute quantification of mitochondrial DNA (*mtDNA*) copy numbers as measured by RTqPCR in placental tissue from PE only (n=5) and PE associated with IUGR (n=5) (A) and IUGR(n=5) (B) matched by age and BMI. All measurements were relative mtDNA copy numbers compared with controls. Data are mean fold change compared with controls.

2.4.7 Senescence Associated Secretory Phenotypes in Maternal Plasma Reveal Different Cytokine Profiles in PE and IUGR

Senescence-associated secretory phenotypes (SASP) consist of a core panel of inflammatory cytokines and mediators including, interferon-γ (INF-γ), interleukins (IL-13, IL-6, IL-8), monocyte chemoattractant protein-1 (MCP-1) and macrophage inflammatory protein 1 alpha (MIP-1α), and matrix metalloproteinase-3 (MMP-3) [333-335]. Of the original panel of seven SASP markers, IL-6 was significantly increased in PE only when compared with controls (0.59 pg/mL ± 0.2 vs. 0.29 pg/mL ± 0.1; p = 0.017) (Figure 2.8A). Expression of the remaining six SASP markers did not differ significantly between PE and controls (Figure 2.8B–G). There was no significant difference in the expression of any SASP marker between PE/IUGR when compared with PE or when compared with controls. Interferon-γ expression was significantly increased (4.6 pg/mL ± 2.2 vs. 2.17 pg/mL ± 0.8; p = 0.002) (Figure 2.9E) in IUGR when compared with controls. There were no other significant changes observed in SASP markers compared with controls (Figure 2.9B–G).

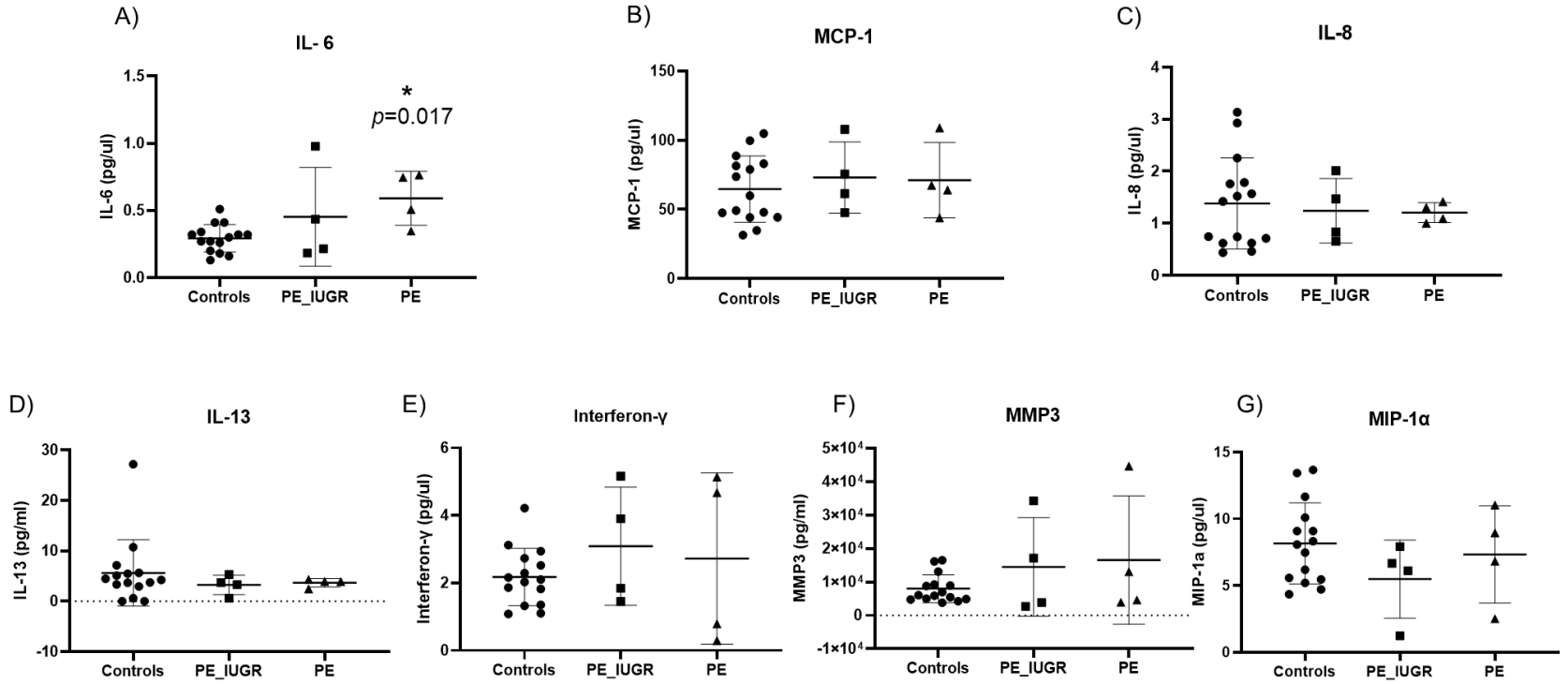


Figure 2.8 Senescence-associated secretory phenotypes (SASP) in PE with or without intrauterine growth restriction. (A) IL-6 was significantly increased in maternal plasma in PE only pregnancies (p = 0.017) when compared with controls. All other cytokines: (B) MCP-1, (C) IL-8, (D) IL-13, (E) Interferon-γ, (F) MMP-3, and (G) MIP-1α showed no significant differences between PE subgroups compared with controls. Data are represented as mean ± SD, $p < 0.05$; p-value < 0.05, (*).

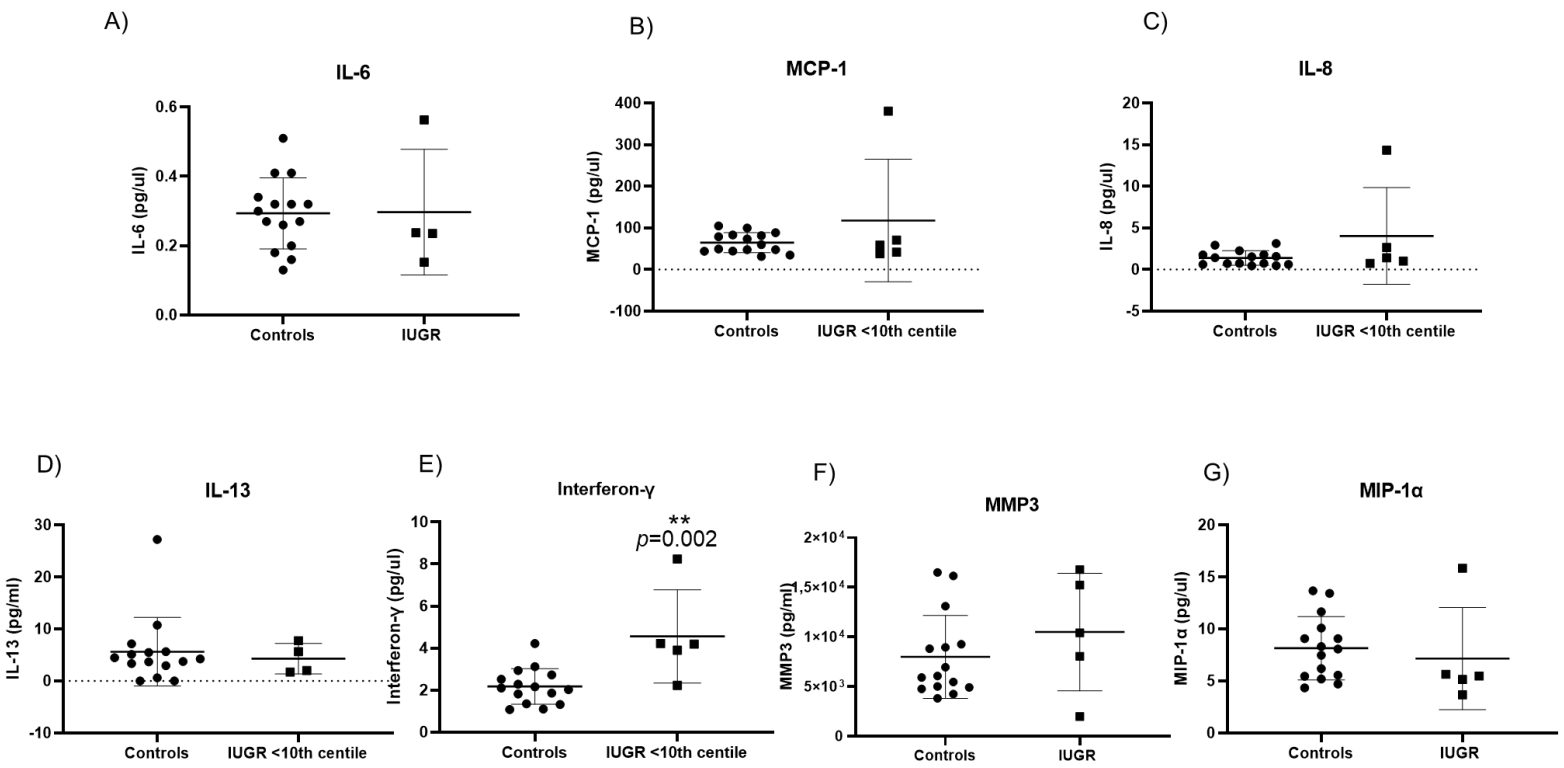


Figure 2.9 Senescence-associated secretory phenotypes (SASP) evident in intrauterine growth restriction IUGR: (E) Interferon-γ (p = 0.002) in IUGR pregnancies were significantly increased in maternal plasma when compared with controls. All other cytokines: (A) IL-6, (B) MCP-1, (C) IL-8, (D) IL-13, (F) MMP-3, and (G) MIP-1α showed no significant difference when compared with controls. Data are represented as mean ± SD, $p < 0.05$; p = 0.002 (**).

2.4 Discussion

Premature placental ageing has been associated with adverse pregnancy outcomes such as PE, intrauterine growth restriction, and stillbirth. Increased oxidative stress and an inadequate antioxidant defense lends to impaired redox signaling and oxidative damage [336]. While the physiological triggers of senescence *in vivo* are not fully understood, evidence of hypoperfusion coupled with oxidative stress and placental insufficiency may orchestrate a multistep cellular senescence response. This study sought to assess the evidence of placental ageing resulting from cellular senescence in both PE and IUGR by evaluating multiple biomarkers of senescence. Cellular senescence is defined as a state of terminal proliferation, accompanied by characteristic metabolic and pro-inflammatory changes. Our results showed a significant decrease in senescence-associated genes ATM, CCNB-1, PCNA, and TBX2 in IUGR placentas, and a significant increase in maternal circulating interferon-γ levels when compared with controls. On the other hand, in PE, we showed a significant increase in placental expression of CHEK-1, CCNB-1, PCNA, CDKN2A, and PTEN accompanied with a significant reduction in p16 placental protein levels, and a significant increase in maternal circulating IL-6 levels when compared with controls. There was no significant difference in absolute placental telomere length between any study groups, when compared with controls.

Initially, the expression of senescent-associated genes was characterised in placental tissue in PE, PE associated with IUGR, and IUGR. There was a significant increase in key regulators of DNA repair and checkpoint surveillance, namely CHEK-1 and PTEN in PE only, with an additional increase in expression of markers promoting proliferation (PCNA and CCNB1). Proliferating cell nuclear antigen

(PCNA) is a proliferation marker, which regulates the replication complex formation and has a role in DNA metabolism, affecting DNA damage repair (DDR) pathways [337]. CHEK-1 is a DDR signalling kinase which arrests cell cycle to allow DNA repair, while the phosphatase and tensin homolog (PTEN), which had the largest increase in expression, equally controls DNA repair and regulates G1/S and G2/M checkpoints in the cell cycle to ensure appropriate cell survival. Cells experiencing DNA damage due to external or internal stressors act through the ATM/ATR pathway. CCNB-1 is downregulated leading to DNA damage-induced cellular senescence via G2 cell cycle arrest [338]. Despite the induction of the DDR, potentially facilitating DNA repair due to exaggerated oxidative stress in PE, the significant increase in CCNB1, a marker of the G2 phase in the cell cycle, and PCNA suggest that placental cells respond to oxidative damage by promoting the required DNA repair and then re-enter the cell cycle rather than inducing senescence.

Conversely, in IUGR, there was a significant reduction in expression of ataxia telangiectasia mutated (ATM), cell proliferation markers CCNB1 and PCNA in placental tissue compared with controls. ATM is activated by double strand break (DSB) in an attempt to repair the damage incurred [339]. TBX-2, a transcription repressor of senescence which plays an important role in the regulation of cellular fate, maintaining cellular proliferation [340-343], was also significantly reduced in IUGR only. The deficiency in the capacity to mount an appropriate DNA damage response, aligned with a significant reduction in cell proliferation, may be indicative of premature terminal differentiation of trophoblasts at a mean GA of <33 weeks, signifying a premature cellular senescence phenotype in this subgroup. While there was no significant difference in placental expression of senescence-associated

genes in the PE associated with IUGR group, there was an obvious heterogeneity in expression of all genes, which was reflective of the individual signature profiles of PE and IUGR.

Further senescent associated genes were also measured including Lysosomal-β-galactosidase (GLB-1) which has been associated as a source of senescence-associated β galactosidase (SA- β-gal) activity, a marker of cellular senescence [344]. ID-1 has been shown to act through the p16ink4a/retinoblastoma (pRb) tumour-suppressor pathway, affecting telomerase activity [345] and Insulin-like growth factor binding protein (IGBP-5) has been shown to regulate apoptosis through DDR and upregulation of the p53 pathway [346]. Superoxide dismutase 2 (SOD-2) is an antioxidant enzyme providing defense against oxidative stress [347]. There was no significant difference in expression of these genes in any of the study groups.

Increased oxidative stress and accumulation of double-stranded DNA damage foci located at telomeres, irrespective of telomerase activity, may simulate premature senescence [348]. In this study, we evaluated absolute telomere length (aTL) in our study groups controlling for maternal age, BMI, gestational age, fetal sex, and fetal ICC. There was no significant difference in absolute telomere length across the three groups compared with controls. However, we identified notable variances in telomere length: PE with/without IUGR had longer placental aTL, whereas IUGR had a much shorter aTL. Multiple studies have failed to show any association between PE and placental telomere length [322, 323, 343]; however, IUGR has been associated with decreased placental telomerase activity and shorter telomere length when compared with healthy uncomplicated pregnancies [243, 252, 255, 256]. Biron-Shental et al. reported shorter telomere length for PE and IUGR placentas compared with

controls [252]. Despite the lack of evidence of significant telomere shortening in this study, it is worth noting that premature senescence can be induced independently of telomere length.

Activation of cyclin-dependent kinase (CDK) inhibitors including p16 and p21 are critical mediators of cell cycle progression and hence have important regulatory roles in promoting premature senescence. Both p21 and p16 are negative modulators of cell proliferation in part due to their control of cyclin-CDK activity in response to extracellular and intracellular signals. In this study, placental expression of p21 was not significantly different in any of the study groups compared with controls. However, placental expression of p16 was significantly reduced in PE only, with no change evident in PE associated with IUGR or IUGR alone.

Conversely, placental CDKN2A gene expression was significantly increased in PE in our study. The CDKN2A gene locus is responsible for production of p16INK4a and p19Arf, which act as cell cycle inhibitors and are expressed at higher levels in senescent cells [318, 349]; however, despite the increase in gene expression, a subsequent increase in p16 activity was not evident in PE. Previous studies have reported increased p16 expression in term placental syncytiotrophoblasts, in PE and IUGR[318]. The reduction of p16 expression in PE in this study suggests that although the evident DDR response mediated via upregulation of CHEK-1 may trigger activation of G2 checkpoint with resultant arrest of cell cycle, entry towards a senescent phenotype is not fully stabilized, which may allow cells to re-enter the cell cycle and maintain cellular mitotic property, which is supported by increase in PCNA and CCNB1 expression in PE [351]. As there was no change in either p21 or p16

expression in PE associated with IUGR or IUGR, it would suggest that growth restriction may induce the alternative senescent phenotype.

Nuclear lamins are structural proteins lining the lamina or inner nuclear envelope surface [352], which provide structural integrity. Senescent cells display enlarged flattened profiles with a distorted nuclear envelope resulting from a reduction in Lamin B1 expression. Loss of Lamin B1 has been reported as a robust marker of cellular senescence but the exact pathway initiating Lamin B1 reduction remains unclear; furthermore, loss of Lamin B1 precedes activation of the SA-β-Gal pathway and the accumulation of SASPs [353]. In this study, there was no significant difference in the placental expression of Lamin B1 in any of the study groups, which suggests that there is no overt disruption to the nuclear structure in response to DDR.

Exaggerated oxidative stress in senescent cells has been associated with the accumulation of dysfunctional mitochondria. Mitochondrial dysfunction has been associated with disease severity and complexity. Mitochondrial DNA (mtDNA) copy numbers is a measure of mtDNA levels per cell and is associated with mitochondrial enzyme activity and adenosine triphosphate (ATP) production. Mitochondria, as the source of ROS production, plays a pivotal role in the pathophysiology of placental hypoperfusion diseases as well as cellular dysfunction and ageing. We subsequently looked for evidence of mitochondrial dysfunction by measuring mtDNA in placental tissue and reported no significant changes across the three study groups. Multiple publications have shown increased mtDNA in maternal circulation and cord blood in pregnancies affected by PE, PE/IUGR, and IUGR [283, 354]. Contrarily, mitochondrial quality and mtDNA copy number is significantly reduced in ageing cells [355-357]. This study did not provide evidence of increased placental mtDNA copy numbers in PE,

PE associated with IUGR, and IUGR, and based on this surrogate marker of mitochondrial dysfunction, we propose that mitochondrial dysfunction is not a significant contributor to the heterogeneity evident in our study.

One of the hallmarks of senescence is the ability of growth-arrested cells to remain metabolically active and secrete SASPs, which affects events within the cell and causes senile modulation of the extra-cellular environment as well as neighboring cells [57]. Our results showed a significant increase in IL-6 levels in maternal plasma in women with PE only. Multiple reports have shown that increased IL-6 levels are associated with both severity and onset of PE [358, 359]. Despite its well-defined role as an inflammatory mediator, IL-6 also has a major role in cell cycle regulation through activation of the Janus kinase-signal transducer and activator of transcription (JAK/STAT) and mitogen-activated protein kinase (MAPK) signal transduction pathways [340, 360]. The classical MAPK/ERK family is an intercellular checkpoint for cellular mitogenesis, controlling cell cycle progression[34]. In this study, the increase in IL-6 may be more indicative of systemic maternal inflammation in PE rather than a direct consequence of a senescent phenotype in PE. Interferon gamma (IFN-γ), a pro-inflammatory cytokine, has been reported to induce cellular senescence through the p53-dependent DNA damage signaling pathway [352, 361, 362]. Our results show significant elevation of circulating IFN-γ in IUGR pregnancies, which may be indicative of premature cellular senescence. Similar to all other senescent biomarkers, there was no significant difference in circulating cytokines in the PE associated with IUGR study group.

The approach of measuring multiple senescence markers in PE, PE associated with IUGR, and IUGR (<10th centile) is a significant strength of this study as it facilitated

a complete investigation of premature senescence phenotypes in these obstetric complications. To date, identifying the physiological stressors of senescence *in vivo* are not fully elucidated. This study has a limited sample size which might influence the overall conclusions drawn in this study. The limited sample number was due to a stringent study design of recruiting nulliparous women with PE, PE associated with IUGR, and IUGR cohorts. The gestational age was matched as closely as possible between cases and controls in the study to overcome the effect of premature births. Women with IUGR pregnancies that were complicated by any fetal abnormalities were excluded.

Despite the limitation of small sample numbers in this study, it is evident that there are significant differences in cell proliferation/senescence phenotypes in PE and IUGR. The heterogeneity of these phenotypes in PE and IUGR alone are equally different in PE associated with IUGR, where an altered molecular profile was evident with no obvious evidence of cellular senescence or altered proliferation.

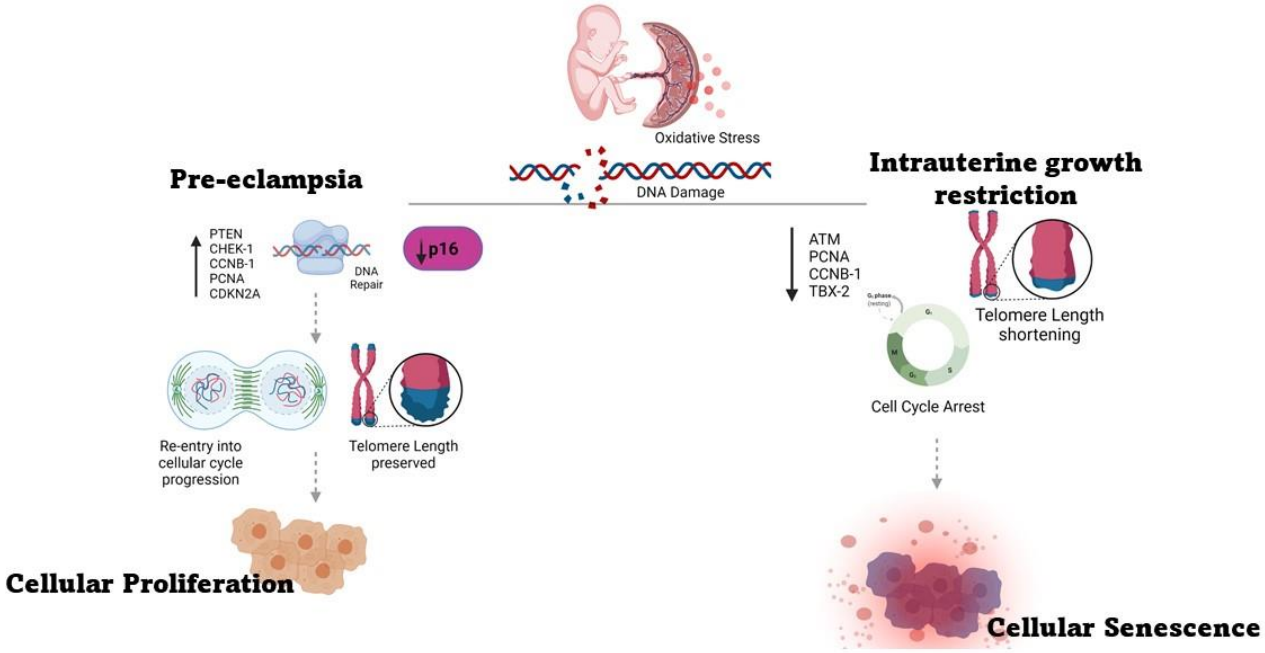


Figure 2.10 Graphical summary of results from Chapter 2 [363]

2.5 Conclusion

In the study we showed that in PE, despite activation of DNA damage response, in part as a result of oxidative damage, the cellular phenotype signified a re-entry into the cell cycle and continued cell proliferation rather than progressing towards senescence. IUGR presented a completely different phenotype, which was representative of significantly reduced cell proliferation and premature terminal differentiation which may progress towards senescence. Despite the assessment of multiple biomarkers of senescence in this study, it highlights the complexity in distinguishing between cellular subtypes at a single cell level as well as between cell types, which may be reflective of the differing orchestrators of placental pathogenesis of these pathologies.

Chapter 3:

A proteomic profile of the healthy human placenta

The text of this chapter has been adapted from the following publication:

Manna S, Scheel J, Noone A, et al. A proteomic profile of the healthy human placenta. Clin Proteomics. 2023;20(1):1. Published 2023 Jan 2. doi:10.1186/s12014-022-09388-4

Abstract

Background: The placenta remains one of the least studied organs within the human body. Yet, placental dysfunction has been associated with various pregnancy complications leading to both maternal and fetal death and long-term health consequences. The aim of this study was to characterise the protein networks of healthy term placental sub-anatomical regions using label free quantification mass spectrometry.

Methods: Three healthy placentae were sampled at five sample sites and each biopsy was dissected into maternal-, middle-, and fetal- sub-anatomical regions. Quadrupole-orbitrap mass spectrometer was used in data dependant analysis mode to identify 1859 unique proteins before detailed differential expression between regions.

Results: Protein profiling identified 1081, 1086, and 1101 proteins in maternal, middle, and fetal sub-anatomical regions respectively. Differentially expressed proteins were identified considering the effect between sample site location and sub-anatomical region on protein expression. Of these, 374 differentially expressed proteins (Two-way ANOVA adjusted p-value < 0.05, HSD Tukey adjusted p-value 0.05) were identified between sample site locations and sub-anatomical regions. The placenta specific disease map NaviCenta (https://www.sbi.uni-rostock.de/minerva/index.xhtml?id=NaviCenta) was used to focus functional analysis results to the placenta specific context. Subsequently, functional analysis with a focus on senescence, and mitochondrial function were performed. Significant differences were observed between sub-anatomical regions in protein

intensity and composition. A decrease in anti-senescent proteins within the maternal sub-anatomical region, and an increase in proteins associated with a switch from ATP to fatty acid consumption as a source of energy between middle and fetal sub-anatomical regions were observed.

Conclusion: These results suggest that normal proteomic variations exist within the anatomical structure of the placenta, thus recommending serial sectioning methodology for consistent placental research.

3.1 Introduction

The placenta is a complex organ playing a critical role in the development and preservation of a healthy pregnancy. It is appropriately defined by Harland Mossman as *"The normal mammalian placenta is an apposition or fusion of the fetal membranes to the uterine mucosa for physiological exchange"* [88, 364]. The placenta is a dynamic organ undergoing rapid growth, and dramatic molecular and histological rearrangements along gestational stages, in order to adapt to fetal requirements [365].

Nevertheless, the placenta remains the least studied organ in the human body, whose structural and functional composition have possible implications for long term maternal and child health outcomes [366, 367]. A healthy placenta at term is a disc shaped organ around 22cm in diameter and weighing approximately 500gms [88]. Although the placenta is a fetal organ, its anatomical regions can be loosely classified as: Maternal and Fetal, based on its proximity to fetus [368, 369]. This multifaceted transient organ is characterised by different anatomical structures; the chorionic plate with umbilical cord attached, at the fetal side (fetal sub-anatomical region), the basal plate which borders the maternal endometrium (maternal sub-anatomical region) and the intermediate region connecting the basal plate and chorionic plate (middle sub-anatomical region) [89, 109]. Placental villi, the core structural unit are classified as stem villi which connect to the chorionic plate with limited exchange functionality; intermediate villi classified as mature or immature consisting of cytotrophoblast subtypes with differing functional roles and the syncytiotrophoblasts layer which acts as principal transfer site especially in first and

second trimester. As pregnancy progresses the terminal villi which are completely formed at 20 weeks' gestation, are the dominant morphological feature with syncytiotrophoblasts being immersed in maternal blood facilitating its functional role in nutrient and gaseous exchange [368, 370]. The placenta ages gradually as the pregnancy proceeds. At 40 weeks of gestation, the placenta is at its verge of decline, exhibiting morphological and physiological senescence [247]. However, in the presence of undesirable oxidative stress, placental aging may be accelerated in certain pregnancy conditions such as PE (PE), intrauterine growth restriction (IUGR) and stillbirth, characterized by both mitochondrial dysfunction and premature cellular senescence [1, 371].

The placental proteome has been used to further our understanding of the molecular mechanisms involved in development of the placenta and in the pathophysiology of placental disorders [365]. Furthermore, this technology has been used in clinical research to aid in the discovery of protein or metabolite biomarkers that can be incorporated into a diagnostic tool for clinical utility [372]. Proteomics has been widely used in pregnancy complication such as PE and IUGR, by using novel methods in specific trimester of pregnancies, for diagnosis, and understanding pathophysiological mechanism to improve maternal and neonatal health outcomes [373].

Uniformity of placental sampling has been lacking in obstetric research with some studies focusing on single placental sampling sites which may not always be representative of the global signature of this large heterogenous metabolic organ. Standardization of placental tissue sampling can improve the quality of placental

research, and facilitate sharing of samples between groups, allowing larger datasets to be generated [326]. Burton et al., summarized factors such as methodological flaws including sampling and processing samples that might be limiting placental research [63]. The aim of this research was to determine the proteomic signature of a healthy term placenta, while investigating proteomic composition and molecular pathways enriched across the placental sub-anatomical regions.

3.2 Materials and Methods

3.2.1 Patient Recruitment and Sample Collection

Participants were recruited as part of the COMRADES Study, a non-interventional cohort study of nulliparous singleton pregnancies with the aim of characterizing placental premature senescence in PE (PE) and Intra-uterine growth restriction (IUGR). The COMRADES study was conducted according to the guidelines laid down in the Declaration of Helsinki, and all the procedures were approved by the Clinical Research Ethics Committee of the Cork Teaching (ECM4 (ff) 04/12/18). All women provided written informed consent to take part in the study. Three normotensive, healthy pregnant participants with no obstetric complications were recruited as a part of the COMRADES Study between February and July 2020. Placental samples were collected from nulliparous, singleton pregnancies undergoing Caesarean section for non-obstetric indications such as breech presentation. Placental sampling was completed within 20 minutes of delivery, snap frozen in liquid nitrogen, and stored at -80°C for long term storage. Placental sectioning was performed in accordance with the standard protocol described by Burton et al [326].

Tissue samples (2-4 cm in diameter) were isolated from 5 different sample sites across the placenta. We defined the sub-anatomical regions of the placenta as: maternal, middle, and fetal to evaluate the basal plate, chorionic plate and the middle part connecting the two surfaces of the placenta. Sectioning was performed by keeping close to the fetal membrane from the chorionic plate, the maternal region was dissected closer to the basal membrane and the middle region was selected from between maternal and fetal sections (Figure 3.1). Fetal membranes were not included in the sectioning [326].

3.2.2 Protein Extraction and Quantification

Processing of placental tissue for proteomics analysis was based on previously established laboratory protocols [374]. Placental tissue (50mg) was homogenized using the TissueLyser II (Qiagen, Germany) and protein isolated using Tetraethylammonium bicarbonate (TEAB) buffer (Sigma-Aldrich, Ireland) in presence of Phosphatase inhibitor (PhosSTOP™, Roche, Ireland) and Protease Inhibitor (Roche, Ireland). Protein quantification was assessed with BCA Assay (Pierce™ Thermo Fisher Scientific, USA) and protein volume adjusted to 50µg/50µl concentration with MS grade dH_2O.

3.2.3 Protein Solubilisation and Desalination

Protein enzymatic digestion was performed using Trypsin (Promega, MyBio, Ireland) with the aid of Rapigest (1%) solution (Waters, Ireland). To aid with Trypsin (Promega, MyBio, Ireland) 50 mM Tris(2-carboxyethyl) phosphine hydrochloride (TCEP) (Sigma-Aldrich, Ireland) solution was added to the denatured proteins and samples reduced for 60 minutes at 60°C, followed by addition of 200mM Indole-3-

acetic acid (IAA) solution (Sigma-Aldrich, Ireland) to alkylate proteins, which were incubated overnight at 37°C with 1:100 sequential grade trypsin according to manufacturer's instruction followed by addition of 1% Formic acid was used to stop digestion. Precipitation of Rapigest was done by centrifuging samples at 13000rpm for 10 minutes and supernatants collected, and air dried on MiVac Quattro sample concentrator (Fisher Scientific, Sweden) followed by resuspension in 0.5% Formic Acid (FA) (Sigma-Aldrich, Ireland). Desalting and sample clean-up was performed using Zip-Tip columns with 0.6 µl binding volume C18 resin (Sigma-Aldrich, Ireland). For maximum binding of protein to resin present on zip-tip column, the tips are equilibrated using 0.1% Trifluoroacetic acid (TFA) in H_2O; followed by washing and binding of protein, and finally the proteins are eluted into 10µl elution solution composed of 50% ACN in 0.1% TFA.

The process was repeated to achieve protein concentration of 1µg/µl. The samples are then re-dried on MiVac Quattro sample concentrator (Fisher Scientific, Sweden) and all samples were resuspended in 0.1% FA to 1µg/µl volume for LC-MS/MS analysis. Equal aliquots of digested proteins in the experiment were pooled into one sample for internal quality control (QC) standard which was injected three times at the beginning of the MS study and throughout the experiment every 10 injections to condition the column and monitor the MS performance. LC-MS/MS analysis was performed in the Proteomics Core in the Conway Institute of Biomolecular and Biomedical Research, UCD, Dublin.

3.2.4 Mass Spectrometry (MS) sample preparation

Proteomic samples were enzymatically digested with Trypsin (Promega sequencing grade) according to manufacturer's instruction and in the presence of Rapigest SF (Waters). Briefly, samples were first reduced with Tris(2-carboxyethyl) phosphine hydrochloride (TCEP) at 60°C for 60 minutes, and alkylated with Iodoacetamide (IAA, final concentration y mM) for 30 mins in the dark, prior to the addition of trypsin in a ratio of enzyme to protein of 1:100 (w/w). The samples were incubated overnight at 37°C followed by addition of 1% Formic acid the next morning to stop digestion and precipitate the Rapigest. Removal of Rapigest by-products was performed by centrifugation of samples at 13000rpm for 10 minutes and supernatants collected and dried under vacuum with a MiVac Quattro sample concentrator (Fisher Scientific, Sweden). The dried digests were resuspended in 0.5% Formic Acid (FA) (Sigma-Aldrich, Ireland) prior to de-salting with C18 ZipTips (Millipore). Finally, the de-salted digests were resuspended in 0.1% FA for LC-MS/MS analysis. Equal aliquots of digested protein from each sample in the experiment were pooled into a single sample for an internal quality control (QC) standard which was injected three times at the beginning of the MS study and throughout the experiment every 10 samples, and to condition the column and monitor the MS performance. LC-MS/MS analysis was performed in the Proteomics Core in the Conway Institute of Biomolecular and Biomedical Research, UCD, Dublin.

3.2.5 Mass Spectrometry

All samples were injected in a randomized sequence combining Internal standards and samples for discovery of sub anatomical region proteomic profiles. 5 µl of each sample was injected in duplicate onto the Thermo Scientific Q-Exactive® connected to a Dionex Ultimate 3000 High-performance Liquid Chromatography (HPLC) system. The digests were loaded onto a fused silica emitter (75 µm ID), pulled using a laser puller (Sutter Instruments P2000) and packed with UChrom C18 (1.8um) reverse phase media (nanoLCMS Solutions LCC). Peptides were separated using an increasing acetonitrile gradient (250nL/min) for 60 mins[374]. The mass spectrometer was operated in data dependent analysis (DDA) mode on a TopN 12 mode with setting: mass range 300-1600Th; resolution for MS1 scan 70000; AGC target 3e6; resolution for MS2 scan 17500; AGC target 2e4; charge exclusion unassigned, 1; dynamic exclusion 40 s.

3.2.6 Bioinformatics and Data pre-processing

Raw data obtained from LC-MS/MS runs were searched against the Uniprot Human reference proteome UP000005640 (downloaded 24-05-2021) with MaxQuant (version 1.6.17) using default settings and additionally including the 'Match Between Runs' and 'Label free quantification (LFQ)' options. The ProteinGroups.txt output file obtained from the MaxQuant analysis was processed in Perseus (version 1.6.15.0). Data was filtered to remove possible contaminants. Samples were categorised by sub-anatomical region. LFQ intensity data was log2 transformed, and proteins not identified in all biological replicates were removed. After rigorous filtering to assure reproducibility, including filtering for valid values in at least 100%

of biological replicates, 70% valid values of samples per sample site, and 70% valid values of samples per sub-anatomical region, these proteomic differences did not persist. Furthermore, proteins absent in 70% of samples in at least one sub-anatomical region/sample site were removed. Missing values were replaced by values from the normal distribution.

3.2.7 Statistical analysis

Statistical analysis was conducted using the built-in statistical tests in Perseus. To analyse the effect of sub-anatomical region and sample site on protein expression a two-way ANOVA was performed. Two-way ANOVA models allow accounting for more than one known source of variation. In this study "sub-anatomical region" and "sample site" were considered independent variables and LFQ protein intensity was the dependent variable (https://www.ncbi.nlm.nih.gov/pmc/articles/PMC2528956/pdf/nihms60473.pdf) . Sample main effects were analysed using simple ANOVA and Tukey's HSD tests. The results were corrected for false discovery ($p < 0.05$) within Perseus [375].

3.2.8 Pathway analysis

Functional analysis of differentially overrepresented gene ontology (GO) terms and pathways associated with differentially expressed proteins, was performed using Cytoscape v 3.9.1 ClueGO plugin [376]. GO and pathway term overrepresentation results were corrected for false discovery using Bonferroni step down correction ($p<0.05$) and considered significantly overrepresented with an adjusted p value < 0.5.

Placenta Specific Characteristics: The term disease map was defined as *"a comprehensive, knowledge-based representation of disease mechanisms*" [377, 378]. The NaviCenta consists of human and machine-readable representations of processes involved in healthy and dysfunctional placentae in SBGN process description and activity flow (https://www.sbi.uni-rostock.de/minerva/index.xhtml?id=NaviCenta). Phenotype predictions based on user defined data uploaded onto the NaviCenta were performed with plugins [379]. The uploaded information consisted of HGNC identifiers for the genes of all identified proteins, their difference score as calculated in Perseus, and adjusted p values.

Mitochondria and senescence specific function analysis: Identified proteins that map to mitochondrial function were filtered using the products of genes associated with mitochondrial functions incorporating information from the Human Protein Atlas mitochondrial sub-cellular location (www.proteinatlas.org) [380], MitoXplorer human interactome [381], and MitoCarta3.0 [382]. The overlap between mitochondrial protein and gene databases, proteins identified in maternal, middle, and fetal regions were visualized using InteractiVenn [383]. Separately, DEPs were filtered to exclusively contain proteins that map to senescence associated molecular process. Senescence associated proteins and genes were identified from the Human Ageing Genomic Resource College Build 20 [384], Cell Senescence Gene Database CSGene [385], and the NCBI gene database with search key "senescence" (https://www.ncbi.nlm.nih.gov/gene/?term=senescence, accessed October 2021). GO biological process terms were visualized using the R Version 4.0.5 and R package GOPlot [386].

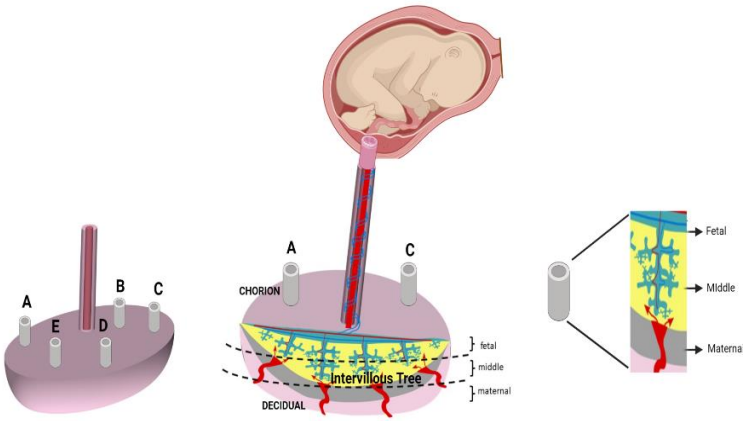
3.3 Results

3.3.1 Study Demographics

Patient demographic and clinical information can be found in Table 3.1. Each placenta had five sample sites (A-E) taken across the placenta. These samples were then separated into three sub-anatomical regions: fetal, middle, and maternal, resulting in a total number of 45 samples. Sub-anatomical regions were confirmed histologically (Figure 3.1).

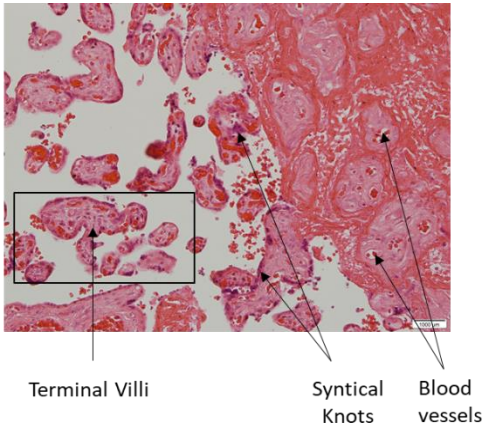
Table 3.1 Patient demographics and clinical parameters of recruited women.

Characteristics	**Mean ± SD**
Maternal Age (years)	34.6 ± 2.5
BMI (kg/m^2))	23.6 ± 4.1
Parity	0
Gestational Age (days)	270.7 ± 5.5
Systolic BP (mm Hg)	122.0 ± 7.5
Diastolic BP (mm Hg)	74.7 ± 5.5
Fetal Weight (kg)	3.3 ± 0.2
Fetal Individualized Customised Centile	52.9 ± 5.4
Maternal Smoking/Tobacco Habit	No

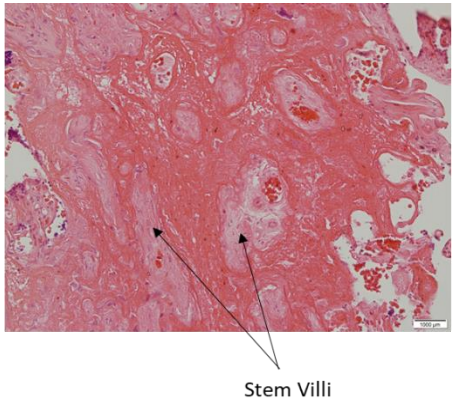


PLACENTAL SECTIONING
(5 sections across placenta)

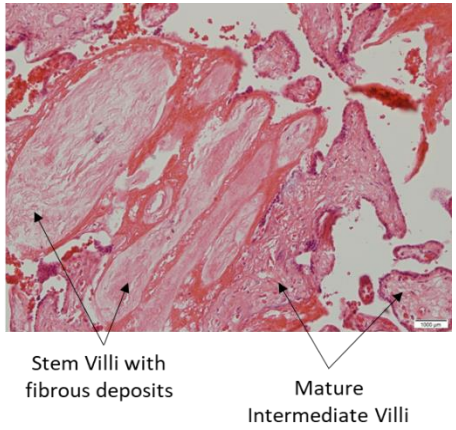
PLACENTAL SUB ANATOMICAL
REGIONS (Fetal, Middle, Maternal)



MATERNAL SUB-ANATOMICAL
REGION



MIDDLE SUB-ANATOMICAL
REGION



FETAL SUB-ANATOMICAL
REGION

Figure 3.1 Histopathological classification of sub-anatomical region sectioning. The maternal region shows evidence of developed terminal villi and arterial vessels, indicating maternal side of the placenta. The fetal sub-anatomical region with mature intermediate villi which provide fetal vascularization for feto-maternal exchange, along with a high fibrous deposition, suggesting it is the fetal side of the placenta. The middle region shows increased evidence of stem villi. Stem Villi are made up of trunks and branches of the villous tree and anchoring villi, depending on caliber and position they assume. At term, they are present mostly in subchorionic areas of the placenta, providing mechanical support to the organ [387].

3.3.2 Proteome Profile shows variation across Placental Regions and Sample sites

In total 1081, 1086, and 1101 proteins were identified in maternal, middle, and fetal sub-anatomical regions, respectively. We identified 14, 8, and 21 proteins as exclusive to the maternal, middle, or fetal sub-anatomical regions, respectively (Figure 3.1).

ClueGO functional analysis showed that in particular proteins aligning with GO terms of membrane organization, protein-containing complex and subunit organization, vesicle-mediated transport, organo-nitrogen compound biosynthetic process, and translation initiation factor activity are overrepresented. All unique proteins to sample site E except SNRPD2, SPP2, EPS8-l1, and ACAA2 were filtered out for the analysis of both sub-anatomical region and sample site considering biological replicates.

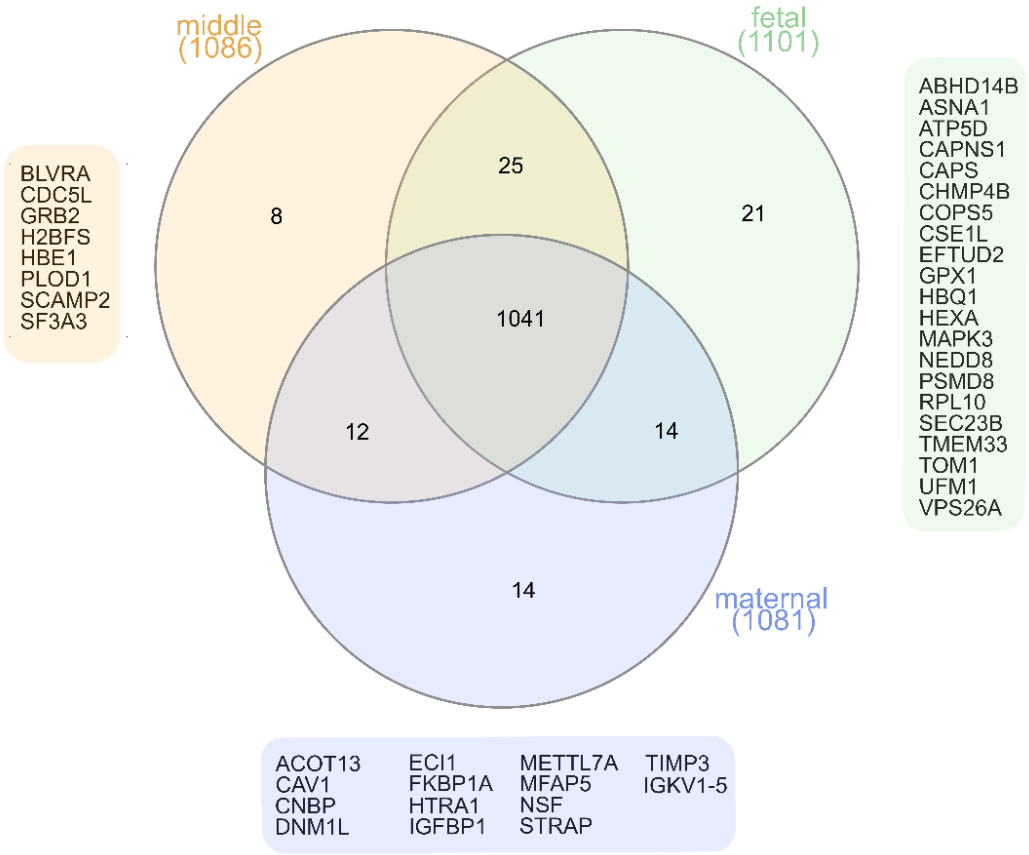


Figure 3.2 Venn diagram of identified proteins in the maternal, middle, and fetal regions. Proteins identified exclusively in one sub-anatomical region are listed next their respective sub-anatomical region.

3.3.3 Placental proteome varies with sub-anatomical region

Adopting a Two-way ANOVA considering both sub-anatomical region and sample site revealed 374 out of 1038 DEPs (adjusted p-value < 0.05) between sub-anatomical regions. Strong interaction between the effect of sample site and sub-anatomical region on LFQ protein intensity was indicated (p-value interaction < 0.05) for some proteins. The intensity of biological replicates of four proteins (CBR1, HBG2, ANXA4, and FHL1) demonstrating the highest interaction between sub-anatomical region and sample site on protein intensity are shown in Figure 3.2. No pattern was apparent, allowing the separate analysis of DEPs between sub-anatomical regions and sample sites.

Simple ANOVAs revealed no significant DEPs between sample sites. Sub-anatomical region comparison maintained the previously identified 374 DEPs. Maternal vs middle sub-anatomical region comparison revealed 128 upregulated, and 152 downregulated DEPs on the maternal side. Maternal vs fetal comparison revealed 115 upregulated, and 123 downregulated DEPs, respectively. Middle vs fetal sub-anatomical region comparison revealed 64 upregulated, and 41 downregulated DEPs in the middle sub-anatomical region (Table 3.2).

The top three up and downregulated DEP are detailed in Table 2. These proteins are associated with an array of molecular functions such as actin binding, protein binding, DNA binding, heparin binding, lipid binding and collagen binding.

Table 3.2 Summary of differentially expressed proteins (HGNC identifier) between maternal, middle, and fetal sub-anatomical regions. Top three DEPs MYH11, NUTF2, CFHr1, COL14A1, NUTF2, PZP, SCIN, LFT based on highest fold change (FC). Adjusted p val < 0.05, up= upregulated, down= downregulated. ***= adjusted p val < 0.001, ** = adjusted p val < 0.01, * = adjusted p val < 0.05. p values adjusted for FDR.

	Up DEP	Top 3 DEP	FC	Down DEP	Top 3 DEP	FC
Maternal vs middle sub-anatomical region	128	MYH11*** NUTF2* CFHR1***	1.48 1.01 0.80	152	PZP*** SCIN*** KDELC2***	-1.41 -1.15 -0.79
Maternal vs fetal sub-anatomical region	115	MYH11*** COL14A1*** NUTF2**	1.24 1.16 1.00	123	KRT19*** SNRPD2** CAPS*	-0.71 -0.69 -0.52
Middle vs fetal	64	PZP*** SCIN*** LTF***	2.29 0.80 0.70	41	DES*** SNRPD2** ERAP1***	-0.74 -0.66 -0.46

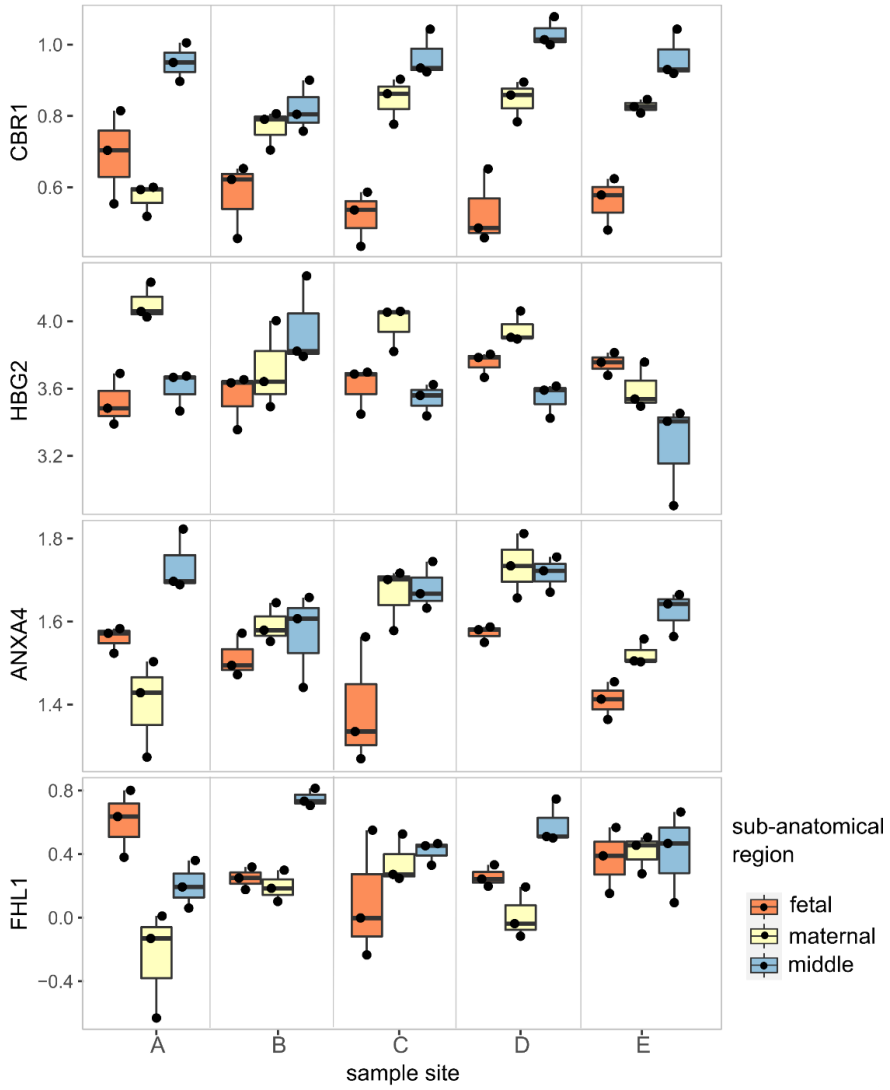


Figure 3.3 The top four proteins FHL1, ANXA4, HBG2, CBR1 show the strongest interaction between protein content in sub-anatomic regions and sample sites. Interaction was defined as two-way ANOVA adj p val < 0.05. Samples were sorted according to sample site and colour coded according to sub-anatomical region.

3.3.4 Functional analysis of placental proteome

To further our understanding of functional differences between sub-anatomical regions based on associated DEP, functional analysis was conducted. DEP of maternal vs fetal, maternal vs middle, middle vs fetal sub-anatomical regions were directly compared within ClueGO for biological process gene ontology (GO), molecular function GO, and cellular component GO overrepresentation. As there

was overlap between up and downregulated DEPs, functional comparisons were separated to consider upregulated DEPs and downregulated DEPs [376].

GO overrepresentation analysis indicated a number of biological processes and molecular functions to be enriched (Figure 3.3). Processes and molecular functions associated with inflammation, humoral and stress responses were overrepresented in both up and down regulated proteins. Processes associated with transcription and translation, such as regulation of RNA, RNA catabolic processes, and regulation of DNA biosynthetic process were primarily overrepresented in downregulated DEPs in the maternal compared to the fetal sub-anatomical region. Processes associated with intracellular transport were primarily enriched in downregulated DEPs in the maternal compared to the middle sub-anatomical region.

Mitochondria and senescence associated processes and functions such as, regulation of G2/M transition mitotic cell cycle, nitric oxide metabolism, oxidoreductase activity, and telomerase activity were overrepresented in downregulated DEPs between maternal and middle sub-anatomical regions. Proteins associated with glyoxylate metabolic processes were overrepresented in downregulated DEPs between maternal and middle or fetal sub-anatomical regions.

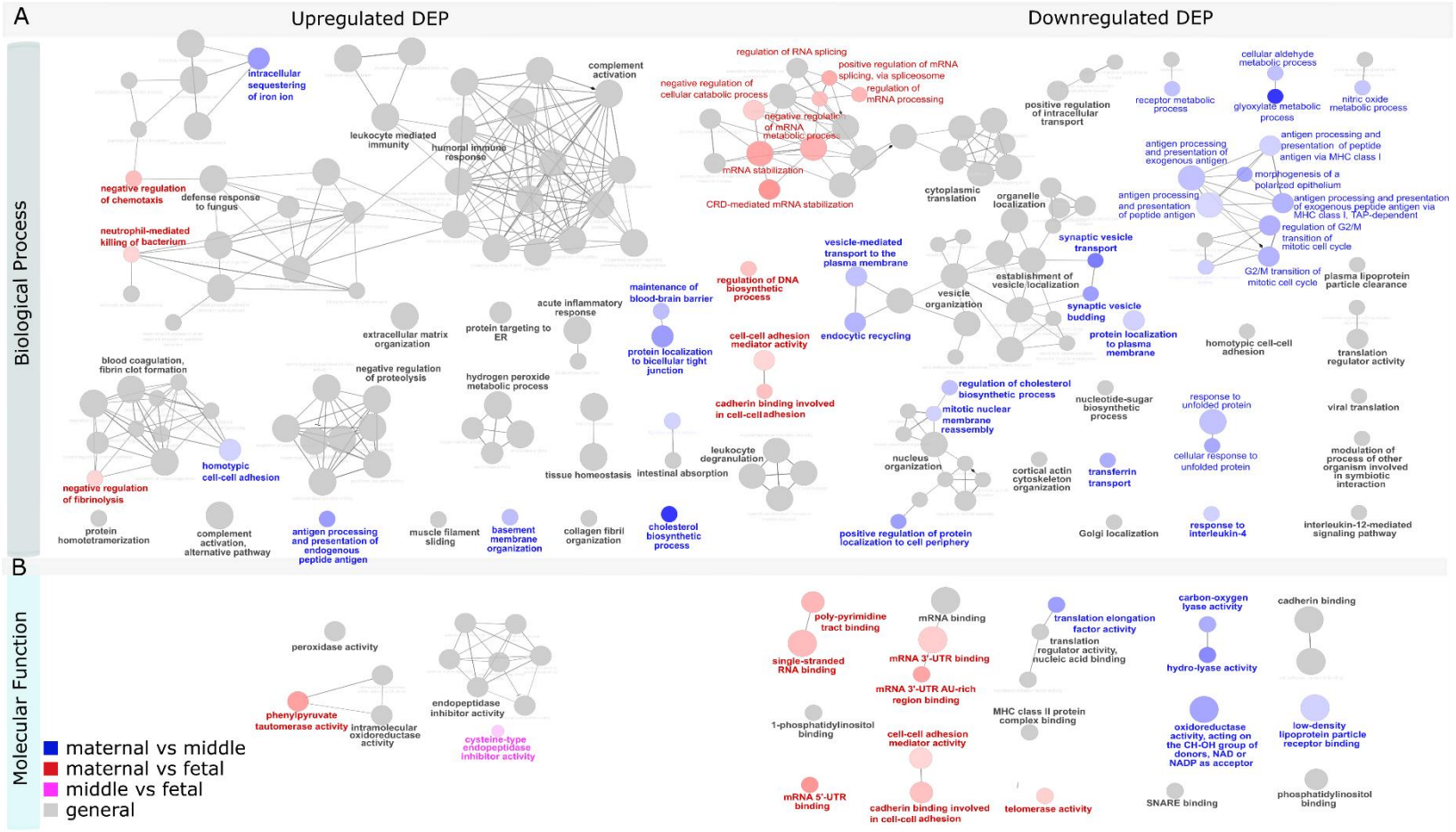


Figure 3.4 ClueGO functional analysis of differentially expressed proteins (DEP) between maternal, middle, and fetal sub-anatomical regions. Significantly (adj. p<0.05) overrepresented biological process (A) and molecular function (B). GO terms can be grouped by similarity, in which case only the group GO term is legible. The size of nodes indicates the number of proteins encoding genes falling into each term. Similarity or hierarchic relationship between GO terms is indicated by edges.

3.3.5 Placenta specific functional analysis

GO overrepresentation analysis revealed a myriad of differentially regulated processes and functions. In order to focus results further, and align them to placental tissue, we used the NaviCenta, a placenta specific disease map. In contrast to traditional methods to characterize the function of deregulated genes or proteins the NaviCenta allows for consideration of DEPs including their respective fold change (Figure 3.4)

Placenta specific phenotype prediction based on NaviCenta, showed that proteins found in the maternal sub-anatomical region are associated with increased endothelial cell (EC) migration, EC apoptosis, and EC proliferation in comparison to both middle and fetal sub-anatomical regions (Table 4). Proteins associated with both the complement cascade and chemotaxis are lower in maternal and middle sub-anatomical regions compared to the fetal sub-anatomical region. Ferritinophagy associated proteins are lower in the maternal than the middle sub-anatomical region, while mRNA splicing is higher in the maternal than the middle sub-anatomical region (Table 3.3).

Table 3.3 NaviCenta differential phenotype prediction based on DEP (Benjamini – Hochberg FDR correction) p-value including adj. Pval < 0.01 between maternal, middle, and fetal sub-anatomical regions and the proteins leading to each phenotype prediction.

Phenotype	Mat-fet log2FC	pval.	Gene Name	Mat-mid log2FC	pval		Mid-fet log2FC	pval	Gene Name
EC migration	0.28	5.94 e^{-24}	PLG	0.18	3.76 e^{-28}	PLG	0	1	
Inflammatory response	-0.26	5.91 e^{-21}	IGHG4	0	1		-0.31	2.30 e^{-35}	IGHG4
contraction	1	1.51 e^{-13}	MYH11	1	5.41 e^{-35}	MYH11, TAGLN	-0.33	3.13 e^{-22}	TAGLN
EC apoptosis	0.2	1.84 e^{-11}	BLVRB	0.15	2.39 e^{-13}	BLVRB	0	1	
EC proliferation	0.2	5.12 e^{-11}	BLVRB	0.15	5.83 e^{-13}	BLVRB	0	1	
Complement cascade	-0.27	1.03 e^{-08}	IGHG4	0	1		-0.31	3.94 e^{-19}	IGHG4
chemotaxis	-0.27	3.91 e^{-08}	IGHG4	0	1		-0.31	5.30 e^{-18}	IGHG4
Antigen clearance	0.41	0.003	IGHA1, IGLC3	-0.05	0.070		0.63	2.22 e^{-11}	IGHA1
Destruction of pathogens	0.15	0.008	MPO	0.07	0.048		0	1	
Ferritinophagy	0.2	0.453		-0.14	0.001	FTL, FTH1	0	1	
mRNA splicing	0	1		0.12	0.003	ACIN1	0	1	

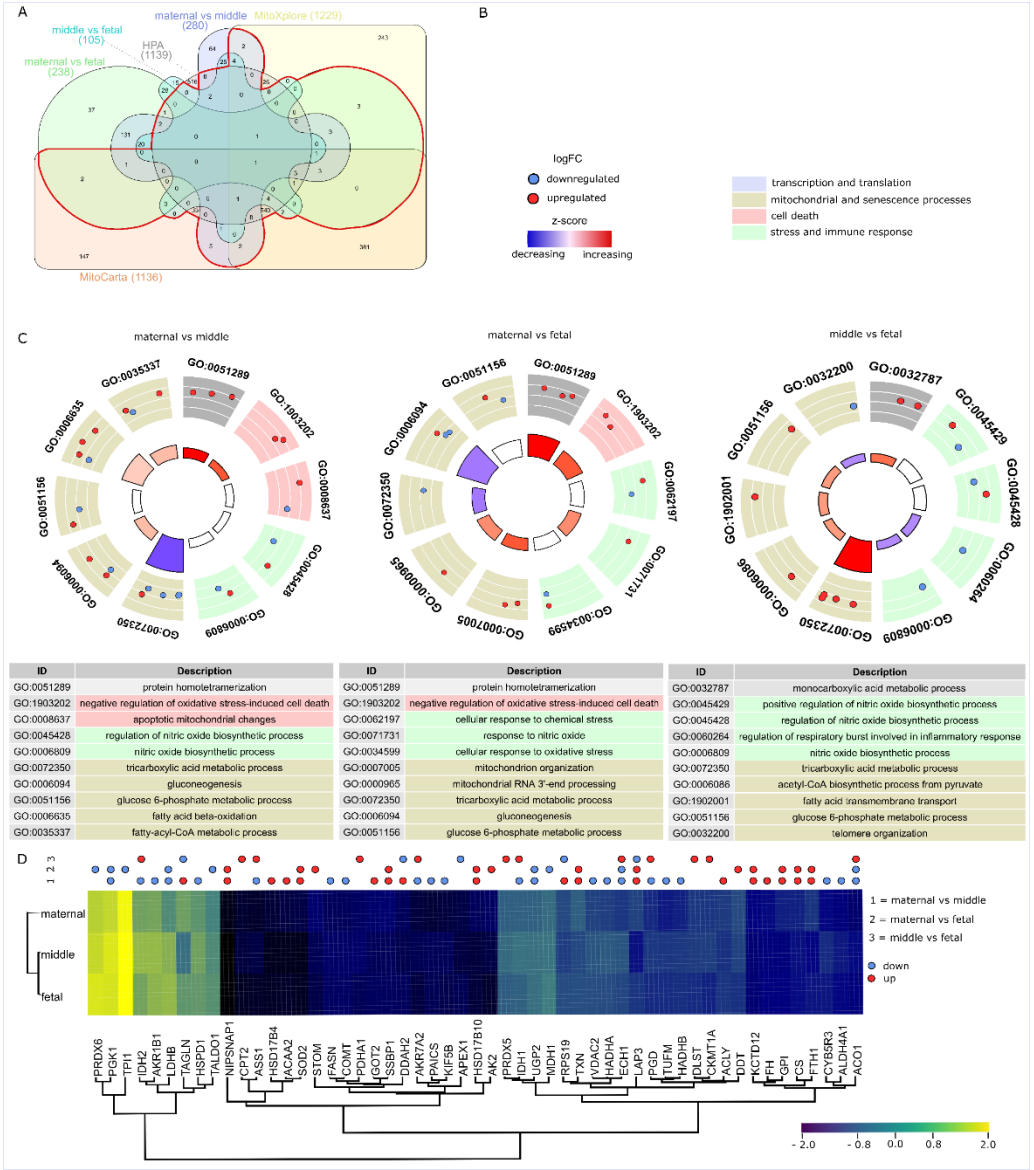
3.3.6 Differing Mitochondrial profile across Placental sub-anatomical regions

The list of all identified proteins was filtered to only include proteins (HGNC IDs) included in the mitochondrial gene and proteome databases Human Protein Atlas mitochondrial sub-cellular location(www.proteinatlas.org), MitoXplorer human interactome [382], and human MitoCarta3.0 [382] (Figure 3.5). HPA contains 1139 proteins associated with mitochondrial function, MitoCarta 3.0 1136, and MitoXplorer 1229, respectively (Figure 3.5). These databases showed overlapping content both with each other and with DEPs identified between sub-anatomical placenta regions. Ensuing functional analysis was conducted using the intersection of any mitochondrial database with placental proteins. Of all identified proteins, 147 out of 1081 in the maternal sub-anatomical region, 144 out of 1086 in the middle sub-anatomical region, and 148 out of 1101 in the fetal sub-anatomical region are associated with mitochondrial function and processes. 53 DEPs out of the previous 374 DEPs are associated with mitochondrial function and processes.

The tricarboxylic acid cycle is indicated in all three conditional comparisons. Downregulated proteins are more evident on the maternal side compared with middle and fetal regions, while upregulated proteins are evident when comparing middle with fetal sub-anatomical region. Protein homotetramerization is indicated by upregulated proteins in the maternal region compared to both the fetal and the middle regions. Proteins associated with the negative regulation of oxidative stress-induced cell death are upregulated in the maternal region compared with both middle and fetal regions. Summarizing the results, a general switch from glucose to

lipid consumption appears to be initiated in the maternal and middle sub-anatomical regions compared to the fetal sub-anatomical region.

Comparing maternal and fetal sub-anatomical region, mitochondrion organization and mitochondrial RNA 3’-end processing are upregulated in the maternal sub-anatomical region, while APEX1 associated with telomere organization is downregulated in the middle sub-anatomical region compared to the fetal sub-anatomical region.



ID	Description
GO:0051289	protein homotetramerization
GO:1903202	negative regulation of oxidative stress-induced cell death
GO:0008637	apoptotic mitochondrial changes
GO:0045428	regulation of nitric oxide biosynthetic process
GO:0006809	nitric oxide biosynthetic process
GO:0072350	tricarboxylic acid metabolic process
GO:0006094	gluconeogenesis
GO:0051156	glucose 6-phosphate metabolic process
GO:0006635	fatty acid beta-oxidation
GO:0035337	fatty-acyl-CoA metabolic process

ID	Description
GO:0051289	protein homotetramerization
GO:1903202	negative regulation of oxidative stress-induced cell death
GO:0062197	cellular response to chemical stress
GO:0071731	response to nitric oxide
GO:0034599	cellular response to oxidative stress
GO:0007005	mitochondrion organization
GO:0000965	mitochondrial RNA 3'-end processing
GO:0072350	tricarboxylic acid metabolic process
GO:0006094	gluconeogenesis
GO:0051156	glucose 6-phosphate metabolic process

ID	Description
GO:0032787	monocarboxylic acid metabolic process
GO:0045429	positive regulation of nitric oxide biosynthetic process
GO:0045428	regulation of nitric oxide biosynthetic process
GO:0060264	regulation of respiratory burst involved in inflammatory response
GO:0006809	nitric oxide biosynthetic process
GO:0072350	tricarboxylic acid metabolic process
GO:0006086	acetyl-CoA biosynthetic process from pyruvate
GO:1902001	fatty acid transmembrane transport
GO:0051156	glucose 6-phosphate metabolic process
GO:0032200	telomere organization

Figure 3.5 Mitochondria associated DEPs and their functional analysis. (A) Venn diagram of DEPs of maternal vs fetal, maternal vs middle, middle vs fetal, and proteins and genes associated with mitochondrial functions and processes from the databases MitoXplorer, human protein atlas (HPA) - mitochondria specific, and MitoCarta V3.0. The section of proteins used for further analysis is within the red border. (B) GO biological processes included and figure legend to (C). GOCircle plots of the 10 most significantly overrepresented mitochondria associated with GO biological process terms, including DEPs falling into each term. Regulation direction is colour coded: upregulated (red), downregulated (blue). Size of the inner segments is indicative of the number of proteins falling into each term. The colour of each inner segment indicates the z-score - general up or downregulation of the GO term considering the number up- and downregulated proteins. (D) Clustered heatmap of average normalized LFQ intensities of mitochondria associated DEPs. Proteins are grouped into samples from maternal, middle, fetal sub-anatomical regions.

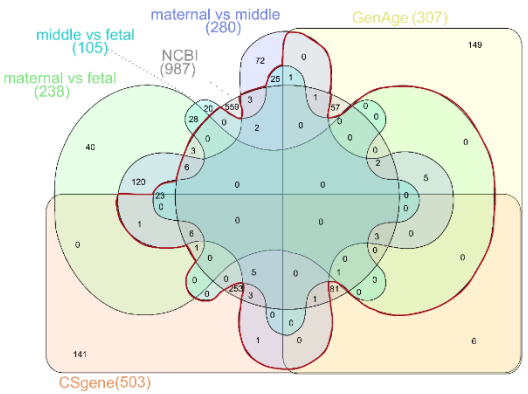
3.3.7 Variation in Senescence status across Placental sub-anatomical regions

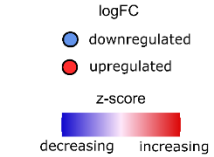
The difference in senescence state between the three sub-anatomical regions was subsequently analysed using three senescence specific databases. Human Ageing Genomic Resource (HAGR) CellAge Build 20, consisting of 307 genes as shown by Avelar et al 2020 [384], Cell Senescence Gene Database (CSGene) consisting of 503 genes, and the National Centre for Biotechnology Information Search database (NCBI) specifically genes associated with senescence in homo sapiens consisting of 988 genes. Of all identified proteins 790 out of 1081 in the maternal sub-anatomical region, 794 out of 1086 in the middle sub-anatomical region, and 804 out of 1101 in the fetal sub-anatomical region were associated with senescence [384].

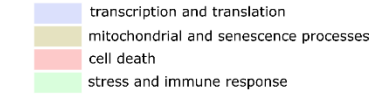
In total, 290 of the previously identified 374 DEPs were associated with senescence (Figure 3.6). Both transcription and translational processes (translation, nuclear-transcribed mRNA catabolic process, gene expression, regulation of mRNA stability) were differentially regulated between maternal and middle sub-anatomical region, with primarily down-regulated proteins on the maternal side, most of which were also downregulated in the middle compared to the fetal sub-anatomical region. Interestingly, proteins associated with negative regulation of, or regulation of cell death and apoptotic processes were primarily downregulated in the maternal compared to the middle sub-anatomical region and upregulated in the middle compared with the fetal sub-anatomical region.

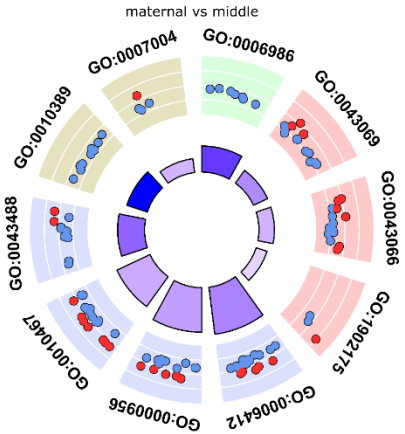
Proteins associated with stress responses were downregulated in the maternal compared to the middle sub-anatomical region and primarily upregulated in the middle compared to the fetal sub-anatomical region. Other senescence associated

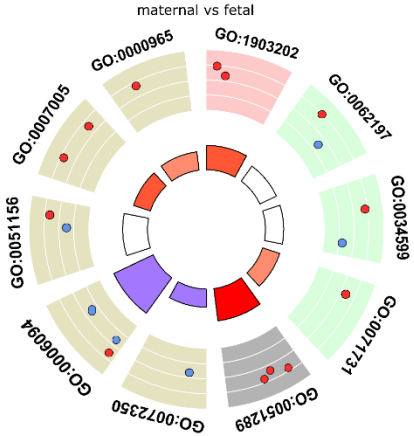
proteins (regulation of G2/M transition of mitotic cell cycle, telomere maintenance) were primarily downregulated in the maternal compared to the middle sub-anatomical region.

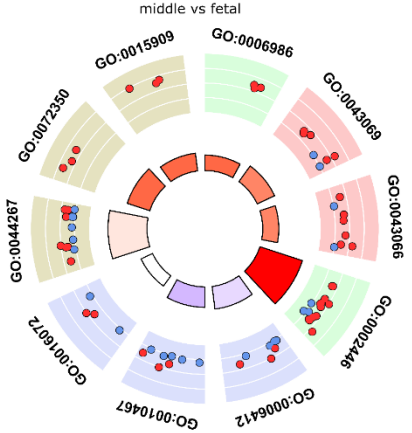












ID	Description
GO:0006986	response to unfolded protein
GO:0043069	negative regulation of programmed cell death
GO:0043066	negative regulation of apoptotic process
GO:1902175	regulation of oxidative stress-induced intrinsic apoptotic signaling pathway
GO:0006412	translation
GO:0000956	nuclear-transcribed mRNA catabolic process
GO:0010467	gene expression
GO:0043488	regulation of mRNA stability
GO:0010389	regulation of G2/M transition of mitotic cell cycle
GO:0007004	telomere maintenance via telomerase

ID	Description
GO:1903202	negative regulation of oxidative stress-induced cell death
GO:0062197	cellular response to chemical stress
GO:0034599	cellular response to oxidative stress
GO:0071731	response to nitric oxide
GO:0051289	protein homotetramerization
GO:0072350	tricarboxylic acid metabolic process
GO:0006094	gluconeogenesis
GO:0051156	glucose 6-phosphate metabolic process
GO:0007005	mitochondrion organization
GO:0000965	mitochondrial RNA 3'-end processing

ID	Description
GO:0006986	response to unfolded protein
GO:0043069	negative regulation of programmed cell death
GO:0043066	negative regulation of apoptotic process
GO:0002446	neutrophil mediated immunity
GO:0006412	translation
GO:0010467	gene expression
GO:0016072	rRNA metabolic process
GO:0044267	cellular protein metabolic process
GO:0072350	tricarboxylic acid metabolic process
GO:0015909	long-chain fatty acid transport

Figure 3.6 Senescence associated DEPs and their functional analysis. (A) Venn diagram of DEPs of maternal vs fetal, maternal vs middle, middle vs fetal, and proteins and genes associated with senescence functions and processes from the databases CellAge, CSGene, and NCBI database results for the keyword senescence. The section of proteins used for further analysis is within the red border. (B) GOCircle plots of the 10 most significantly overrepresented GO biological process terms, including senescence associated DEPs falling into each term. Regulation direction is colour coded: upregulated (red), downregulated (blue). Size of the inner segments is indicative of the number of proteins falling into each term. The colour of each inner segment indicates the z-score - general up or downregulation of the GO term considering the number up- and downregulated proteins.

3.4 Discussion

The placenta is a highly complex organ and crucial for embryo development, however molecular interactions and their association with pregnancy complications remain poorly understood [389, 390]. In this study, for the first time, the proteomic structure of healthy placentae was investigated. Three placentae from healthy uncomplicated pregnancies were sampled at five sample sites, and further categorised into three sub-anatomical regions. We ensured reproducibility by ensuring that the 5 identical cross sections collected from the placenta which were further divided into three sub-anatomical regions, represented approximate sub-anatomical regions, i.e., maternal, middle, and fetal through histopathological confirmation. Subsequent LFQ mass spectrometry analysis revealed distinct protein signatures of placental sub-anatomical regions. Resulting functional differences were characterized by functional analysis.

Based on the heterogeneity in senescent phenotypes identified in PE and IUGR in Chapter 2, in this chapter we wanted to explore mitochondrial, and senescence associated proteins in normal healthy placenta using a more in-depth proteomic approach. Mitochondria and senescence associated processes and functions such as, regulation of G2/M transition mitotic cell cycle, nitric oxide metabolism, and telomere maintenance are overrepresented in downregulated DEPs between maternal and middle sub-anatomical regions, indicating increased cell-cycle arrest of cells in the maternal sub-anatomical region compared with the middle sub-anatomical region. Additionally, proteins associated with glyoxylate metabolic processes were overrepresented in upregulated DEPs between middle and fetal

sub-anatomical regions, suggesting an age induced switch from glucose to fatty acids via the activation of glyoxylate cycle, as a source of energy [391]. A high number of DEPs were also associated with senescence, in part due to an overlap with mitochondria associated proteins. Interestingly both maternal versus fetal and maternal versus middle sub-anatomical region comparison indicate a decrease in senescence associated protein levels. Specifically, DEPs such as DEAD-Box Helicase 17 (DDX17), and heterogeneous nuclear ribonucleoprotein A1 (HNRNPA1), which differ between maternal and fetal sub-anatomical regions do not possess pro-senescent qualities but are protective against senescence [392, 393].

Similarly, the DEPs trifunctional enzyme subunit alpha and beta (HADHA) and (HADHB), 3-hydroxyacyl-CoA dehydrogenase type-2 (HSD17B10), and L-lactate dehydrogenase B chain (LHDB) are associated with senescence, mitochondrial dysfunction, and the beta-oxidation pathway [394, 395]. Downregulation of HADHA, HADHB, and HSD17B10 have been shown to induce mitochondrial dysfunction and senescence [396]. LHDB is involved in the conversion of pyruvate to (S)-lactate; its downregulation reduces mitochondrial function. Whereas the induction of LDHB expression causes enhanced mitochondrial function- including positive changes in mitochondrial respiratory subunits, mitochondrial membrane potential, ATP, NAD+/NADH ratio [397]. This indicates that the more senescent phenotype within the maternal sub-anatomical region is caused by the downregulation of mitochondrial proteins with anti-senescent properties.

The placentas collected are from term gestation (>37 weeks of gestation), hence the ageing changes seen in the maternal sub-anatomical region is more

physiologically rather than pathological. This hypothesis is also supplemented by lower ferritinophagy in the maternal sub-anatomical region. Ferritinophagy is a ferroptosis regulator and associated with iron-dependent regulated necrosis usually caused by massive lipid peroxidation-mediated membrane damage [398]. Moreover, we also report mitochondrial dysfunction in the form of glucose to lipid oxidation shift for energy production within the maternal sub-anatomical region compared to middle, or fetal sub-anatomical regions. This change can be indicative of change in trophoblastic microenvironment as a consequence of higher oxidative stress within this region [399].

Mitochondrial-related DEPs were predominantly down-regulated on the maternal side compared with the middle sub-anatomical regions, and predominantly upregulated proteins when comparing the middle with the fetal sub-anatomical region. The upregulated proteins in the middle versus fetal sub-anatomical region, included IDH1, IDH2, ALDH4A1 and PDHA1. Isocitrate dehydrogenases (IDH) protein 1 found in the cytosol, while IDH2 is found in mitochondria and converts isocitrate to alpha-ketoglutarate (α-KG) in the TCA cycle and production of NADPH [400]. Upregulated protein expression of IDH1 and IDH2 levels in the middle region compared to maternal or fetal regions, suggests a higher production of NADPH and higher mitochondrial activity in this sub-anatomical region. In fact, studies have shown that IDH2 in pregnancy is inversely related to pregnancy conditions such as IUGR and high maternal BMI [401, 402]. Superoxide dismutase 2 (SOD2), which is upregulated in the middle sub-anatomical region compared to the fetal sub-anatomical region, is an enzymatic antioxidant that regulates oxidative stress, lack of antioxidant defence can lead to increased oxidative stress which in turn can

damage cells, proteins, as well as DNA and accelerate aging. In pregnancy, this may lead to placental insufficiency linked to PE and IUGR [157, 249]. The increased expression of SOD2 along with IDH1, IDH2 indicate altered energy homeostasis and metabolism, along with antioxidant defence in the middle sub-anatomical region [403, 404].

Apurinic/apyrimidinic endodeoxyribonuclease 1 or APEX-1 is a multifunctional protein usually associated to DNA Damage Repair (DDR) functionality in cells experiencing oxidative insults [405]. Our results indicate that APEX-1 is downregulated in the middle sub-anatomical region compared to the fetal region. This might be indicative of higher oxidative stress experienced by this sub-anatomical region, causing telomere damage.

Independent analysis of unique proteins identified in placental sample sites revealed a myriad of proteins solely identified in one sample site E (Figure 3.1) before normalisation. These were filtered out when adjusted for consideration of sub-anatomical regions. Additionally, strong interaction between the effect of sample site and sub-anatomical region on LFQ protein intensity was shown. This suggests that the effect between sub-anatomical region on LFQ proteins intensity is not the same for all sample sites. This may have been caused by individual variations and the placenta not being geometrically oval and stresses the importance of sampling several placenta sites from the same patient and recruiting an increased study number to compensate for the extremely high individual variability of placental shapes, size, and structure [326, 407].

Our sample collection protocol has been based on recommendation detailed by Burton et al., 2014 where we selected five different sites across the placenta [326]. As our results show, there is minute variations across the different sampling sites, with one site in particular showcasing unique proteins. We, therefore, concur with published recommendation for proteomic analysis by including at least five sites while sampling for both qualitative and quantitative validity [326]. We also identified proteomic differences between sub-anatomical regions, which we recommend considering in future studies. However, we did not include fetal and maternal membranes for sub-anatomical proteomic analysis. Through our results, we demonstrate a variable protein composition between sub-anatomical regions, with higher senescence associated protein and upregulated translation and transcription proteins in maternal and middle compared to fetal sub-anatomical region, hence we conclude separating these regions for a robust placental analysis.

Traditional functional analysis techniques such as GO terms are not tissue specific but consider all biological processes and molecular functions present within the human body. Traditional functional analysis is unbiased. Although this is an advantage, in the context of placenta research, a more placenta focused approach is useful. The NaviCenta is a human and machine readable multiscale computational model. The NaviCenta consists of information regarding processes and cell interactions within the placenta, and of relevance to healthy placentation, including molecular interactions between proteins, RNA, and DNA, enriched with regulatory factors, such as transcription factors, miRNA, and lncRNA, which can be used for network-based analyses [377]. The NaviCenta enables network based *in silico* perturbations and the integration of log2FC, and p-value information. The

NaviCenta indicated deregulated apoptosis, non-apoptotic cell death, and cell proliferation associated phenotypes of endothelial cells in particular [378]. These have been shown to be governed by mitochondrial function [408] and are associated with a more senescent state [409].

3.5 Conclusion

This study provides a comprehensive proteomic assessment of separate sub-anatomical regions of healthy placentae, while allowing a specific insight into mitochondrial functioning and placental ageing. The proteome differences between placental sub-anatomical regions, referred to as maternal, middle, and fetal side, indicate cell senescence, mitochondrial dysfunction, and specifically activities of endothelial cells. Our results indicate a pronounced increase in senescence in both the maternal and middle sub-anatomical regions mediated by downregulation of proteins protective against senescence. Additionally, DEPs indicate a senescence associated switch from ATP to fatty acids as a source of energy in the placenta.

Chapter 4:

Characterisation of placental proteomic profile in Pre-eclampsia and IUGR

Abstract

Background: The placenta remains a key instigator of maternal adverse pregnancy outcomes such as Pre-eclampsia (PE) and Intrauterine growth restriction (IUGR), however the exact pathophysiology for both PE and IUGR remains elusive. The aim of this study was to characterize the key proteomic variations between PE and IUGR, to better understand these outcomes.

Methods: Placental tissue collected at term from nulliparous PE and IUGR affected pregnancies were matched for maternal age with healthy controls. Quadrupole-orbitrap mass spectrometer was used in data dependent analysis mode to identify differentially expressed proteins (DEP) between PE and IUGR. Functional analysis was conducted using Perseus, ClusterCompare, NaviCenta disease map and TriplexRNA database. A core regulatory network based on log2FC and rewiring scores including regulating miRNAs and transcription factors was constructed using Cytoscape DyNet.

Results: In total 314, 391, and 378 proteins were identified in healthy control, PE, and IUGR placenta, respectively. Venn diagram analysis revealed that 35 placental proteins were unique to PE, 17 placental proteins were unique to IUGR, and 3 placental proteins were unique to healthy controls. Further interrogation, by applying a log2FC >0.5 threshold, nine DEPs were identified between these adverse pregnancy outcomes. Functional analysis combining ClusterCompare and NaviCenta, showed that the identified regulatory elements are predominantly involved in the complement cascade and antioxidant activities. Our results further

highlight two RNA triplexes involved in the core regulatory module in PE and IUGR placentas, both targeting PSAP mRNA.

Conclusion: Our results identify new potential regulatory proteins in PE and IUGR pathology. The identified miRNA triplexes further open a novel avenue of investigation for placenta research.

4.1 Introduction

The placenta is the key organ orchestrating maternal and fetal well-being during pregnancy. Placental dysfunction has been associated with various adverse pregnancy outcomes including PE (PE) and intrauterine growth restriction (IUGR) [366, 413].

PE is defined as de novo hypertension after 20 weeks of gestation in presence of proteinuria and maternal organ/uteroplacental dysfunction [66]. PE has been associated with an increased risk of stillbirth, preterm births, and fetal growth restriction. Moreover, longitudinal studies have shown various chronic disease outcomes in both mother and baby affected by PE pregnancy [414, 415]. PE can occur with comorbidities such as hypertension, proteinuria and uteroplacental dysfunction, further challenging the determination of causative factors [416]. IUGR is defined as estimated fetal weight below 10th centile for gestational age [166].

Maternal risk factors contributing to IUGR include maternal malnutrition, smoking, drugs use during pregnancy, while more common fetal causes include malformations such as aneuploidy, uniparental disomy, single-gene mutations, partial deletions or duplications, ring chromosome, aberrant genomic imprinting, and trisomy of certain genes, and placental insufficiency [166, 417]. More recently, accelerated placental aging as a result of reduced blood flow and elevated oxidative stress has been associated with adverse pregnancy outcomes such as PE and IUGR. These oxidative insults are irreversible in nature and often lead to deleterious molecular dynamics [1, 371]. Yet, the exact pathophysiology of PE and IUGR remain poorly understood.

Understanding the underlying molecular pathways might provide insight into the variations between these adverse pregnancy outcomes [418]. Placental insufficiency as a result of improper maternal spiral artery remodelling due to persistent elevated oxidative stress (OS) and lack of antioxidant defence, have been implicated as the primary pathophysiology for both PE and IUGR [280]. Molecular regulators of placental growth and functionality such as insulin like growth factor acting AKT/mTOR pathway which regulate cell proliferation are downregulated in both IUGR and PE [418, 419]. Moreover, stress response pathways such as Unfolded Protein Response (UPR) has been implicated in both PE and IUGR [420]. However, a distinct feature of PE is the presence of a systemic inflammatory response indicating close contact between maternal immune cells and trophoblasts. Systemic inflammation is a major regulator in driving the pathology in PE and PE associated with IUGR, but not in pregnancies complicated with IUGR only [418, 421].

Stereologically, the main effects of placental morphology was not associated with PE whereas IUGR (with or without PE) has been associated with reduced volumes of placental intervillous space and villi, along with reduced exchange surface area and thickened trophoblast, which could be conclusive that these substantial alterations in placental morphology disrupts fetoplacental angiogenesis in IUGR but not in PE [422-424]. Previous studies have reported that the placenta in PE is usually characterized as smaller size, lower weight and overall thickness when compared to controls, additionally PE associated with IUGR are significantly lower weight and thickness of placenta compared with the group without IUGR [425, 426]. These histopathological characteristics would indicate that PE, PE associated to IUGR and IUGR are possibly three distinct pathogenetic entities.

The placental proteome has been used to improve our understanding of molecular mechanisms involved in the pathophysiology of placental disorders [427, 428]. Moreover, proteomics in association with other omics methodologies such as metabolomic and transcriptomic may provide a more integrated insight of disease aetiology, identify biomarkers to predict and diagnose pregnancy outcomes at early stages in pregnancy and ultimately improve overall maternal and neonatal health outcomes [429, 430].

To date, expression level studies primarily treat samples at hand as static systems. However, cells and tissues are highly dynamic. It is therefore crucial to identify and understand the governing regulatory network underlying each condition [431] . To that end, in this study we created networks including identified DEPs, regulatory miRNAs and transcription factors (TF) and focused on elements with the highest variance and rewiring, including integration of miRNA couples acting in synergy on the same mRNA target [432].

In this study, placental proteomics was used to evaluate the placental protein composition of PE and IUGR pregnancies, in consideration of sub-anatomical regions. These differences were then interpreted using a functional level leveraging systems biology approach, such as the placenta specific disease map NaviCenta [378].

4.2 Material and Methods:

4.2.1 Study Design

Participants (n=12) were recruited as part of the COMRADES Study, a non-interventional cohort study of nulliparous singleton pregnancies with the aim of characterizing placental premature senescence in PE (PE) and Intrauterine growth restriction (IUGR). Participants were recruited from Cork University Maternity Hospital, Ireland between 2020 and 2021. The COMRADES study was conducted according to the guidelines laid down in the Declaration of Helsinki. All procedures were approved by the Clinical Research Ethics Committee of the Cork Teaching (ECM4 (ff) 04/12/18), and all women provided written informed consent. After receiving consent, placental samples were collected from nulliparous, singleton pregnancies undergoing pre-labour Caesarean section, PE (n=4), IUGR (n=4) and healthy controls (n=4). The mean gestational age was matched as closely as possible for healthy controls (38 ± 0.9 weeks) and cases: PE (35 ± 3.4 weeks) and IUGR (35.5 ± 2.6 weeks) pregnancies. PE was defined according to ISSHP 2018 guidelines as de-novo hypertension with BP ≥140 mm Hg systolic or ≥90 mm Hg diastolic, after 20 weeks of gestation, associated with 3+ proteinuria or 2500mg/24 hours proteinuria[66]. IUGR was defined according to RCOG guidelines as an estimated fetal weight less than 10th centile for gestational age[166].

Placental tissue was dissected within 20 minutes of delivery, 5 tissue sections (2-4 cm diameter each) taken from identified regions (as in Chapter 3) across including the entire width from maternal to fetal surface of the placenta. All samples were snap frozen in liquid nitrogen and stored in -80°C .

4.2.2 Protein Extraction and Sample preparation

Proteomic samples were prepared and analysed according to standardised protocol described previously [428, 433]. Homogenised placental tissue (50 mg) in Tetraethylammonium bicarbonate (TEAB) buffer (Sigma-Aldrich, Ireland) were subjected to protein extraction in presence of Phosphatase inhibitor (PhosSTOP™, Roche, Ireland) and Protease Inhibitor (Roche, Ireland) and quantified using the BCA Assay (Pierce™ Thermo Fisher Scientific, USA). 50µg/50µl denatured protein samples, in presence of Rapigest (1%) solution (Waters, Ireland) samples were then treated with 200 mM Indole-3-acetic acid (IAA) solution (Sigma-Aldrich, Ireland) after reduction for 60 min at 60°C and incubated overnight at 37°C with 1:100 sequential grade Trypsin (Promega, MyBio, Ireland) for enzymatic digestion. 1% Formic Acid (Sigma-Aldrich, Ireland) was added to the samples to stop further protein digestion followed by centrifugation of the samples at 13,000 rpm for 10 mins and supernatant collected. The collected supernatant was then air dried on MiVac Quattro sample concentrator (Fisher Scientific, Sweden) and resuspended in 0.5% Formic Acid (FA) (Sigma-Aldrich, Ireland). Samples were then cleaned and desalinated using Zip-Tip columns with 0.6 µl binding volume C18 resin (Sigma-Aldrich, Ireland), described in detail previously [428]. An aliquot of quality control (QC) was prepared by pooling equal quantities from all samples, which was injected throughout mass spectrometry (MS) run for conditioning of the columns and efficient MS performance.

4.2.3 Mass Spectrometry

5µl of sample were injected onto the Thermo Scientific Q-Exactive® connected to a Dionex Ultimate 3000 High-performance Liquid Chromatography (HPLC) system at random, combined with internal standards for proteomic profile of PE and IUGR placentas when compared to controls. An increasing acetonitrile gradient (250 mL/min) was used to separate the peptides. Data Dependent Analysis (DDA) mode was used on the MS using a 12-mode with setting: mass range 300-1600Th; resolution for MS1 scan 70000; AGC target 3e6; resolution for MS2 scan 17500; AGC target 2e4; charge exclusion unassigned, 1; dynamic exclusion 40 s [433].

4.2.4 Bioinformatics and Statistical Analysis

LC-MS/MS raw files were uploaded to the MaxQuant (version 1.6.17) interface, where parameters were inputted for 'Match Between Runs' and "Label free quantification" (LFQ) [433, 434]. Samples with extremely low yields (<100 proteins) were excluded from each group to maintain data robustness. MaxQuant results were uploaded to Perseus (version 1.6.15.0). The overlap between proteins identified in samples per condition were visualized using InteracitVenn [383]. The data were filtered to remove contaminants. LFQ intensity data were processed via log2 transformation. To ensure reproducibility, results were filtered to include exclusively valid sample measurements in 100% of biological replicates, 70% of measurements per sub-anatomical region (as discussed in Chapter 3), and 70% measurements per condition. Measurements were then z-score normalized. Normalized LFQ intensity, considering correlation with internal standards, were used for differential expression analysis. Two-way ANOVA considering condition

and sub-anatomical region, with follow up single ANOVA with permutation-based FDR (0.05) and Tukey's HSD tests with FDR were performed [375, 435]. Significant results with an adjusted p-value < 0.05 were further filtered for a log2FC > | 0.5 |. Hierarchical Clustering was based on Euclidean distance with the default cluster number of 300.

4.2.5 Functional Analysis

Gene ontology (GO) term overrepresentation analysis was performed and visualized using the R (R Core Team (2022). R: A language and environment for statistical computing. R Foundation for Statistical Computing, Vienna, Austria. URL https://www.R-project.org/) package ClusterProfiler 4.0 [436, 437]. Additionally, placenta specific phenotype analysis was performed using the DMNaviCenta [378] (https://www.sbi.uni-rostock.de/minerva/index.xhtml?id=NaviCenta) and a DM phenotype plugin [379].

4.2.6 Regulatory module identification

The comparison between regulatory networks for each condition was constructed using identified DEPs. There is a strong evidence that MicroRNAs are responsible for the regulation of the genes of each DEP were obtained from miRTarBase v8.0 [438]. Transcription factors were obtained from TRRUST and transcription factor - miRNA interactions were obtained from TransmiR v2.0 [439, 440]. The interaction networks were visualized in Cytoscape v3.9.1. Once the networks were generated, Cytoscape plugin Dynet was used to compress the networks. Thus, all networks were visualized in one regulatory network. The network was overlaid with the rewiring and variance (between log2FC) scores [441]. MiRNA couples of miRNAs indicated in

the regulatory module acting on a DEP within the regulatory module were identified using the web interface of TriplexRNA database V2 (https://triplexrna.org/, accessed 2022.12.12). 2D structure visualization were also obtained from the TriplexRNA database [442]

4.3 Results

4.3.1 Study Demographics

Twelve participants were grouped as: PE (n=4), IUGR (<10th centile) (n=4) and maternal age-matched normotensive controls (n=4) as shown in Table 4.1. There were no significance differences in maternal age, maternal BMI, gestational age and mean arterial blood pressure (MAP) at 10-12 weeks between study groups. There was a non-significant increase in MAP at 20-24 weeks in the PE group when compared to normotensive controls. There was a significant decrease in mean birth weight for PE (p=0.017) and IUGR (p=0.02) study groups, compared to normotensive controls. Similarly, fetal individualized customized centile (ICC) was significantly reduced in the IUGR group (p=0.037) compared to normotensive controls.

Table 4.1 Patient demographics in study cohort. Data is represented as Mean ± SD. Mean Arterial Pressure has been calculated as MAP= [Systolic BP + (2 X Diastolic BP)]/3. Statistically Significant values have been denoted as ***** compared to controls with $p < 0.05$.

Type	Data	PE (n=4)	IUGR (n=4)	Control (n=4)
Maternal	Mean Age (years ± SD)	33.75 ± 1.5	32.5 ± 3	33.8 ± 2.16
	Mean BMI (kg/m^2 ± SD)	26.26 ± 4.7	25.95 ± 5.87	25.56 ± 4.9
	Mean Arterial Blood Pressure (mmHg) ± SD (10-12 weeks)	89.5 ± 6.9	93.7 ± 8.4	88.25 ± 7.04
	Mean Arterial Blood Pressure (mmHG) ± SD (20-24 weeks)	101.1 ± 18.1	81.3 ± 4	85.9 ± 8.1
	Mean Gestational Age at delivery (weeks ± SD)	35 ± 3.4	35.5 ± 2.6	38 ± 0.9
Fetal	Mean birth weight (grams ± SD)	1908 ± 553.1*	1955 ± 762.2*	3213 ± 230.6
	Fetal Sex (M=Male; F=Female)	F = 4 M = 0	F = 2 M = 2	F = 2 M = 2
	Fetal Individualized Customized Centile (± SD)	14.4 ± 25.3	4.55 ± 5*	42.63 ± 21.15

4.3.2 Proteome Profile of healthy, PE and IUGR placenta

The relative proteome profile of sub-anatomical regions of placental tissue from healthy, PE, and IUGR pregnancies, was measured using LFQ mass spectrometry. In total 314, 391, and 378 proteins were identified in normal, PE, and IUGR placental tissue samples respectively. Overlapping and unique proteins identified in each condition are shown in Figure 4.1. 35 placental proteins were unique to PE, 17 placental proteins were unique to IUGR, and 3 placental proteins were unique to healthy controls. 72 proteins were shared between PE and IUGR placentas with only 5 proteins shared between healthy and IUGR and 7 shared proteins between healthy and PE. There were 263 proteins common for all three phenotypes.

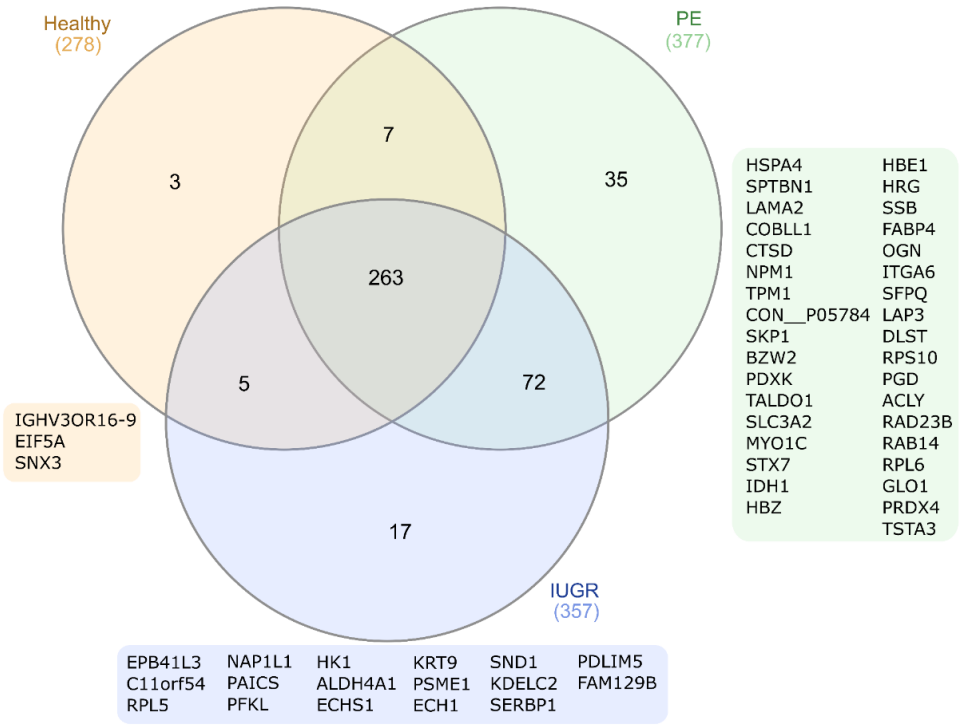


Figure 4.1 Venn diagram of proteins identified in placental tissue from normal, PE, and IUGR pregnancies. Proteins identified in exclusively one condition are listed next to their respective condition.

4.3.3 Functional analysis of protein profiles from healthy, PE and IUGR placenta

Further examination of biological functions of identified unique and shared proteins revealed that although unique proteins were identified between conditions, their biological functions fall into a similar group. Proteins uniquely identified in PE or IUGR and shared placental proteins between PE and IUGR are primarily involved in cell-cell adhesion, while additional shared proteins between PE and IUGR are also associated with ribosome rRNA binding, structural constituents of ribosome and chaperone binding. Proteins uniquely identified in healthy controls were associated with phosphatidylinositol's and translation elongation factor activity. Shared proteins identified in IUGR, and healthy samples are associated with immunoglobulin receptor binding and au-rich element-binding. Similarly, common

proteins identified in PE and healthy samples are associated with glycosaminoglycan binding, annealing and ribosomal small subunit binding (Figure 4.2).

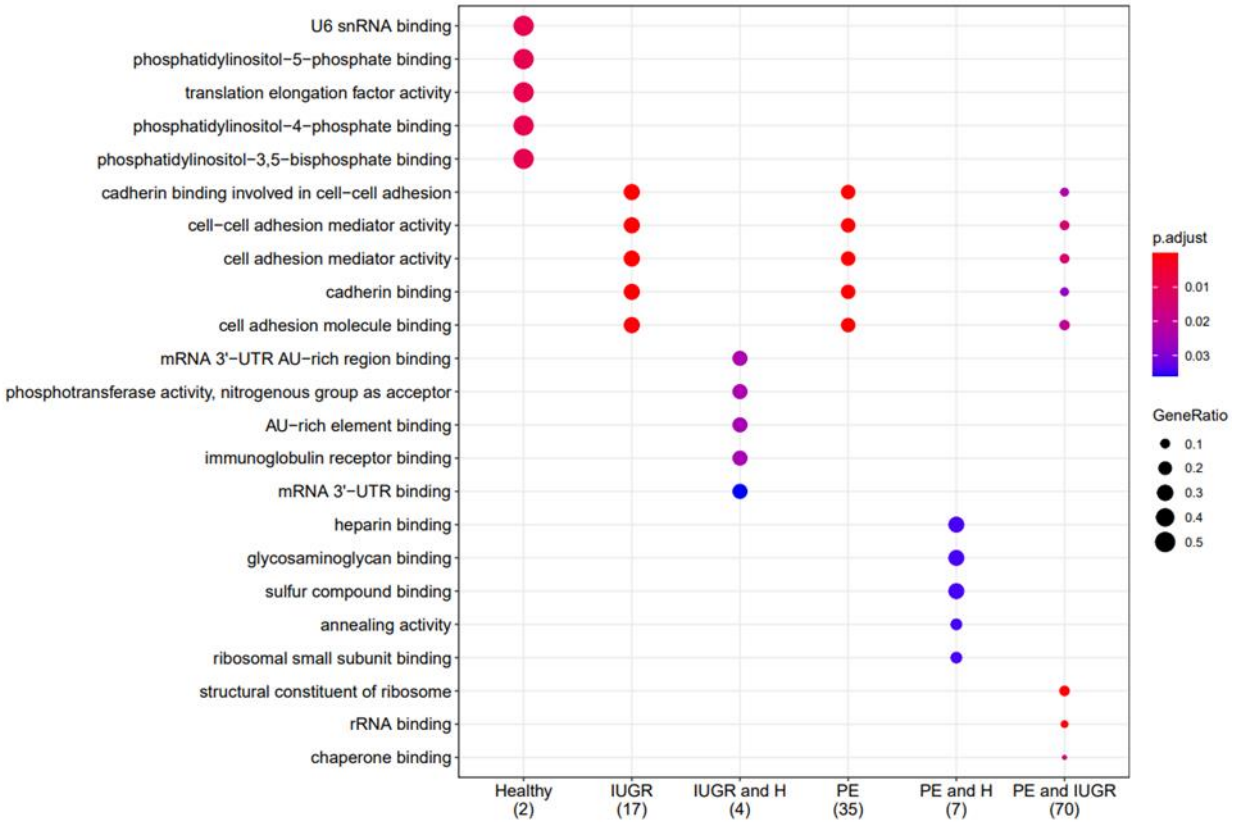


Figure 4.2 GO biological function analysis of placental proteins identified in PE, IUGR. Proteins were grouped as follows; unique to condition (Healthy, PE, IUGR) and shared combinations (PE and Healthy, IUGR and Healthy, PE and IUGR). The dot size indicated protein ratio (number of proteins versus number of all proteins associated per binding protein (BP) function).

4.3.4 Differentially expressed protein differences between healthy, PE, and IUGR

Further interrogation of DEP was performed using two-way ANOVA taking both condition and sub-anatomical regions in consideration. This analysis identified 60 DEP between conditions and 40 DEP between sub-anatomical regions. As some DEPs presented with high interaction between the condition and sub-anatomical region (p interaction < 0.05), additional one-way ANOVAs with post hoc Tukey's HSD test were conducted. Following this analysis, 18 out of 60 DEP remained significant between conditions while none of 40 DEP were significant between sub-anatomical regions. Results were further filtered according to 0.5 > log2FC < - 0.5. After this 9 out of 18 DEP remained between conditions (Figure 4.3, Table 2: DEPs between PE, IUGR, and normal placenta). Hierarchical clustering of DEP normalized LFQ intensities showed that after strict filtering and normalization of the data to support reproducibility, greater correlation exists between IUGR and PE proteins than between IUGR and healthy, or PE and healthy proteomic comparisons (Figure 4.3).

We further analysed for both upregulated and downregulated DEPs across study groups as shown in Table 2. Prosaposin (PSAP) is a glycoprotein which codes for saposins (p=0.046), fibronectin 1 (FN1) and Fibulin 1 (FBLN1) which are both extracellular matrix glycoproteins and Collagen type XIV alpha 1 chain (COL14A1) which is a fibril-associated collagen were significantly upregulated in PE placentas compared to controls (p=0.048, 0.015 and 0.017 respectively). Immune regulatory proteins, including Immunoglobulin Heavy Constant Gamma 4 protein (IGHG4) and Immunoglobulin heavy constant alpha 1 (IGHA1) were significantly downregulated

(p=0.004 and 0.015 respectively) in PE placentas. Additionally, mitochondrial proteins creatine kinase mitochondrial 1A (CKMT1A) and antioxidant haptoglobin (HP) were also significantly downregulated in PE placentas compared to controls (p=0.038 and 0.016 respectively). FBLN1 (p=0.015) and PSAP (p=0,046) were also significantly upregulated in IUGR placentas. Amine oxidase copper containing 1 (AOC1), which is involved in metabolism and oxidation (p=0.016), HP (p=0.016) and IGHA1 (p=0.014) were significantly downregulated in IUGR compared to control placentas.

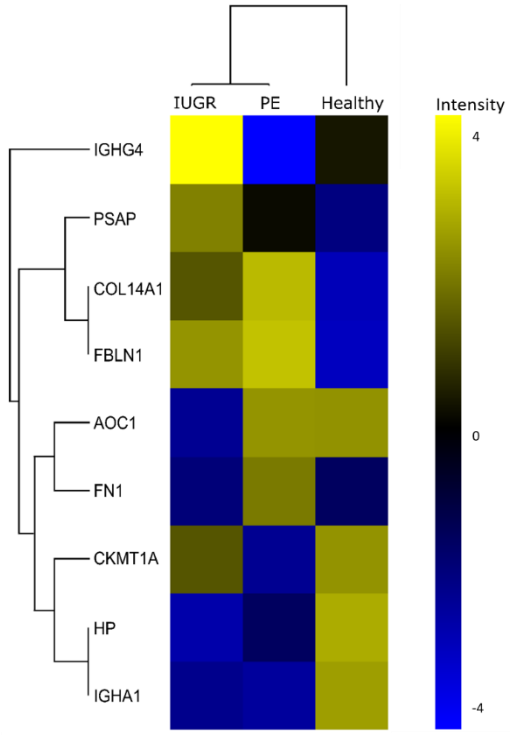


Figure 4.3 Clustered heatmap of normalized LFQ intensities of DEPs between PE, IUGR, and healthy placentas.

Table 4.2 DEPs between PE, IUGR, and healthy placentas. The comparisons include PE vs normal, IUGR vs normal, and IUGR vs PE. DEP are defined as adj p < 0.05 and log2FC > 0.5 and < - 0.5.

	PE vs Normal	log2FC	Adj p-val	**IUGR vs Normal**	log2FC	Adj p-val	**IUGR vs PE**	log2FC	Adj p-val
Up	PSAP, FN1, FBLN1, COL14A1	0.57 0.80 0.87 0.53	0.046 0.048 0.015 0.017	FBLN1, PSAP	0.73 0.67	0.015 0.046	CKMT1A, IGHG4	0.56 1.08	0.038 0.004
Down	IGHG4, IGHA1, CKMT1A, HP	-0.92 -0.65 -0.79 -0.59	0.004 0.015 0.038 0.016	HP, AOC1, IGHA1	-0.84 -0.71 -0.61	0.016 0.016 0.014	FN1, AOC1	-0.92 -0.72	0.048 0.016

4.3.5 Functional Analyses of DEP between healthy, PE, and IUGR

To advance our understanding of differences between IUGR, PE, and healthy placental tissue, functional analysis based on associated DEPs, was conducted. DEPs of PE, IUGR and healthy placentas were directly compared using the R packages compareCluster and enrichGO. As there is overlap between up and downregulated DEPs, functional comparison was performed additionally considering the direction of fold change (FC).

GO biological process functional analysis revealed 20 significantly (adj p < 0.001) overrepresented GO terms (Figure 4.4). Antigen binding, chemotaxis and antioxidant activity were downregulated in both PE and IUGR compared with healthy placentas. Placenta specific phenotype prediction showed the proteins

found in PE placentas indicate decreased functionality of antigen clearance, complement cascade, chemotaxis, and inflammatory response compared to normal placentas. Antigen clearance has also been indicated to be decreased in IUGR compared to healthy placentas. We used both CompareCluster and NaviCenta platforms for similar functional group and decided to focus on the overlap in functionality to highlight DEPs of importance (Figure 4.5). Both functional analyses revealed overrepresented terms associated with antioxidant activity such as oxidoreductase activity, actin on the CH-NH2 group of donors and oxygen acceptor, oxidoreductase activity acting on the CH-NH2 group of donors with the DEPs HP and AOC1.

Table 4.3 NaviCenta differential phenotype prediction based on DEP including ad. P value < 0.05 between conditions.

Phenotype	**PE vs Normal**	Adj pval	**IUGR vs Normal**	Adj pval	**IUGR vs PE**	Adj pval
antigen clearance	-0.65 IGHA1	2.38E-42	-0.61	2.38E-42	0	1
complement cascade	-0.92 iGHG4	4.77E-07	0	1	1	1
chemotaxis	-0.92 IGHG4	6.09E-07	0	1	1	1
inflammatory response	-0.49 IGHG4	0.015299	0	1	0.54	1

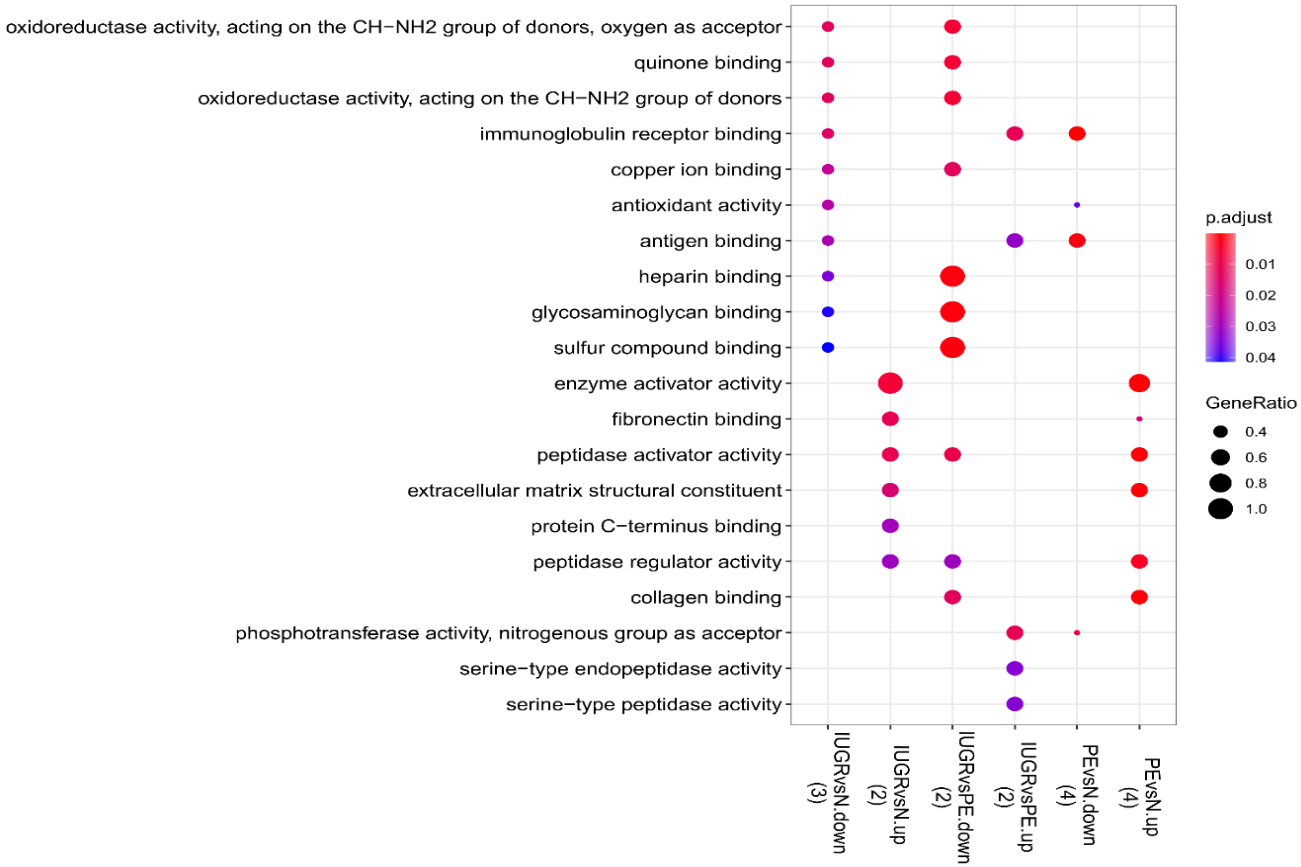


Figure 4.4 DEGs analysis and GO biological function annotation in PE, IUGR and healthy placentas. Up- and downregulation were considered. Dots colour indicated the significance of the enrichment. The dot size indicated protein ration (number of DEPs against number of all proteins associated per BP function).

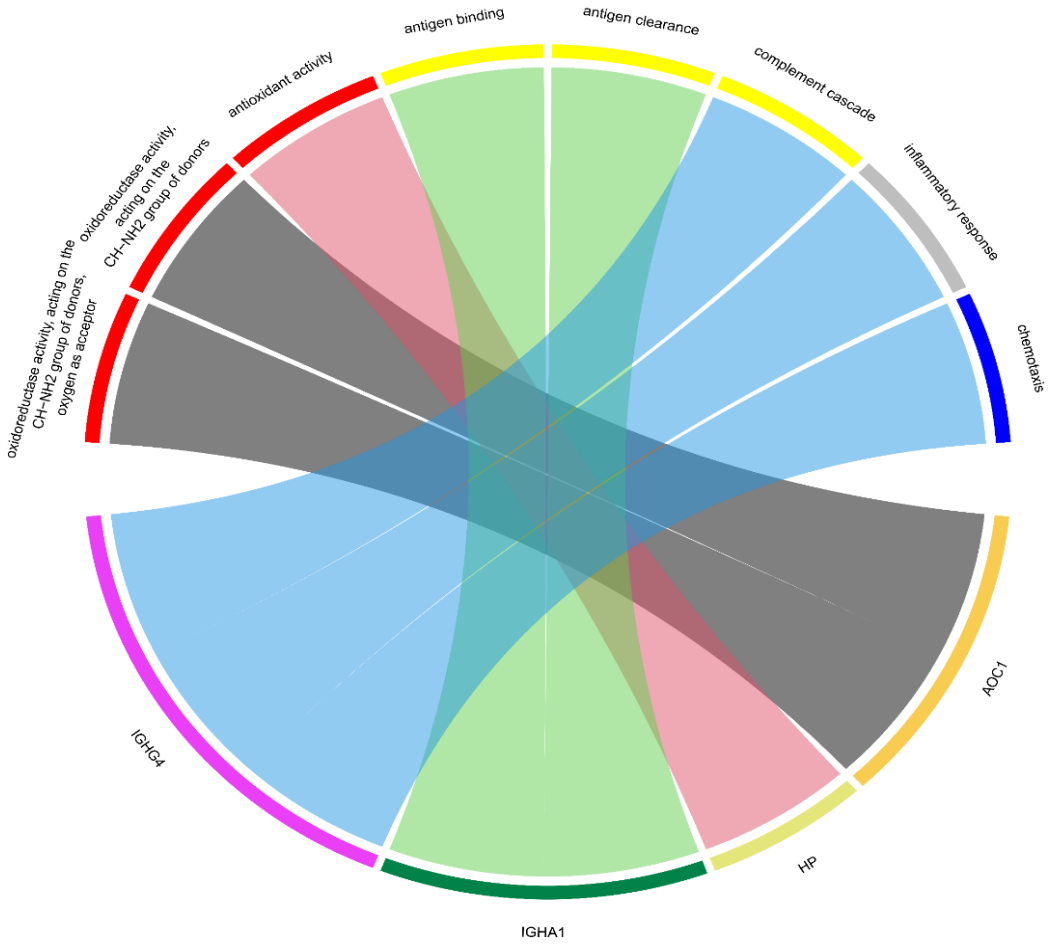


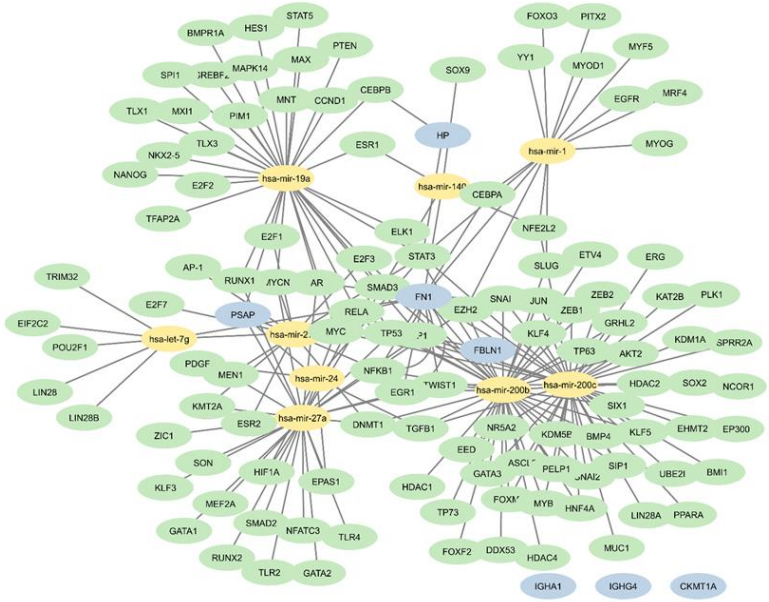
Figure 4.5 Overrepresented GO terms, overlapping with NaviCenta phenotype prediction results including DEPs falling into these terms. Antioxidant associated terms contain red bars, complement cascade associated terms contain yellow bars. Chords are coloured according to the protein.

4.2.6 Regulatory Motifs of dysregulated Proteins in PE and IUGR and healthy placentas

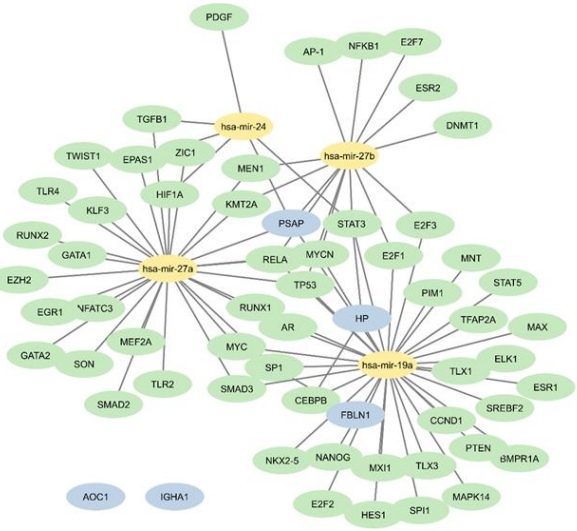
Network inference enables the transformation of OMICs data into biological knowledge. Reverse engineering of gene regulatory networks from i.e. proteomics data allows the identification of regulatory elements responsible for the resulting proteomics phenotype [443]. To this end the regulatory networks of dysregulated proteins were constructed (Figure 4.6 A-C, including all DEPs, miRNAs, TFs). To enable a direct comparison of networks, the regulatory networks, including log2FC were condensed using DyNet (Figure 4.6 D) [441]. The elements in the condensed network were filtered to contain only elements with a rewiring score higher than 0.5 or a variance score higher than 0.4. The rewiring score is based on node attributes which infers that elements with a high rewiring score either do not exist in all original regulatory networks, or contain different edges i.e., do not connect to the same nodes in all original regulatory networks. Given the high number of elements within the original regulatory networks, this makes the identification of core regulatory elements more intuitive.

The DEPs indicated by rewiring scores are HP, PSAP, and FN1. AOC1, although not indicated by rewiring score, shows a high variance score. Other regulatory elements are the miRNAs hsa-mir-27a, hsa-mir-19a, hsa-mir-27b, hsa-mir-24, hsa-let-7g, hsa-mir-140, hsa-mir-200c, hsa-mir-1, and hsa-mir-200b. Furthermore, TFs AR, MYC, SMAD3, SP1, TWIST1, FNE2L2, EZH2, SLUG, SNAI1, TGFB1, EGR1, STAT3, NFKB1, TP53, E2F3, RELA, and MYCN remain in the core regulatory network.

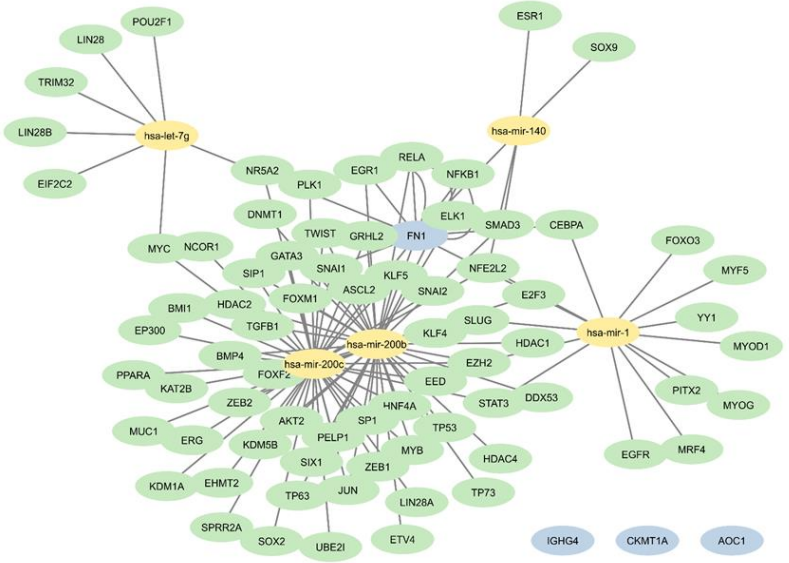
PE vs N



IUGR vs N



IUGR vs PE



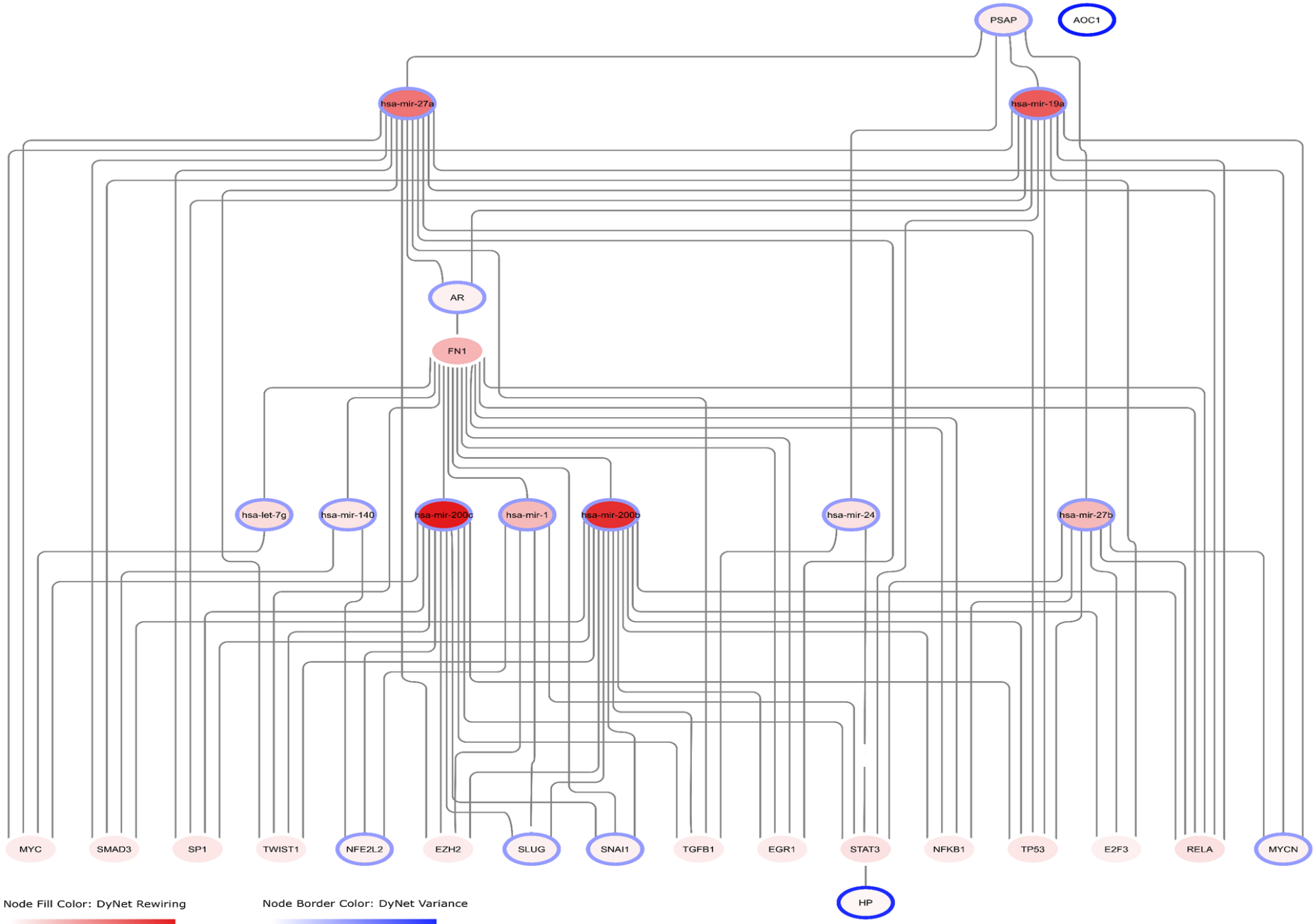

PSAP
AOC1
hsa-mir-27a
hsa-mir-19a
AR
FN1
hsa-let-7g
hsa-mir-140
hsa-mir-200c
hsa-mir-1
hsa-mir-200b
hsa-mir-24
hsa-mir-27b
MYC
SMAD3
SP1
TWIST1
NFE2L2
EZH2
SLUG
SNAI1
TGFB1
EGR1
STAT3
NFKB1
TP53
E2F3
RELA
MYCN
HP
Node Fill Color: DyNet Rewiring
0.00
15.30
Node Border Color: DyNet Variance
0.00
0.76

Figure 4.6 Interaction networks of dysregulated Proteins including TFs and miRNAs regulating their genes. Interaction network of DEPs identified in PE vs N (A). Interaction network of DEPs identified in IUGR vs N (B). Interaction network of DEPs identified in IUGR vs PE (C). Blue: DEP, green: TF, yellow: miRNA. Interactions are shown as lines. The networks were condensed into a dynamic molecular interaction network (D). FC variance is indicated as node border colour. Node rewiring degree is shown as node colour.

Finally, we further analysed the core regulatory network for involvement of triplexes, miRNA couples acting on a common DEP gene target and resulting in an increased inhibitory effect, using the TriplexRNA database. We identified two triplexes, working on the same target PSAP (Figure 4.7).

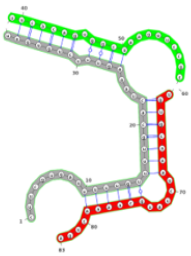
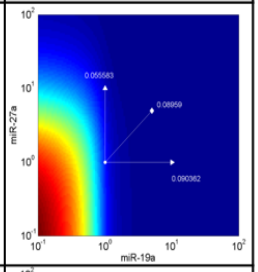
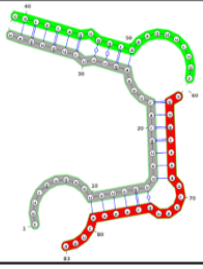
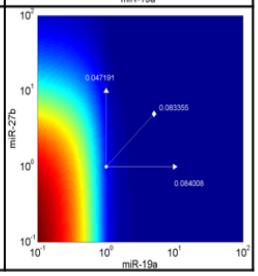
Gene	Details		2D Structure	Target respression simulation
PSAP	miRNA 1: miRNA 2: Triplex ID: Free energy (Kcal/mol): Energy gain (Kcal/mol): Pattern:	hsa-mir-19a hsa-mir-27a 134612 -26.26 -11.08 canonical triplex		
PSAP	miRNA 1: miRNA 2: Triplex ID: Free energy (Kcal/mol): Energy gain (Kcal/mol): Pattern:	hsa-mir-19a hsa-mir-27b 134613 -26.26 -11.08 canonical triplex		

Figure 4.7 RNA triplexes involved in the core regulatory network including DEPs and miRNAs. 2D structure is shown in the third column, with miRNA1 in red, miRNA2 in green, and target mRNA (of DEP) in grey. Target repression simulation is shown in column four.

4.4 Discussion

PE and IUGR share some similar pathophysiological features, wherein placental development is abnormal due to lack of trophoblast invasion of the maternal spiral artery and failure to establish adequate blood flow to the fetus [444]. The distinction of pathophysiological mechanisms responsible for specific placental diseases remains challenging due to limited studies, but also common comorbidities [445]. Even though PE and IUGR share similarities in their predispositions and pathophysiology, the main difference between the two disorders is that PE has higher degree of endothelial dysfunction, inflammation and metabolic dysregulation [444]. This study characterised the placental proteomic variations and similarities in PE and IUGR pregnancies. Although this study excluded pregnancies with comorbidities, unsurprisingly, placental proteomic phenotypes of PE and IUGR aligned closely compared with healthy placentas. Our results show that 72 proteins are shared between PE and IUGR, confirming that these diseases share a common pathophysiological origin, while 17 unique proteins were identified in IUGR and 35 unique proteins were identified in PE.

Interestingly, although there were specific protein differences between PE and IUGR, functional analysis of both unique and shared proteins in PE and IUGR fall into the same categories. Proteins uniquely identified in either PE or IUGR, and shared between PE and IUGR placentas, are primarily involved in cell-cell adhesion. Additionally, some shared proteins between PE and IUGR are also associated with the ribosome function (rRNA binding, structural constituent of ribosome, chaperone binding). Impaired cell-cell adhesion can lead to abnormal placental

development [446] and has previously been shown to be a pathogenic factor in PE [447]. These findings indicate that the same biological processes are altered in PE and IUGR, albeit in different ways on a molecular level. Additionally both post-transcriptional modification and post-translational mechanisms such as AU-rich element binding [448], phosphatidylinositol binding [449], ribosomal small subunit binding, translation elongation factor activity [450], and annealing [451] differ between conditions.

Placental DEPs included mitochondrial creatine kinase (CKMT1A) and immunoglobulin heavy constant gamma 4 (IGHG4) were upregulated in IUGR compared to PE, while fibronectin 1 (FN1), and Amine Oxidase Copper Containing 1 (AOC1) were downregulated in IUGR compared to PE placentas. IGHG4 is a part of the IgG4 complex and is transported across the placenta to the fetus [452]. It has been previously identified to be deregulated in plasma and other bodily secretions in women with PE [453]. Furthermore, IGHG4 gene and protein expression has been shown to be downregulated in PE and upregulated in IUGR human decidua [454]. IgG4 has been shown to have various immuno-regulatory effects, both directly pathogenic while also being protective against inflammation [455]. CKMT1A is responsible for the transfer of energy across mitochondria membrane by transferring phosphate groups from mitochondrial ATP to creatine [456]. Increased expression of CKMT1A has been associated with various cancers; however, in this study it was downregulated in PE compared to healthy placentas, while significantly upregulated in IUGR in comparison to PE placentas. This indicates reduced expression of CKMT1A expression maybe specific to PE. Although CKMT1A has not previously been associated with placental diseases, it has been shown to negatively

affect cell migration [456, 457]. Moreover, the association of mitochondrial dysfunction with PE as a result of damage to mitochondrial membranes and mtDNA due to the persistent presence of high OS have previously being reported [280]. Our results here showing significant downregulation of mitochondrial creatine kinase CKMT1A in PE compared to controls might suggest mitochondrial damage and induction of apoptosis[458]. Conversely there was a significant upregulation of CKMT1A in IUGR compared to healthy placentas. Upregulation of CKMT1A has been frequently associated with breast and cervical cancers, ensuring survival of cells through the generation of increased ATP and tumor growth [459]. Nevertheless, deregulation of CKMT1A in both PE and IUGR suggest altered cellular metabolism in these adverse pregnancy outcomes and requires further investigation.

FN1 and AOC1 were downregulated in IUGR compared to PE placentas. Fibronectin 1 (FN1) protein encodes a glycoprotein present within both cellular plasma and cell membrane [460] and influences a myriad of functions including cellular migration, adhesion, proliferations as well as wound healing, blood coagulation and host defence [460]. As previously discussed, FN1 has been shown to be significantly upregulated in PE placentas and has previously shown to be unaffected in IUGR pregnancies [461]. Overexpression of FN1 is commonly associated with cancer progression and expression of FN1 has been shown to be regulated by natural killer (NK) cell [462]. NK cells have been found to be regulator of normal placental development and maintenance of pregnancy, with presence of NK cells being significantly elevated in maternal circulation in pregnant women compared to non-pregnant women [463].

AOC1 protein is a metal-binding membrane glycoprotein, also associated with multiple cancers, promoting cellular proliferation and tumor progression [465]. Although AOC1 has been shown to be dysregulated in PE in previous studies on a transcriptomic level [466], in this study we found significant downregulation of AOC1 in IUGR when compared to healthy placentas. Downregulation of AOC1 in IUGR placentas maybe associated with inhibition of cell proliferation and induction of apoptosis, features often associated with placental pathology in IUGR [363, 467]. This study proposes that FN1 and AOC1 are candidate biomarkers to distinguish between PE and IUGR.

Functional analysis of proteomic data identified that the significant elevation of DEPs IGHG4 and IGHA1 are associated with an inflammatory response, specifically the complement cascade and antigen binding and clearance. These DEPs are over-represented in PE and IUGR when compared to controls, whereas chemotaxis is overrepresented when comparing IUGR with PE. These indicated functionalities have been shown to interact with each other under pathological and/or physiological conditions [468]. Complement activation in the placenta is hypothesized to be related to inflammatory events within trophoblasts, as a consequence of deficient placental angiogenesis [469].

Major histopathological complexes or MHC molecules are essential immune mediators involved in detecting self and non-self-antigens. The human fetus is 50% allogeneic, hence, maternal cells need to be immunologically tolerant for optimum fetal development. In healthy pregnancy, T-cells and NK Cells play a coordinated role in spiral artery remodelling, prevention of infections and maintenance of

maternal-fetal immunological tolerance [470]. Antigen binding by MHC complexes is thought to be dysregulated in PE pregnancies resulting in improper maternal artery remodelling, creating a state of placental hypoxia that might result in activation of complement cascade [471]. Within the endothelium, complement activation can result in a loss of vascular homeostasis, creating a pro-inflammatory state via altering cytokine activity [468]. Miao et al., showed differences in the complement system, cell adhesion, and ribosomal functions in PE placenta [475]. The association of complement system in PE has also been associated with both Stage 1 and Stage 2 of Redman's model, contributing to placental malformation and presentation of maternal clinical symptoms [480]. Endothelial dysfunction as a result of placental inflammation may contribute to further increases in activity of the placental complement cascade in PE [480, 481]. Our results are in accordance with previously published data, illustrating the role of antigen binding, activation of complement cascade and a resultant inflammatory response, in both PE and IUGR phenotypes, when compared to healthy controls.

Our results indicate significant upregulation in Prosaposin (PSAP) in PE and IUGR placentas when compared to healthy controls. PSAP is a glycoprotein which encodes saposins (A to D) which are involved in the metabolism of various sphingolipids through the activation of several lysosomal hydrolases [483]. PSAP has been shown to inhibit both Mammalian target of rapamycin (mTOR) and Sphingosine Kinase 1 (SK1) pathways [474, 484]. mTOR has been shown to regulate cell growth and proliferation, acting through the PTEN/AKT pathway [485], whereas sphingolipids have opposing effects and are associated with apoptosis, oxidative stress, angiogenesis and autophagy [486]. Elevated placental PSAP has previously been

associated with early onset PE [487]. In a recent circulating miRNA study, PSAP was overrepresented in the target gene with shared DEmiRNA associated with PE [488]. We report significant upregulation of PSAP in PE and IUGR when compared to healthy placenta. We can hypothesize that the significant increase in placental PSAP in PE, may be resultant of elevated levels of sphingolipids , which has been commonly associated in metabolomics studies of PE and IUGR pregnancies, and may have pathophysiological role in part by contributing to defective placental angiogenesis [486, 489]. PSAP has also been identified as a novel marker of cellular senescence, with upregulation of PSAP evident in hydrogen peroxide associated premature cellular senescence [490, 491]. This is in line with our data from Chapter 2 [363]. None of the identified DEPs, apart from FN1, are official biomarkers for PE, or IUGR (https://www.disgenet.org/; accessed on 19-March-2023) [482].

Most miRNAs and TFs identified within the core regulatory network have previously been associated with either PE and/or IUGR [492, 493]. The exact function of these miRNAs in the context of placental function, in particular molecular changes due to miRNA treatment are yet to be fully investigated. TFs were not shown to be differentially expressed in this study. However, TFs can be regulated not only at a concentration level, but also on an activity level. TF activity is often regulated by phosphorylation meaning TF activity can be altered without any change in TF abundance [494]. TFs are the most direct regulators of gene transcription and therefore not to be neglected within the regulatory core. In fact, some of the identified TFs such as nuclear factor, erythroid 2 like 2 (NFE2L2) have previously been demonstrated to have placental differential activity in pregnancy complications [495, 496]. Other TFs such as nuclear factor-kappa B (NF-κB) activation

within trophoblast-like cell line as a result of OS has been associated with PE [497]. Recent research has suggested that altered DNAm in HIF1α and HIF3α in PE placentas and correlation of DNAm in HIF1α and its expression, might suggests a possible role of interactions between HIF1α and HIF3α in the pathogenesis of PE [498].

Our results highlight two RNA triplexes involved in the core regulatory module in PE and IUGR placentas, both targeting PSAP mRNA. hsa-miR-19a has previously been shown to be downregulated in placental tissue in PE [499], while there is no current evidence for either hsa-miR-27a nor hsa-miR-27b in placental tissue. However, hsa-miR-27b has been shown to be increased in maternal blood plasma of PE and IUGR women [500]. Hsa-miR-27a has been shown to inhibit trophoblast cell migration and invasion *in vitro* [500].

The main study limitation was our small sample size which might impact the DEPs expression in PE and IUGR phenotypes and overall conclusions. The small sample size was due to strict study design for participant recruitment, including nulliparous pregnancies, matching gestational age as closely as possible. Any pathologies or fetal abnormalities associated with any pregnancy were also excluded. This was also a single site study with Irish-Caucasian population, thereby limiting the extrapolation of our findings to other ethnicities. The main strengths of this study were the computational biology approach which included NaviCenta, which provided a placenta specific phenotype prediction, while considering protein fold change, which the general functional analysis was integrated into, enabling a more meaningful and intuitive interpretation of results. Furthermore, regulatory gene networks can be used to investigate the underlying molecular mechanisms of

conditions. In this study, DEPs identified between healthy, PE, and IUGR placentas were used to start the regulatory network in Cytoscape V3.9.1 [503]. Subsequently, miRNAs regulating the transcription of their respective genes were recovered from miRTarBase V8.0 [438], and associated transcription factors of each miRNA were recovered from TransmiR v2.0 [504]. Finally, interactions between identified transcription factors with genes of interest were recovered from TRRUST V2 [439].

Finally, this study highlights several new research directions. In particular, synergistically working miRNAs acting on a single mRNA have not been previously explored in placenta research. TFs identified in the core regulatory network for PE and IUGR warrant further interrogation. The constructed core regulatory network serves as template for further research into the exact molecular mechanisms leading to PE and IUGR.

4.5 Conclusion

This study provides a comprehensive placental proteomic assessment of healthy, IUGR, and PE pregnancies, identifying the importance of complement system, inflammatory response, and antioxidant activity in placental function. Differences in proteomic profiles based solely on identified proteins between conditions further indicate deregulated proteins involved in cell-adhesion and post-translational and post-transcriptional modifications We additionally identified novel targets for further research such as transcription factor activity and synergistic miRNAs of elements within the core regulatory network in the context of PE and IUGR.

Chapter 5:

General Discussion

5.1 Overview and Interpretations of key findings

The placenta is a complex transient organ that acts as an interface between the mother and fetus during pregnancy, serving as focal points for exchange of gases, nutrients, immunoglobulins and hormones for the growth and development of the fetus [196]. The human placenta is a unique organ with a lifespan equal to the length of human pregnancy, goes through various transformations though its lifetime to facilitate and maintain the pregnancy and development of the fetus [89]. The placenta is formed of the maternal component comprising of the endometrium that transforms into the decidua and incorporated into the basal plate of the placenta [88, 364]. The fetal part of the placenta is formed of trophoblast cells, and is responsible for remodelling of maternal spiral arteries to establish maternal – fetal circulation, as well as acting as an endocrine organ to alter the maternal metabolism in order to meet the metabolic demands for the fetus [88]. In Chapter 1 this thesis highlights the important role of placenta in pregnancy and establishes how placental insufficiency contributes to the pathophysiology of adverse pregnancy outcomes such as PE and IUGR.

During the early stages of the pregnancy, the placenta and fetus coexists in a hypoxic condition, which controls the amount of maternal blood entering the organ [99]. In adverse pregnancy outcomes such as PE, elevated OS at end of first trimester leads to shallow placentation and failure to establish sufficient pO_2 uptake by the organ which results in hypoxia-reoxygenation of placental cells [99]. Moreover, the presence of systemic inflammation and maternal multi-organ dysfunction including endothelial dysfunction, and generalized vasoconstriction, is a consequence of

exposure to the shedding placental trophoblasts [99]. Contrarily, in IUGR, the growth of the fetus is restricted as a result of increased OS and lack of proper placentation limits the damage to the placenta and the fetus without systemic maternal disturbances [422]. Various studies have also reported that alterations in placental villous and capillary surface area is more characteristic of IUGR than PE [422-424]. However, trophoblast shedding in the form of aponecrosis and loss of membrane-bound fragments and microparticles are higher in PE compared to IUGR [422]. Elevated OS is associated with both PE and IUGR, however, differences in morphological villous diffusion raises the possibility of either fetal hypoxia or uteroplacental hypoxia which is possibly distorted by confounding pathophysiological factors [422].

This thesis strives to understand the variations between PE and IUGR complicated pregnancies through the assessment of placental senescence status in these adverse pregnancy outcomes. Additionally, in this thesis we have added further evidence of these differential features through proteomic variability in healthy pregnancy contrasted to adverse pregnancy outcomes. In Chapter 2 we evaluated the molecular signatures of cellular senescence in PE, PE associated with IUGR and IUGR phenotypes compared to control pregnancies. In Chapter 3, we aimed to identify the protein composition of a normal healthy placenta and characterise compositional differences related to placental ageing between the maternal and fetal sub anatomical regions. Finally in Chapter 4, we mapped the dynamic and functional pathways and interaction networks of differentially expressed placental proteins associated with immune regulation and cellular senescence in PE & IUGR compared to healthy controls.

In Chapter 2 we focused on evaluating a number of previously defined biomarkers of cellular senescence to determine if premature cellular senescence was evident in pregnancies complicated with PE, IUGR or PE and IUGR. Premature cellular senescence is defined as a state of terminal proliferation mediated in part by altered cell cycle kinetics and accompanied by characteristic metabolic and pro-inflammatory changes. Initially we provided evidence of a significant decrease in senescence associated genes ATM, CCNB-1, PCNA and TBX2 in IUGR placentas, and significant increase in maternal circulating Interferon-γ levels when compared to controls. Downregulation of these genes which are associated with DNA metabolism, DNA damage repair (DDR) and cell cycle arrest are frequently associated with senile changes within a cell [507-509]. Additionally, TBX-2 is frequently increased in proliferating cells and increases resistance to apoptotic stimuli and inhibits senescence in certain cancer types. In IUGR the reduction in expression of the TBX-2 transcription factor indicates a halt in cellular proliferation and induction of a more senile phenotype[510, 511]. Increased circulating levels of IFN-γ secretion have previously been linked to cellular senescence acting via p53 dependant pathway and DNA damage signalling pathway [361, 512].

Our results showed no significant difference in p21 and p16 levels in IUGR placentas when compared to controls. Cell cycle arrest is induced by p53 through binding to CDK inhibitor gene p21, p53/p21WAF1 activated in response to DNA damage caused by telomere attrition and DDR signalling leads to cellular senescence [513]. In a transient stress condition there is induction of p53 gene which allows the cells to continue proliferation, however in persistent altered redox conditions, p53 acts as pro-oxidative gene worsening the condition and leading to cellular death [514].

Moreover, our results failed to show significant attrition of absolute telomere length in IUGR placentas compared to healthy placentas. From the evidence in Chapter 2, we can conclude that premature cellular senescence is a pathophysiological feature of this adverse pregnancy outcome. More in-depth research is required to understand the molecular pathways involved in causing placental senescence in IUGR placentas.

In our PE study group, we reported a significant increase in placental expression of CHEK-1, CCNB-1, PCNA, CDKN2A and PTEN accompanied by a significant reduction in p16 protein expression, and a significant increase in maternal circulating IL-6 levels in PE compared to the control group. In contrast to IUGR, these mediators are more consistent with cellular proliferation and cell survival phenotype rather than a senile phenotype in PE affected placentas [319-322, 343, 348]. Additionally, we quantified Lamin-B1, a nuclear lamin, a structural protein involved in senescence through the SA-β-Gal pathway activation and SASPs accumulation [353]. Placental Lamin-B1 level showed no significant differences in all groups compared to controls. Similarly, we failed to see association of placental mtDNA copy numbers or absolute telomere length in all study groups compared to controls, which indicated that an alternative signalling might be causative of accelerated cellular senescence. The stark difference in cell survival between PE and IUGR placentas might be key to understanding the specific differences in pathophysiology of these pregnancy complications. Somewhat surprisingly, the key phenotypic indicators identified in PE or IUGR were not reflected in pregnancies where PE is also complicated with IUGR. This equally suggests that this PE subtype has a unique pathophysiology compared to both PE and IUGR presented in isolation. Research by Srinivas et al.,

evaluating differences between PE and IUGR, and the dependence of maternal hypertension, summarized that development of IUGR is independent of PE onset [515]. They outlined that chronic maternal hypertension and other co-morbid maternal factors such as obesity, diabetes, might be drivers for development of PE associated with IUGR compared to the development of PE or IUGR alone [515]. Malnourishment and low BMI before and during pregnancy are an underlying maternal factor frequently associated with IUGR [516].

In Chapter 2, even though there were no significant variations in maternal BMI across study groups compared to controls, maternal BMI was higher in PE only, following the earlier trend [517, 518]. Moreover, mothers affected by PE have been linked with cardiovascular diseases and hypertension later in life [415, 519]. The difference in pathophysiology in the three distinct phenotypes for PE, PE associated IUGR and IUGR might be linked to maternal factors such as genetics, socio-economic and lifestyle. Further larger studies with additional clinical descriptions are required to intrinsically evaluate cellular aging markers and provide a deeper understanding of senescence profiles and associated pathways in these adverse pregnancy outcomes.

In Chapter 3 we investigated the placental proteomic composition of healthy uncomplicated pregnancies to determine if normal physiological placental ageing is evident in these placental tissues. We further divided the placental sections into three sub anatomical regions: maternal, middle, and fetal to explore the variation between the maternal and fetal surfaces of the placenta. We observed no significant variabilities in protein abundance between sub-anatomical regions,

however functional analysis of placental sub-anatomical regions and sample site proteome showed a myriad of differentially regulated processes and functions. We provided evidence of an age or senescence-associated shift in energy metabolism from glucose to fatty acids, in part by the overrepresentation of glyoxylate metabolic processes in upregulated DEPs within the middle and fetal sub-anatomical regions when compared to maternal sub-anatomical region.

The glyoxylate pathway and gluconeogenesis are an alternative to the tricarboxylate acid (TCA) cycle for production of ATP in absence of glucose [520]. Glyoxylate metabolites have been previously associated with various pregnancy complications including PE, IUGR and early pregnancy loss [428, 521-523]. Moreover, our results pointed towards a more senescent phenotype in the maternal sub-anatomical region where DEPs were associated with mitochondrial dysfunction and lack of antioxidant or anti-senescent activity.

The proteomic profile and associated functional analysis suggest an advanced ageing profile in the maternal sub-anatomical region of a healthy placenta at term. This senile change was not reflected in the fetal or middle sub-anatomical region suggesting that placental ageing morphologically migrates from maternal towards the fetal surface of the organ [428, 524] (Chapter 3). Increased mitochondrial metabolism was evident following functional analysis of DEPs in the middle sub-anatomical region with significant expression of IDH1, IDH2, ALDH4A1 and PDHA1 protein when compared to maternal and fetal regions. The middle sub-anatomical region also appeared protected from DNA damage and telomere shortening due to greater energy homeostasis and antioxidant defence when compared to the other

two sub-anatomical regions. In Chapter 3, we investigated the proteomic structure and functional variabilities between sub-anatomical regions within healthy placenta for the first time. We chose five identical sample sites and divided each section into approximate maternal, middle, and fetal sub-anatomical region, and ensured reproducibility by histopathological confirmation. Our results from individual section sites and sub-anatomical region showed phenotypic differences and served as a proof of concept that optimal placental research should be standardized by including multiple tissue sites to discern the global signature of this large heterogenous metabolic organ. Additionally, our proteomic assessment of healthy control placentas provided a unique insight into the functioning, including mitochondrial status and senescence in term placentas uncomplicated by underlying pathologies.

In Chapter 4 we performed a comprehensive proteomic profile of placental tissues from healthy uncomplicated compared to PE and IUGR affected pregnancies. We showed that despite the heterogeneity in phenotypes evident in Chapter 2, there were 72 shared proteins between PE and IUGR placentas, with similar protein pathways and potentially some shared pathophysiology between both complications. However, we provided evidence of uniquely identified proteins in PE (35 proteins) and IUGR (14 proteins) which may explain the variations in disease pathology and progression. Upon evaluation of DEPs, we identified that immune-regulatory proteins such as IgG4 and IGHG4 were downregulated in PE compared to controls, whereas these proteins were upregulated in IUGR when compared to controls. IgG4 is a unique class of immunoglobulin which cross the placental barrier efficiently, yet its role is not fully understood in pregnancy. There is transfer of

maternal IgG antibodies from the mother to fetus through the placenta, which provides protection to the developing fetus while its immune defence develops [527]. Research has shown that IgG4 has the strongest correlation between maternal and cord IgG concentration [528]. However the presence of increased levels of IgG4 in maternal plasma would indicate the presence of a pathology, whereas low plasma levels of IgG4 have been associated with miscarriages in part due to the presence of high levels of interferon gamma (IFN-γ), as shown in chapter 2 of this thesis [529]. Increased levels of IFN-γ inhibits the production of IgG4 responsible for maternal tolerance to the fetus and maintenance of pregnancy[528,529]. Mitochondrial dysfunction has been frequently associated with PE as a result of elevated OS coupled with lack of antioxidant defence and a reduction in ATP production and increased mtDNA damage [156]. Mitochondrial creatine kinase 1A (CKMT1A) is a mitochondrial protein responsible for regulation of apoptosis through mitochondrial permeability transition and was downregulated in PE and upregulated in IUGR placental tissue when compared to controls [458]. The CKMT group of proteins maybe altered as a result of oxidative and radical induced molecular damage. This result would also complement our findings from Chapter 2, reflecting that in IUGR, trophoblasts are at end stage of cellular division and are undergoing senescence or apoptosis [530].

Prosaposin (PSAP) is another mitochondrial associated protein responsible for induction of apoptosis, acting through the caspase-8 and caspase-9 mitochondrial apoptotic factors [531]. We showed a significant upregulation of PSAP in PE whereas PSAP was significant downregulated in IUGR. These findings agree with various publications [488, 532-534]. Contrarily, PSAP has also been associated with ERK

phosphorylation and prevention of cellular apoptosis [535].The exact mechanism of how PSAP contributes to the pathology of PE &IUGR, and its effect on inducing cellular senescence has not yet fully understood [532]. However, upregulation of PSAP in PE may indicate an apoptotic phenotype whereas in IUGR it suggests a senescence phenotype compared to matched controls. We also identified two RNA triplexes involved in regulation of PSAP mRNA in both PE & IUGR which requires further evaluation to fully comprehend the role of this protein in pathophysiology of these adverse pregnancy outcomes.

Amine oxidase copper-containing 1 (AOC1) protein was shown to be downregulated in IUGR when compared to PE. AOC1 is frequently associated with cancer, where overexpression of AOC1 has been involved in the regulation of proliferation, migration, and apoptosis of cells by catalysing the deamination of polyamines, which produces reactive oxygen species [536]. Spermidine, a substrate of AOC1 has been associated with preservation of mitochondrial functioning against ROS insults, while also displaying anti-inflammatory properties and preventing cellular senescence [537, 538]. The downregulation of AOC1 in IUGR maybe associated with cellular senescence through the lack of protective action of spermidine. However, more in-depth interrogation is required to understand the mechanism of action of AOC1 in IUGR and PE pregnancies.

5.2 Strengths and Limitations

This thesis has many strengths. Firstly, the robustness of the samples collected from term first time mothers through a well-defined pregnancy cohort. Furthermore, as this study recruited nulliparous women it allowed us to explore the

pathophysiology of both PE and IUGR, without the confounding effects of adaptive maternal physiological responses to previous pregnancies. The analysis of senescent mediators and proteomic signatures were further supported by correlating outcomes with clinical variables for each participant in the study.

One of the key strengths of this thesis is the segregation of the study cohorts into PE, PE associated with IUGR and IUGR only for evaluation of cellular senescence This allowed us to explore the shared and diverse senescence/cell proliferation pathways, placental cells undergo in each pathology. To our knowledge, this is the first time that multiple biomarkers of cellular senescence have been examined in these complications. Another major strength of this thesis is the evaluation of protein composition in healthy placentas from uncomplicated pregnancies which we divided into three sub-anatomical regions.

A further strength of this thesis is the proteomic characterisation using Label free quantification. Relative quantification in mass spectrometry uses stable isotopes (2H, 13C, 15N, 18O) as labels, which could be chemical, metabolic or enzymatic and are often used in *in vitro* studies but not routinely used in clinical proteomic research [539]. Label-free quantification encompassing two quantitative methods, namely a spectral counting approach and an ion-intensity-based approach are used to determine peptide abundance by evaluating chromatographic peaks [539]. The major advantage of Label-free LC-MS quantification is the higher dynamic range of quantification and identifying alterations in abundance across samples. However, samples need to be run consecutively which makes this process time consuming [505, 540].

Systems biology and the use of computational biology to analyse genomic, proteomic and metabolomic data to construct cohesive disease model seeks to understand complex disease process through vast biology and mathematical tools [428]. In this thesis we used NaViCenta, a placenta specific disease mapping system, a human and machine-readable computational model. This mode works on the data collected from multiomics databases including information with placental processes and cell interactions, relevance to healthy placentation, various molecular interactions between proteins, RNA, and DNA, enriched with regulatory factors, transcription factors, miRNA, and lncRNA, which can be used for network-based analyses. A further key strength of this thesis is the use of NaviCenta model to perform placenta specific phenotype prediction, functional analysis, and provides a robust and meaningful interpretation of proteomic data.

There are equally limitations to this research. One of the limitations is the limited sample size consisting of largely Caucasian (Irish) population. The sample size was limited due to strict recruitment criteria. Moreover, due to Covid-19 pandemic there were additional restrictions in the CUMH during participant recruitment, which impacted participant recruitment. Another limitation was that biological samples were collected at a single timepoint at the end of pregnancy, which makes it difficult to accurately determine if the identified pathogenic mediators are contributing or consequential factors in PE and IUGR.

5.3 Future Research

Pregnancy-related research entails many challenges. The inherent vulnerability of the patient groups, as well as common comorbidities in pregnancy complications,

increase the required number of biological samples for robust statistical analysis. Nonetheless, the use of cell lines, explant cultures, animal models, and computational modelling are useful circumventions [305, 541].

While we evaluated multiple biomarkers of senescence in placental samples including senescence associated genes, telomere length, mtDNA, p16 and p21 protein expression, Lamin B1, and circulating SASPs in maternal blood, we were unable to measure one integral marker of senescence due to poor yields of primary trophoblasts. Future studies are required to evaluate senescence-associated-β-galactosidase (SA-β-gal) in primary trophoblasts across our study groups. SA-β-gal is a histochemical assay to measure lysosomal enzyme β-galactosidase, which can be detected at an acidic pH 6 or lower in senescent cells. Increased SA-β-gal activity has been linked to upregulation of SASP and cell cycle inhibitors, which resonates with our results [54, 363].

Redox signalling plays a major role in both successful and complicated pregnancies. We have shown the plethora of processes falling under the term “redox signalling” and associated maternal and fetal outcomes. The complexity of redox signalling requires consideration of more than one biomarker to obtain meaningful results. On the experimental side, this requires more integrative approaches considering both pro- and antioxidant reactions with a higher sensitivity to physiological variation. Assessment of ROS *in vivo* is particularly challenging and while quantitation of ROS in primary cells using fluorescent dyes is feasible it equally has its flaws. One surrogate marker of oxidative stress-induced damage would be to

measure mitochondrial metabolism using the Seahorse XFp Analyzer Mito Stress Test.

Additionally, proteomic analysis of isolated placental mitochondria would provide insight into mitochondrial function in healthy and adverse pregnancy outcomes. Mitochondrial dysfunction has frequently been associated with cellular senescence and while we examined mtDNA as a marker of mitochondrial dysfunction, a more robust and global assessment of mitochondrial function is required to correlate its involvement in mediating senescence in these pregnancy complications. Another potential method to assess redox signalling is through the use of computational modelling and machine learning. Although computational modelling of redox-related processes is often utilized in health sciences, these models have not been exploited in the context of feto-maternal health research. Notwithstanding computational modelling reduces the need for experimental replicates by identifying biomarker candidates [305, 541]. The combination of existing models to a larger network, including other redox-signalling pathways, may lead to deeper insights and provide opportunities to explore interventions and their effects on complex biological processes [305, 542].

Currently there are limited therapeutic options available to treat adverse pregnancy outcomes. Recent work assessing the therapeutic benefit of aspirin treatment of women with suspected PE using untargeted metabolomics profiles of plasma samples from pregnant women at high risk of PE before and after aspirin/placebo treatment, hypothesised that aspirin treatment prevented PE by delaying the metabolic clock and estimated gestational age [543, 544]. Additionally, there was a

reversal of wide range of metabolic changes over advancing gestational age in aspirin treated pregnancies compared to healthy pregnancies [543, 544]. Our results showed a stark contrast between PE and IUGR pregnancy outcomes when assessing placental premature ageing. These differences could potentially be related to the effect of aspirin treatment of women with PE; however, further research is required to assess if aspirin directly alters cellular senescence.

Methodologically, future research in placental proteomic assessment might be performed using Bruker's high throughput LC/MS system. In 2021, Bruker's added a new dimension to proteomic research by addition of gas separation phase within the linear accelerator which made possible to detect around 4,000 to 8,000 proteins/µl in 20 minutes, making it the highest performing MS technique in the world. Re-running the samples on the Bruker's system would yield higher protein quantification, providing us with an extensive placental proteomic database and increased identification of proteins of interest, which might have not been detected the first time.

In addition to insight into placental ageing in adverse pregnancy outcomes, this thesis provides understanding of the heterogenous proteomic profiles of the healthy placenta and diseased placentas. Placental research, though diverse, is still in its infancy with incomplete genetic and proteomic information that could shed light into physiological and disrupted signalling pathways in healthy placentas compared to placental conditions. Therefore, placental disease mapping utilizing the data provided in this thesis for adverse pregnancy outcomes such as PE and IUGR could fill in the gaps for understanding the pathophysiology of the placental

and systemic conditions for both mother and the baby. Moreover, it could also provide novel biomarkers for early diagnosis of PE & IUGR and potentially identify a therapeutic target. Additionally, continued research into investigation of pathways and markers responsible for maternal and fetal long term health consequences of both these obstetric complications is warranted as a future research directive.

6.0 Conclusion

In my thesis I have provided novel insight into the heterogenous differences in cellular senescent phenotypes in PE, PE associated with IUGR, and IUGR following quantitative assessment of multiple biomarkers of senescence. This work showcases the distinction between PE and IUGR placental phenotypes compared to healthy pregnancy, even though these adverse pregnancy outcomes share some common pathophysiology. Additionally, this thesis provides novel insights into proteomic signature of healthy placental tissues including variations between sub-anatomical regions of healthy placenta. Finally in this thesis I characterised the proteomic profile of PE and IUGR placentas compared to healthy controls and identified the significance of mitochondrial proteins including their antioxidant activity, which might uncover novel therapeutic targets and enhance biomarker discovery in adverse pregnancy outcomes.

7.0 Bibliography

1. Manna S, McCarthy C, McCarthy FP. Placental Ageing in Adverse Pregnancy Outcomes: Telomere Shortening, Cell Senescence, and Mitochondrial Dysfunction. Oxidative Medicine and Cellular Longevity. 2019;2019:3095383.

2. Vermeulen K, Van Bockstaele DR, Berneman ZN. The cell cycle: a review of regulation, deregulation and therapeutic targets in cancer. Cell proliferation. 2003;36(3):131-49.

3. Maes A, Menu E, Veirman KD, Maes K, Vand Erkerken K, De Bruyne E. The therapeutic potential of cell cycle targeting in multiple myeloma. Oncotarget. 2017;8(52):90501-20.

4. McIntosh JR. Mitosis. Cold Spring Harbor perspectives in biology. 2016;8(9):a023218.

5. Shay JW, Wright WE. Hayflick, his limit, and cellular ageing. Nature Reviews Molecular Cell Biology. 2000;1(1):72-6.

6. López-Otín C, Blasco MA, Partridge L, Serrano M, Kroemer G. The hallmarks of aging. Cell. 2013;153(6):1194-217.

7. Taylor RC, Dillin A. Aging as an event of proteostasis collapse. Cold Spring Harb Perspect Biol. 2011;3(5).

8. Trifunovic A, Larsson NG. Mitochondrial dysfunction as a cause of ageing. J Intern Med. 2008;263(2):167-78.

9. McHugh D, Gil J. Senescence and aging: Causes, consequences, and therapeutic avenues. J Cell Biol. 2018;217(1):65-77.

10. Childs BG, Baker DJ, Kirkland JL, Campisi J, van Deursen JM. Senescence and apoptosis: dueling or complementary cell fates? EMBO Rep. 2014;15(11):1139-53.

11. Thannickal VJ, Fanburg BL. Reactive oxygen species in cell signaling. Am J Physiol Lung Cell Mol Physiol. 2000;279(6):L1005-28.

12. Finkel T. Signal transduction by reactive oxygen species. J Cell Biol. 2011;194(1):7-15.

13. Cross CE, Halliwell B, Borish ET, Pryor WA, Ames BN, Saul RL, McCord JM, Harman D. Oxygen radicals and human disease. Ann Intern Med. 1987;107(4):526-45.

14. Starkov AA. The role of mitochondria in reactive oxygen species metabolism and signaling. Ann N Y Acad Sci. 2008;1147:37-52.

15. Murphy MP. How mitochondria produce reactive oxygen species. Biochem J. 2009;417(1):1-13.

16. Guengerich FP. Mechanisms of Cytochrome P450-Catalyzed Oxidations. ACS Catalysis. 2018;8(12):10964-76.

17. Murad F. The 1996 Albert Lasker Medical Research Awards. Signal transduction using nitric oxide and cyclic guanosine monophosphate. Jama. 1996;276(14):1189-92.

18. Förstermann U, Sessa WC. Nitric oxide synthases: regulation and function. Eur Heart J. 2012;33(7):829-37, 37a-37d.

19. Xue Q, Yan Y, Zhang R, Xiong H. Regulation of iNOS on Immune Cells and Its Role in Diseases. Int J Mol Sci. 2018;19(12).

20. Francis SH, Busch JL, Corbin JD, Sibley D. cGMP-dependent protein kinases and cGMP phosphodiesterases in nitric oxide and cGMP action. Pharmacol Rev. 2010;62(3):525-63.

21. Bolaños JP, Heales SJ, Peuchen S, Barker JE, Land JM, Clark JB. Nitric oxide-mediated mitochondrial damage: a potential neuroprotective role for glutathione. Free Radic Biol Med. 1996;21(7):995-1001.

22. Adams L, Franco MC, Estevez AG. Reactive nitrogen species in cellular signaling. Experimental biology and medicine (Maywood, NJ). 2015;240(6):711-7.

23. Halliwell B. How to characterize an antioxidant: an update. Biochem Soc Symp. 1995;61:73-101.

24. Krinsky NI. Mechanism of action of biological antioxidants. Proc Soc Exp Biol Med. 1992;200(2):248-54.

25. Lü JM, Lin PH, Yao Q, Chen C. Chemical and molecular mechanisms of antioxidants: experimental approaches and model systems. J Cell Mol Med. 2010;14(4):840-60.

26. Csire G, Canabady-Rochelle L, Averlant-Petit M-C, Selmeczi K, Stefan L. Both metal-chelating and free radical-scavenging synthetic pentapeptides as efficient inhibitors of reactive oxygen species generation†. Metallomics. 2020;12(8):1220-9.

27. Poljšak B, Dahmane R. Free radicals and extrinsic skin aging. Dermatol Res Pract. 2012;2012:135206.

28. Wang Y, Branicky R, Noë A, Hekimi S. Superoxide dismutases: Dual roles in controlling ROS damage and regulating ROS signaling. The Journal of cell biology. 2018;217(6):1915-28.

29. Goyal MM, Basak A. Human catalase: looking for complete identity. Protein & cell. 2010;1(10):888-97.

30. Saccoccia F, Angelucci F, Boumis G, Carotti D, Desiato G, Miele AE, Bellelli A. Thioredoxin reductase and its inhibitors. Current protein & peptide science. 2014;15(6):621-46.

31. Deponte M. Glutathione catalysis and the reaction mechanisms of glutathione-dependent enzymes. Biochimica et Biophysica Acta (BBA) - General Subjects. 2013;1830(5):3217-66.

32. Mieyal JJ, Gallogly MM, Qanungo S, Sabens EA, Shelton MD. Molecular mechanisms and clinical implications of reversible protein S-glutathionylation. Antioxidants & redox signaling. 2008;10(11):1941-88.

33. Birch-Machin MA, Bowman A. Oxidative stress and ageing. British Journal of Dermatology. 2016;175(S2):26-9.

34. Austad SN, Hoffman JM. Is antagonistic pleiotropy ubiquitous in aging biology? Evolution, Medicine, and Public Health. 2018;2018(1):287-94.

35. Jin K. Modern Biological Theories of Aging. Aging Dis. 2010;1(2):72-4.

36. Blagosklonny MV. Why the disposable soma theory cannot explain why women live longer and why we age. Aging (Albany NY). 2010;2(12):884-7.

37. Giorgio M, Trinei M, Migliaccio E, Pelicci PG. Hydrogen peroxide: a metabolic by-product or a common mediator of ageing signals? Nature reviews Molecular cell biology. 2007;8(9):722-8.

38. Schieber M, Chandel NS. ROS function in redox signaling and oxidative stress. Current biology. 2014;24(10):R453-R62.

39. Gladyshev VN. The free radical theory of aging is dead. Long live the damage theory! Antioxidants & redox signaling. 2014;20(4):727-31.

40. Liguori I, Russo G, Curcio F, Bulli G, Aran L, Della-Morte D, Gargiulo G, Testa G, Cacciatore F, Bonaduce D, Abete P. Oxidative stress, aging, and diseases. Clin Interv Aging. 2018;13:757-72.

41. Hayflick L, Moorhead PS. The serial cultivation of human diploid cell strains. Experimental cell research. 1961;25(3):585-621.

42. Campisi J. Cellular senescence as a tumor-suppressor mechanism. Trends in Cell Biology. 2001;11:S27-S31.

43. De Lange T. How telomeres solve the end-protection problem. Science. 2009;326(5955):948-52.

44. Zhu Y, Liu X, Ding X, Wang F, Geng X. Telomere and its role in the aging pathways: telomere shortening, cell senescence and mitochondria dysfunction. Biogerontology. 2019;20(1):1-16.

45. Bernadotte A, Mikhelson VM, Spivak IM. Markers of cellular senescence. Telomere shortening as a marker of cellular senescence. Aging (Albany NY). 2016;8(1):3.

46. Guirro M, Costa A, Gual-Grau A, Mayneris-Perxachs J, Torrell H, Herrero P, Canela N, Arola L. Multi-omics approach to elucidate the gut microbiota activity: Metaproteomics and metagenomics connection. Electrophoresis. 2018;39(13):1692-701.

47. Glousker G, Lingner J. When telomerase causes telomere loss. Developmental cell. 2018;44(3):281-3.

48. Anderson R, Lagnado A, Maggiorani D, Walaszczyk A, Dookun E, Chapman J, Birch J, Salmonowicz H, Ogrodnik M, Jurk D, Proctor C, Correia-Melo C, Victorelli S, Fielder E, Berlinguer-Palmini R, Owens A, Greaves LC, Kolsky KL, Parini A, Douin-Echinard V, LeBrasseur NK, Arthur HM, Tual-Chalot S, Schafer MJ, Roos CM, Miller JD, Robertson N, Mann J, Adams PD, Tchkonia T, Kirkland JL, Mialet-Perez J, Richardson GD, Passos JF. Length-independent telomere damage drives post-mitotic cardiomyocyte senescence. The EMBO journal. 2019;38(5):e100492.

49. Ball AJ, Levine F. Telomere-independent cellular senescence in human fetal cardiomyocytes. Aging Cell. 2005;4(1):21-30.

50. Liu J, Wang L, Wang Z, Liu J-P. Roles of Telomere Biology in Cell Senescence, Replicative and Chronological Ageing. Cells. 2019;8(1):54.

51. Victorelli S, Passos JF. Telomeres and Cell Senescence - Size Matters Not. EBioMedicine. 2017;21:14-20.

52. Shiloh Y. TheATM-mediatedDNA-damageresponse: takingshape. Trends; 2006.

53. Taylor RC, Cullen SP, Martin SJ. Apoptosis: controlled demolition at the cellular level. Nature reviews Molecular cell biology. 2008;9(3):231-41.

54. Di Micco R, Krizhanovsky V, Baker D, d'Adda di Fagagna F. Cellular senescence in ageing: from mechanisms to therapeutic opportunities. Nature Reviews Molecular Cell Biology. 2021;22(2):75-95.

55. Passos JF, Saretzki G, von Zglinicki T. DNA damage in telomeres and mitochondria during cellular senescence: is there a connection? Nucleic Acids Research. 2007;35(22):7505-13.

56. d'Adda di Fagagna F. Living on a break: cellular senescence as a DNA-damage response. Nature Reviews Cancer. 2008;8(7):512-22.

57. Kumari R, Jat P. Mechanisms of Cellular Senescence: Cell Cycle Arrest and Senescence Associated Secretory Phenotype. Frontiers in Cell and Developmental Biology. 2021;9(485).

58. Lopes-Paciencia S, Saint-Germain E, Rowell M-C, Ruiz AF, Kalegari P, Ferbeyre G. The senescence-associated secretory phenotype and its regulation. Cytokine. 2019;117:15-22.

59. Coppé J-P, Rodier F, Patil CK, Freund A, Desprez P-Y, Campisi J. Tumor suppressor and aging biomarker p16(INK4a) induces cellular senescence without the associated inflammatory secretory phenotype. The Journal of biological chemistry. 2011;286(42):36396-403.

60. Muñoz-Espín D, Serrano M. Cellular senescence: from physiology to pathology. Nature Reviews Molecular Cell Biology. 2014;15(7):482-96.

61. Sousa-Victor P, Gutarra S, Garcia-Prat L, Rodriguez-Ubreva J, Ortet L, Ruiz-Bonilla V, Jardi M, Ballestar E, Gonzalez S, Serrano AL. Geriatric muscle stem cells switch reversible quiescence into senescence. Nature. 2014;506(7488):316-21.

62. Molofsky AV, Slutsky SG, Joseph NM, He S, Pardal R, Krishnamurthy J, Sharpless NE, Morrison SJ. Increasing p16 INK4a expression decreases forebrain progenitors and neurogenesis during ageing. Nature. 2006;443(7110):448-52.

63. Burton DGA, Krizhanovsky V. Physiological and pathological consequences of cellular senescence. Cellular and Molecular Life Sciences. 2014;71(22):4373-86.

64. Streuli C. Extracellular matrix remodelling and cellular differentiation. Current opinion in cell biology. 1999;11(5):634-40.

65. Millis AJ, Hoyle M, McCue HM, Martini H. Differential expression of metalloproteinase and tissue inhibitor of metalloproteinase genes in aged human fibroblasts. Experimental cell research. 1992;201(2):373-9.

66. Brown MA, Magee LA, Kenny LC, Karumanchi SA, McCarthy FP, Saito S, Hall DR, Warren CE, Adoyi G, Ishaku S. The hypertensive disorders of pregnancy: ISSHP classification, diagnosis & management recommendations for international practice. Pregnancy Hypertension. 2018;13:291-310.

67. Ives CW, Sinkey R, Rajapreyar I, Tita ATN, Oparil S. Preeclampsia—Pathophysiology and Clinical Presentations: JACC State-of-the-Art Review. Journal of the American College of Cardiology. 2020;76(14):1690-702.

68. Haram K, Svendsen E, Abildgaard U. The HELLP syndrome: clinical issues and management. A Review. BMC Pregnancy Childbirth. 2009;9:8.

69. Erez O, Othman M, Rabinovich A, Leron E, Gotsch F, Thachil J. DIC in Pregnancy - Pathophysiology, Clinical Characteristics, Diagnostic Scores, and Treatments. J Blood Med. 2022;13:21-44.

70. Taylor Jr FB, Toh C-H, Hoots KW, Wada H, Levi M. Towards definition, clinical and laboratory criteria, and a scoring system for disseminated intravascular coagulation. Thrombosis and haemostasis. 2001;86(11):1327-30.

71. Jeyabalan A. Epidemiology of preeclampsia: impact of obesity. Nutrition reviews. 2013;71 Suppl 1(0 1):S18-S25.

72. Fox A, McHugh S, Browne J, Kenny LC, Fitzgerald A, Khashan AS, Dempsey E, Fahy C, O'Neill C, Kearney PM. Estimating the Cost of Preeclampsia in the Healthcare System. Hypertension. 2017;70(6):1243-9.

73. English FA, Kenny LC, McCarthy FP. Risk factors and effective management of preeclampsia. Integr Blood Press Control. 2015;8:7-12.

74. Ghojazadeh M, Azami-Aghdash S, Mohammadi M, Vosoogh S, Mohammadi S, Naghavi-Behzad M. Prognostic risk factors for early diagnosing of Preeclampsia in Nulliparas. Niger Med J. 2013;54(5):344-8.

75. Aliyu MH, Salihu HM, Lynch O, Alio AP, Marty PJ. Fetal sex and differential survival in preeclampsia and eclampsia. Arch Gynecol Obstet. 2012;285(2):361-5.

76. Trogstad L, Magnus P, Moffett A, Stoltenberg C. The effect of recurrent miscarriage and infertility on the risk of pre-eclampsia. Bjog. 2009;116(1):108-13.

77. Tranquilli AL, Brown MA, Zeeman GG, Dekker G, Sibai BM. The definition of severe and early-onset preeclampsia. Statements from the International Society for the Study of Hypertension in Pregnancy (ISSHP). Pregnancy Hypertension: An International Journal of Women's Cardiovascular Health. 2013;3(1):44-7.

78. Huppertz B. Placental origins of preeclampsia: challenging the current hypothesis. Hypertension. 2008;51(4):970-5.

79. Thilaganathan B. Placental syndromes: getting to the heart of the matter. Ultrasound Obstet Gynecol. 2017;49(1):7-9.

80. Redman C. The six stages of pre-eclampsia. Pregnancy Hypertension: An International Journal of Women's Cardiovascular Health. 2014;4(3):246.

81. Roberts JM, Hubel CA. The two stage model of preeclampsia: variations on the theme. Placenta. 2009;30:32-7.

82. Thilaganathan B. Pre-eclampsia is primarily a placental disorder: AGAINST: Pre-eclampsia: the heart matters. BJOG: An International Journal of Obstetrics & Gynaecology. 2017;124(11):1763-.

83. Roberts JM, Hubel CA. The two stage model of preeclampsia: variations on the theme. Placenta. 2009;30 Suppl A(Suppl A):S32-7.

84. Redman C. Pre-eclampsia and the placenta. Placenta. 1991;12(4):301-8.

85. Staff AC. The two-stage placental model of preeclampsia: An update. Journal of Reproductive Immunology. 2019;134-135:1-10.

86. Pankiewicz K, Szczerba E, Maciejewski T, Fijałkowska A. Non-obstetric complications in preeclampsia. Przeglad menopauzalny= Menopause review. 2019;18(2):99.

87. Rana S, Lemoine E, Granger JP, Karumanchi SA. Preeclampsia: Pathophysiology, Challenges, and Perspectives. Circ Res. 2019;124(7):1094-112.

88. Burton GJ, Fowden AL. The placenta: a multifaceted, transient organ. Philosophical Transactions of the Royal Society B: Biological Sciences. 2015;370(1663):20140066.

89. Burton GJ, Jauniaux E. What is the placenta? American journal of obstetrics and gynecology. 2015;213(4):S6. e1-S6. e4.

90. Goldman-Wohl D, Yagel S. Regulation of trophoblast invasion: from normal implantation to pre-eclampsia. Molecular and cellular endocrinology. 2002;187(1-2):233-8.

91. Windsperger K, Dekan S, Pils S, Golletz C, Kunihs V, Fiala C, Kristiansen G, Knöfler M, Pollheimer J. Extravillous trophoblast invasion of venous as well as lymphatic vessels is altered in idiopathic, recurrent, spontaneous abortions. Human reproduction. 2017;32(6):1208-17.

92. Kasprzak JD, Kłosińska M, Drozdz J. Clinical aspects of assessment of endothelial function. Pharmacological reports: PR. 2006;58:33-40.

93. Incalza MA, D'Oria R, Natalicchio A, Perrini S, Laviola L, Giorgino F. Oxidative stress and reactive oxygen species in endothelial dysfunction associated with cardiovascular and metabolic diseases. Vascular Pharmacology. 2018;100:1-19.

94. Bonetti PO, Lerman LO, Lerman A. Endothelial Dysfunction. Arteriosclerosis, Thrombosis, and Vascular Biology. 2003;23(2):168-75.

95. Lerman A, Burnett Jr J. Intact and altered endothelium in regulation of vasomotion. Circulation. 1992;86(6 Suppl):III12-9.

96. Bdolah Y, Karumanchi SA, Sachs BP. Recent advances in understanding of preeclampsia. Croatian medical journal. 2005;46(5).

97. Damsky CH, Fitzgerald M, Fisher S. Distribution patterns of extracellular matrix components and adhesion receptors are intricately modulated during first trimester cytotrophoblast differentiation along the invasive pathway, in vivo. The Journal of clinical investigation. 1992;89(1):210-22.

98. Genbacev O, Zhou Y, Ludlow JW, Fisher SJ. Regulation of human placental development by oxygen tension. Science. 1997;277(5332):1669-72.

99. Myatt L, Cui X. Oxidative stress in the placenta. Histochemistry and cell biology. 2004;122(4):369-82.

100. Tomimatsu T, Mimura K, Endo M, Kumasawa K, Kimura T. Pathophysiology of preeclampsia: an angiogenic imbalance and long-lasting systemic vascular dysfunction. Hypertension research. 2017;40(4):305-10.

101. Shah DA, Khalil RA. Bioactive factors in uteroplacental and systemic circulation link placental ischemia to generalized vascular dysfunction in hypertensive pregnancy and preeclampsia. Biochemical pharmacology. 2015;95(4):211-26.

102. Irani RA, Xia Y. The Functional Role of the Renin–Angiotensin System in Pregnancy and Preeclampsia. Placenta. 2008;29(9):763-71.

103. Koga K, Osuga Y, Yoshino O, Hirota Y, Ruimeng X, Hirata T, Takeda S, Yano T, Tsutsumi O, Taketani Y. Elevated serum soluble vascular endothelial growth factor receptor 1 (sVEGFR-1) levels in women with preeclampsia. The Journal of Clinical Endocrinology & Metabolism. 2003;88(5):2348-51.

104. Craici IM, Wagner SJ, Weissgerber TL, Grande JP, Garovic VD. Advances in the pathophysiology of pre-eclampsia and related podocyte injury. Kidney international. 2014;86(2):275-85.

105. Soma H, Yoshida K, Mukaida T, Tabuchi Y. Morphologic changes in the hypertensive placenta. Contributions to gynecology and obstetrics. 1982;9:58-75.

106. Loukeris K, Sela R, Baergen RN. Syncytial knots as a reflection of placental maturity: reference values for 20 to 40 weeks' gestational age. Pediatr Dev Pathol. 2010;13(4):305-9.

107. Heazell AEP, Moll SJ, Jones CJP, Baker PN, Crocker IP. Formation of Syncytial Knots is Increased by Hyperoxia, Hypoxia and Reactive Oxygen Species. Placenta. 2007;28:S33-S40.

108. Falco ML, Sivanathan J, Laoreti A, Thilaganathan B, Khalil A. Placental histopathology associated with pre-eclampsia: systematic review and meta-analysis. Ultrasound in Obstetrics & Gynecology. 2017;50(3):295-301.

109. Roberts RM, Green JA, Schulz LC. The evolution of the placenta. Reproduction (Cambridge, England). 2016;152(5):R179-R89.

110. Zhang P, Schmidt M, Cook L. Maternal vasculopathy and histologic diagnosis of preeclampsia: Poor correlation of histologic changes and clinical manifestation. American Journal of Obstetrics and Gynecology. 2006;194(4):1050-6.

111. VINNARS M-T, NASIELL J, GHAZI S, WESTGREN M, PAPADOGIANNAKIS N. The severity of clinical manifestations in preeclampsia correlates with the amount of placental infarction. Acta Obstetricia et Gynecologica Scandinavica. 2011;90(1):19-25.

112. Pittara T, Vyrides A, Lamnisos D, Giannakou K. Pre-eclampsia and long-term health outcomes for mother and infant: an umbrella review. BJOG: An International Journal of Obstetrics & Gynaecology. 2021;128(9):1421-30.

113. Bellamy L, Casas J-P, Hingorani AD, Williams DJ. Pre-eclampsia and risk of cardiovascular disease and cancer in later life: systematic review and meta-analysis. BMJ. 2007;335(7627):974.

114. Lykke JA, Langhoff-Roos J, Sibai BM, Funai EF, Triche EW, Paidas MJ. Hypertensive pregnancy disorders and subsequent cardiovascular morbidity and type 2 diabetes mellitus in the mother. Hypertension. 2009;53(6):944-51.

115. Brown DW, Dueker N, Jamieson DJ, Cole JW, Wozniak MA, Stern BJ, Giles WH, Kittner SJ. Preeclampsia and the risk of ischemic stroke among young women: results from the Stroke Prevention in Young Women Study. Stroke. 2006;37(4):1055-9.

116. Poulter N, Chang C. Haemorrhagic stroke, overall stroke risk, and combined oral contraceptives: Results of an. The Lancet. 1996;348(9026):505-10.

117. Poulter N, Chang C, Farley T, Meirik O, Marmot M. Contraceptives: results of international multicentre case-control study. Lancet. 1995;346:1575-82.

118. Turbeville HR, Sasser JM. Preeclampsia beyond pregnancy: long-term consequences for mother and child. Am J Physiol Renal Physiol. 2020;318(6):F1315-f26.

119. Vikse BE, Irgens LM, Leivestad T, Skjærven R, Iversen BM. Preeclampsia and the risk of end-stage renal disease. New England Journal of Medicine. 2008;359(8):800-9.

120. Mule G, Castiglia A, Cusumano C, Scaduto E, Geraci G, Altieri D, Natale ED, Cacciatore O, Cerasola G, Cottone S. Subclinical kidney damage in hypertensive patients: a renal window opened on the cardiovascular system. Focus on microalbuminuria. Hypertension: from basic research to clinical practice. 2016:279-306.

121. Ärnlöv J, Evans JC, Meigs JB, Wang TJ, Fox CS, Levy D, Benjamin EJ, D'Agostino RB, Vasan RS. Low-grade albuminuria and incidence of cardiovascular disease events in nonhypertensive and nondiabetic individuals: the Framingham Heart Study. Circulation. 2005;112(7):969-75.

122. McDonald S, Yusuf S, Walsh M, Lonn E, Teo K, Anand S, Pogue J, Islam S, Devereaux P, Gerstein H. Increased cardiovascular risk after pre-eclampsia in women with dysglycaemia. Diabetic Medicine. 2013;30(1):e1-e7.

123. Johnson AC, Cipolla MJ. The cerebral circulation during pregnancy: adapting to preserve normalcy. Physiology (Bethesda). 2015;30(2):139-47.

124. Postma IR, Slager S, Kremer HPH, de Groot JC, Zeeman GG. Long-term Consequences of the Posterior Reversible Encephalopathy Syndrome in Eclampsia and Preeclampsia: A Review of the Obstetric and Nonobstetric Literature. Obstetrical & Gynecological Survey. 2014;69(5):287-300.

125. Aukes AM, Arion K, Bone JN, Li J, Vidler M, Bellad MB, Charantimath U, Goudar SS, Hoodbhoy Z, Katageri G, Macuacua S, Mallapur AA, Munguambe K, Qureshi RN, Sacoor C, Sevene E, Sheikh S, Valá A, Lewis G, Bhutta ZA, von Dadelszen P, Magee LA, Woo Kinshella M-L, Wong H, von Dadelszen P, Vilanculo F, Vidler M, Valá A, Ukah UV, Tu DK, Thabane L, Tchavana C, Thornton J, Sotunsa JO, Singer J, Sheikh S, Sharma S, Sevene E, Schuurman N, Sawchuck D, Sacoor C, Revankar AP, Raza F, Ramdurg UY, Qureshi RN, Pires R, Payne BA, Nobela V, Nkumbula C, Nhancolo A, Nhamirre Z, Munguambe K, Mungarwadi GI, Mulungo D, Mocumbi S, Mitton C, Merialdi M, Memon J, Matavele A, Mastiholi SS, Mandlate E, Mallapur AA, Magee LA, Maculuve S, Macuacua S, Macete E, Macamo M, Lui M, Li J, Lewis G, Lewin S, Lee T, Langer A, Kudachi US, Kodkany BS, Knight M, Kengapur GS, Kavi AJ, Katageri G, Kariya C, Karadiguddi CC, Kamble NA, Joshi AM, Hutton E, Hussain A, Honnungar NV, Hoodbhoy Z, Grobman W, Goudar SS, Gonçálves E, Firoz T, Fillipi V, Filimone P, Engelbrecht SM, Dunsmuir DT, Dumont G, Drebit SK, Donnay F, Dharamsi S, Dhamanekar VB, Derman R, Darlow B, Cutana S, Chougala KS, Chiaú R, Charantimath U, Byaruhanga RN, Bone JN, Boene H, Biz AI, Bique C, Bhutta ZA, Betrán AP, Bellad MB, Bannale SG, Aukes AM, Augusto O, Arion K, Ansermino JM, Amose F, Ahmed I, Adetoro OO. Causes and circumstances of maternal death: a secondary analysis of the Community-Level Interventions for Pre-eclampsia (CLIP) trials cohort. The Lancet Global Health. 2021;9(9):e1242-e51.

126. Zeeman GG, editor Neurologic complications of pre-eclampsia. Seminars in perinatology; 2009: Elsevier.

127. Obstetricians ACo, Gynecologists. ACOG Practice Bulletin No. 204: fetal growth restriction. Obstetrics and gynecology. 2019;133(2):e97-e109.

128. Institute of Medicine Committee on Understanding Premature B, Assuring Healthy O. The National Academies Collection: Reports funded by National Institutes of Health. In: Behrman RE, Butler AS, editors. Preterm Birth: Causes, Consequences, and Prevention. Washington (DC): National Academies Press (US)

Copyright © 2007, National Academy of Sciences.; 2007.

129. Harmon QE, Huang L, Umbach DM, Klungsøyr K, Engel SM, Magnus P, Skjærven R, Zhang J, Wilcox AJ. Risk of fetal death with preeclampsia. Obstetrics and gynecology. 2015;125(3):628-35.

130. Simpson LL, editor Maternal medical disease: risk of antepartum fetal death. Seminars in perinatology; 2002: Elsevier.

131. Backes CH, Markham K, Moorehead P, Cordero L, Nankervis CA, Giannone PJ. Maternal preeclampsia and neonatal outcomes. Journal of pregnancy. 2011;2011:214365-.

132. Bastek JA, Elovitz MA. The role and challenges of biomarkers in spontaneous preterm birth and preeclampsia. Fertility and Sterility. 2013;99(4):1117-23.

133. Fortunato SJ, Menon R, Lombardi SJ. Role of tumor necrosis factor-α in the premature rupture of membranes and preterm labor pathways. American journal of obstetrics and gynecology. 2002;187(5):1159-62.

134. O'Shea JE, Davis PG, Doyle LW, for the Victorian Infant Collaborative Study G. Maternal preeclampsia and risk of bronchopulmonary dysplasia in preterm infants. Pediatric Research. 2012;71(2):210-4.

135. Shin SH, Shin SH, Kim SH, Kim Y-J, Cho H, Kim E-K, Kim H-S. The Association of Pregnancy-induced Hypertension with Bronchopulmonary Dysplasia – A

Retrospective Study Based on the Korean Neonatal Network database. Scientific Reports. 2020;10(1):5600.

136. Wiedmeier SE, Henry E, Sola-Visner M, Christensen R. Platelet reference ranges for neonates, defined using data from over 47 000 patients in a multihospital healthcare system. Journal of perinatology. 2009;29(2):130-6.

137. Sola MC, Del Vecchio A, Rimsza LM. Evaluation and treatment of thrombocytopenia in the neonatal intensive care unit. Clinics in perinatology. 2000;27(3):655-79.

138. Burrows RF, Andrew M. Neonatal thrombocytopenia in the hypertensive disorders of pregnancy. Obstet Gynecol. 1990;76(2):234-8.

139. Wang A, Rana S, Karumanchi SA. Preeclampsia: the role of angiogenic factors in its pathogenesis. Physiology. 2009;24(3):147-58.

140. Strand KM, Heimstad R, Iversen A-C, Austgulen R, Lydersen S, Andersen GL, Irgens LM, Vik T. Mediators of the association between pre-eclampsia and cerebral palsy: population based cohort study. Bmj. 2013;347.

141. Gumusoglu SB, Chilukuri ASS, Santillan DA, Santillan MK, Stevens HE. Neurodevelopmental Outcomes of Prenatal Preeclampsia Exposure. Trends in Neurosciences. 2020;43(4):253-68.

142. Gumusoglu SB, Chilukuri ASS, Santillan DA, Santillan MK, Stevens HE. Neurodevelopmental Outcomes of Prenatal Preeclampsia Exposure. Trends Neurosci. 2020;43(4):253-68.

143. Barron A, Manna S, McElwain CJ, Musumeci A, McCarthy FP, O'Keeffe GW, McCarthy CM. Maternal pre-eclampsia serum increases neurite growth and

mitochondrial function through a potential IL-6-dependent mechanism in differentiated SH-SY5Y cells. Frontiers in Physiology. 2023;13.

144. Report of the National High Blood Pressure Education Program Working Group on High Blood Pressure in Pregnancy. American Journal of Obstetrics & Gynecology. 2000;183(1):s1-s22.

145. August P. Preeclampsia: New Thoughts on an Ancient Problem. J Clin Hypertens (Greenwich). 2000;2(2):115-23.

146. Force UPST. Aspirin Use to Prevent Preeclampsia and Related Morbidity and Mortality: US Preventive Services Task Force Recommendation Statement. JAMA. 2021;326(12):1186-91.

147. Too GT, Hill JB. Hypertensive crisis during pregnancy and postpartum period. Semin Perinatol. 2013;37(4):280-7.

148. Prins JR, Boelens HM, Heimweg J, Van der Heide S, Dubois AE, Van Oosterhout AJ, Erwich JJ. Preeclampsia is associated with lower percentages of regulatory T cells in maternal blood. Hypertens Pregnancy. 2009;28(3):300-11.

149. Amaral LM, Wallace K, Owens M, LaMarca B. Pathophysiology and Current Clinical Management of Preeclampsia. Curr Hypertens Rep. 2017;19(8):61.

150. Hyppönen E, Cavadino A, Williams D, Fraser A, Vereczkey A, Fraser WD, Bánhidy F, Lawlor D, Czeizel AE. Vitamin D and Pre-Eclampsia: Original Data, Systematic Review and Meta-Analysis. Annals of Nutrition and Metabolism. 2013;63(4):331-40.

151. Chappell LC, Seed PT, Briley AL, Kelly FJ, Lee R, Hunt BJ, Parmar K, Bewley SJ, Shennan AH, Steer PJ, Poston L. Effect of antioxidants on the occurrence of pre-

eclampsia in women at increased risk: a randomised trial. Lancet. 1999;354(9181):810-6.

152. Kasawara KT, do Nascimento SL, Costa ML, Surita FG, e Silva JL. Exercise and physical activity in the prevention of pre-eclampsia: systematic review. Acta Obstet Gynecol Scand. 2012;91(10):1147-57.

153. Paulis L, Šimko F. Blood pressure modulation and cardiovascular protection by melatonin: potential mechanisms behind. Physiological research. 2007;56(6).

154. Langston-Cox A, Marshall SA, Lu D, Palmer KR, Wallace EM. Melatonin for the Management of Preeclampsia: A Review. Antioxidants (Basel, Switzerland). 2021;10(3):376.

155. Yang Y, Xu P, Zhu F, Liao J, Wu Y, Hu M, Fu H, Qiao J, Lin L, Huang B, Jin H, Liu X, Zheng Y, Wen L, Saffery R, Kilby MD, Yan J, Kenny LC, Qi H, Tong C, Baker PN. The Potent Antioxidant MitoQ Protects Against Preeclampsia During Late Gestation but Increases the Risk of Preeclampsia When Administered in Early Pregnancy. Antioxid Redox Signal. 2021;34(2):118-36.

156. McCarthy C, Kenny LC. Therapeutically targeting mitochondrial redox signalling alleviates endothelial dysfunction in preeclampsia. Scientific Reports. 2016;6(1):32683.

157. Williamson RD, McCarthy FP, Manna S, Groarke E, Kell DB, Kenny LC, McCarthy CM. L-(+)-Ergothioneine Significantly Improves the Clinical Characteristics of Preeclampsia in the Reduced Uterine Perfusion Pressure Rat Model. Hypertension. 2020;75(2):561-8.

158. Mandruzzato G, Antsaklis A, Botet F, Chervenak FA, Figueras F, Grunebaum A, Puerto B, Skupski D, Stanojevic M. Intrauterine restriction (IUGR). Journal of Perinatal Medicine. 2008;36(4):277-81.

159. Sharma D, Shastri S, Farahbakhsh N, Sharma P. Intrauterine growth restriction – part 1. The Journal of Maternal-Fetal & Neonatal Medicine. 2016;29(24):3977-87.

160. Sharma D, Farahbakhsh N, Shastri S, Sharma P. Intrauterine growth restriction - part 2. J Matern Fetal Neonatal Med. 2016;29(24):4037-48.

161. Kesavan K, Devaskar SU. Intrauterine Growth Restriction: Postnatal Monitoring and Outcomes. Pediatric Clinics of North America. 2019;66(2):403-23.

162. Figueras F, Gardosi J. Intrauterine growth restriction: new concepts in antenatal surveillance, diagnosis, and management. American Journal of Obstetrics & Gynecology. 2011;204(4):288-300.

163. Platz E, Newman R. Diagnosis of IUGR: Traditional Biometry. Seminars in Perinatology. 2008;32(3):140-7.

164. Dashe JS, McIntire DD, Lucas MJ, Leveno KJ. Effects of symmetric and asymmetric fetal growth on pregnancy outcomes. Obstet Gynecol. 2000;96(3):321-7.

165. Fry FJ. Ultrasound: its applications in medicine and biology: Elsevier; 2013.

166. Suhag A, Berghella V. Intrauterine Growth Restriction (IUGR): Etiology and Diagnosis. Current Obstetrics and Gynecology Reports. 2013;2(2):102-11.

167. Resnik R. Intrauterine growth restriction. Obstetrics & Gynecology. 2002;99(3):490-6.

168. Lin C-C, Santolaya-Forgas J. Current concepts of fetal growth restriction: part I. Causes, classification, and pathophysiology. Obstetrics & Gynecology. 1998;92(6):1044-55.

169. Abuzzahab MJ, Schneider A, Goddard A, Grigorescu F, Lautier C, Keller E, Kiess W, Klammt J, Kratzsch J, Osgood D. IGF-I receptor mutations resulting in intrauterine and postnatal growth retardation. New England Journal of Medicine. 2003;349(23):2211-22.

170. Neerhof MG. Causes of intrauterine growth restriction. Clinics in perinatology. 1995;22(2):375-85.

171. Nardozza LMM, Caetano ACR, Zamarian ACP, Mazzola JB, Silva CP, Marçal VMG, Lobo TF, Peixoto AB, Araujo Júnior E. Fetal growth restriction: current knowledge. Archives of Gynecology and Obstetrics. 2017;295(5):1061-77.

172. Sharma D, Shastri S, Sharma P. Intrauterine Growth Restriction: Antenatal and Postnatal Aspects. Clinical medicine insights Pediatrics. 2016;10:67-83.

173. Sharma D, Shastri S, Sharma P. Intrauterine Growth Restriction: Antenatal and Postnatal Aspects. Clinical Medicine Insights: Pediatrics. 2016;10:CMPed.S40070.

174. Puccio G, Giuffré M, Piccione M, Piro E, Malerba V, Corsello G. Intrauterine growth pattern and birthweight discordance in twin pregnancies: a retrospective study. Italian Journal of Pediatrics. 2014;40(1):43.

175. Heinonen S, Taipale P, Saarikoski S. Weights of placentae from small-for-gestational age infants revisited. Placenta. 2001;22(5):399-404.

176. Pardi G, Marconi AM, Cetin I. Pathophysiology of intrauterine growth retardation: role of the placenta. Acta Paediatrica. 1997;86(S423):170-2.

177. Zygmunt M. Placental circulation: Clinical significance. Early Pregnancy (Online). 2001;5(1):72-3.

178. Djakovic A, Rieger L, Wirbelauer J, Kalla J, Dietl J. Severe foetal growth retardation in a patient with uterus bicornis, velamentous insertion and partial placental abruption in the 26th week of gestation--a case report. Zeitschrift fur Geburtshilfe und Neonatologie. 2007;211(4):169-73.

179. Bjøro Jr K, editor Gross pathology of the placenta in intrauterine growth retardation. Annales chirurgiae et gynaecologiae; 1981.

180. Seitz J, Morales-Prieto DM, Favaro RR, Schneider H, Markert UR. Molecular Principles of Intrauterine Growth Restriction in Plasmodium Falciparum Infection. Frontiers in Endocrinology. 2019;10(98).

181. Netchine I, Azzi S, Le Bouc Y, Savage MO. IGF1 molecular anomalies demonstrate its critical role in fetal, postnatal growth and brain development. Best practice & research Clinical endocrinology & metabolism. 2011;25(1):181-90.

182. Agrogiannis GD, Sifakis S, Patsouris ES, Konstantinidou AE. Insulin-like growth factors in embryonic and fetal growth and skeletal development. Molecular medicine reports. 2014;10(2):579-84.

183. Jakó M, Surányi A, Kaizer L, Németh G, Bártfai G. Maternal Hematological Parameters and Placental and Umbilical Cord Histopathology in Intrauterine Growth Restriction. Med Princ Pract. 2019;28(2):101-8.

184. Macara L, Kingdom JC, Kaufmann P, Kohnen G, Hair J, More IA, Lyall F, Greer IA. Structural analysis of placental terminal villi from growth-restricted pregnancies with abnormal umbilical artery Doppler waveforms. Placenta. 1996;17(1):37-48.

185. Redline RW, Patterson P. Patterns of placental injury. Correlations with gestational age, placental weight, and clinical diagnoses. Arch Pathol Lab Med. 1994;118(7):698-701.

186. Smith SC, Baker PN, Symonds EM. Increased placental apoptosis in intrauterine growth restriction. American journal of obstetrics and gynecology. 1997;177(6):1395-401.

187. Park S-Y, Kim MY, Kim YJ, Chun YK, Kim HS, Kim HS, Hong SR. Placental pathology in intrauterine growth retardation. 대한병리학회지: 제. 2002;36(1).

188. Krebs C, Macara LM, Leiser R, Bowman AW, Greer IA, Kingdom JC. Intrauterine growth restriction with absent end-diastolic flow velocity in the umbilical artery is associated with maldevelopment of the placental terminal villous tree. American journal of obstetrics and gynecology. 1996;175(6):1534-42.

189. McCowan LM, Craigie S, Taylor RS, Ward C, McLintock C, North RA. Inherited thrombophilias are not increased in “idiopathic” small-for-gestational-age pregnancies. American journal of obstetrics and gynecology. 2003;188(4):981-5.

190. Li B, Chang S, Liu C, Zhang M, Zhang L, Liang L, Li R, Wang X, Qin C, Zhang T, Niu B, Wang L. Low Maternal Dietary Folate Alters Retrotranspose by Methylation Regulation in Intrauterine Growth Retardation (IUGR) Fetuses in a Mouse Model. Medical science monitor : international medical journal of experimental and clinical research. 2019;25:3354-65.

191. Rolfo A, Nuzzo AM, De Amicis R, Moretti L, Bertoli S, Leone A. Fetal-Maternal Exposure to Endocrine Disruptors: Correlation with Diet Intake and Pregnancy Outcomes. Nutrients. 2020;12(6):1744.

192. Sebastiani G, Herranz Barbero A, Borrás-Novell C, Alsina Casanova M, Aldecoa-Bilbao V, Andreu-Fernández V, Pascual Tutusaus M, Ferrero Martínez S, Gómez Roig MD, García-Algar O. The Effects of Vegetarian and Vegan Diet during Pregnancy on the Health of Mothers and Offspring. Nutrients. 2019;11(3):557.

193. Sebastiani G, Borrás-Novell C, Casanova MA, Pascual Tutusaus M, Ferrero Martínez S, Gómez Roig MD, García-Algar O. The Effects of Alcohol and Drugs of Abuse on Maternal Nutritional Profile during Pregnancy. Nutrients. 2018;10(8):1008.

194. Rasmussen C, Andrew G, Zwaigenbaum L, Tough S. Neurobehavioural outcomes of children with fetal alcohol spectrum disorders: A Canadian perspective. Paediatrics & child health. 2008;13(3):185-91.

195. Liu AJ, Sithamparanathan S, Jones MP, Cook CM, Nanan R. Growth restriction in pregnancies of opioid-dependent mothers. Arch Dis Child Fetal Neonatal Ed. 2010;95(4):F258-62.

196. Griffiths SK, Campbell JP. Placental structure, function and drug transfer. Continuing Education in Anaesthesia Critical Care & Pain. 2015;15(2):84-9.

197. Timalsina U, Andrasovich A, Kupferman FE, Viswanathan K, Ericksen K. Reversal of Opioid Intoxication in an Infant With Intrauterine Growth Restriction With a Single Dose of Naloxone. Cureus. 2021;13(10):e18908.

198. Ganapathy V. Drugs of abuse and human placenta. Life sciences. 2011;88(21-22):926-30.

199. Ballester F, Estarlich M, Iñiguez C, Llop S, Ramón R, Esplugues A, Lacasaña M, Rebagliato M. Air pollution exposure during pregnancy and reduced birth size: a

prospective birth cohort study in Valencia, Spain. Environmental Health. 2010;9(1):1-11.

200. Estarlich M, Ballester F, Aguilera I, Fernández-Somoano A, Lertxundi A, Llop S, Freire C, Tardón A, Basterrechea M, Sunyer J. Residential exposure to outdoor air pollution during pregnancy and anthropometric measures at birth in a multicenter cohort in Spain. Environmental health perspectives. 2011;119(9):1333-8.

201. Familari M, Naav A, Erlandsson L, de Iongh RU, Isaxon C, Strandberg B, Lundh T, Hansson SR, Malmqvist E. Exposure of trophoblast cells to fine particulate matter air pollution leads to growth inhibition, inflammation and ER stress. PLoS One. 2019;14(7):e0218799.

202. Rich DQ, Demissie K, Lu S-E, Kamat L, Wartenberg D, Rhoads GG. Ambient air pollutant concentrations during pregnancy and the risk of fetal growth restriction. Journal of Epidemiology & Community Health. 2009;63(6):488-96.

203. Nethery E, Teschke K, Brauer M. Predicting personal exposure of pregnant women to traffic-related air pollutants. Science of the total environment. 2008;395(1):11-22.

204. Dutta A, Alexander D, Karrison T, Morhasson-Bello O, Wilson N, Atalabi OM, Adu D, Ibigbami T, Adekunle S, Adepoju D, Olamijulo J, Akinwunmi O, Afolabi OS, Deji-Abiodun O, Adedokun B, Aschebrook-Kilfoy B, Ojengbede O, Olopade CO. Household air pollution, ultrasound measurement, fetal biometric parameters and intrauterine growth restriction. Environmental health : a global access science source. 2021;20(1):74-.

205. Gabory A, Attig L, Junien C. Developmental programming and epigenetics. The American Journal of Clinical Nutrition. 2011;94(suppl_6):1943S-52S.

206. Januar V, Desoye G, Novakovic B, Cvitic S, Saffery R. Epigenetic regulation of human placental function and pregnancy outcome: considerations for causal inference. American Journal of Obstetrics and Gynecology. 2015;213(4, Supplement):S182-S96.

207. Koukoura O, Sifakis S, Zaravinos A, Apostolidou S, Jones A, Hajiioannou J, Widschwendter M, Spandidos DA. Hypomethylation along with increased H19 expression in placentas from pregnancies complicated with fetal growth restriction. Placenta. 2011;32(1):51-7.

208. Yuen RK, Jiang R, Penaherrera MS, McFadden DE, Robinson WP. Genome-wide mapping of imprinted differentially methylated regions by DNA methylation profiling of human placentas from triploidies. Epigenetics & chromatin. 2011;4(1):1-16.

209. Crider KS, Whitehead N, Buus RM. Genetic variation associated with preterm birth: a HuGE review. Genetics in Medicine. 2005;7(9):593-604.

210. Beard JR, Lincoln D, Donoghue D, Taylor D, Summerhayes R, Dunn TM, Earnest A, Morgan G. Socioeconomic and maternal determinants of small-for-gestational age births: Patterns of increasing disparity. Acta Obstetricia et Gynecologica Scandinavica. 2009;88(5):575-83.

211. Baschat A. Neurodevelopment following fetal growth restriction and its relationship with antepartum parameters of placental dysfunction. Ultrasound in obstetrics & gynecology. 2011;37(5):501-14.

212. Johansson I-M, Birzniece V, Lindblad C, Olsson T, Bäckström T. Allopregnanolone inhibits learning in the Morris water maze. Brain research. 2002;934(2):125-31.

213. Sedlmayr P, Blaschitz A, Stocker R. The Role of Placental Tryptophan Catabolism. Frontiers in Immunology. 2014;5(230).

214. Fleiss B, Wong F, Brownfoot F, Shearer IK, Baud O, Walker DW, Gressens P, Tolcos M. Knowledge Gaps and Emerging Research Areas in Intrauterine Growth Restriction-Associated Brain Injury. Frontiers in Endocrinology. 2019;10(188).

215. Figueras F, Cruz-Martinez R, Sanz-Cortes M, Arranz A, Illa M, Botet F, Costas-Moragas C, Gratacos E. Neurobehavioral outcomes in preterm, growth-restricted infants with and without prenatal advanced signs of brain-sparing. Ultrasound Obstet Gynecol. 2011;38(3):288-94.

216. Murray E, Fernandes M, Fazel M, Kennedy SH, Villar J, Stein A. Differential effect of intrauterine growth restriction on childhood neurodevelopment: a systematic review. Bjog. 2015;122(8):1062-72.

217. Hernandez-Andrade E, Figueroa-Diesel H, Jansson T, Rangel-Nava H, Gratacos E. Changes in regional fetal cerebral blood flow perfusion in relation to hemodynamic deterioration in severely growth-restricted fetuses. Ultrasound Obstet Gynecol. 2008;32(1):71-6.

218. Tolsa CB, Zimine S, Warfield SK, Freschi M, Rossignol AS, Lazeyras F, Hanquinet S, Pfizenmaier M, Hüppi PS. Early alteration of structural and functional brain development in premature infants born with intrauterine growth restriction. Pediatric research. 2004;56(1):132-8.

219. Rees S, Harding R, Walker D. The biological basis of injury and neuroprotection in the fetal and neonatal brain. Int J Dev Neurosci. 2011;29(6):551-63.

220. Poudel R, McMillen IC, Dunn SL, Zhang S, Morrison JL. Impact of chronic hypoxemia on blood flow to the brain, heart, and adrenal gland in the late-gestation IUGR sheep fetus. Am J Physiol Regul Integr Comp Physiol. 2015;308(3):R151-62.

221. Lister JP, Blatt GJ, DeBassio WA, Kemper TL, Tonkiss J, Galler JR, Rosene DL. Effect of prenatal protein malnutrition on numbers of neurons in the principal cell layers of the adult rat hippocampal formation. Hippocampus. 2005;15(3):393-403.

222. Mallard C, Loeliger M, Copolov D, Rees S. Reduced number of neurons in the hippocampus and the cerebellum in the postnatal guinea-pig following intrauterine growth-restriction. Neuroscience. 2000;100(2):327-33.

223. Hayakawa M, Mimura S, Sasaki J, Watanabe K. Neuropathological changes in the cerebrum of IUGR rat induced by synthetic thromboxane A2. Early Hum Dev. 1999;55(2):125-36.

224. Dezateux C, Lum S, Hoo AF, Hawdon J, Costeloe K, Stocks J. Low birth weight for gestation and airway function in infancy: exploring the fetal origins hypothesis. Thorax. 2004;59(1):60-6.

225. Pike KC, Crozier SR, Lucas JS, Inskip HM, Robinson S, Roberts G, Godfrey KM. Patterns of fetal and infant growth are related to atopy and wheezing disorders at age 3 years. Thorax. 2010;65(12):1099-106.

226. Morsing E, Gustafsson P, Brodszki J. Lung function in children born after foetal growth restriction and very preterm birth. Acta Paediatr. 2012;101(1):48-54.

227. Kotecha SJ, Watkins WJ, Henderson AJ, Kotecha S. The effect of birth weight on lung spirometry in white, school-aged children and adolescents born at term: a

longitudinal population based observational cohort study. J Pediatr. 2015;166(5):1163-7.

228. Maritz GS, Cock ML, Louey S, Suzuki K, Harding R. Fetal growth restriction has long-term effects on postnatal lung structure in sheep. Pediatr Res. 2004;55(2):287-95.

229. Joss-Moore LA, Lane RH, Albertine KH. Epigenetics and the developmental origins of lung disease. The Lung. 2014:299-308.

230. Rehan VK, Sakurai R, Li Y, Karadag A, Corral J, Bellusci S, Xue YY, Belperio J, Torday JS. Effects of maternal food restriction on offspring lung extracellular matrix deposition and long term pulmonary function in an experimental rat model. Pediatric pulmonology. 2012;47(2):162-71.

231. O'Brien EA, Barnes V, Zhao L, McKnight RA, Yu X, Callaway CW, Wang L, Sun J, Dahl MJ, Wint A. Uteroplacental insufficiency decreases p53 serine-15 phosphorylation in term IUGR rat lungs. American Journal of Physiology-Regulatory, Integrative and Comparative Physiology. 2007;293(1):R314-R22.

232. Rozance PJ, Seedorf GJ, Brown A, Roe G, O'Meara MC, Gien J, Tang J-R, Abman SH. Intrauterine growth restriction decreases pulmonary alveolar and vessel growth and causes pulmonary artery endothelial cell dysfunction in vitro in fetal sheep. American Journal of Physiology-Lung Cellular and Molecular Physiology. 2011;301(6):L860-L71.

233. Corstius HB, Zimanyi MA, Maka N, Herath T, Thomas W, Van Der Laarse A, Wreford NG, Black MJ. Effect of intrauterine growth restriction on the number of cardiomyocytes in rat hearts. Pediatric research. 2005;57(6):796-800.

234. Wadley GD, McConell GK, Goodman CA, Siebel AL, Westcott KT, Wlodek ME. Growth restriction in the rat alters expression of metabolic genes during postnatal cardiac development in a sex-specific manner. Physiological genomics. 2013;45(3):99-105.

235. Crispi F, Bijnens B, Figueras F, Bartrons J, Eixarch E, Le Noble F, Ahmed A, Gratacós E. Fetal growth restriction results in remodeled and less efficient hearts in children. Circulation. 2010;121(22):2427-36.

236. Sarvari SI, Rodriguez-Lopez M, Nuñez-Garcia M, Sitges M, Sepulveda-Martinez A, Camara O, Butakoff C, Gratacos E, Bijnens B, Crispi F. Persistence of Cardiac Remodeling in Preadolescents With Fetal Growth Restriction. Circ Cardiovasc Imaging. 2017;10(1).

237. ACOG Practice bulletin no. 134: fetal growth restriction. Obstet Gynecol. 2013;121(5):1122-33.

238. Reece EA, Smikle C, O'Connor TZ, Holford T, Nelson-Robinson L, Degennaro N, Hobbins JC. A longitudinal study comparing growth in diabetic pregnancies with growth in normal gestations: I. The fetal weight. Obstet Gynecol Surv. 1990;45(3):161-4.

239. Nabhan AF, Abdelmoula YA. Amniotic fluid index versus single deepest vertical pocket as a screening test for preventing adverse pregnancy outcome. Cochrane Database Syst Rev. 2008;2008(3):Cd006593.

240. Lausman A, Kingdom J. Intrauterine growth restriction: screening, diagnosis, and management. J Obstet Gynaecol Can. 2013;35(8):741-8.

241. Sweet DG, Carnielli V, Greisen G, Hallman M, Ozek E, Te Pas A, Plavka R, Roehr CC, Saugstad OD, Simeoni U. European consensus guidelines on the

management of respiratory distress syndrome–2019 update. Neonatology. 2019;115(4):432-50.

242. Hallows SE, Regnault TR, Betts DH. The long and short of it: the role of telomeres in fetal origins of adult disease. Journal of pregnancy. 2012;2012.

243. Biron-Shental T, Sadeh-Mestechkin D, Amiel A. Telomere homeostasis in IUGR placentas – A review. Placenta. 2016;39:21-3.

244. Ietta F, Wu Y, Winter J, Xu J, Wang J, Post M, Caniggia I. Dynamic HIF1A regulation during human placental development. Biology of reproduction. 2006;75(1):112-21.

245. Nishi H, Nakada T, Kyo S, Inoue M, Shay JW, Isaka K. Hypoxia-inducible factor 1 mediates upregulation of telomerase (hTERT). Molecular and cellular biology. 2004;24(13):6076-83.

246. Vrijens K, Tsamou M, Madhloum N, Gyselaers W, Nawrot TS. Placental hypoxia-regulating network in relation to birth weight and ponderal index: the ENVIR ON AGE Birth Cohort Study. Journal of translational medicine. 2018;16(1):1-8.

247. Fox H. Aging of the placenta. Archives of disease in childhood Fetal and neonatal edition. 1997;77(3):F171-F5.

248. Guller S. Role of the syncytium in placenta-mediated complications of preeclampsia. Thrombosis research. 2009;124(4):389-92.

249. Roland L, Beauchemin D, Acteau G, Fradette C, St-Pierre I, Bilodeau JF. Effects of labor on placental expression of superoxide dismutases in preeclampsia. Placenta. 2010;31(5):392-400.

250. Roland CS, Hu J, Ren C-E, Chen H, Li J, Varvoutis MS, Leaphart LW, Byck DB, Zhu X, Jiang S-W. Morphological changes of placental syncytium and their implications for the pathogenesis of preeclampsia. Cellular and molecular life sciences. 2016;73(2):365-76.

251. Biron-Shental T, Sukenik-Halevy R, Naboani H, Liberman M, Kats R, Amiel A. Telomeres are shorter in placentas from pregnancies with uncontrolled diabetes. Placenta. 2015;36(2):199-203.

252. Biron-Shental T, Sukenik Halevy R, Goldberg-Bittman L, Kidron D, Fejgin MD, Amiel A. Telomeres are shorter in placental trophoblasts of pregnancies complicated with intrauterine growth restriction (IUGR). Early Human Development. 2010;86(7):451-6.

253. Yang X, Benny PA, Cervera-Marzal E, Wu B, Lassiter C, Astern J, Garmire LX. Placental telomere length shortening is not associated with preeclampsia but the gestational age. medRxiv. 2022:2022.02.28.22271630.

254. Cindrova-Davies T, Fogarty NME, Jones CJP, Kingdom J, Burton GJ. Evidence of oxidative stress-induced senescence in mature, post-mature and pathological human placentas. Placenta. 2018;68:15-22.

255. Toutain J, Prochazkova-Carlotti M, Cappellen D, Jarne A, Chevret E, Ferrer J, Idrissi Y, Pelluard F, Carles D, Maugey-Laulon B, Lacombe D, Horovitz J, Merlio J-P, Saura R. Reduced Placental Telomere Length during Pregnancies Complicated by Intrauterine Growth Restriction. PLOS ONE. 2013;8(1):e54013.

256. Biron-Shental T, Sukenik-Halevy R, Sharon Y, Goldberg-Bittman L, Kidron D, Fejgin MD, Amiel A. Short telomeres may play a role in placental dysfunction in

preeclampsia and intrauterine growth restriction. American Journal of Obstetrics & Gynecology. 2010;202(4):381.e1-.e7.

257. Roggensack AM, Zhang Y, Davidge ST. Evidence for peroxynitrite formation in the vasculature of women with preeclampsia. Hypertension. 1999;33(1):83-9.

258. Nuzzo AM, Giuffrida D, Masturzo B, Mele P, Piccoli E, Eva C, Todros T, Rolfo A. Altered expression of G1/S phase cell cycle regulators in placental mesenchymal stromal cells derived from preeclamptic pregnancies with fetal-placental compromise. Cell Cycle. 2017;16(2):200-12.

259. Sharp AN, Heazell AEP, Baczyk D, Dunk CE, Lacey HA, Jones CJP, Perkins JE, Kingdom JCP, Baker PN, Crocker IP. Preeclampsia is associated with alterations in the p53-pathway in villous trophoblast. PloS one. 2014;9(1):e87621-e.

260. Gao Q, Zhu X, Chen J, Mao C, Zhang L, Xu Z. Upregulation of P53 promoted G1arrest and apoptosis in human umbilical cord vein endothelial cells from preeclampsia. Journal of hypertension. 2016;34(7):1380.

261. Leavey K, Wilson SL, Bainbridge SA, Robinson WP, Cox BJ. Epigenetic regulation of placental gene expression in transcriptional subtypes of preeclampsia. Clinical epigenetics. 2018;10(1):1-13.

262. Mirbahai L, Chipman JK. Epigenetic memory of environmental organisms: a reflection of lifetime stressor exposures. Mutation Research/Genetic Toxicology and Environmental Mutagenesis. 2014;764:10-7.

263. Maccani MA, Marsit CJ. Epigenetics in the placenta. American Journal of Reproductive Immunology. 2009;62(2):78-89.

264. Eddy AC, Chapman H, George EM. Acute hypoxia and chronic ischemia induce differential total changes in placental epigenetic modifications. Reproductive Sciences. 2019;26(6):766-73.

265. Gabbe SG, Niebyl JR, Simpson JL, Landon MB, Galan HL, Jauniaux ER, Driscoll DA, Berghella V, Grobman WA. Obstetrics: normal and problem pregnancies e-book: Elsevier Health Sciences; 2016.

266. Burton G, Yung H, Murray A. Mitochondrial–endoplasmic reticulum interactions in the trophoblast: stress and senescence. Placenta. 2017;52:146-55.

267. McCarthy CM, Kenny LC. Mitochondrial [dys] function; culprit in pre-eclampsia? Clinical Science. 2016;130(14):1179-84.

268. Ježek P, Hlavatá L. Mitochondria in homeostasis of reactive oxygen species in cell, tissues, and organism. The international journal of biochemistry & cell biology. 2005;37(12):2478-503.

269. Luo X, Yao Z-w, Qi H-b, Liu D-d, Chen G-q, Huang S, Li Q-s. Gadd45α as an upstream signaling molecule of p38 MAPK triggers oxidative stress-induced sFlt-1 and sEng upregulation in preeclampsia. Cell and tissue research. 2011;344(3):551-65.

270. Wang Y, Walsh S. Placental mitochondria as a source of oxidative stress in pre-eclampsia. Placenta. 1998;19(8):581-6.

271. Fujimaki A, Watanabe K, Mori T, Kimura C, Shinohara K, Wakatsuki A. Placental oxidative DNA damage and its repair in preeclamptic women with fetal growth restriction. Placenta. 2011;32(5):367-72.

272. Repetto M, Semprine J, Boveris A. Lipid peroxidation: chemical mechanism, biological implications and analytical determination. Lipid peroxidation. 2012;1:3-30.

273. Spiteller G. Lipid peroxidation in aging and age-dependent diseases. Experimental gerontology. 2001;36(9):1425-57.

274. Lyall F, Bulmer JN, Kelly H, Duffie E, Robson SC. Human trophoblast invasion and spiral artery transformation: the role of nitric oxide. The American journal of pathology. 1999;154(4):1105-14.

275. Kossenjans W, Eis A, Sahay R, Brockman D, Myatt L. Role of peroxynitrite in altered fetal-placental vascular reactivity in diabetes or preeclampsia. American Journal of Physiology-Heart and Circulatory Physiology. 2000;278(4):H1311-H9.

276. Seo AY, Joseph A-M, Dutta D, Hwang JC, Aris JP, Leeuwenburgh C. New insights into the role of mitochondria in aging: mitochondrial dynamics and more. Journal of cell science. 2010;123(15):2533-42.

277. Sun N, Youle RJ, Finkel T. The mitochondrial basis of aging. Molecular cell. 2016;61(5):654-66.

278. Chen H, Detmer SA, Ewald AJ, Griffin EE, Fraser SE, Chan DC. Mitofusins Mfn1 and Mfn2 coordinately regulate mitochondrial fusion and are essential for embryonic development. The Journal of cell biology. 2003;160(2):189-200.

279. Zhang L, Han L, Ma R, Hou X, Yu Y, Sun S, Xu Y, Schedl T, Moley KH, Wang Q. Sirt3 prevents maternal obesity-associated oxidative stress and meiotic defects in mouse oocytes. Cell Cycle. 2015;14(18):2959-68.

280. Williamson RD, McCarthy C, McCarthy FP, Kenny LC. Oxidative stress in pre-eclampsia; have we been looking in the wrong place? Pregnancy Hypertension: An International Journal of Women's Cardiovascular Health. 2017;8:1-5.

281. Lobo V, Patil A, Phatak A, Chandra N. Free radicals, antioxidants and functional foods: Impact on human health. Pharmacognosy reviews. 2010;4(8):118.

282. Qiu C, Hevner K, Enquobahrie DA, Williams MA. A case-control study of maternal blood mitochondrial DNA copy number and preeclampsia risk. International journal of molecular epidemiology and genetics. 2012;3(3):237.

283. Williamson RD, McCarthy FP, Khashan AS, Totorika A, Kenny LC, McCarthy C. Exploring the role of mitochondrial dysfunction in the pathophysiology of pre-eclampsia. Pregnancy Hypertens. 2018;13:248-53.

284. Marschalek J, Wohlrab P, Ott J, Wojta J, Speidl W, Klein KU, Kiss H, Pateisky P, Zeisler H, Kuessel L. Maternal serum mitochondrial DNA (mtDNA) levels are elevated in preeclampsia–a matched case-control study. Pregnancy Hypertension. 2018;14:195-9.

285. Marquez CMD, Ibana JA, Velarde MC. The female reproduction and senescence nexus. American Journal of Reproductive Immunology. 2017;77(5):e12646.

286. Kupferminc MJ, Peaceman AM, Wigton TR, Rehnberg KA, Socol ML. Tumor necrosis factor-α is elevated in plasma and amniotic fluid of patients with severe preeclampsia. American journal of obstetrics and gynecology. 1994;170(6):1752-9.

287. Altara R, Ghali R, Mallat Z, Cataliotti A, Booz GW, Zouein FA. Conflicting vascular and metabolic impact of the IL-33/sST2 axis. Cardiovascular research. 2018;114(12):1578-94.

288. Romero R, Chaemsaithong P, Tarca AL, Korzeniewski SJ, Maymon E, Pacora P, Panaitescu B, Chaiyasit N, Dong Z, Erez O. Maternal plasma-soluble ST2 concentrations are elevated prior to the development of early and late onset preeclampsia–a longitudinal study. The Journal of Maternal-Fetal & Neonatal Medicine. 2018;31(4):418-32.

289. Shi X, Sun M, Liu H, Yao Y, Song Y. Long non-coding RNAs: a new frontier in the study of human diseases. Cancer letters. 2013;339(2):159-66.

290. Munjas J, Sopić M, Stefanović A, Košir R, Ninić A, Joksić I, Antonić T, Spasojević-Kalimanovska V, Prosenc Zmrzljak U. Non-Coding RNAs in Preeclampsia-Molecular Mechanisms and Diagnostic Potential. Int J Mol Sci. 2021;22(19).

291. Tan Y, Xiao D, Xu Y, Wang C. Long non-coding RNA DLX6-AS1 is upregulated in preeclampsia and modulates migration and invasion of trophoblasts through the miR-376c/GADD45A axis. Experimental Cell Research. 2018;370(2):718-24.

292. Robinson JM, Ackerman WEt, Kniss DA, Takizawa T, Vandre DD. Proteomics of the human placenta: promises and realities. Placenta. 2008;29(2):135-43.

293. Rice GE, Georgiou HM, Ahmed N, Shi G, Kruppa G. Translational Proteomics: Developing a Predictive Capacity – A Review. Placenta. 2006;27:76-86.

294. Mary S, Kulkarni MJ, Malakar D, Joshi SR, Mehendale SS, Giri AP. Placental Proteomics Provides Insights into Pathophysiology of Pre-Eclampsia and Predicts Possible Markers in Plasma. J Proteome Res. 2017;16(2):1050-60.

295. Erez O, Romero R, Maymon E, Chaemsaithong P, Done B, Pacora P, Panaitescu B, Chaiworapongsa T, Hassan SS, Tarca AL. The prediction of late-onset preeclampsia: Results from a longitudinal proteomics study. PLoS One. 2017;12(7):e0181468.

296. Tarca AL, Romero R, Benshalom-Tirosh N, Than NG, Gudicha DW, Done B, Pacora P, Chaiworapongsa T, Panaitescu B, Tirosh D, Gomez-Lopez N, Draghici S, Hassan SS, Erez O. The prediction of early preeclampsia: Results from a longitudinal proteomics study. PLOS ONE. 2019;14(6):e0217273.

297. Myers JE, Tuytten R, Thomas G, Laroy W, Kas K, Vanpoucke G, Roberts CT, Kenny LC, Simpson NA, Baker PN, North RA. Integrated proteomics pipeline yields novel biomarkers for predicting preeclampsia. Hypertension. 2013;61(6):1281-8.

298. Carty DM, Delles C, Dominiczak AF. Novel Biomarkers for Predicting Preeclampsia. Trends in Cardiovascular Medicine. 2008;18(5):186-94.

299. Rana S, Lemoine E, Granger JP, Karumanchi SA. Preeclampsia. Circulation Research. 2019;124(7):1094-112.

300. Martinez-Fierro ML, Hernández-Delgadillo GP, Flores-Morales V, Cardenas-Vargas E, Mercado-Reyes M, Rodriguez-Sanchez IP, Delgado-Enciso I, Galván-Tejada CE, Galván-Tejada JI, Celaya-Padilla JM, Garza-Veloz I. Current model systems for the study of preeclampsia. Exp Biol Med (Maywood). 2018;243(6):576-85.

301. Moufarrej MN, Vorperian SK, Wong RJ, Campos AA, Quaintance CC, Sit RV, Tan M, Detweiler AM, Mekonen H, Neff NF, Baruch-Gravett C, Litch JA, Druzin ML, Winn VD, Shaw GM, Stevenson DK, Quake SR. Early prediction of preeclampsia in pregnancy with cell-free RNA. Nature. 2022;602(7898):689-94.

302. MacDonald TM, Walker SP, Hannan NJ, Tong S, Kaitu'u-Lino TJ. Clinical tools and biomarkers to predict preeclampsia. EBioMedicine. 2022;75:103780.

303. Breitling R. What is systems biology? Front Physiol. 2010;1:9.

304. Colquitt RB, Colquhoun DA, Thiele RH. In silico modelling of physiologic systems. Best Pract Res Clin Anaesthesiol. 2011;25(4):499-510.

305. Manna S, Ruano CSM, Hegenbarth J-C, Vaiman D, Gupta S, McCarthy FP, Méhats C, McCarthy C, Apicella C, Scheel J. Computational Models on Pathological Redox Signalling Driven by Pregnancy: A Review. Antioxidants. 2022;11(3):585.

306. Barh D, Chaitankar V, Yiannakopoulou EC, Salawu EO, Chowbina S, Ghosh P, Azevedo V. In Silico Models: From Simple Networks to Complex Diseases: Animal Biotechnology. 2014:385-404. doi: 10.1016/B978-0-12-416002-6.00021-3. Epub 2013 Nov 15.

307. Leemis LM, editor Computational probability applications. Proceedings of the Winter Simulation Conference 2014; 2014: IEEE.

308. Paauw ND, Lely AT. Cardiovascular Sequels During and After Preeclampsia. Adv Exp Med Biol. 2018;1065:455-70.

309. Calcinotto A, Kohli J, Zagato E, Pellegrini L, Demaria M, Alimonti A. Cellular Senescence: Aging, Cancer, and Injury. Physiological Reviews. 2019;99(2):1047-78.

310. Sultana Z, Maiti K, Dedman L, Smith R. Is there a role for placental senescence in the genesis of obstetric complications and fetal growth restriction? American Journal of Obstetrics and Gynecology. 2018;218(2, Supplement):S762-S73.

311. Ho JH, Chen Y-F, Ma W-H, Tseng T-C, Chen M-H, Lee OK. Cell Contact Accelerates Replicative Senescence of Human Mesenchymal Stem Cells Independent of Telomere Shortening and p53 Activation: Roles of Ras and Oxidative Stress. Cell Transplantation. 2011;20(8):1209-20.

312. Morgan RG, Ives SJ, Walker AE, Cawthon RM, Andtbacka RHI, Noyes D, Lesniewski LA, Richardson RS, Donato AJ. Role of arterial telomere dysfunction in

hypertension: relative contributions of telomere shortening and telomere uncapping. Journal of hypertension. 2014;32(6):1293-9.

313. Farr JN, Khosla S. Cellular senescence in bone. Bone. 2019;121:121-33.

314. Chocron ES, Munkácsy E, Pickering AM. Cause or casualty: The role of mitochondrial DNA in aging and age-associated disease. Biochimica et Biophysica Acta (BBA) - Molecular Basis of Disease. 2019;1865(2):285-97.

315. Sanchez-Contreras M, Kennedy SR. The Complicated Nature of Somatic mtDNA Mutations in Aging. Frontiers in Aging. 2022;2.

316. Birch J, Gil J. Senescence and the SASP: many therapeutic avenues. Genes & development. 2020;34(23-24):1565-76.

317. Feringa FM, Raaijmakers JA, Hadders MA, Vaarting C, Macurek L, Heitink L, Krenning L, Medema RH. Persistent repair intermediates induce senescence. Nature Communications. 2018;9(1):3923.

318. Baker DJ, Jin F, van Deursen JM. The yin and yang of the Cdkn2a locus in senescence and aging. Cell cycle (Georgetown, Tex). 2008;7(18):2795-802.

319. Poehlmann A, Habold C, Walluscheck D, Reissig K, Bajbouj K, Ullrich O, Hartig R, Gali-Muhtasib H, Diestel A, Roessner A, Schneider-Stock R. Cutting edge: Chk1 directs senescence and mitotic catastrophe in recovery from G_2 checkpoint arrest. J Cell Mol Med. 2011;15(7):1528-41.

320. González-Gualda E, Baker AG, Fruk L, Muñoz-Espín D. A guide to assessing cellular senescence in vitro and in vivo. The FEBS Journal. 2021;288(1):56-80.

321. Wijaya JC, Khanabdali R, Georgiou HM, Kalionis B. Ageing in human parturition: impetus of the gestation clock in the decidua†. Biology of Reproduction. 2020;103(4):695-710.

322. Cox LS, Redman C. The role of cellular senescence in ageing of the placenta. Placenta. 2017;52:139-45.

323. Chuprin A, Gal H, Biron-Shental T, Biran A, Amiel A, Rozenblatt S, Krizhanovsky V. Cell fusion induced by ERVWE1 or measles virus causes cellular senescence. Genes & development. 2013;27(21):2356-66.

324. Harville EW, Williams MA, Qiu C-F, Mejia J, Risques RA. Telomere length, pre-eclampsia, and gestational diabetes. BMC research notes. 2010;3:113-.

325. Broady AJ, Loichinger MH, Ahn HJ, Davy PMC, Allsopp RC, Bryant-Greenwood GD. Protective proteins and telomere length in placentas from patients with pre-eclampsia in the last trimester of gestation. Placenta. 2017;50:44-52.

326. Burton GJ, Sebire NJ, Myatt L, Tannetta D, Wang YL, Sadovsky Y, Staff AC, Redman CW. Optimising sample collection for placental research. Placenta. 2014;35(1):9-22.

327. Ajaz S, Czajka A, Malik A. Accurate measurement of circulating mitochondrial DNA content from human blood samples using real-time quantitative PCR. Methods Mol Biol. 2015;1264:117-31.

328. Li B, Kalinowski P, Kim B, Pauls AD, Poburko D. Emerging methods for and novel insights gained by absolute quantification of mitochondrial DNA copy number and its clinical applications. Pharmacology & Therapeutics. 2022;232:107995.

329. Meller M, Vadachkoria S, Luthy DA, Williams MA. Evaluation of housekeeping genes in placental comparative expression studies. Placenta. 2005;26(8):601-7.

330. Lanoix D, St-Pierre J, Lacasse AA, Viau M, Lafond J, Vaillancourt C. Stability of reference proteins in human placenta: General protein stains are the benchmark. Placenta. 2012;33(3):151-6.

331. Li S-C, Lan K-C, Hung H-N, Huang W-T, Lai Y-J, Cheng H-H, Tsai C-C, Huang K-L, You H-L, Hsu T-Y. HSPA4 Is a Biomarker of Placenta Accreta and Enhances the Angiogenesis Ability of Vessel Endothelial Cells. International Journal of Molecular Sciences. 2022;23(10):5682.

332. McIntyre KR, Vincent KMM, Hayward CE, Li X, Sibley CP, Desforges M, Greenwood SL, Dilworth MR. Human placental uptake of glutamine and glutamate is reduced in fetal growth restriction. Sci Rep. 2020;10(1):16197.

333. Alimbetov D, Davis T, Brook AJ, Cox LS, Faragher RG, Nurgozhin T, Zhumadilov Z, Kipling D. Suppression of the senescence-associated secretory phenotype (SASP) in human fibroblasts using small molecule inhibitors of p38 MAP kinase and MK2. Biogerontology. 2016;17(2):305-15.

334. Hudgins AD, Tazearslan C, Tare A, Zhu Y, Huffman D, Suh Y. Age- and Tissue-Specific Expression of Senescence Biomarkers in Mice. Frontiers in Genetics. 2018;9.

335. Coppé JP, Desprez PY, Krtolica A, Campisi J. The senescence-associated secretory phenotype: the dark side of tumor suppression. Annu Rev Pathol. 2010;5:99-118.

336. Raijmakers MTM, Dechend R, Poston L. Oxidative Stress and Preeclampsia. Hypertension. 2004;44(4):374-80.

337. Tanase DM, Gosav EM, Radu S, Ouatu A, Rezus C, Ciocoiu M, Costea CF, Floria M. Arterial Hypertension and Interleukins: Potential Therapeutic Target or

Future Diagnostic Marker? International journal of hypertension. 2019;2019:3159283-.

338. Nakayama Y, Yamaguchi N. Chapter Seven - Role of Cyclin B1 Levels in DNA Damage and DNA Damage-Induced Senescence. In: Jeon KW, editor. International Review of Cell and Molecular Biology. 305: Academic Press; 2013. p. 303-37.

339. Maréchal A, Zou L. DNA damage sensing by the ATM and ATR kinases. Cold Spring Harbor perspectives in biology. 2013;5(9):a012716.

340. Moran DM, Mattocks MA, Cahill PA, Koniaris LG, McKillop IH. Interleukin-6 mediates G(0)/G(1) growth arrest in hepatocellular carcinoma through a STAT 3-dependent pathway. The Journal of surgical research. 2008;147(1):23-33.

341. Zhang W, Liu HT. MAPK signal pathways in the regulation of cell proliferation in mammalian cells. Cell Research. 2002;12(1):9-18.

342. Freeman DJ, McManus F, Brown EA, Cherry L, Norrie J, Ramsay JE, Clark P, Walker ID, Sattar N, Greer IA. Short-and long-term changes in plasma inflammatory markers associated with preeclampsia. Hypertension. 2004;44(5):708-14.

343. Seif F, Khoshmirsafa M, Aazami H, Mohsenzadegan M, Sedighi G, Bahar M. The role of JAK-STAT signaling pathway and its regulators in the fate of T helper cells. Cell Communication and Signaling. 2017;15(1):23.

344. Wagner J, Damaschke N, Yang B, Truong M, Guenther C, McCormick J, Huang W, Jarrard D. Overexpression of the novel senescence marker β-galactosidase (GLB1) in prostate cancer predicts reduced PSA recurrence. PLoS One. 2015;10(4):e0124366.

345. Alani RM, Young AZ, Shifflett CB. Id1 regulation of cellular senescence through transcriptional repression of p16/Ink4a. Proc Natl Acad Sci U S A. 2001;98(14):7812-6.

346. Sanada F, Taniyama Y, Muratsu J, Otsu R, Shimizu H, Rakugi H, Morishita R. IGF Binding Protein-5 Induces Cell Senescence. Front Endocrinol (Lausanne). 2018;9:53.

347. Velarde MC, Flynn JM, Day NU, Melov S, Campisi J. Mitochondrial oxidative stress caused by Sod2 deficiency promotes cellular senescence and aging phenotypes in the skin. Aging (Albany NY). 2012;4(1):3-12.

348. Hewitt G, Jurk D, Marques FDM, Correia-Melo C, Hardy T, Gackowska A, Anderson R, Taschuk M, Mann J, Passos JF. Telomeres are favoured targets of a persistent DNA damage response in ageing and stress-induced senescence. Nature Communications. 2012;3(1):708.

349. He S, Sharpless NE. Senescence in Health and Disease. Cell. 2017;169(6):1000-11.

350. Davy P, Nagata M, Bullard P, Fogelson N, Allsopp R. Fetal growth restriction is associated with accelerated telomere shortening and increased expression of cell senescence markers in the placenta. Placenta. 2009;30(6):539-42.

351. Müllers E, Silva Cascales H, Burdova K, Macurek L, Lindqvist A. Residual Cdk1/2 activity after DNA damage promotes senescence. Aging cell. 2017;16(3):575-84.

352. Wang S, Zhou M, Lin F, Liu D, Hong W, Lu L, Zhu Y, Xu A. Interferon-γ Induces Senescence in Normal Human Melanocytes. PLOS ONE. 2014;9(3):e93232.

353. Freund A, Laberge R-M, Demaria M, Campisi J. Lamin B1 loss is a senescence-associated biomarker. Molecular Biology of the Cell. 2012;23(11):2066-75.

354. Novielli C, Mandò C, Tabano S, Anelli GM, Fontana L, Antonazzo P, Miozzo M, Cetin I. Mitochondrial DNA content and methylation in fetal cord blood of pregnancies with placental insufficiency. Placenta. 2017;55:63-70.

355. Foote K, Reinhold J, Yu EPK, Figg NL, Finigan A, Murphy MP, Bennett MR. Restoring mitochondrial DNA copy number preserves mitochondrial function and delays vascular aging in mice. Aging Cell. 2018;17(4):e12773.

356. Spano L, Etain B, Meyrel M, Hennion V, Gross G, Laplanche JL, Bellivier F, Marie-Claire C. Telomere length and mitochondrial DNA copy number in bipolar disorder: identification of a subgroup of young individuals with accelerated cellular aging. Translational Psychiatry. 2022;12(1):135.

357. Castellani CA, Longchamps RJ, Sumpter JA, Newcomb CE, Lane JA, Grove ML, Bressler J, Brody JA, Floyd JS, Bartz TM, Taylor KD, Wang P, Tin A, Coresh J, Pankow JS, Fornage M, Guallar E, O'Rourke B, Pankratz N, Liu C, Levy D, Sotoodehnia N, Boerwinkle E, Arking DE. Mitochondrial DNA copy number can influence mortality and cardiovascular disease via methylation of nuclear DNA CpGs. Genome Medicine. 2020;12(1):84.

358. Xiao JP, Yin YX, Gao YF, Lau S, Shen F, Zhao M, Chen Q. The increased maternal serum levels of IL-6 are associated with the severity and onset of preeclampsia. Cytokine. 2012;60(3):856-60.

359. Udenze I, Amadi C, Awolola N, Makwe CC. The role of cytokines as inflammatory mediators in preeclampsia. The Pan African medical journal. 2015;20:219-.

360. Kojima H, Kunimoto H, Inoue T, Nakajima K. The STAT3-IGFBP5 axis is critical for IL-6/gp130-induced premature senescence in human fibroblasts. Cell Cycle. 2012;11(4):730-9.

361. Kim KS, Kang KW, Seu YB, Baek S-H, Kim J-R. Interferon-γ induces cellular senescence through p53-dependent DNA damage signaling in human endothelial cells. Mechanisms of Ageing and Development. 2009;130(3):179-88.

362. Hubackova S, Kucerova A, Michlits G, Kyjacova L, Reinis M, Korolov O, Bartek J, Hodny Z. IFNγ induces oxidative stress, DNA damage and tumor cell senescence via TGFβ/SMAD signaling-dependent induction of Nox4 and suppression of ANT2. Oncogene. 2016;35(10):1236-49.

363. Manna S, Elwain CJM, Maher GM, Giralt Martín M, Musumeci A, McCarthy FP, McCarthy C. Heterogenous Differences in Cellular Senescent Phenotypes in Pre-Eclampsia and IUGR following Quantitative Assessment of Multiple Biomarkers of Senescence. International Journal of Molecular Sciences. 2023;24(4):3101.

364. Mossman HW. Comparative morphogenesis of the fetal membranes and accessory uterine structures. Placenta. 1991;12(1):1-5.

365. Khorami Sarvestani S, Shojaeian S, Vanaki N, Ghresi-Fard B, Amini M, Gilany K, Soltanghoraee H, Arefi S, Jeddi-Tehrani M, Zarnani A-H. Proteome profiling of human placenta reveals developmental stage-dependent alterations in protein signature. Clinical Proteomics. 2021;18(1):18.

366. Woods L, Perez-Garcia V, Hemberger M. Regulation of Placental Development and Its Impact on Fetal Growth—New Insights From Mouse Models. Frontiers in Endocrinology. 2018;9(570).

367. Maltepe E, Penn AA. Development, Function, and Pathology of the Placenta. In: Gleason CA, Juul SE, editors. Avery's Diseases of the Newborn (Tenth Edition). Philadelphia: Elsevier; 2018. p. 40-60.e8.

368. Holder B, Aplin JD, Gomez-Lopez N, Heazell AEP, James JL, Jones CJP, Jones H, Lewis RM, Mor G, Roberts CT, Robertson SA, Zenclussen AC. 'Fetal side' of the placenta: anatomical mis-annotation of carbon particle 'transfer' across the human placenta. Nature Communications. 2021;12(1):7049.

369. Bové H, Bongaerts E, Slenders E, Bijnens EM, Saenen ND, Gyselaers W, Van Eyken P, Plusquin M, Roeffaers MBJ, Ameloot M, Nawrot TS. Ambient black carbon particles reach the fetal side of human placenta. Nature Communications. 2019;10(1):3866.

370. Wang Y, Zhao S. Integrated Systems Physiology: from Molecules to Function to Disease. Vascular Biology of the Placenta. San Rafael (CA): Morgan & Claypool Life Sciences

Copyright © 2010 by Morgan & Claypool Life Sciences.; 2010.

371. Sultana Z, Maiti K, Aitken J, Morris J, Dedman L, Smith R. Oxidative stress, placental ageing-related pathologies and adverse pregnancy outcomes. American Journal of Reproductive Immunology. 2017;77(5):e12653.

372. Law KP, Han TL, Tong C, Baker PN. Mass spectrometry-based proteomics for pre-eclampsia and preterm birth. Int J Mol Sci. 2015;16(5):10952-85.

373. Nguyen TPH, Patrick CJ, Parry LJ, Familari M. Using proteomics to advance the search for potential biomarkers for preeclampsia: A systematic review and meta-analysis. PloS one. 2019;14(4):e0214671-e.

374. English JA, Lopez LM, O'Gorman A, Föcking M, Hryniewiecka M, Scaife C, Sabherwal S, Wynne K, Dicker P, Rutten BPF, Lewis G, Zammit S, Cannon M, Cagney G, Cotter DR. Blood-Based Protein Changes in Childhood Are Associated With Increased Risk for Later Psychotic Disorder: Evidence From a Nested Case-Control Study of the ALSPAC Longitudinal Birth Cohort. Schizophr Bull. 2018;44(2):297-306.

375. Tyanova S, Temu T, Sinitcyn P, Carlson A, Hein MY, Geiger T, Mann M, Cox J. The Perseus computational platform for comprehensive analysis of (prote)omics data. Nat Methods. 2016;13(9):731-40.

376. Bindea G, Mlecnik B, Hackl H, Charoentong P, Tosolini M, Kirilovsky A, Fridman W-H, Pagès F, Trajanoski Z, Galon J. ClueGO: a Cytoscape plug-in to decipher functionally grouped gene ontology and pathway annotation networks. Bioinformatics (Oxford, England). 2009;25(8):1091-3.

377. Mazein A, Ostaszewski M, Kuperstein I, Watterson S, Le Novère N, Lefaudeux D, De Meulder B, Pellet J, Balaur I, Saqi M, Nogueira MM, He F, Parton A, Lemonnier N, Gawron P, Gebel S, Hainaut P, Ollert M, Dogrusoz U, Barillot E, Zinovyev A, Schneider R, Balling R, Auffray C. Systems medicine disease maps: community-driven comprehensive representation of disease mechanisms. npj Systems Biology and Applications. 2018;4(1):21.

378. Scheel J, Gupta S, Wolkenhauer O. NaviCenta: Navigate the placenta. Placenta. 2021;112:e35.

379. Hoch M, Smita S, Cesnulevicius K, Lescheid D, Schultz M, Wolkenhauer O, Gupta S. Network- and enrichment-based inference of phenotypes and targets from large-scale disease maps. npj Systems Biology and Applications. 2022;8(1):13.

380. Uhlén M, Fagerberg L, Hallström BM, Lindskog C, Oksvold P, Mardinoglu A, Sivertsson Å, Kampf C, Sjöstedt E, Asplund A, Olsson I, Edlund K, Lundberg E, Navani S, Szigyarto CA, Odeberg J, Djureinovic D, Takanen JO, Hober S, Alm T, Edqvist PH, Berling H, Tegel H, Mulder J, Rockberg J, Nilsson P, Schwenk JM, Hamsten M, von Feilitzen K, Forsberg M, Persson L, Johansson F, Zwahlen M, von Heijne G, Nielsen J, Pontén F. Proteomics. Tissue-based map of the human proteome. Science. 2015;347(6220):1260419.

381. Yim A, Koti P, Bonnard A, Marchiano F, Dürrbaum M, Garcia-Perez C, Villaveces J, Gamal S, Cardone G, Perocchi F, Storchova Z, Habermann BH. mitoXplorer, a visual data mining platform to systematically analyze and visualize mitochondrial expression dynamics and mutations. Nucleic Acids Res. 2020;48(2):605-32.

382. Rath S, Sharma R, Gupta R, Ast T, Chan C, Durham TJ, Goodman RP, Grabarek Z, Haas ME, Hung WHW, Joshi PR, Jourdain AA, Kim SH, Kotrys AV, Lam SS, McCoy JG, Meisel JD, Miranda M, Panda A, Patgiri A, Rogers R, Sadre S, Shah H, Skinner OS, To TL, Walker MA, Wang H, Ward PS, Wengrod J, Yuan CC, Calvo SE, Mootha VK. MitoCarta3.0: an updated mitochondrial proteome now with sub-organelle localization and pathway annotations. Nucleic Acids Res. 2021;49(D1):D1541-d7.

383. Heberle H, Meirelles GV, da Silva FR, Telles GP, Minghim R. InteractiVenn: a web-based tool for the analysis of sets through Venn diagrams. BMC Bioinformatics. 2015;16(1):169.

384. Avelar RA, Ortega JG, Tacutu R, Tyler EJ, Bennett D, Binetti P, Budovsky A, Chatsirisupachai K, Johnson E, Murray A, Shields S, Tejada-Martinez D, Thornton D, Fraifeld VE, Bishop CL, de Magalhães JP. A multidimensional systems biology analysis of cellular senescence in aging and disease. Genome Biology. 2020;21(1):91.

385. Zhao M, Chen L, Qu H. CSGene: a literature-based database for cell senescence genes and its application to identify critical cell aging pathways and associated diseases. Cell Death & Disease. 2016;7(1):e2053-e.

386. Walter W, Sánchez-Cabo F, Ricote M. GOplot: an R package for visually combining expression data with functional analysis. Bioinformatics. 2015;31(17):2912-4.

387. Baergen RN. Chorionic Villi: Histology and Villous Development. Manual of Pathology of the Human Placenta: Second Edition. Boston, MA: Springer US; 2011. p. 69-83.

388. Zhang X, Lan Y, Xu J, Quan F, Zhao E, Deng C, Luo T, Xu L, Liao G, Yan M, Ping Y, Li F, Shi A, Bai J, Zhao T, Li X, Xiao Y. CellMarker: a manually curated resource of cell markers in human and mouse. Nucleic Acids Research. 2018;47(D1):D721-D8.

389. Burton GJ, Jauniaux E. Oxidative stress. Best practice & research Clinical obstetrics & gynaecology. 2011;25(3):287-99.

390. Burton GJ, Fowden AL. Review: The placenta and developmental programming: balancing fetal nutrient demands with maternal resource allocation. Placenta. 2012;33 Suppl:S23-7.

391. Samokhvalov V, Ignatov V, Kondrashova M. Inhibition of Krebs cycle and activation of glyoxylate cycle in the course of chronological aging of Saccharomyces cerevisiae. Compensatory role of succinate oxidation. Biochimie. 2004;86(1):39-46.

392. Wang H, Han L, Zhao G, Shen H, Wang P, Sun Z, Xu C, Su Y, Li G, Tong T, Chen J. hnRNP A1 antagonizes cellular senescence and senescence-associated secretory phenotype via regulation of SIRT1 mRNA stability. Aging Cell. 2016;15(6):1063-73.

393. Jia Q, Nie H, Yu P, Xie B, Wang C, Yang F, Wei G, Ni T. HNRNPA1-mediated 3' UTR length changes of HN1 contributes to cancer- and senescence-associated phenotypes. Aging (Albany NY). 2019;11(13):4407-37.

394. Djouadi F, Bastin J. Mitochondrial Genetic Disorders: Cell Signaling and Pharmacological Therapies. Cells. 2019;8(4).

395. Li S, Zhan J-K, Wang Y-J, Lin X, Zhong J-Y, Wang Y, Tan P, He J-Y, Cui X-J, Chen Y-Y, Huang W, Liu Y-S. Exosomes from hyperglycemia-stimulated vascular endothelial cells contain versican that regulate calcification/senescence in vascular smooth muscle cells. Cell & Bioscience. 2019;9(1):1.

396. Dahl ES, Buj R, Leon KE, Newell JM, Imamura Y, Bitler BG, Snyder NW, Aird KM. Targeting IDH1 as a Prosenescent Therapy in High-grade Serous Ovarian Cancer. Molecular Cancer Research. 2019;17(8):1710-20.

397. Tian C, Kim YJ, Hali S, Choo O-S, Lee J-S, Jung S-K, Choi Y-U, Park CB, Choung Y-H. Suppressed expression of LDHB promotes age-related hearing loss via aerobic glycolysis. Cell Death & Disease. 2020;11(5):375.

398. Mazhar M, Din AU, Ali H, Yang G, Ren W, Wang L, Fan X, Yang S. Implication of ferroptosis in aging. Cell Death Discovery. 2021;7(1):149.

399. Munir R, Lisec J, Swinnen JV, Zaidi N. Lipid metabolism in cancer cells under metabolic stress. British Journal of Cancer. 2019;120(12):1090-8.

400. Charitou P, Rodriguez-Colman M, Gerrits J, van Triest M, Groot Koerkamp M, Hornsveld M, Holstege F, Verhoeven-Duif NM, Burgering BM. FOXOs support the metabolic requirements of normal and tumor cells by promoting IDH1 expression. EMBO Rep. 2015;16(4):456-66.

401. Chen F, Wang T, Feng C, Lin G, Zhu Y, Wu G, Johnson G, Wang J. Proteome Differences in Placenta and Endometrium between Normal and Intrauterine Growth Restricted Pig Fetuses. PLOS ONE. 2015;10(11):e0142396.

402. Mitsuya K, Parker AN, Liu L, Ruan J, Vissers MCM, Myatt L. Alterations in the placental methylome with maternal obesity and evidence for metabolic regulation. PLoS One. 2017;12(10):e0186115.

403. Mondesir J, Willekens C, Touat M, de Botton S. IDH1 and IDH2 mutations as novel therapeutic targets: current perspectives. J Blood Med. 2016;7:171-80.

404. DeBerardinis Ralph J, Thompson Craig B. Cellular Metabolism and Disease: What Do Metabolic Outliers Teach Us? Cell. 2012;148(6):1132-44.

405. Tummanatsakun D, Proungvitaya T, Roytrakul S, Limpaiboon T, Wongkham S, Wongkham C, Silsirivanit A, Somintara O, Sangkhamanon S, Proungvitaya S. Serum Apurinic/Apyrimidinic Endodeoxyribonuclease 1 (APEX1) Level as a Potential Biomarker of Cholangiocarcinoma. Biomolecules. 2019;9(9).

406. Rackham O, Filipovska A. Organization and expression of the mammalian mitochondrial genome. Nature Reviews Genetics. 2022;23(10):606-23.

407. Yampolsky M, Salafia CM, Shlakhter O, Haas D, Eucker B, Thorp J. Modeling the variability of shapes of a human placenta. Placenta. 2008;29(9):790-7.

408. Antico Arciuch VG, Elguero ME, Poderoso JJ, Carreras MC. Mitochondrial regulation of cell cycle and proliferation. Antioxidants & redox signaling. 2012;16(10):1150-80.

409. Sabbatinelli J, Prattichizzo F, Olivieri F, Procopio AD, Rippo MR, Giuliani A. Where Metabolism Meets Senescence: Focus on Endothelial Cells. Frontiers in Physiology. 2019;10(1523).

410. Ong SE, Blagoev B, Kratchmarova I, Kristensen DB, Steen H, Pandey A, Mann M. Stable isotope labeling by amino acids in cell culture, SILAC, as a simple and accurate approach to expression proteomics. Mol Cell Proteomics. 2002;1(5):376-86.

411. Thompson A, Schäfer J, Kuhn K, Kienle S, Schwarz J, Schmidt G, Neumann T, Hamon C. Tandem Mass Tags: A Novel Quantification Strategy for Comparative Analysis of Complex Protein Mixtures by MS/MS. Analytical Chemistry. 2003;75(8):1895-904.

412. Bantscheff M, Schirle M, Sweetman G, Rick J, Kuster B. Quantitative mass spectrometry in proteomics: a critical review. Anal Bioanal Chem. 2007;389(4):1017-31.

413. Maltepe E, Penn AA. 5 - Development, Function, and Pathology of the Placenta. In: Gleason CA, Juul SE, editors. Avery's Diseases of the Newborn (Tenth Edition). Philadelphia: Elsevier; 2018. p. 40-60.e8.

414. Lu HQ, Hu R. Lasting Effects of Intrauterine Exposure to Preeclampsia on Offspring and the Underlying Mechanism. AJP Rep. 2019;9(3):e275-e91.

415. Giorgione V, Jansen G, Kitt J, Ghossein-Doha C, Leeson P, Thilagalathan B. Peripartum and Long-Term Maternal Cardiovascular Health After Preeclampsia. Hypertension. 2022.

416. Booker WA, Ananth CV, Wright JD, Siddiq Z, D'Alton ME, Cleary KL, Goffman D, Friedman AM. Trends in comorbidity, acuity, and maternal risk associated with preeclampsia across obstetric volume settings. J Matern Fetal Neonatal Med. 2019;32(16):2680-7.

417. Albu AR, Anca AF, Horhoianu VV, Horhoianu IA. Predictive factors for intrauterine growth restriction. J Med Life. 2014;7(2):165-71.

418. Burton GJ, Jauniaux E. American Journal of Obstetrics & Gynecology. 2018;218(2):S745-S61.

419. Tsai K, Tullis B, Jensen T, Graff T, Reynolds P, Arroyo J. Differential expression of mTOR related molecules in the placenta from gestational diabetes mellitus (GDM), intrauterine growth restriction (IUGR) and preeclampsia patients. Reproductive Biology. 2021;21(2):100503.

420. Yung HW, Atkinson D, Campion-Smith T, Olovsson M, Charnock-Jones DS, Burton GJ. Differential activation of placental unfolded protein response pathways implies heterogeneity in causation of early- and late-onset pre-eclampsia. J Pathol. 2014;234(2):262-76.

421. Geldenhuys J, Rossouw TM, Lombaard HA, Ehlers MM, Kock MM. Disruption in the Regulation of Immune Responses in the Placental Subtype of Preeclampsia. Front Immunol. 2018;9:1659.

422. Mayhew TM, Manwani R, Ohadike C, Wijesekara J, Baker PN. The Placenta in Pre-eclampsia and Intrauterine Growth Restriction: Studies on Exchange Surface

Areas, Diffusion Distances and Villous Membrane Diffusive Conductances. Placenta. 2007;28(2):233-8.

423. Mayhew TM, Wijesekara J, Baker PN, Ong SS. Morphometric evidence that villous development and fetoplacental angiogenesis are compromised by intrauterine growth restriction but not by pre-eclampsia. Placenta. 2004;25(10):829-33.

424. Egbor M, Ansari T, Morris N, Green CJ, Sibbons PD. Pre-eclampsia and Fetal Growth Restriction: How Morphometrically Different is the Placenta? Placenta. 2006;27(6):727-34.

425. Dahlstrøm B, Romundstad P, Øian P, Vatten LJ, Eskild A. Placenta weight in pre-eclampsia. Acta Obstetricia et Gynecologica Scandinavica. 2008;87(6):608-11.

426. Milosevic-Stevanovic J, Krstic M, Radovic-Janosevic D, Stefanovic M, Antic V, Djordjevic I. Preeclampsia with and without intrauterine growth restriction–Two pathogenetically different entities? Hypertension in Pregnancy. 2016;35(4):573-82.

427. Khorami Sarvestani S, Shojaeian S, Vanaki N, Ghresi-Fard B, Amini M, Gilany K, Soltanghoraee H, Arefi S, Jeddi-Tehrani M, Zarnani AH. Proteome profiling of human placenta reveals developmental stage-dependent alterations in protein signature. Clin Proteomics. 2021;18(1):18.

428. Manna S, Scheel J, Noone A, McElwain CJ, Scaife C, Gupta S, English J, McCarthy C, McCarthy FP. A proteomic profile of the healthy human placenta. Clinical Proteomics. 2023;20(1):1.

429. Burchard J, Polpitiya AD, Fox AC, Randolph TL, Fleischer TC, Dufford MT, Garite TJ, Critchfield GC, Boniface JJ, Saade GR, Kearney PE. Clinical Validation of a

Proteomic Biomarker Threshold for Increased Risk of Spontaneous Preterm Birth and Associated Clinical Outcomes: A Replication Study. J Clin Med. 2021;10(21).

430. Klein J, Buffin-Meyer B, Mullen W, Carty DM, Delles C, Vlahou A, Mischak H, Decramer S, Bascands J-L, Schanstra JP. Clinical proteomics in obstetrics and neonatology. Expert Review of Proteomics. 2014;11(1):75-89.

431. You G, Zu B, Wang B, Fu Q, Li F. Identification of miRNA–mRNA–TFs Regulatory Network and Crucial Pathways Involved in Tetralogy of Fallot. Frontiers in Genetics. 2020;11.

432. Schmitz U, Lai X, Winter F, Wolkenhauer O, Vera J, Gupta SK. Cooperative gene regulation by microRNA pairs and their identification using a computational workflow. Nucleic Acids Res. 2014;42(12):7539-52.

433. English JA, Lopez LM, O'Gorman A, Föcking M, Hryniewiecka M, Scaife C, Sabherwal S, Wynne K, Dicker P, Rutten BPF, Lewis G, Zammit S, Cannon M, Cagney G, Cotter DR. Blood-Based Protein Changes in Childhood Are Associated With Increased Risk for Later Psychotic Disorder: Evidence From a Nested Case–Control Study of the ALSPAC Longitudinal Birth Cohort. Schizophrenia Bulletin. 2018;44(2):297-306.

434. Drabovich AP, Pavlou MP, Batruch I, Diamandis EP. Chapter 2 - Proteomic and Mass Spectrometry Technologies for Biomarker Discovery. In: Issaq HJ, Veenstra TD, editors. Proteomic and Metabolomic Approaches to Biomarker Discovery. Boston: Academic Press; 2013. p. 17-37.

435. Oberg AL, Mahoney DW, Eckel-Passow JE, Malone CJ, Wolfinger RD, Hill EG, Cooper LT, Onuma OK, Spiro C, Therneau TM, Bergen HR, 3rd. Statistical analysis of

relative labeled mass spectrometry data from complex samples using ANOVA. J Proteome Res. 2008;7(1):225-33.

436. Wu T, Hu E, Xu S, Chen M, Guo P, Dai Z, Feng T, Zhou L, Tang W, Zhan L, Fu X, Liu S, Bo X, Yu G. clusterProfiler 4.0: A universal enrichment tool for interpreting omics data. Innovation (Camb). 2021;2(3):100141.

437. Yu G, Wang LG, Han Y, He QY. clusterProfiler: an R package for comparing biological themes among gene clusters. Omics. 2012;16(5):284-7.

438. Huang H-Y, Lin Y-C-D, Cui S, Huang Y, Tang Y, Xu J, Bao J, Li Y, Wen J, Zuo H, Wang W, Li J, Ni J, Ruan Y, Li L, Chen Y, Xie Y, Zhu Z, Cai X, Chen X, Yao L, Chen Y, Luo Y, LuXu S, Luo M, Chiu C-M, Ma K, Zhu L, Cheng G-J, Bai C, Chiang Y-C, Wang L, Wei F, Lee T-Y, Huang H-D. miRTarBase update 2022: an informative resource for experimentally validated miRNA–target interactions. Nucleic Acids Research. 2022;50(D1):D222-D30.

439. Han H, Shim H, Shin D, Shim JE, Ko Y, Shin J, Kim H, Cho A, Kim E, Lee T, Kim H, Kim K, Yang S, Bae D, Yun A, Kim S, Kim CY, Cho HJ, Kang B, Shin S, Lee I. TRRUST: a reference database of human transcriptional regulatory interactions. Scientific Reports. 2015;5(1):11432.

440. Tong Z, Cui Q, Wang J, Zhou Y. TransmiR v2.0: an updated transcription factor-microRNA regulation database. Nucleic Acids Research. 2018;47(D1):D253-D8.

441. Goenawan IH, Bryan K, Lynn DJ. DyNet: visualization and analysis of dynamic molecular interaction networks. Bioinformatics. 2016;32(17):2713-5.

442. Lai X, Schmitz U, Gupta SK, Bhattacharya A, Kunz M, Wolkenhauer O, Vera J. Computational analysis of target hub gene repression regulated by multiple and cooperative miRNAs. Nucleic Acids Res. 2012;40(18):8818-34.

443. Buetti-Dinh A, Herold M, Christel S, El Hajjami M, Delogu F, Ilie O, Bellenberg S, Wilmes P, Poetsch A, Sand W, Vera M, Pivkin IV, Friedman R, Dopson M. Reverse engineering directed gene regulatory networks from transcriptomics and proteomics data of biomining bacterial communities with approximate Bayesian computation and steady-state signalling simulations. BMC Bioinformatics. 2020;21(1):23.

444. Ness RB, Sibai BM. Shared and disparate components of the pathophysiologies of fetal growth restriction and preeclampsia. Am J Obstet Gynecol. 2006;195(1):40-9.

445. Surico D, Bordino V, Cantaluppi V, Mary D, Gentilli S, Oldani A, Farruggio S, Melluzza C, Raina G, Grossini E. Preeclampsia and intrauterine growth restriction: Role of human umbilical cord mesenchymal stem cells-trophoblast cross-talk. PLoS One. 2019;14(6):e0218437.

446. Nagao K, Zhu J, Heneghan MB, Hanson JC, Morasso MI, Tessarollo L, Mackem S, Udey MC. Abnormal Placental Development and Early Embryonic Lethality in EpCAM-Null Mice. PLOS ONE. 2010;4(12):e8543.

447. Atigan A, Tan S, Cetin H, Guler OT, Ozdamar S, Karakaya YA. CD97 expression level and its effect on cell adhesion in Preeclampsia. BMC Pregnancy and Childbirth. 2022;22(1):967.

448. Dolicka D, Sobolewski C, Correia de Sousa M, Gjorgjieva M, Foti M. mRNA Post-Transcriptional Regulation by AU-Rich Element-Binding Proteins in Liver

Inflammation and Cancer. International Journal of Molecular Sciences. 2020;21(18):6648.

449. Jeganathan S, Lee JM. Binding of Elongation Factor eEF1A2 to Phosphatidylinositol 4-Kinase β Stimulates Lipid Kinase Activity and Phosphatidylinositol 4-Phosphate Generation *. Journal of Biological Chemistry. 2007;282(1):372-80.

450. Xu B, Liu L, Song G. Functions and Regulation of Translation Elongation Factors. Frontiers in Molecular Biosciences. 2022;8.

451. Kishkevich A, Tamang S, Nguyen MO, Oehler J, Bulmaga E, Andreadis C, Morrow CA, Osman F, Whitby MC. Rad52's DNA annealing activity drives template switching associated with restarted DNA replication. Nature Communications. 2022;13(1):7293.

452. Garty BZ, Ludomirsky A, Danon YL, Peter JB, Douglas SD. Placental transfer of immunoglobulin G subclasses. Clin Diagn Lab Immunol. 1994;1(6):667-9.

453. Hian Tan K, Sim Tan S, Sze SK, Ryan Lee WK, Jack Ng M, Kiang Lim S. Plasma biomarker discovery in preeclampsia using a novel differential isolation technology for circulating extracellular vesicles. American Journal of Obstetrics and Gynecology. 2014;211(4):380.e1-.e13.

454. Freed KA, Brennecke SP, Moses EK. Gene expression of the constant region of the heavy chain of immunoglobulin G (IgG CRHC) is down-regulated in human decidua in association with preeclampsia. Journal of Reproductive Immunology. 2005;68(1):105-20.

455. Trampert DC, Hubers LM, van de Graaf SFJ, Beuers U. On the role of IgG4 in inflammatory conditions: lessons for IgG4-related disease. Biochim Biophys Acta Mol Basis Dis. 2018;1864(4 Pt B):1401-9.

456. Yang M, Liu S, Xiong Y, Zhao J, Deng W. An integrative pan-cancer analysis of molecular characteristics and oncogenic role of mitochondrial creatine kinase 1A (CKMT1A) in human tumors. Scientific Reports. 2022;12(1):10025.

457. Ellery SJ, Murthi P, Gatta PAD, May AK, Davies-Tuck ML, Kowalski GM, Callahan DL, Bruce CR, Wallace EM, Walker DW, Dickinson H, Snow RJ. The Effects of Early-Onset Pre-Eclampsia on Placental Creatine Metabolism in the Third Trimester. Int J Mol Sci. 2020;21(3).

458. Datler C, Pazarentzos E, Mahul-Mellier AL, Chaisaklert W, Hwang MS, Osborne F, Grimm S. CKMT1 regulates the mitochondrial permeability transition pore in a process that provides evidence for alternative forms of the complex. J Cell Sci. 2014;127(Pt 8):1816-28.

459. Kurmi K, Hitosugi S, Yu J, Boakye-Agyeman F, Wiese EK, Larson TR, Dai Q, Machida YJ, Lou Z, Wang L, Boughey JC, Kaufmann SH, Goetz MP, Karnitz LM, Hitosugi T. Tyrosine Phosphorylation of Mitochondrial Creatine Kinase 1 Enhances a Druggable Tumor Energy Shuttle Pathway. Cell Metabolism. 2018;28(6):833-47.e8.

460. Geng QS, Huang T, Li LF, Shen ZB, Xue WH, Zhao J. Over-Expression and Prognostic Significance of FN1, Correlating With Immune Infiltrates in Thyroid Cancer. Front Med (Lausanne). 2021;8:812278.

461. Fruscalzo A, Londero AP, Orsaria M, Marzinotto S, Driul L, Di Loreto C, Mariuzzi L. Placental fibronectin staining is unaffected in pregnancies complicated

by late-onset intrauterine growth restriction and small for gestational age fetuses. Int J Gynaecol Obstet. 2020;148(2):253-60.

462. Glasner A, Levi A, Enk J, Isaacson B, Viukov S, Orlanski S, Scope A, Neuman T, Enk CD, Hanna JH, Sexl V, Jonjic S, Seliger B, Zitvogel L, Mandelboim O. NKp46 Receptor-Mediated Interferon-γ Production by Natural Killer Cells Increases Fibronectin 1 to Alter Tumor Architecture and Control Metastasis. Immunity. 2018;48(1):107-19.e4.

463. Fukui A, Yokota M, Funamizu A, Nakamua R, Fukuhara R, Yamada K, Kimura H, Fukuyama A, Kamoi M, Tanaka K, Mizunuma H. Changes of NK Cells in Preeclampsia. American Journal of Reproductive Immunology. 2012;67(4):278-86.

464. Zhao S, Lv N, Li Y, Liu T, Sun Y, Chu X. Identification and characterization of methylation-mediated transcriptional dysregulation dictate methylation roles in preeclampsia. Human Genomics. 2020;14(1):5.

465. Liu F, Ou W, Tang W, Huang Z, Zhu Z, Ding W, Fu J, Zhu Y, Liu C, Xu W, Du P. Increased AOC1 Expression Promotes Cancer Progression in Colorectal Cancer. Frontiers in Oncology. 2021;11.

466. Mary S, Small H, Herse F, Carrick E, Flynn A, Mullen W, Dechend R, Delles C. Preexisting hypertension and pregnancy-induced hypertension reveal molecular differences in placental proteome in rodents. Physiological Genomics. 2021;53(6):259-68.

467. Ding Q, Lin D, Zhou Y, Li F, Lai J, Duan J, Chen J, Jiang C. Downregulation of amine oxidase copper containing 1 inhibits tumor progression by suppressing IL-6/JAK/STAT3 pathway activation in hepatocellular carcinoma. Oncology Letters. 2021;22(6):1-9.

468. Hart ML, Walsh MC, Stahl GL. Initiation of complement activation following oxidative stress. In vitro and in vivo observations. Mol Immunol. 2004;41(2-3):165-71.

469. Tincani A, Cavazzana I, Ziglioli T, Lojacono A, De Angelis V, Meroni P. Complement activation and pregnancy failure. Clin Rev Allergy Immunol. 2010;39(3):153-9.

470. Aisagbonhi O, Morris GP. Human Leukocyte Antigens in Pregnancy and Preeclampsia. Frontiers in Genetics. 2022;13.

471. Aneman I, Pienaar D, Suvakov S, Simic TP, Garovic VD, McClements L. Mechanisms of Key Innate Immune Cells in Early- and Late-Onset Preeclampsia. Frontiers in Immunology. 2020;11.

472. Thway TM, Shlykov SG, Day M-C, Sanborn BM, Gilstrap LC, Xia Y, Kellems RE. Antibodies From Preeclamptic Patients Stimulate Increased Intracellular Ca²⁺ Mobilization Through Angiotensin Receptor Activation. Circulation. 2004;110(12):1612-9.

473. Markiewski MM, Lambris JD. The role of complement in inflammatory diseases from behind the scenes into the spotlight. Am J Pathol. 2007;171(3):715-27.

474. Ancuța E, Zamfir R, Martinescu G, Crauciuc DV, Ancuța C. The Complement System, T Cell Response, and Cytokine Shift in Normotensive versus Pre-Eclamptic and Lupus Pregnancy. J Clin Med. 2021;10(24).

475. Miao Z, Chen M, Wu H, Ding H, Shi Z. Comparative proteomic profile of the human placenta in normal and fetal growth restriction subjects. Cell Physiol Biochem. 2014;34(5):1701-10.

476. Valent D, Yeste N, Hernández-Castellano LE, Arroyo L, Wu W, García-Contreras C, Vázquez-Gómez M, González-Bulnes A, Bendixen E, Bassols A. SWATH-MS quantitative proteomic investigation of intrauterine growth restriction in a porcine model reveals sex differences in hippocampus development. J Proteomics. 2019;204:103391.

477. Wang J, Chen L, Li D, Yin Y, Wang X, Li P, Dangott LJ, Hu W, Wu G. Intrauterine Growth Restriction Affects the Proteomes of the Small Intestine, Liver, and Skeletal Muscle in Newborn Pigs. The Journal of Nutrition. 2008;138(1):60-6.

478. Wölter M, Röwer C, Koy C, Reimer T, Rath W, Pecks U, Glocker MO. A proteome signature for intrauterine growth restriction derived from multifactorial analysis of mass spectrometry-based cord blood serum profiling. Electrophoresis. 2012;33(12):1881-93.

479. Okai CA, Russ M, Wölter M, Andresen K, Rath W, Glocker MO, Pecks U. Precision Diagnostics by Affinity-Mass Spectrometry: A Novel Approach for Fetal Growth Restriction Screening During Pregnancy. J Clin Med. 2020;9(5).

480. Regal JF, Burwick RM, Fleming SD. The Complement System and Preeclampsia. Curr Hypertens Rep. 2017;19(11):87.

481. Pierik E, Prins JR, van Goor H, Dekker GA, Daha MR, Seelen MAJ, Scherjon SA. Dysregulation of Complement Activation and Placental Dysfunction: A Potential Target to Treat Preeclampsia? Front Immunol. 2019;10:3098.

482. Piñero J, Ramírez-Anguita JM, Saüch-Pitarch J, Ronzano F, Centeno E, Sanz F, Furlong LI. The DisGeNET knowledge platform for disease genomics: 2019 update. Nucleic Acids Res. 2020;48(D1):D845-d55.

483. Kishimoto Y, Hiraiwa M, O'Brien JS. Saposins: structure, function, distribution, and molecular genetics. J Lipid Res. 1992;33(9):1255-67.

484. Darmoise A, Maschmeyer P, Winau F. Chapter 2 - The Immunological Functions of Saposins. In: Alt FW, editor. Advances in Immunology. 105: Academic Press; 2010. p. 25-62.

485. Zou Z, Tao T, Li H, Zhu X. mTOR signaling pathway and mTOR inhibitors in cancer: progress and challenges. Cell & Bioscience. 2020;10(1):31.

486. Charkiewicz K, Goscik J, Blachnio-Zabielska A, Raba G, Sakowicz A, Kalinka J, Chabowski A, Laudanski P. Sphingolipids as a new factor in the pathomechanism of preeclampsia – Mass spectrometry analysis. PLOS ONE. 2017;12(5):e0177601.

487. Ashar-Patel A, Kaymaz Y, Rajakumar A, Bailey JA, Karumanchi SA, Moore MJ. FLT1 and transcriptome-wide polyadenylation site (PAS) analysis in preeclampsia. Sci Rep. 2017;7(1):12139.

488. Zhang W, Wu Q, Su J, Wang W, Zhao X, Cao P. Circulating miRNAs as Epigenetic Mediators of Periodontitis and Preeclampsia Association. Dis Markers. 2022;2022:2771492.

489. Del Gaudio I, Sasset L, Di Lorenzo A, Wadsack C. Sphingolipid Signature of Human Feto-Placental Vasculature in Preeclampsia. International Journal of Molecular Sciences. 2020;21(3):1019.

490. Zhang Y, Yang J-m. The impact of cellular senescence in cancer therapy: is it true or not? Acta Pharmacologica Sinica. 2011;32(10):1199-207.

491. Kim N-Y, Woo A-M, Kim J-R, Lee C. Exploration of senescence-associated genes by differential display reverse transcription polymerase chain reaction:

Prosaposin as a novel senescence-associated gene. Archives of Pharmacal Research. 2009;32(5):737-45.

492. Hu X-Q, Zhang L. MicroRNAs in Uteroplacental Vascular Dysfunction. Cells. 2019;8(11):1344.

493. Jaszczuk I, Koczkodaj D, Kondracka A, Kwaśniewska A, Winkler I, Filip A. The role of miRNA-210 in pre-eclampsia development. Annals of Medicine. 2022;54(1):1350-6.

494. CALKHOVEN CF, AB G. Multiple steps in the regulation of transcription-factor level and activity. Biochemical Journal. 1996;317(2):329-42.

495. Wu J, He Z, Gao Y, Zhang G, Huang X, Fang Q. Placental NFE2L2 is discordantly activated in monochorionic twins with selective intrauterine growth restriction and possibly regulated by hypoxia. Free Radic Res. 2017;51(4):351-9.

496. Meakin AS, Clifton VL. Review: Understanding the role of androgens and placental AR variants: Insight into steroid-dependent fetal-placental growth and development. Placenta. 2019;84:63-8.

497. Vaughan JE, Walsh SW. Activation of NF-κB in placentas of women with preeclampsia. Hypertension in pregnancy. 2012;31(2):243-51.

498. Kaur L, Sundrani D, Dave K, Randhir K, Mehendale S, Bayyana S, Kalyanaraman K, Chandak GR, Joshi S. Hypoxia Inducible Factors (HIF1α and HIF3α) are differentially methylated in preeclampsia placentae and are associated with birth outcomes. Molecular and Cellular Biochemistry. 2023.

499. Xu P, Zhao Y, Liu M, Wang Y, Wang H, Li YX, Zhu X, Yao Y, Wang H, Qiao J, Ji L, Wang YL. Variations of microRNAs in human placentas and plasma from preeclamptic pregnancy. Hypertension. 2014;63(6):1276-84.

500. Tagliaferri S, Cepparulo P, Vinciguerra A, Campanile M, Esposito G, Maruotti GM, Zullo F, Annunziato L, Pignataro G. miR-16-5p, miR-103-3p, and miR-27b-3p as Early Peripheral Biomarkers of Fetal Growth Restriction. Frontiers in Pediatrics. 2021;9.

501. Leisegang MS, Bains JK, Seredinski S, Oo JA, Krause NM, Kuo C-C, Günther S, Sentürk Cetin N, Warwick T, Cao C, Boos F, Izquierdo Ponce J, Haydar S, Bednarz R, Valasarajan C, Fuhrmann DC, Preussner J, Looso M, Pullamsetti SS, Schulz MH, Jonker HRA, Richter C, Rezende F, Gilsbach R, Pflüger-Müller B, Wittig I, Grummt I, Ribarska T, Costa IG, Schwalbe H, Brandes RP. HIF1α-AS1 is a DNA:DNA:RNA triplex-forming lncRNA interacting with the HUSH complex. Nature Communications. 2022;13(1):6563.

502. Devi G, Zhou Y, Zhong Z, Toh DF, Chen G. RNA triplexes: from structural principles to biological and biotech applications. Wiley Interdiscip Rev RNA. 2015;6(1):111-28.

503. Shannon P, Markiel A Fau - Ozier O, Ozier O Fau - Baliga NS, Baliga Ns Fau - Wang JT, Wang Jt Fau - Ramage D, Ramage D Fau - Amin N, Amin N Fau - Schwikowski B, Schwikowski B Fau - Ideker T, Ideker T. Cytoscape: a software environment for integrated models of biomolecular interaction networks. (1088-9051 (Print)).

504. Wang J, Lu M, Qiu C, Cui Q. TransmiR: a transcription factor-microRNA regulation database. Nucleic Acids Res. 2010;38(Database issue):D119-22.

505. Patel VJ, Thalassinos K, Slade SE, Connolly JB, Crombie A, Murrell JC, Scrivens JH. A comparison of labeling and label-free mass spectrometry-based proteomics approaches. J Proteome Res. 2009;8(7):3752-9.

506. Al Shweiki MHDR, Mönchgesang S, Majovsky P, Thieme D, Trutschel D, Hoehenwarter W. Assessment of Label-Free Quantification in Discovery Proteomics and Impact of Technological Factors and Natural Variability of Protein Abundance. Journal of Proteome Research. 2017;16(4):1410-24.

507. Correia-Melo C, Jurk D, Passos JF. Robust multiparametric assessment of cellular senescence. Methods Mol Biol. 2013;965:409-19.

508. Zhao J, Zhang L, Lu A, Han Y, Colangelo D, Bukata C, Scibetta A, Yousefzadeh MJ, Li X, Gurkar AU, McGowan SJ, Angelini L, O'Kelly R, Li H, Corbo L, Sano T, Nick H, Pola E, Pilla SPS, Ladiges WC, Vo N, Huard J, Niedernhofer LJ, Robbins PD. ATM is a key driver of NF-κB-dependent DNA-damage-induced senescence, stem cell dysfunction and aging. Aging (Albany NY). 2020;12(6):4688-710.

509. Zhang H, Zhang X, Li X, Meng W-B, Bai Z-T, Rui S-Z, Wang Z-F, Zhou W-C, Jin X-D. Effect of CCNB1 silencing on cell cycle, senescence, and apoptosis through the p53 signaling pathway in pancreatic cancer. Journal of Cellular Physiology. 2019;234(1):619-31.

510. Lv Y, Si M, Chen N, Li Y, Ma X, Yang H, Zhang L, Zhu H, Xu GY, Wu GP, Cao C. TBX2 over-expression promotes nasopharyngeal cancer cell proliferation and invasion. Oncotarget. 2017;8(32):52699-707.

511. Martin N, Benhamed M, Nacerddine K, Demarque MD, van Lohuizen M, Dejean A, Bischof O. Physical and functional interaction between PML and TBX2 in the establishment of cellular senescence. The EMBO Journal. 2012;31(1):95-109.

512. Homann L, Rentschler M, Brenner E, Böhm K, Röcken M, Wieder T. IFN-γ and TNF Induce Senescence and a Distinct Senescence-Associated Secretory Phenotype in Melanoma. Cells. 2022;11(9).

513. Kulaberoglu Y, Hergovich A, Gómez V. Chapter 15 - The role of p53/p21/p16 in DNA damage signaling and DNA repair. In: Kovalchuk I, Kovalchuk O, editors. Genome Stability (Second Edition). 26. Boston: Academic Press; 2021. p. 257-74.

514. Liu D, Xu Y. p53, oxidative stress, and aging. (1557-7716 (Electronic)).

515. Srinivas SK, Edlow AG, Neff PM, Sammel MD, Andrela CM, Elovitz MA. Rethinking IUGR in preeclampsia: dependent or independent of maternal hypertension? J Perinatol. 2009;29(10):680-4.

516. Armengaud JB, Yzydorczyk C, Siddeek B, Peyter AC, Simeoni U. Intrauterine growth restriction: Clinical consequences on health and disease at adulthood. Reproductive Toxicology. 2021;99:168-76.

517. Motedayen M, Rafiei M, Rezaei Tavirani M, Sayehmiri K, Dousti M. The relationship between body mass index and preeclampsia: A systematic review and meta-analysis. Int J Reprod Biomed. 2019;17(7):463-72.

518. Lopez-Jaramillo P, Barajas J, Rueda-Quijano SM, Lopez-Lopez C, Felix C. Obesity and Preeclampsia: Common Pathophysiological Mechanisms. Front Physiol. 2018;9:1838.

519. Lisowska M, Pietrucha T, Sakowicz A. Preeclampsia and Related Cardiovascular Risk: Common Genetic Background. Curr Hypertens Rep. 2018;20(8):71.

520. Chew SY, Chee WJY, Than LTL. The glyoxylate cycle and alternative carbon metabolism as metabolic adaptation strategies of Candida glabrata: perspectives from Candida albicans and Saccharomyces cerevisiae. J Biomed Sci. 2019;26(1):52.

521. Zheng Y, Pan J, Xia C, Chen H, Zhou H, Ju W, Wegiel J, Myatt L, Roberts JM, Guo X, Zhong N. Characterization of placental and decidual cell development in

early pregnancy loss by single-cell RNA sequencing. Cell & Bioscience. 2022;12(1):168.

522. Wang X, Liu J, Hui X, Song Y. Metabolomics Applied to Cord Serum in Preeclampsia Newborns: Implications for Neonatal Outcomes. Front Pediatr. 2022;10:869381.

523. Yao M, Yang Z, Rong X, Hu X, Yao N, Zhu M, Wang X, Zhu X, Yin J. The Exploration of Fetal Growth Restriction Based on Metabolomics: A Systematic Review. Metabolites. 2022;12(9).

524. Ma Y, Li J. Metabolic shifts during aging and pathology. Compr Physiol. 2015;5(2):667-86.

525. Aalberse RC, Schuurman J. IgG4 breaking the rules. Immunology. 2002;105(1):9-19.

526. Davies AM, Sutton BJ. Human IgG4: a structural perspective. Immunological reviews. 2015;268(1):139-59.

527. Palmeira P, Quinello C, Silveira-Lessa AL, Zago CA, Carneiro-Sampaio M. IgG placental transfer in healthy and pathological pregnancies. Clin Dev Immunol. 2012;2012:985646.

528. Clements T, Rice TF, Vamvakas G, Barnett S, Barnes M, Donaldson B, Jones CE, Kampmann B, Holder B. Update on Transplacental Transfer of IgG Subclasses: Impact of Maternal and Fetal Factors. Frontiers in Immunology. 2020;11.

529. Shakerian B, Moghtaderi M, Heidari N. Immunoglobulin G4 deficiency can be a new entity for primary recurrent miscarriage: Successful pregnancy in two cases after treatment with intravenous immunoglobulin. Turk J Obstet Gynecol. 2019;16(4):274-7.

530. Gasek NS, Kuchel GA, Kirkland JL, Xu M. Strategies for targeting senescent cells in human disease. Nature Aging. 2021;1(10):870-9.

531. Li T, Zeng L, Gao W, Cui M-Z, Fu X, Xu X. PSAP induces a unique Apaf-1 and Smac-dependent mitochondrial apoptotic pathway independent of Bcl-2 family proteins. Biochimica et Biophysica Acta (BBA) - Molecular Basis of Disease. 2013;1832(3):453-74.

532. Majewska M, Lipka A, Paukszto L, Jastrzebski JP, Szeszko K, Gowkielewicz M, Lepiarczyk E, Jozwik M, Majewski MK. Placenta Transcriptome Profiling in Intrauterine Growth Restriction (IUGR). International Journal of Molecular Sciences. 2019;20(6):1510.

533. Motta M, Tatti M, Furlan F, Celato A, Di Fruscio G, Polo G, Manara R, Nigro V, Tartaglia M, Burlina A, Salvioli R. Clinical, biochemical and molecular characterization of prosaposin deficiency. Clinical Genetics. 2016;90(3):220-9.

534. Ashar-Patel A, Kaymaz Y, Rajakumar A, Bailey JA, Karumanchi SA, Moore MJ. FLT1 and transcriptome-wide polyadenylation site (PAS) analysis in preeclampsia. Scientific Reports. 2017;7(1):12139.

535. Misasi R, Garofalo T, Di Marzio L, Mattei V, Gizzi C, Hiraiwa M, Pavan A, Grazia Cifone M, Sorice M. Prosaposin: a new player in cell death prevention of U937 monocytic cells. Experimental Cell Research. 2004;298(1):38-47.

536. Xu F, Xu Y, Xiong JH, Zhang JH, Wu J, Luo J, Xiong JP. AOC1 Contributes to Tumor Progression by Promoting the AKT and EMT Pathways in Gastric Cancer. Cancer Manag Res. 2020;12:1789-98.

537. Madeo F, Eisenberg T, Pietrocola F, Kroemer G. Spermidine in health and disease. Science. 2018;359(6374).

538. Ding Y, Feng Y, Huang Z, Zhang Y, Li X, Liu R, Li H, Wang T, Ding Y, Jia Z, Yang J. SOX15 transcriptionally increases the function of AOC1 to modulate ferroptosis and progression in prostate cancer. Cell Death & Disease. 2022;13(8):673.

539. Megger DA, Bracht T, Meyer HE, Sitek B. Label-free quantification in clinical proteomics. Biochimica et Biophysica Acta (BBA) - Proteins and Proteomics. 2013;1834(8):1581-90.

540. Mann M. Comparative analysis to guide quality improvements in proteomics. Nature Methods. 2009;6(10):717-9.

541. Brodland GW. How computational models can help unlock biological systems. Seminars in Cell & Developmental Biology. 2015;47-48:62-73.

542. Pereira EJ, Smolko CM, Janes KA. Computational models of reactive oxygen species as metabolic byproducts and signal-transduction modulators. Frontiers in pharmacology. 2016;7:457.

543. Wright D, Nicolaides KH. Aspirin delays the development of preeclampsia. American journal of obstetrics and gynecology. 2019;220(6):580. e1-. e6.

544. Li X, Milosavljevic A, Elsea SH, Wang CC, Scaglia F, Syngelaki A, Nicolaides KH, Poon LC. Effective Aspirin Treatment of Women at Risk for Preeclampsia Delays the Metabolic Clock of Gestation. Hypertension. 2021;78(5):1398-410.

545. Varesi AA-O, Chirumbolo SA-O, Campagnoli LA-OX, Pierella EA-O, Piccini GA-O, Carrara AA-O, Ricevuti GA-O, Scassellati C, Bonvicini CA-O, Pascale AA-O. The Role of Antioxidants in the Interplay between Oxidative Stress and Senescence. LID - 10.3390/antiox11071224 [doi] LID - 1224. (2076-3921 (Print)).

546. Liao N, Shi Y, Zhang C, Zheng Y, Wang Y, Zhao B, Zeng Y, Liu X, Liu J. Antioxidants inhibit cell senescence and preserve stemness of adipose tissue-

derived stem cells by reducing ROS generation during long-term in vitro expansion. Stem Cell Research & Therapy. 2019;10(1):306.

547. Tian X, Thorne JL, Moore JB. Ergothioneine: an underrecognised dietary micronutrient required for healthy ageing?

548. Firuzi O, Miri R, Tavakkoli M, Saso L. Antioxidant therapy: current status and future prospects. Curr Med Chem. 2011;18(25):3871-88.

549. Fuchs R, Ellinger I. Endocytic and transcytotic processes in villous syncytiotrophoblast: role in nutrient transport to the human fetus. Traffic. 2004;5(10):725-38.

550. Han E-S, Wu Y, McCarter R, Nelson JF, Richardson A, Hilsenbeck SG. Reproducibility, Sources of Variability, Pooling, and Sample Size: Important Considerations for the Design of High-Density Oligonucleotide Array Experiments. The Journals of Gerontology: Series A. 2004;59(4):B306-B15.

551. Leung DTH, Chu S. Measurement of Oxidative Stress: Mitochondrial Function Using the Seahorse System. In: Murthi P, Vaillancourt C, editors. Preeclampsia : Methods and Protocols. New York, NY: Springer New York; 2018. p. 285-93.

552. Wiley Christopher D, Velarde Michael C, Lecot P, Liu S, Sarnoski Ethan A, Freund A, Shirakawa K, Lim Hyung W, Davis Sonnet S, Ramanathan A, Gerencser Akos A, Verdin E, Campisi J. Mitochondrial Dysfunction Induces Senescence with a Distinct Secretory Phenotype. Cell Metabolism. 2016;23(2):303-14.

553. Wan, M., Gray-Gaillard, E.F. & Elisseeff, J.H. Cellular senescence in musculoskeletal homeostasis, diseases, and regeneration. Bone Res 9, 41 (2021). https://doi.org/10.1038/s41413-021-00164-y

8.0 Appendix: Published Manuscript

Hindawi
Oxidative Medicine and Cellular Longevity
Volume 2019, Article ID 3095383, 11 pages
https://doi.org/10.1155/2019/3095383

Review Article

Placental Ageing in Adverse Pregnancy Outcomes: Telomere Shortening, Cell Senescence, and Mitochondrial Dysfunction

Samprikta Manna,[1] **Cathal McCarthy**,[1,2] **and Fergus P. McCarthy**[1]

[1]*Irish Centre for Fetal and Neonatal Translational Research (INFANT), Cork University Maternity Hospital, Cork, Ireland*
[2]*Department of Pharmacology and Therapeutics, University College Cork, Western Gateway Building, Cork, Ireland*

Correspondence should be addressed to Samprikta Manna; samprikta.manna@ucc.ie

Received 21 January 2019; Revised 8 April 2019; Accepted 6 May 2019; Published 22 May 2019

Guest Editor: Valentina Giorgio

Copyright © 2019 Samprikta Manna et al. This is an open access article distributed under the Creative Commons Attribution License, which permits unrestricted use, distribution, and reproduction in any medium, provided the original work is properly cited.

Preeclampsia is a multisystemic pregnancy disorder and a major cause of maternal and neonatal morbidity and mortality worldwide. The exact pathophysiology of preeclampsia remains unclear; however, it is speculated that the various pathologies can be attributed to impaired vascular remodelling and elevated oxidative stress within the placenta. Oxidative stress plays a key role in cell ageing, and the persistent presence of elevated oxidative stress precipitates cellular senescence and mitochondrial dysfunction, resulting in premature ageing of the placenta. Premature ageing of the placenta is associated with placental insufficiency, which reduces the functional capacity of this critical organ and leads to abnormal pregnancy outcomes. The changes brought about by oxidative insults are irreversible and often lead to deleterious modifications in macromolecules such as lipids and proteins, DNA mutations, and alteration of mitochondrial functioning and dynamics. In this review, we have summarized the current knowledge of placental ageing in the aetiology of adverse pregnancy outcomes and discussed the hallmarks of ageing which could be potential markers for preeclampsia and fetal growth restriction.

1. Introduction

Preeclampsia can be defined as de novo hypertension after 20 weeks of gestation in the presence of proteinuria and maternal organ/uteroplacental dysfunction [1]. It is one of the leading causes of maternal and neonatal morbidity and mortality affecting about 3 to 8% of pregnancies worldwide [2]. Preterm birth as a result of iatrogenic delivery is a common factor in preeclampsia with up to 25% of babies born to preeclamptic mothers being growth restricted [2, 3]. Preeclampsia and IUGR are pregnancy-specific disorders that are associated with placental insufficiency [4]. Complications associated with preeclampsia are responsible for about 15% of maternal deaths and high perinatal mortality rates worldwide [5]. Ageing is experienced inevitably by organs; however, in preeclampsia, the presence of persistent oxidative stress accelerates this process resulting in premature ageing of the placenta [6]. It has been reported by various studies that premature placental ageing is associated with telomere shortening, cellular senescence, and mitochondrial dysfunction [7–10].

2. Physiology of Ageing

Ageing is a unidirectional phenomenon experienced inevitably by every tissue. It can be characterised as cellular senescence through decline in functionality and mitochondrial dysfunction through altered metabolism and signalling.

2.1. Cellular Senescence. Cells are capable of replication, dividing into two exact copies of the parent cell. This includes division of the genetic material by unwinding and splitting of the DNA strands, in order to form two new copies as daughter strands. Telomeres are cap-like nucleotide repeats (TTAG GG) present on the end of each strand. Damage to DNA strands activates signalling cascades (ataxia telangiectasia-mutated (ATM) and ataxia telangiectasia and Rad3-related (ATR) pathways) that arrest cell division, induce cellular

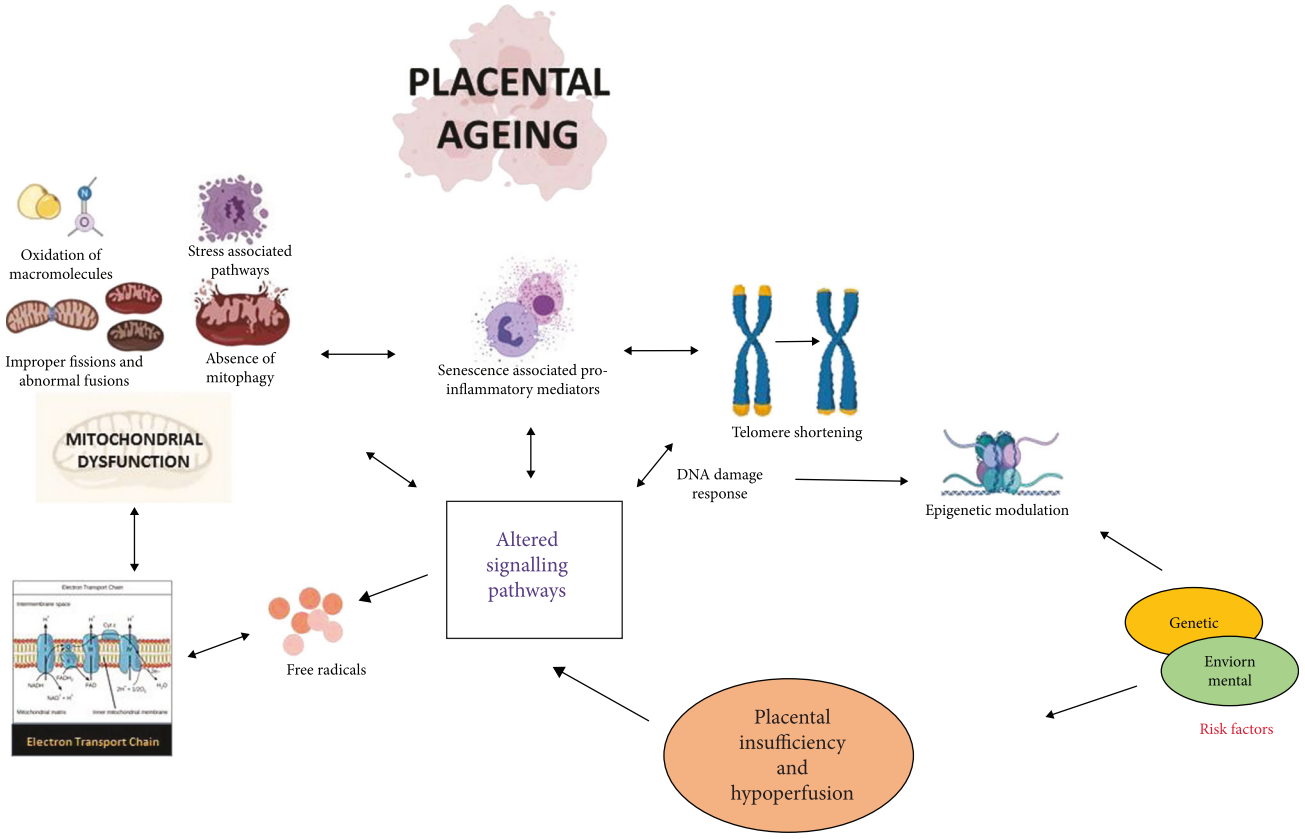


Figure 1: Cause and consequence of placental ageing: the pathophysiology of placental conditions such as preeclampsia and fetal growth restriction is often associated with internal and external factors such as oxidative stress, genetic, immunological, and environmental. This can result in placental insufficiency with further evidence of premature ageing of the placenta as a consequence of cellular senescence and mitochondrial dysfunction [130, 131].

senescence, and promote cell death [11]. Telomeres with other proteins like shelterin protect the end of nuclei from being recognised as a double-strand damaged region (DDR) [11]. It has been shown that telomeres shorten after every replication cycle [12]. With the increase in proliferation and decrease in telomere size, cells enter senescence or a growth retardation phase (Hayflick limit) which ultimately results in cellular death [12]. Telomere shortening has been associated with various genetic diseases such as progeria or premature ageing and Hutchinson-Gilford syndrome [13].

In some cases, such as cancer, cells can bypass senescence and keep proliferating, becoming immortal. However, even cancer cells do not divide indefinitely, and they enter a crisis stage which results in either cellular death or telomere length stabilization with a consequent upregulation of the telomerase enzyme to maintain telomere length [14]. Telomerase is a RNA-protein complex that replenishes the lost nucleotides to preserve the length of the telomere [15]. In somatic cells, telomerases are turned off as a protective mechanism to prevent neoplastic changes [16], but their activity is more pronounced in germ cells, stem cells, and 90% of cancer cells [17].

2.2. Mitochondrial Dysfunction. Mitochondria are key regulators of metabolism, redox balance, and apoptosis. During the electron transport chain (ETC), electrons are pumped across the inner mitochondrial membrane (from reduced compounds to molecular oxygen) to create an efflux for synthesis of energy [18]. According to the free radical or oxidative stress hypothesis of ageing, there are a number of timeline events occurring during oxidative phosphorylation resulting in leaching of electrons from mitochondrial membranes which reacts with oxygen, forming free radicals such as superoxide, ultimately impairing redox balance [19, 20]. The free radical theory has been succeeded by the damage theory hypothesis which suggests that ageing can be associated with the frequent and inevitable cumulative damage at a molecular level caused by accumulated reactive oxygen species (ROS) and its by-products and enzymes [21]. Accumulated reactive oxygen species (ROS) leads to reversible and irreversible changes within cells, resulting in loss of molecular functioning and increased oxidative stress, a phenomenon frequently associated with senescence, as shown in Figure 1 [19, 20].

Mitochondrial functioning in ageing has been studied extensively; it has been reported by a number of articles that mitochondrial density, respiratory capacity, and ATP production decline with cellular ageing [22–24]. Apart from reduced functionality, ageing is accompanied with damaged mitochondrial DNA (mtDNA), mutations, and mitophagy [22, 25].

Impaired redox signalling induces various modifications within the macromolecules and mutations within mtDNA; however, deleterious effects of these mtDNA mutations are still not fully elucidated [26–28]. The bottleneck effect, which explains genetic drifts and variations in small population subsets, as is the case with mtDNA mutations, may transmit small variations in germlines which are amplified in later stages of oogenesis [29, 30]. A few studies have reported that mutations in yeast mtDNA result in a shorter lifespan when mitophagy is inhibited [31, 32]. Reduced mtDNA copy numbers have been associated with ageing and associated diseases including cardiovascular disease (cardiomyopathy, atherosclerosis), neurodegenerative disease (Alzheimer's disease, Parkinson's disease), cancer, and premature ageing of ovaries in women [33, 34].

Mitophagy is a protective mechanism to maintain mitochondrial quality, remove mutated mtDNA, and ensure mitochondrial homeostasis [35]. Furthermore, mitochondrial dynamics are maintained through frequent mitochondrial fission and fusion [36]. Oxidative damage to the mitochondria can cause impaired fission with asymmetric membrane potentials of daughter mitochondria which fail to fuse effectively, resulting in accumulated malformed mitochondrial proteins with decreased autophagic capacity [37]. Palikaras et al. showed that mitophagy is required for longevity in *C. elegans* as a result of reduced insulin/IGF-1 signalling or impaired mitochondrial function [38].

Furthermore, loss of mitochondrial biogenesis through an imbalance of mitophagy and mitochondrial fission/fusion and accumulation of mitochondrial debris leads to cardiac ageing in mice [39, 40].

Impaired mitochondrial functioning is reflective of the mitochondrial unfolded protein response (UPR^{mt}) [41] which is regulated by communication between mitochondrial and nuclear proteins, where nuclear remodelling is required for the activation of UPR^{mt} [42]. When stress is induced within cells, UPR^{mt} is upregulated to promote repairs, but in cases of prolonged UPR^{mt} action, mutations may be induced within the mtDNA [42]. Experiments on *C. elegans* have shown that UPR^{mt} upregulation and imbalance in mitonuclear response induce longevity [43, 44].

Cell senescence is a result of nuclear damage usually associated with high oxidative stress and accumulation of ROS, debris, or misfolded proteins. Innate immune mediators with Senescence-Associated Secretory Phenotypes (SASPs) including cytokines, chemokines, growth factors, and proteases are responsible for clearing debris from dead or dying cells which might activate proapoptotic p53 and AKT signalling pathways [45–47]. In several studies, removal of inflammatory mediators and consequent signalling caused a reversal in cellular ageing, indicating that inflammation might be both cause and consequence in cellular senescence [48–50].

3. Pathophysiology of Preeclampsia

The pathophysiology of preeclampsia, even after decades of research, is not completely understood. Preeclampsia can be characterised as early onset, comprising or less than 20% of all cases, or late onset, comprising the remaining 80% [51]. Several hypotheses have been proposed to fully elucidate the underlying pathological mechanisms [51–54]. The placental origin of preeclampsia hypothesis describes inefficient trophoblast invasion and remodelling of maternal spiral arteries, causing "placental syndrome," subsequently resulting in preeclampsia and fetal growth restriction [51, 54].

A more recent theory proposed by Thilaganathan implicated abnormal cardiovascular function driving the abnormal placentation that occurs within preeclampsia, and the placental origin of preeclampsia only holds true in the case of early onset of the disease [52, 54]. Late-onset preeclampsia can be attributed to underlying maternal cardiovascular dysfunction which fails to meet the haemodynamic and metabolic needs of the pregnancy and also results in adverse postpartum cardiovascular outcomes in over 50% of patients, possibly due to the fact that both preeclampsia and cardiovascular diseases share similar genetic and environmental risk factors [52].

Supporting the link between placental-mediated pathophysiology of early-onset PE, Yung et al. examined placental samples from preterm, term, and second trimester pregnancies and demonstrated that in early-onset preeclampsia, placental pathology is associated with upregulation of the unfolded protein response (UPR) pathway and ER stress activation along with depression of the AKT pathway, reducing cellular proliferation [55]. These authors demonstrated molecular differences between the two phenotypes of term and preterm preeclampsia [55].

Roberts and Hubel, amongst others, proposed a two-stage model of preeclampsia which was later modified to six stages by Redman et al. [53, 56]. Redman explains that stages 1 and 2 could be an early phenomenon such as preconception tolerance of the mother towards paternal semen or short duration between coitus and conception, leading to poor placentation and affecting the health and growth of the fetus [53]. Stage 3 begins at around 8 weeks of pregnancy where in uncomplicated cases, trophoblastic plugs sealing the maternal spiral arteries recede and the establishment of uteroplacental circulation begins [53, 57]. However, in preeclampsia, there is premature opening of trophoblastic plugs with the influx of arterial blood increasing stress within the placenta and leading to defective placentation [53]. Stage 4 of Redman's model is characterised by decrease in placental growth factors in cases of preeclampsia, leading to impaired vascular remodelling of maternal spiral arteries into larger vessels with low resistance to blood flow by trophoblast [53, 58, 59]. Furthermore, Redman also states that with increased placental and endothelial damage, clinical symptoms of preeclampsia are evident in stages 5 and 6 [53].

The development of the placenta begins with a decidual reaction evoked by the blastocyst in the maternal endometrium, eventually leading to the formation of the basal plate [60, 61]. Trophoblasts differentiate into two types: the invasive extravillous cytotrophoblast (EVT) or the villous cytotrophoblast which later fuse to form the multinucleated syncytiotrophoblast [61, 62]. The extravillous cytotrophoblasts are responsible for establishment of uteroplacental circulation and regulation of the maternal innate immune

system [63, 64]. In uncomplicated pregnancy, extravillous cytotrophoblasts (EVT) invade maternal spiral arteries, veins, and lymphatic vessels of the endometrium during the first trimester [65, 66]. EVT accumulations have also localised in lymph nodes without any neoplastic changes suggesting immune cell regulation by trophoblasts [65, 66].

Defective placentation results in a decrease in the angiogenic vascular endothelial growth factor (VEGF) and placental growth factor (PLGF) and the release of deleterious placental factors like soluble fms-like tyrosine kinase 1 (sFIt1) into the maternal circulation causing generalized endothelial dysfunction [56, 57]. Circulating sFlt1 is abundant in preeclamptic women which is attributed to vascular resistance and increase in arterial blood pressure [67]. Recent studies in women with fetal growth restriction (FGR) with no symptoms of preeclampsia have provided evidence of a high sFlt1/PLGF ratio [68, 69]. Proteinuria in preeclampsia can also be associated with high levels of placental factors like sFlt1, precipitating glomerular endotheliosis [70]. Altered haemodynamic and decreased vascular flow leads to persistent hypoxic-oxygenated states, resulting in high oxidative stress within the placental tissue [55, 71–74]. Even though elevated oxidative stress is evident in trophoblasts during uncomplicated pregnancy, prolonged oxidative stress suppresses trophoblast activity, worsening the situation in pregnancy complications [75].

The syncytiotrophoblast is the outermost layer of the villous trophoblast, in direct contact with maternal blood, and syncytial debris in the form of knots or nuclear aggregates can be detected in maternal circulation with increasing gestational age [76, 77]. Constant vascular flow to the syncytiotrophoblast causes rapid ageing changes and requires activation of autophagy for their removal in uncomplicated pregnancies [8, 78, 79]. During preeclampsia, the syncytiotrophoblast experiences accelerated ageing with upregulation of the apoptotic cascade, necrotic breakdown with release of necrotic debris, and increase in syncytial aggregates [77, 80]. It has been observed that the syncytiotrophoblast secretes Senescence-Associated Beta-Galactosidase (SAβ-Gal) along with elevation of proapoptotic p53 and CDK inhibitors, indicating cessation of cell cycle and senescence [81, 82].

A recent review by Cox and Redman outlines the biochemical pathway and the mechanism of ageing of placental cells following oxidative stress [8]. They outline that the early onset of senescence in preeclampsia can be due to excessive ROS accumulation and oxidative/endoplasmic reticulum (ER) stress leading to mTORC pathway (cell cycle regulator) activation and production of Senescence-Associated Secretory Phenotype (SASP) proteins which then activates the cyclooxygenase pathway and enhances generation of proinflammatory cytokines and chemokines [8].

4. Cellular Senescence in Adverse Pregnancy Outcomes

Trophoblasts mimic cancer cells by displaying invasiveness in order to support growth of the fetus. Like neoplastic cells, trophoblasts maintain their telomere length and Human Telomerase Reverse Transcriptase (hTERT) level in uncomplicated pregnancies [83, 84]. During the first trimester, the trophoblast experiences low oxygen tension or a physiologic hypoxic state, associated with the upregulation of HIF-1α. This low oxygen tension state is responsible for the modelling of villous architecture and maintenance of cellular integrity by preservation of telomere length and upregulation of telomerase enzymes [85, 86]. This physiologic state is altered at the end of the first trimester when the placenta becomes oxygenated [87]. The telomere length remains constant throughout normal pregnancy, but in certain conditions like fetal growth restriction and uncontrolled diabetes, telomere length is significantly reduced [88, 89]. Telomere changes could be associated with increased oxidative stress, leading to DNA damage and activation of damage response (DDR) through the p53 pathway and promoting senescence of the trophoblast [9, 84]. In 2010, Biron-Shental et al. were the first to report evidence of cellular senescence in preeclampsia and fetal growth restriction. They demonstrated that in preeclampsia and IUGR pregnancies, telomeres are significantly shorter in the trophoblast with reduced expression of hTERTs with increased frequency of telomere aggregates when compared to uncomplicated pregnancies [90]. These placental alterations were not present at 37-41 weeks' gestation, indicating premature ageing of the placenta in these pregnancy complications [90].

The placenta ages gradually, and the presence of senescence markers such as p21, p16, p53, and Rb proteins towards the term supports the ageing hypothesis of the normal placenta [91]. Recently, a study by Nuzzo et al. shows cell cycle changes with upregulated cyclin D1 (cell cycle regulator) and PARP1 (expressed on DNA damage and age-related changes) with downregulation of JunB (senescence suppressor gene) in placental mesenchymal stromal cells (PMSC) extracted from the preeclamptic placenta when compared to the normal placenta [92]. Additionally, Sharp et al. found an imbalance between p53 (senescence-inducing and proapoptotic gene) and MDM2 (p53 suppressor) signalling in placental proteins in the syncytiotrophoblast but not in the cytotrophoblast in patients with early-onset preeclampsia [93]. Finally, Gao et al. reported the upregulation of p53 signalling and cell cycle arrest with activation of proapoptotic BAX and caspase proteins in human umbilical vein endothelial cells (HUVEC) taken from patients with preeclampsia when compared to that from uncomplicated pregnancy controls [94].

Activation of DDR pathways, mtDNA mutations, and endogenous stress like ROS accumulation and redox signalling can cause epigenetic modifications. Epigenetics can be defined as physiologic changes which cannot be attributed to the genetic code but rather modifications like phosphorylation, acetylation, or methylation of DNA or histone proteins in the nucleus [95]. Either these changes could be an adaptive response to persistent stimuli or they could be virulent modifications leading to irreversible alterations in germ cells [96]. The link between epigenetics, ageing, and age-related disorders has been demonstrated in several studies. Remodelling of chromatin may include methylation or demethylation of histone residues at specific sites, which can induce epigenetic changes within the cells [95, 96]. Lowe

et al., through their research on endothelial cells collected from the coronary artery of a 19-year-old male, discussed that cellular ageing can be estimated precisely through intrinsic properties of cells known as the epigenetic clock indicated by specific DNA methylation or cytosine methylation of CpG islands, which may speed up ageing under certain conditions [97]. Madrigano et al., through their longitudinal study in an elderly population, showed that gene-specific DNA methylation is strongly associated with ageing and age-related disorders [98].

Epigenetic changes have been demonstrated within placental tissue including DNA methylation patterns, binding ability of DNA-binding proteins or DBP (especially in the cytochrome p450 gene), methylation patterns on imprinted regions in H19/IGF2 genes, and methylation of histone proteins within the human growth hormone in placental chromatin [99]. In a recent study by Eddy et al., histone modifications were evident in the BeWo placental trophoblast when exposed to hypoxic conditions with marked hypomethylation of cytosine, an epigenetic change usually evident in age-related pathologies [100].

5. Mitochondrial Dysfunction-Associated Ageing Changes in the Placenta

The placenta is a highly metabolic organ, requiring robust mitochondrial activity. Even with normal mitochondrial function, continuous changes within the extravillous trophoblast (EVT) and vascular remodelling lead to increased ATP production through oxidative phosphorylation [101, 102].

Accumulation of ROS such as superoxide, nitric oxides, and peroxynitrite results in oxidative stress during early pregnancy [101]. ROS are signalling molecules which have predominance over apoptotic, redox, and inflammatory-mediated signalling pathways, respectively [103, 104]. ROS can be generated from a number of sources including mitochondria (mROS), NADPH oxidases, xanthine oxidase, or p450 enzyme [105, 106]. Reactive oxygen species (ROS) alter macromolecules through oxidative damage to proteins affecting gene functioning, lipid peroxidation with increased polyunsaturated fatty acid circulation, and loss of cellular membrane integrity [107–109]. Upregulation of ROS and its by-product generation, lack of clearance, and redox signalling have direct links to both mitochondrial and cellular ageing. In addition to these changes, oxidative stress activates the Mitogen-Activated Protein Kinase (MAPK) pathway via the Stress-Activated Protein Kinase/Jun N-Terminal Kinase (SAPK/JNK) or p38 pathway in response to DNA damage, which further leads to cessation of cell proliferation, and cellular senescence [110].

Within the placenta, protein nitration and lipid peroxidation have been shown to be significantly higher in tissue isolated from preeclampsia patients compared with uncomplicated pregnancy [111–113]. Lipid peroxidation can be either enzymatic, catalysed by lipoxygenase enzymes, or nonenzymatic in the presence of free radicals [114]. Nonenzymatic lipid peroxidation is upregulated with ageing, and its products are highly expressed in age-related diseases such as atherosclerosis [115]. In 1998, Wang and Walsh described that placental lipid peroxidation was significantly higher in preeclampsia [111]. They established that high lipid peroxidation levels are a result of escalated mitochondrial mass in poor vascular flow to meet energy requirements in preeclampsia [111].

Various systematic reviews have indicated elevated lipid oxidation levels in preeclamptic maternal serum and plasma, usually associated with impaired antioxidant defence when compared with uncomplicated pregnancies [116, 117].

Low vascularization of the placenta results in a reduction in mitochondrial size, number, and activity [118, 119]. A recent study by Venkata et al., using the reduced uterine perfusion pressure (RUPP) model of preeclampsia in rats, showed significant reduction in mitochondrial respiration, especially in stage 3, and increased hydrogen peroxide production when compared to control rats [118].

Nitric oxide signalling regulates cell processes such as apoptosis, differentiation, and division [120]. Extravillous trophoblastic activity such as migration and invasion could be affected by two subtypes of nitric oxides, eNOS (endothelial nitric oxide synthase) and iNOS (inducible nitric oxide synthase) [120]. Nitration of proteins may either have no effect or exhibit loss/gain of functionality. In the placenta, peroxynitrite may alter vascular reactivity and uteroplacental circulation in pregnancy complications such as preeclampsia [91, 121]. Upregulation of NOS activity and peroxynitrite accumulation in preeclampsia may result in depression of mitochondrial activity by inhibiting the electron transport chain and nitration of mitochondrial proteins and antioxidants such as mitochondrial superoxide dismutase (MnSOD) along with activation of trophoblastic apoptosis [122].

As shown in Figure 1, ageing is usually associated with mitochondrial dysfunction as a direct consequence of loss of mitochondrial dynamics and increased mitochondrial damage [122, 123]. Mitochondria undergo continuous fission and fusion to maintain mitochondrial dynamics, failure of which may lead to accumulation of mitochondrial debris and deteriorate mitochondrial functioning [122, 123]. It is believed that mitochondrial dynamics are altered in preeclampsia with altered expression of mitochondrial autophagy regulator genes like OPA1, SIRT3, and MNF2/1, but limited research has been conducted to fully understand the signalling process [124, 125]. Recently, Ausman et al. reported that mitochondrial dynamics in preeclampsia is inclined towards mitochondrial fission with increased phosphorylation of the DERP1 gene in mitochondria isolated from preeclamptic placentas [126]. These changes were accompanied by accumulation of ceramides which upregulated BOK, a proapoptotic protein in preeclamptic placental tissues when compared with normal placenta indicating increased trophoblastic autophagy in preeclampsia and IUGR [126].

Antioxidants are produced by cells to neutralise ROS products by converting them to oxygen and hydrogen peroxide, which is further broken down to form water. Antioxidants are also considered as antiageing agents and can be classified into subtypes: enzymatic such as superoxide dismutases (SODs), catalases, and peroxidases or nonenzymatic such as vitamins (A, C, and E), bilirubin, and uric acid

Table 1: Senescence markers associated with placental ageing in adverse pregnancy outcomes.

Maternal plasma/serum	(1) Mitochondrial dysfunction (2) Inflammatory marker (IL33/ST2 signalling pathway)	↑ mtDNA copy numbers ↑ sST2 level
Trophoblastic cell lines	(1) Cell cycle regulators (2) miRNA/lncRNA (3) DNA damage response (4) Senescence regulators (5) Epigenetic changes	↑ Cyclin D1 ↑ Mir-376 ↑ PARP1 ↑ p53 ↓ JunB ↓ MDM2 ↑Hypomethylation of cytosine
Placenta	(1) DNA damage response (2) Cell cycle regulators (3) Mitochondrial dysfunction	↑ p53 ↓ hTERT ↑ Telomere aggregates ↑ BAX ↑Lipid peroxidation ↑ NOS activity ↑ Peroxynitrite synthesis ↑ Phosphorylated DERP1 gene

[127, 128]. Oxidative stress ensues when there is an imbalance between the ROS by-products produced and those scavenged by antioxidants [128, 129]. All major antioxidants are localised in the placenta to reduce oxidative stress, and their activity is dependent on the amount of stress experienced by the cells [71]. In preeclampsia and IUGR, antioxidant activity is attenuated when compared to uncomplicated pregnancies, as shown in Figure 1 [127].

6. Senescence Markers in Adverse Pregnancy Outcomes

A major obstetric challenge has been to establish biomarkers for detection of pregnancy complications such as preeclampsia and IUGR in maternal body fluids. Various markers of mitochondrial dysfunction and oxidative stress have been investigated as early biomarkers for pregnancy disorders, as shown in Table 1. In 2012, Qiu et al. were the first to report elevated mtDNA levels in the maternal peripheral blood in preeclampsia indicating high oxidative stress and mitochondrial dysfunction [132]. A recent case-control study by Williamson and McCarthy and Kenny found elevated mtDNA copy numbers in maternal plasma at 15-20 weeks' gestation in preeclamptic cases compared to those in uncomplicated pregnancy controls [133, 134]. Furthermore, this study also demonstrated significant reduction in the antioxidant mitochondrial superoxide dismutase (mSOD) level at 15 weeks' gestation in women who later developed preeclampsia, thus vindicating mitochondrial dysfunction as a pathophysiological event in preeclampsia [134]. Another similar study by Marschalek et al. indicated similar results with elevated mtDNA copy numbers in maternal serum detectable in early-onset preeclampsia [135].

Apart from mitochondrial dysfunction, inflammation and inflammatory mediators are evident in premature ageing of the placenta. Certain ageing-associated inflammatory markers such as Senescence-Associated Secretory Phenotypes (SASPs) are elevated in preeclampsia [136].

Kupferminc et al. showed that TNF-α is significantly elevated in amniotic fluid and maternal plasma in severe preeclampsia [137]. sST2 (soluble ST2) is a member of the interleukin-1 family, expressed abundantly in endothelial cells, and usually associated with age-related disorders such as cardiac diseases [138]. In the case of elevated cell death and necrotic signalling, the IL33/STL2 pathway is triggered by Toll-Like Receptor-1 (TLR1) activation which leads to upregulation of the cytokine and chemokine influx [139]. A recent longitudinal study by Romero et al. reported significant elevation of sST2 levels in maternal plasma in risk patients almost 6 weeks prior to development of preeclampsia [140].

MicroRNAs (miRNA) and long noncoding RNAs (lncRNA) are noncoding RNAs that have the potential for gene regulation [141]. miRNAs are available in bodily fluids and are now being regularly investigated as both biomarkers and perspective therapeutics. In the uterus, miRNAs are controlled by steroidal hormones and they are responsible for efficient placentation. Recent work by Tan et al. stated that in adverse placental conditions like preeclampsia, long noncoding RNA, lncRNA DLX6-AS1, is overexpressed in trophoblastic cell lines, resulting in upregulation of mir-376c which is responsible for cell cycle arrest [142].

7. Potential Therapeutics and Future Perspectives for Adverse Pregnancy Outcomes

Ageing is a unidirectional process which cannot be reversed; however, research focused on reducing oxidative stress by restoring mitochondrial fitness could be a potential therapy for adverse pregnancy outcomes [143]. Mitochondrial fitness is acknowledged as the key regulator for cell cycle progression and metabolism with mitochondrial interactions with other organelles including the nucleus and endoplasmic reticulum (ER) ensuring homeostasis of cellular dynamics and viability. In pregnancy complications, chronic oxidative

stress leads to mitochondrial dysfunction resulting in loss of mitochondrial signalling stability [102]. Antioxidant supplements such as vitamins C and E given during pregnancy have not demonstrated any significant effects in reducing oxidative stress.

However, continued research for more effective antioxidants have shed light on a few cytoprotective agents targeting the mitochondria.

A recent study has demonstrated that a mitochondria targeting antioxidant, MitoTEMPO, is cytoprotective against ROS-induced cell death [134]. When HUVEC cells were pretreated with MitoTEMPO before exposure to 3% plasma from preeclampsia pregnancies, it resulted in significant reduction in cellular superoxide production, normalization of mitochondrial functioning, and reduction in inflammatory influx [134]. Recently, another study done by Nuzzo et al. demonstrates that mitochondrial-targeting antioxidant MitoQ-treated pregnant rats exhibit normalized placental volumes and rescued fetal growth restriction in hypoxic conditions [144]. Furthermore, they discussed that MitoQ has the potential to regulate the cell cycle through the MAPK proliferation signalling pathway [144].

Finally, ergothioneine is a water soluble amino acid that has been shown to be cytoprotective. Ergothioneine primarily targets the mitochondria and can scavenge ROS, induce cellular proliferation, and repair through upregulated antioxidant pathways [145]. The multitude of benefits of antioxidants targeting and normalizing mitochondrial functioning and dynamics may become potential prenatal therapeutics for adverse pregnancy outcomes [145].

8. Conclusion

Senescence is beneficial to multicellular organisms especially for elimination of mutations and prevention of cancers. However, in the presence of persistent undesirable stress, this process can accelerate unnaturally and result in serious health complications. In adverse pregnancy outcomes such as preeclampsia and fetal growth restriction, placental insufficiency is accompanied with aberrant signalling for premature placental senescence and apoptosis. As summarized through Figure 1, this review has highlighted the current knowledge on the role of placental mitochondrial dysfunction, cellular senescence, and the placental ageing axis in adverse pregnancy outcomes.

Future research should focus on furthering our understanding of premature placental ageing as a pathophysiology in pregnancy disorders and investigating novel ways to improve outcomes such as preeclampsia and fetal growth restriction.

Conflicts of Interest

The authors declare no conflict of interest.

Authors' Contributions

Cathal McCarthy and Fergus P. McCarthy contributed equally.

Acknowledgments

This project is funded by the European Union's Horizon 2020 research and innovation programme under Marie Skłodowska-Curie Actions Innovative Training Network (H2020-MSCA-ITN 2017), Grant No. 765274, acronym iPLACENTA (http://www.iplacenta.eu).

References

[1] A. L. Tranquilli, G. Dekker, L. Magee et al., "The classification, diagnosis and management of the hypertensive disorders of pregnancy: a revised statement from the ISSHP," *Pregnancy Hypertension: An International Journal of Women's Cardiovascular Health*, vol. 4, no. 2, pp. 97–104, 2014.

[2] A. Jeyabalan, "Epidemiology of pre-eclampsia: impact of obesity," *Nutrition Reviews*, vol. 71, Supplement 1, pp. S18–S25, 2013.

[3] L. Duley, "The global impact of pre-eclampsia and eclampsia," *Seminars in Perinatology*, vol. 33, no. 3, pp. 130–137, 2009.

[4] V. Chaddha, S. Viero, B. Huppertz, and J. Kingdom, "Developmental biology of the placenta and the origins of placental insufficiency," *Seminars in Fetal and Neonatal Medicine*, vol. 9, no. 5, pp. 357–369, 2004.

[5] F. P. McCarthy, S. Drewlo, F. A. English et al., "Evidence implicating peroxisome proliferator-activated receptor-γ in the pathogenesis of pre-eclampsia," *Hypertension*, vol. 58, no. 5, pp. 882–887, 2011.

[6] G. C. Kujoth, A. Hiona, T. D. Pugh et al., "Mitochondrial DNA mutations, oxidative stress, and apoptosis in mammalian aging," *Science*, vol. 309, no. 5733, pp. 481–484, 2005.

[7] C. W. G. Redman and I. L. Sargent, "Placental stress and pre-eclampsia: a revised view," *Placenta*, vol. 30, pp. 38–42, 2009.

[8] L. S. Cox and C. Redman, "The role of cellular senescence in ageing of the placenta," *Placenta*, vol. 52, pp. 139–145, 2017.

[9] T. Cindrova-Davies, N. M. E. Fogarty, C. J. P. Jones, J. Kingdom, and G. J. Burton, "Evidence of oxidative stress-induced senescence in mature, post-mature and pathological human placentas," *Placenta*, vol. 68, pp. 15–22, 2018.

[10] P. Davy, M. Nagata, P. Bullard, N. S. Fogelson, and R. Allsopp, "Fetal growth restriction is associated with accelerated telomere shortening and increased expression of cell senescence markers in the placenta," *Placenta*, vol. 30, no. 6, pp. 539–542, 2009.

[11] T. de Lange, "How telomeres solve the end-protection problem," *Science*, vol. 326, no. 5955, pp. 948–952, 2009.

[12] Y. Zhu, X. Liu, X. Ding, F. Wang, and X. Geng, "Telomere and its role in the aging pathways: telomere shortening, cell senescence and mitochondria dysfunction," *Biogerontology*, vol. 20, no. 1, pp. 1–16, 2019.

[13] J. W. Shay, "Role of telomeres and telomerase in aging and cancer," *Cancer Discovery*, vol. 6, no. 6, pp. 584–593, 2016.

[14] M. O'Reilly, S. A. Teichmann, and D. Rhodes, "Telomerases," *Current Opinion in Structural Biology*, vol. 9, no. 1, pp. 56–65, 1999.

[15] A. Bernadotte, V. M. Mikhelson, and I. M. Spivak, "Markers of cellular senescence. Telomere shortening as a marker of cellular senescence," *Aging*, vol. 8, no. 1, pp. 3–11, 2016.

[16] G. Glousker and J. Lingner, "When telomerase causes telomere loss," *Developmental Cell*, vol. 44, no. 3, pp. 281–283, 2018.

[17] P. Margalef, P. Kotsantis, V. Borel, R. Bellelli, S. Panier, and S. J. Boulton, "Stabilization of reversed replication forks by telomerase drives telomere catastrophe," *Cell*, vol. 172, no. 3, pp. 439–453.e14, 2018.

[18] J. W. Shay and W. E. Wright, "Hayflick, his limit, and cellular ageing," *Nature Reviews Molecular Cell Biology*, vol. 1, no. 1, pp. 72–76, 2000.

[19] M. Giorgio, M. Trinei, E. Migliaccio, and P. G. Pelicci, "Hydrogen peroxide: a metabolic by-product or a common mediator of ageing signals?," *Nature Reviews Molecular Cell Biology*, vol. 8, no. 9, pp. 722–728, 2007.

[20] M. Schieber and N. S. Chandel, "ROS function in redox signaling and oxidative stress," *Current Biology*, vol. 24, no. 10, pp. R453–R462, 2014.

[21] V. N. Gladyshev, "The free radical theory of aging is dead. Long live the damage theory!," *Antioxidants and Redox Signaling*, vol. 20, no. 4, pp. 727–731, 2014.

[22] P. Theurey and P. Pizzo, "The aging mitochondria," *Genes*, vol. 9, no. 1, p. 22, 2018.

[23] K. Boengler, M. Kosiol, M. Mayr, R. Schulz, and S. Rohrbach, "Mitochondria and ageing: role in heart, skeletal muscle and adipose tissue," *Journal of Cachexia, Sarcopenia and Muscle*, vol. 8, no. 3, pp. 349–369, 2017.

[24] G. Lenaz, "Role of mitochondria in oxidative stress and ageing," *Biochimica et Biophysica Acta (BBA) - Bioenergetics*, vol. 1366, no. 1-2, pp. 53–67, 1998.

[25] A. Trifunovic, A. Wredenberg, M. Falkenberg et al., "Premature ageing in mice expressing defective mitochondrial DNA polymerase," *Nature*, vol. 429, no. 6990, pp. 417–423, 2004.

[26] Y. Mikhed, A. Daiber, and S. Steven, "Mitochondrial oxidative stress, mitochondrial DNA damage and their role in age-related vascular dysfunction," *International Journal of Molecular Sciences*, vol. 16, no. 7, pp. 15918–15953, 2015.

[27] J. B. Stewart, C. Freyer, J. L. Elson, and N. G. Larsson, "Purifying selection of mtDNA and its implications for understanding evolution and mitochondrial disease," *Nature Reviews Genetics*, vol. 9, no. 9, pp. 657–662, 2008.

[28] G. L. Norddahl, C. J. Pronk, M. Wahlestedt et al., "Accumulating mitochondrial DNA mutations drive premature hematopoietic aging phenotypes distinct from physiological stem cell aging," *Cell Stem Cell*, vol. 8, no. 5, pp. 499–510, 2011.

[29] T. Su, D. Turnbull, and L. Greaves, "Roles of mitochondrial DNA mutations in stem cell ageing," *Genes*, vol. 9, no. 4, p. 182, 2018.

[30] S. Abel, P. Abel zur Wiesch, B. M. Davis, and M. K. Waldor, "Analysis of bottlenecks in experimental models of infection," *PLoS Pathogens*, vol. 11, no. 6, article e1004823, 2015.

[31] Y. Kurihara, T. Kanki, Y. Aoki et al., "Mitophagy plays an essential role in reducing mitochondrial production of reactive oxygen species and mutation of mitochondrial DNA by maintaining mitochondrial quantity and quality in yeast," *Journal of Biological Chemistry*, vol. 287, no. 5, pp. 3265–3272, 2012.

[32] I. Kim, S. Rodriguez-Enriquez, and J. J. Lemasters, "Selective degradation of mitochondria by mitophagy," *Archives of Biochemistry and Biophysics*, vol. 462, no. 2, pp. 245–253, 2007.

[33] C. Tatone, F. Amicarelli, M. C. Carbone et al., "Cellular and molecular aspects of ovarian follicle ageing," *Human Reproduction Update*, vol. 14, no. 2, pp. 131–142, 2008.

[34] R. K. Lane, T. Hilsabeck, and S. L. Rea, "The role of mitochondrial dysfunction in age-related diseases," *Biochimica et Biophysica Acta (BBA) - Bioenergetics*, vol. 1847, no. 11, pp. 1387–1400, 2015.

[35] A. Diot, K. Morten, and J. Poulton, "Mitophagy plays a central role in mitochondrial ageing," *Mammalian Genome*, vol. 27, no. 7-8, pp. 381–395, 2016.

[36] L. Tilokani, S. Nagashima, V. Paupe, and J. Prudent, "Mitochondrial dynamics: overview of molecular mechanisms," *Essays In Biochemistry*, vol. 62, no. 3, pp. 341–360, 2018.

[37] G. Twig, A. Elorza, A. J. A. Molina et al., "Fission and selective fusion govern mitochondrial segregation and elimination by autophagy," *The EMBO Journal*, vol. 27, no. 2, pp. 433–446, 2008.

[38] K. Palikaras, E. Lionaki, and N. Tavernarakis, "Coordination of mitophagy and mitochondrial biogenesis during ageing in *C. elegans*," *Nature*, vol. 521, no. 7553, pp. 525–528, 2015.

[39] A. Hoshino, Y. Mita, Y. Okawa et al., "Cytosolic p53 inhibits Parkin-mediated mitophagy and promotes mitochondrial dysfunction in the mouse heart," *Nature Communications*, vol. 4, no. 1, article 2308, 2013.

[40] M. Song, K. Mihara, Y. Chen, L. Scorrano, and G. W. Dorn II, "Mitochondrial fission and fusion factors reciprocally orchestrate mitophagic culling in mouse hearts and cultured fibroblasts," *Cell Metabolism*, vol. 21, no. 2, pp. 273–286, 2015.

[41] V. Jovaisaite and J. Auwerx, "The mitochondrial unfolded protein response - synchronizing genomes," *Current Opinion in Cell Biology*, vol. 33, pp. 74–81, 2015.

[42] R. H. Houtkooper, L. Mouchiroud, D. Ryu et al., "Mitonuclear protein imbalance as a conserved longevity mechanism," *Nature*, vol. 497, no. 7450, pp. 451–457, 2013.

[43] F. Urano, M. Calfon, T. Yoneda et al., "A survival pathway for *Caenorhabditis elegans* with a blocked unfolded protein response," *Journal of Cell Biology*, vol. 158, no. 4, pp. 639–646, 2002.

[44] S. Wolff and A. Dillin, "Ageing: beneficial miscommunication," *Nature*, vol. 497, no. 7450, pp. 442-443, 2013.

[45] F. Licastro, G. Candore, D. Lio et al., "Innate immunity and inflammation in ageing: a key for understanding age-related diseases," *Immunity & Ageing*, vol. 2, no. 1, p. 8, 2005.

[46] G. Pawelec, D. Goldeck, and E. Derhovanessian, "Inflammation, ageing and chronic disease," *Current Opinion in Immunology*, vol. 29, pp. 23–28, 2014.

[47] N. Loaiza and M. Demaria, "Cellular senescence and tumor promotion: is aging the key?," *Biochimica et Biophysica Acta (BBA) - Reviews on Cancer*, vol. 1865, no. 2, pp. 155–167, 2016.

[48] M. E. Poynter and R. A. Daynes, "Peroxisome proliferator-activated receptor α activation modulates cellular redox status, represses nuclear factor-κB signaling, and reduces inflammatory cytokine production in aging," *Journal of Biological Chemistry*, vol. 273, no. 49, pp. 32833–32841, 1998.

[49] A. Freund, A. V. Orjalo, P. Y. Desprez, and J. Campisi, "Inflammatory networks during cellular senescence: causes and consequences," *Trends in Molecular Medicine*, vol. 16, no. 5, pp. 238–246, 2010.

[50] E. Montecino-Rodriguez, B. Berent-Maoz, and K. Dorshkind, "Causes, consequences, and reversal of immune system

aging," *The Journal of Clinical Investigation*, vol. 123, no. 3, pp. 958–965, 2013.

[51] B. Huppertz, "Placental origins of preeclampsia," *Hypertension*, vol. 51, no. 4, pp. 970–975, 2008.

[52] B. Thilaganathan, "Pre-eclampsia is primarily a placental disorder," *BJOG: An International Journal of Obstetrics & Gynaecology*, vol. 124, no. 11, pp. 1763–1763, 2017.

[53] C. W. G. Redman, "The six stages of pre-eclampsia," *Pregnancy Hypertension: An International Journal of Women's Cardiovascular Health*, vol. 4, no. 3, p. 246, 2014.

[54] B. Thilaganathan, "Placental syndromes: getting to the heart of the matter," *Ultrasound in Obstetrics & Gynecology*, vol. 49, no. 1, pp. 7–9, 2017.

[55] H. W. Yung, D. Atkinson, T. Campion-Smith, M. Olovsson, D. S. Charnock-Jones, and G. J. Burton, "Differential activation of placental unfolded protein response pathways implies heterogeneity in causation of early- and late-onset pre-eclampsia," *The Journal of Pathology*, vol. 234, no. 2, pp. 262–276, 2014.

[56] J. M. Roberts and C. A. Hubel, "The two stage model of pre-eclampsia: variations on the theme," *Placenta*, vol. 30, pp. 32–37, 2009.

[57] T. Tomimatsu, K. Mimura, M. Endo, K. Kumasawa, and T. Kimura, "Pathophysiology of preeclampsia: an angiogenic imbalance and long-lasting systemic vascular dysfunction," *Hypertension Research*, vol. 40, no. 4, pp. 305–310, 2017.

[58] F. Reister, H. G. Frank, J. C. P. Kingdom et al., "Macrophage-induced apoptosis limits endovascular trophoblast invasion in the uterine wall of preeclamptic women," *Laboratory Investigation*, vol. 81, no. 8, pp. 1143–1152, 2001.

[59] F. Colucci, "The role of KIR and HLA interactions in pregnancy complications," *Immunogenetics*, vol. 69, no. 8-9, pp. 557–565, 2017.

[60] B. Pansky, "Chapter 41, Placental physiology," *Review of Medical Embyology*, 1982.

[61] J. S. Lowe and P. G. Anderson, "Chapter 17 - female reproductive system," in *Stevens & Lowe's Human Histology (Fourth Edition)*, J. S. Lowe and P. G. Anderson, Eds., pp. 337–362, Mosby, Philadelphia, 2015.

[62] A. Tarrade, R. Lai Kuen, A. Malassiné et al., "Characterization of human villous and extravillous trophoblasts isolated from first trimester placenta," *Laboratory Investigation*, vol. 81, no. 9, pp. 1199–1211, 2001.

[63] G. J. Burton and A. L. Fowden, "The placenta: a multifaceted, transient organ," *Philosophical Transactions of the Royal Society B: Biological Sciences*, vol. 370, no. 1663, article 20140066, 2015.

[64] G. J. Burton and E. Jauniaux, "What is the placenta?," *American Journal of Obstetrics and Gynecology*, vol. 213, no. 4, pp. - S6.e1–S6.e4, 2015.

[65] D. Goldman-Wohl and S. Yagel, "Regulation of trophoblast invasion: from normal implantation to pre-eclampsia," *Molecular and Cellular Endocrinology*, vol. 187, no. 1-2, pp. 233–238, 2002.

[66] K. Windsperger, S. Dekan, S. Pils et al., "Extravillous trophoblast invasion of venous as well as lymphatic vessels is altered in idiopathic, recurrent, spontaneous abortions," *Human Reproduction*, vol. 32, no. 6, pp. 1208–1217, 2017.

[67] K. Koga, Y. Osuga, O. Yoshino et al., "Elevated serum soluble vascular endothelial growth factor receptor 1 (sVEGFR-1) levels in women with pre-eclampsia," *The Journal of Clinical Endocrinology & Metabolism*, vol. 88, no. 5, pp. 2348–2351, 2003.

[68] S. Shinohara, Y. Uchida, M. Kasai, and R. Sunami, "Association between the high soluble fms-like tyrosine kinase-1 to placental growth factor ratio and adverse outcomes in asymptomatic women with early-onset fetal growth restriction," *Hypertension in Pregnancy*, vol. 36, no. 3, pp. 269–275, 2017.

[69] I. Herraiz, M. S. Quezada, J. Rodriguez-Calvo, E. Gómez-Montes, C. Villalaín, and A. Galindo, "Longitudinal change of sFlt-1/PlGF ratio in singleton pregnancy with early-onset fetal growth restriction," *Ultrasound in Obstetrics & Gynecology*, vol. 52, no. 5, pp. 631–638, 2018.

[70] I. M. Craici, S. J. Wagner, T. L. Weissgerber, J. P. Grande, and V. D. Garovic, "Advances in the pathophysiology of pre-eclampsia and related podocyte injury," *Kidney International*, vol. 86, no. 2, pp. 275–285, 2014.

[71] L. Myatt and X. Cui, "Oxidative stress in the placenta," *Histochemistry and Cell Biology*, vol. 122, no. 4, pp. 369–382, 2004.

[72] C. W. G. Redman and I. L. Sargent, "Placental debris, oxidative stress and pre-eclampsia," *Placenta*, vol. 21, no. 7, pp. 597–602, 2000.

[73] O. Genbacev, Y. Zhou, J. W. Ludlow, and S. J. Fisher, "Regulation of human placental development by oxygen tension," *Science*, vol. 277, no. 5332, pp. 1669–1672, 1997.

[74] C. H. Damsky, M. L. Fitzgerald, and S. J. Fisher, "Distribution patterns of extracellular matrix components and adhesion receptors are intricately modulated during first trimester cytotrophoblast differentiation along the invasive pathway, in vivo," *Journal of Clinical Investigation*, vol. 89, no. 1, pp. 210–222, 1992.

[75] M. H. Schoots, S. J. Gordijn, S. A. Scherjon, H. van Goor, and J. L. Hillebrands, "Oxidative stress in placental pathology," *Placenta*, vol. 69, pp. 153–161, 2018.

[76] S. Guller, "Role of the syncytium in placenta-mediated complications of preeclampsia," *Thrombosis Research*, vol. 124, no. 4, pp. 389–392, 2009.

[77] C. S. Roland, J. Hu, C. E. Ren et al., "Morphological changes of placental syncytium and their implications for the pathogenesis of preeclampsia," *Cellular and Molecular Life Sciences*, vol. 73, no. 2, pp. 365–376, 2016.

[78] S. J. Coleman, L. Gerza, C. J. P. Jones, C. P. Sibley, J. D. Aplin, and A. E. P. Heazell, "Syncytial nuclear aggregates in normal placenta show increased nuclear condensation, but apoptosis and cytoskeletal redistribution are uncommon," *Placenta*, vol. 34, no. 5, pp. 449–455, 2013.

[79] C. P. Chen, K. G. Wang, C. Y. Chen, C. Yu, H. C. Chuang, and H. Chen, "Altered placental syncytin and its receptor ASCT2 expression in placental development and pre-eclampsia," *BJOG: An International Journal of Obstetrics & Gynaecology*, vol. 113, no. 2, pp. 152–158, 2006.

[80] H. Soma, K. Yoshida, T. Mukaida, and Y. Tabuchi, "Morphologic changes in the hypertensive placenta," *Contributions to Gynecology and Obstetrics*, vol. 9, pp. 58–75, 1982.

[81] S. Roberge, K. Nicolaides, S. Demers, J. Hyett, N. Chaillet, and E. Bujold, "The role of aspirin dose on the prevention of pre-eclampsia and fetal growth restriction: systematic review and meta-analysis," *American Journal of Obstetrics and Gynecology*, vol. 216, no. 2, pp. 110–120.e6, 2017.

[82] A. N. Sharp, A. E. P. Heazell, D. Baczyk et al., "Preeclampsia is associated with alterations in the p53-pathway in villous trophoblast," *PLoS One*, vol. 9, no. 1, article e87621, 2014.

[83] S. E. Hallows, T. R. H. Regnault, and D. H. Betts, "The long and short of it: the role of telomeres in fetal origins of adult disease," *Journal of Pregnancy*, vol. 2012, Article ID 638476, 8 pages, 2012.

[84] T. Biron-Shental, D. Sadeh-Mestechkin, and A. Amiel, "Telomere homeostasis in IUGR placentas - a review," *Placenta*, vol. 39, pp. 21–23, 2016.

[85] F. Ietta, Y. Wu, J. Winter et al., "Dynamic HIF1A regulation during human placental development," *Biology of Reproduction*, vol. 75, no. 1, pp. 112–121, 2006.

[86] H. Nishi, T. Nakada, S. Kyo, M. Inoue, J. W. Shay, and K. Isaka, "Hypoxia-inducible factor 1 mediates upregulation of telomerase (hTERT)," *Molecular and Cellular Biology*, vol. 24, no. 13, pp. 6076–6083, 2004.

[87] K. Vrijens, M. Tsamou, N. Madhloum, W. Gyselaers, and T. S. Nawrot, "Placental hypoxia-regulating network in relation to birth weight and ponderal index: the ENVIRONAGE Birth Cohort Study," *Journal of Translational Medicine*, vol. 16, no. 1, p. 2, 2018.

[88] T. Biron-Shental, R. Sukenik-Halevy, H. Naboani, M. Liberman, R. Kats, and A. Amiel, "Telomeres are shorter in placentas from pregnancies with uncontrolled diabetes," *Placenta*, vol. 36, no. 2, pp. 199–203, 2015.

[89] J. Toutain, M. Prochazkova-Carlotti, D. Cappellen et al., "Reduced placental telomere length during pregnancies complicated by intrauterine growth restriction," *PLoS One*, vol. 8, no. 1, article e54013, 2013.

[90] T. Biron-Shental, R. Sukenik-Halevy, Y. Sharon et al., "Short telomeres may play a role in placental dysfunction in preeclampsia and intrauterine growth restriction," *American Journal of Obstetrics and Gynecology*, vol. 202, no. 4, pp. 381.e1–381.e7, 2010.

[91] A. M. Roggensack, Y. Zhang, and S. T. Davidge, "Evidence for peroxynitrite formation in the vasculature of women with pre-eclampsia," *Hypertension*, vol. 33, no. 1, pp. 83–89, 1999.

[92] A. M. Nuzzo, D. Giuffrida, B. Masturzo et al., "Altered expression of G1/S phase cell cycle regulators in placental mesenchymal stromal cells derived from preeclamptic pregnancies with fetal-placental compromise," *Cell Cycle*, vol. 16, no. 2, pp. 200–212, 2017.

[93] A. N. Sharp, A. E. P. Heazell, D. Baczyk et al., "Pre-eclampsia is associated with alterations in the p53-pathway in villous trophoblast," *PLoS One*, vol. 9, no. 1, article e87621, 2014.

[94] Q. Gao, X. Zhu, J. Chen, C. Mao, L. Zhang, and Z. Xu, "Upregulation of P53 promoted G1 arrest and apoptosis in human umbilical cord vein endothelial cells from preeclampsia," *Journal of Hypertension*, vol. 34, no. 7, pp. 1380–1388, 2016.

[95] L. Mirbahai and J. K. Chipman, "Epigenetic memory of environmental organisms: a reflection of lifetime stressor exposures," *Mutation Research/Genetic Toxicology and Environmental Mutagenesis*, vol. 764-765, pp. 10–17, 2014.

[96] K. Leavey, S. L. Wilson, S. A. Bainbridge, W. P. Robinson, and B. J. Cox, "Epigenetic regulation of placental gene expression in transcriptional subtypes of pre-eclampsia," *Clinical Epigenetics*, vol. 10, no. 1, p. 28, 2018.

[97] D. Lowe, S. Horvath, and K. Raj, "Epigenetic clock analyses of cellular senescence and ageing," *Oncotarget*, vol. 7, no. 8, pp. 8524–8531, 2016.

[98] J. Madrigano, A. A. Baccarelli, M. A. Mittleman et al., "Aging and epigenetics: longitudinal changes in gene-specific DNA methylation," *Epigenetics*, vol. 7, no. 1, pp. 63–70, 2012.

[99] M. A. Maccani and C. J. Marsit, "Review article: epigenetics in the placenta," *American Journal of Reproductive Immunology*, vol. 62, no. 2, pp. 78–89, 2009.

[100] A. C. Eddy, H. Chapman, and E. M. George, "Acute hypoxia and chronic ischemia induce differential total changes in placental epigenetic modifications," *Reproductive Sciences*, no. - article 1933719118799193, 2018.

[101] G. J. Burton, C. P. Sibley, E. R. M. Jauniaux, S. G. Gabbe, J. R. Niebyl, J. L. Simpson, M. B. Landon, H. L. Galan, D. A. Driscoll, V. Berghella, and W. A. Grobman, Eds., "Chapter 1: placental anatomy and physiology," in *Obstetrics: Normal and Problem Pregnancies*, Elsevier, 7th edition, 2016.

[102] G. J. Burton, H. W. Yung, and A. J. Murray, "Mitochondrial-endoplasmic reticulum interactions in the trophoblast: stress and senescence," *Placenta*, vol. 52, pp. 146–155, 2017.

[103] J. Zhang, X. Wang, V. Vikash et al., "ROS and ROS-mediated cellular signaling," *Oxidative Medicine and Cellular Longevity*, vol. 2016, Article ID 4350965, 18 pages, 2016.

[104] T. Finkel, "Signal transduction by reactive oxygen species," *Journal of Cell Biology*, vol. 194, no. 1, pp. 7–15, 2011.

[105] C. M. McCarthy and L. C. Kenny, "Mitochondrial [dys]function; culprit in preeclampsia?," *Clinical Science*, vol. 130, no. 14, pp. 1179–1184, 2016.

[106] P. Jezek and L. Hlavata, "Mitochondria in homeostasis of reactive oxygen species in cell, tissues, and organism," *The International Journal of Biochemistry & Cell Biology*, vol. 37, no. 12, pp. 2478–2503, 2005.

[107] T. Finkel and N. J. Holbrook, "Oxidants, oxidative stress and the biology of ageing," *Nature*, vol. 408, no. 6809, pp. 239–247, 2000.

[108] M. Ott, V. Gogvadze, S. Orrenius, and B. Zhivotovsky, "Mitochondria, oxidative stress and cell death," *Apoptosis*, vol. 12, no. 5, pp. 913–922, 2007.

[109] G. J. Burton and E. Jauniaux, "Oxidative stress," *Best Practice & Research Clinical Obstetrics & Gynaecology*, vol. 25, no. 3, pp. 287–299, 2011.

[110] X. Luo, Z. W. Yao, H. B. Qi et al., "Gadd45α as an upstream signaling molecule of p38 MAPK triggers oxidative stress-induced sFlt-1 and sEng upregulation in preeclampsia," *Cell and Tissue Research*, vol. 344, no. 3, pp. 551–565, 2011.

[111] Y. Wang and S. W. Walsh, "Placental mitochondria as a source of oxidative stress in pre-eclampsia," *Placenta*, vol. 19, no. 8, pp. 581–586, 1998.

[112] V. Toescu, S. L. Nuttall, U. Martin, M. J. Kendall, and F. Dunne, "Oxidative stress and normal pregnancy," *Clinical Endocrinology*, vol. 57, no. 5, pp. 609–613, 2002.

[113] A. Fujimaki, K. Watanabe, T. Mori, C. Kimura, K. Shinohara, and A. Wakatsuki, "Placental oxidative DNA damage and its repair in preeclamptic women with fetal growth restriction," *Placenta*, vol. 32, no. 5, pp. 367–372, 2011.

[114] M. Repetto, J. Semprine, and A. Boveris, "Lipid peroxidation: chemical mechanism, biological implications and analytical determination," in *Lipid Peroxidation*, IntechOpen, 2012.

[115] G. Spiteller, "Lipid peroxidation in aging and age-dependent diseases," *Experimental Gerontology*, vol. 36, no. 9, pp. 1425–1457, 2001.

[116] S. Gupta, N. Aziz, L. Sekhon et al., "Lipid peroxidation and antioxidant status in preeclampsia: a systematic review,"

Obstetrical & Gynecological Survey, vol. 64, no. 11, pp. 750–759, 2009.

[117] E. Llurba, E. Gratacós, P. Martín-Gallán, L. Cabero, and C. Dominguez, "A comprehensive study of oxidative stress and antioxidant status in preeclampsia and normal pregnancy," *Free Radical Biology & Medicine*, vol. 37, no. 4, pp. 557–570, 2004.

[118] V. R. Vaka, K. M. McMaster, M. W. Cunningham Jr et al., "Role of mitochondrial dysfunction and reactive oxygen species in mediating hypertension in the reduced uterine perfusion pressure rat model of preeclampsia," *Hypertension*, vol. 72, no. 3, pp. 703–711, 2018.

[119] S. S. Salgado and M. K. R. Salgado, "Structural changes in preeclamptic and eclamptic placentas—an ultrastructural study," *Journal of the College of Physicians and Surgeons Pakistan*, vol. 21, no. 8, pp. 482–486, 2011.

[120] F. Lyall, J. N. Bulmer, H. Kelly, E. Duffie, and S. C. Robson, "Human trophoblast invasion and spiral artery transformation: The Role of Nitric Oxide," *The American Journal of Pathology*, vol. 154, no. 4, pp. 1105–1114, 1999.

[121] W. Kossenjans, A. Eis, R. Sahay, D. Brockman, and L. Myatt, "Role of peroxynitrite in altered fetal-placental vascular reactivity in diabetes or preeclampsia," *American Journal of Physiology-Heart and Circulatory Physiology*, vol. 278, no. 4, pp. H1311–H1319, 2000.

[122] A. Y. Seo, A. M. Joseph, D. Dutta, J. C. Y. Hwang, J. P. Aris, and C. Leeuwenburgh, "New insights into the role of mitochondria in aging: mitochondrial dynamics and more," *Journal of Cell Science*, vol. 123, no. 15, pp. 2533–2542, 2010.

[123] N. Sun, R. J. Youle, and T. Finkel, "The mitochondrial basis of aging," *Molecular Cell*, vol. 61, no. 5, pp. 654–666, 2016.

[124] H. Chen, S. A. Detmer, A. J. Ewald, E. E. Griffin, S. E. Fraser, and D. C. Chan, "Mitofusins Mfn1 and Mfn2 coordinately regulate mitochondrial fusion and are essential for embryonic development," *Journal of Cell Biology*, vol. 160, no. 2, pp. 189–200, 2003.

[125] L. Zhang, L. Han, R. Ma et al., "Sirt3 prevents maternal obesity-associated oxidative stress and meiotic defects in mouse oocytes," *Cell Cycle*, vol. 14, no. 18, pp. 2959–2968, 2015.

[126] J. Ausman, J. Abbade, L. Ermini et al., "Ceramide-induced BOK promotes mitochondrial fission in pre-eclampsia," *Cell Death & Disease*, vol. 9, no. 3, p. 298, 2018.

[127] R. D. Williamson, C. McCarthy, F. P. McCarthy, and L. C. Kenny, "Oxidative stress in pre-eclampsia; have we been looking in the wrong place?," *Pregnancy Hypertension: An International Journal of Women's Cardiovascular Health*, vol. 8, pp. 1–5, 2017.

[128] V. Lobo, A. Patil, A. Phatak, and N. Chandra, "Free radicals, antioxidants and functional foods: Impact on human health," *Pharmacognosy Reviews*, vol. 4, no. 8, pp. 118–126, 2010.

[129] A. M. R. Salles, T. F. Galvao, M. T. Silva, L. C. D. Motta, and M. G. Pereira, "Antioxidants for preventing preeclampsia: a systematic review," *The Scientific World Journal*, vol. 2012, Article ID 243476, 10 pages, 2012.

[130] Created using: https://biorender.com/.

[131] J. M. Roberts and C. Escudero, "The placenta in preeclampsia," *Pregnancy Hypertension*, vol. 2, no. 2, pp. 72–83, 2012.

[132] C. Qiu, K. Hevner, D. A. Enquobahrie, and M. A. Williams, "A case-control study of maternal blood mitochondrial DNA copy number and preeclampsia risk," *Int J Mol Epidemiol Genet*, vol. 3, no. 3, pp. 237–244, 2012.

[133] R. Williamson, C. McCarthy, F. McCarthy, A. Khashan, and L. Kenny, "OP 15 Investigating the role of mitochondrial dysfunction as a biomarker of pre-eclampsia," *Pregnancy Hypertension: An International Journal of Women's Cardiovascular Health*, vol. 9, p. 15, 2017.

[134] C. McCarthy and L. C. Kenny, "Therapeutically targeting mitochondrial redox signalling alleviates endothelial dysfunction in pre-eclampsia," *Scientific Reports*, vol. 6, no. 1, article 32683, 2016.

[135] J. Marschalek, P. Wohlrab, J. Ott et al., "Maternal serum mitochondrial DNA (mtDNA) levels are elevated in preeclampsia – a matched case-control study," *Pregnancy Hypertension*, vol. 14, pp. 195–199, 2018.

[136] C. M. D. Marquez, J. A. Ibana, and M. C. Velarde, "The female reproduction and senescence nexus," *American Journal of Reproductive Immunology*, vol. 77, no. 5, article e12646, 2017.

[137] M. J. Kupferminc, A. M. Peaceman, T. R. Wigton, K. A. Rehnberg, and M. L. Socol, "Tumor necrosis factor-α is elevated in plasma and amniotic fluid of patients with severe preeclampsia," *American Journal of Obstetrics and Gynecology*, vol. 170, no. 6, pp. 1752–1759, 1994.

[138] R. Altara, R. Ghali, Z. Mallat, A. Cataliotti, G. W. Booz, and F. A. Zouein, "Conflicting vascular and metabolic impact of the IL-33/sST2 axis," *Cardiovascular Research*, vol. 114, no. 12, pp. 1578–1594, 2018.

[139] B. Dieplinger and T. Mueller, "Soluble ST2 in heart failure," *Clinica Chimica Acta*, vol. 443, pp. 57–70, 2015.

[140] R. Romero, P. Chaemsaithong, A. L. Tarca et al., "Maternal plasma-soluble ST2 concentrations are elevated prior to the development of early and late onset pre-eclampsia – a longitudinal study," *The Journal of Maternal-Fetal & Neonatal Medicine*, vol. 31, no. 4, pp. 418–432, 2018.

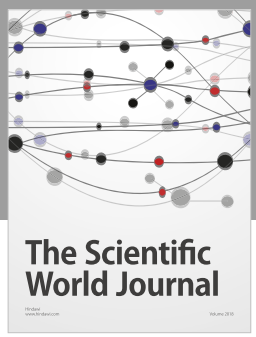
[141] X. Shi, M. Sun, H. Liu, Y. Yao, and Y. Song, "Long noncoding RNAs: a new frontier in the study of human diseases," *Cancer Letters*, vol. 339, no. 2, pp. 159–166, 2013.

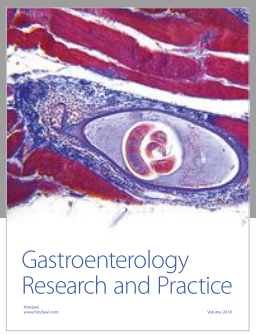
[142] Y. Tan, D. Xiao, Y. Xu, and C. Wang, "Long non-coding RNA DLX6-AS1 is upregulated in preeclampsia and modulates migration and invasion of trophoblasts through the miR-376c/GADD45A axis," *Experimental Cell Research*, vol. 370, no. 2, pp. 718–724, 2018.

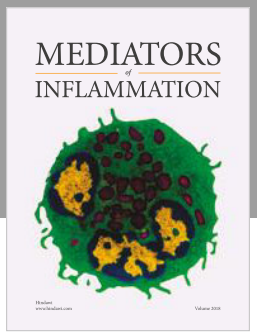
[143] A. E. Covarrubias, E. Lecarpentier, A. Lo et al., "AP39, a modulator of mitochondrial bioenergetics, reduces antiangiogenic response and oxidative stress in hypoxia-exposed trophoblasts: relevance for pre-eclampsia pathogenesis," *The American Journal of Pathology*, vol. 189, no. 1, pp. 104–114, 2019.

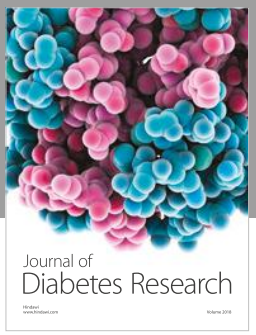
[144] A. M. Nuzzo, E. J. Camm, A. N. Sferruzzi-Perri et al., "Placental adaptation to early-onset hypoxic pregnancy and mitochondria-targeted antioxidant therapy in a rodent model," *The American Journal of Pathology*, vol. 188, no. 12, pp. 2704–2716, 2018.

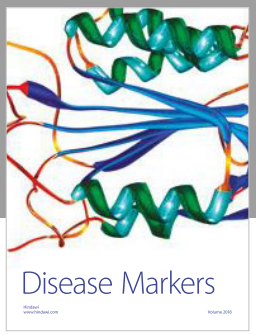
[145] R. N. Kerley, C. McCarthy, D. B. Kell, and L. C. Kenny, "The potential therapeutic effects of ergothioneine in pre-eclampsia," *Free Radical Biology & Medicine*, vol. 117, pp. 145–157, 2018.



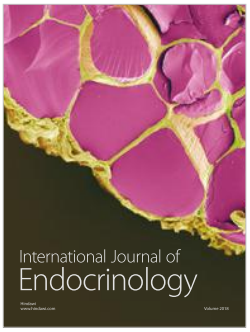








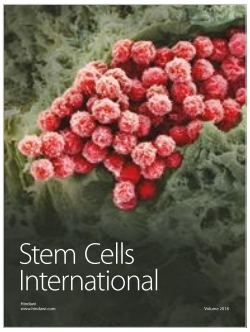


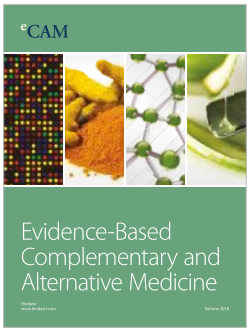






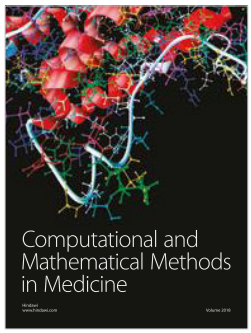


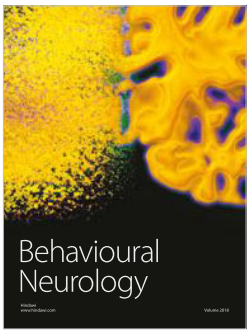




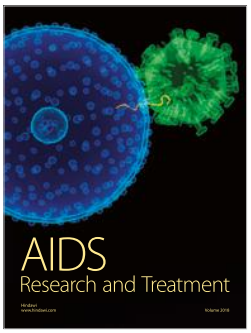














Hindawi

Submit your manuscripts at
www.hindawi.com

antioxidants

MDPI

Review

Computational Models on Pathological Redox Signalling Driven by Pregnancy: A Review

Samprikta Manna [1,*,†], Camino S. M. Ruano [2,†], Jana-Charlotte Hegenbarth [3,4,†], Daniel Vaiman [2], Shailendra Gupta [5], Fergus P. McCarthy [1], Céline Méhats [2], Cathal McCarthy [6,‡], Clara Apicella [2,‡] and Julia Scheel [5,‡]

1 Department of Obstetrics and Gynaecology, Cork University Maternity Hospital, University College Cork, T12 YE02 Cork, Ireland; fergus.mccarthy@ucc.ie
2 Institut Cochin, Inserm U1016, UMR8104 CNRS, Université de Paris, 75014 Paris, France; camino.ruano@inserm.fr (C.S.M.R.); daniel.vaiman@inserm.fr (D.V.); celine.mehats@inserm.fr (C.M.); clara.apicella@inserm.fr (C.A.)
3 Department of Molecular Genetics, Faculty of Science and Engineering, Faculty of Health, Medicine and Life Sciences, Maastricht University, 6211 KH Maastricht, The Netherlands; j.hegenbarth@maastrichtuniversity.nl
4 Department of Cardiology, CARIM School for Cardiovascular Diseases, Faculty of Health, Medicine and Life Sciences, Maastricht University, 6229 ER Maastricht, The Netherlands
5 Department of Systems Biology and Bioinformatics, Rostock University, 18051 Rostock, Germany; shailendra.gupta@uni-rostock.de (S.G.); julia.scheel@uni-rostock.de (J.S.)
6 Department of Pharmacology and Therapeutics, Western Gateway Building, University College Cork, T12 K8AF Cork, Ireland; cmccarthy@ucc.ie
* Correspondence: samprikta.manna@ucc.ie
† These authors contributed equally to this work.
‡ These authors contributed equally to this work.

check for updates

Citation: Manna, S.; Ruano, C.S.M.; Hegenbarth, J.-C.; Vaiman, D.; Gupta, S.; McCarthy, F.P.; Méhats, C.; McCarthy, C.; Apicella, C.; Scheel, J. Computational Models on Pathological Redox Signalling Driven by Pregnancy: A Review. *Antioxidants* **2022**, *11*, 585. https://doi.org/10.3390/antiox11030585

Academic Editor: Alessandra Napolitano

Received: 21 January 2022
Accepted: 16 March 2022
Published: 18 March 2022

Publisher's Note: MDPI stays neutral with regard to jurisdictional claims in published maps and institutional affiliations.

Copyright: © 2022 by the authors. Licensee MDPI, Basel, Switzerland. This article is an open access article distributed under the terms and conditions of the Creative Commons Attribution (CC BY) license (https://creativecommons.org/licenses/by/4.0/).

Abstract: Oxidative stress is associated with a myriad of diseases including pregnancy pathologies with long-term cardiovascular repercussions for both the mother and baby. Aberrant redox signalling coupled with deficient antioxidant defence leads to chronic molecular impairment. Abnormal placentation has been considered the primary source for reactive species; however, placental dysfunction has been deemed secondary to maternal cardiovascular maladaptation in pregnancy. While various therapeutic interventions, aimed at combating deregulated oxidative stress during pregnancy have shown promise in experimental models, they often result as inconclusive or detrimental in clinical trials, warranting the need for further research to identify candidates. The strengths and limitations of current experimental methods in redox research are discussed. Assessment of redox status and oxidative stress in experimental models and in clinical practice remains challenging; the state-of-the-art of computational models in this field is presented in this review, comparing static and dynamic models which provide functional information such as protein-protein interactions, as well as the impact of changes in molecular species on the redox-status of the system, respectively. Enhanced knowledge of redox biology in during pregnancy through computational modelling such as generation of Systems Biology Markup Language model which integrates existing models to a larger network in the context of placenta physiology.

Keywords: oxidative stress; preeclampsia; systems biology; antioxidant therapy; integrative modelling; cardio-obstetrics

1. Introduction

Reactive oxygen and nitrogen species (RONS) are recognised as important signalling molecules within cells. Redox signalling occurs when a biological system alters in response to a change in the level of a particular reactive species (RS) or the shift in redox state of a redox-sensitive group. RONS are physiological signalling molecules at low levels but cause

oxidative stress (OS) at high levels, resulting in damage to cell organelles, especially mitochondria. The role of OS has been extensively proven in pathological outcomes, including but not limited to aging, diabetes, cancer, and cardiovascular diseases (CVD) [1–4].

OS is considered a hallmark of pregnancy pathologies such as preeclampsia (PE), defined by de novo hypertension and proteinuria after 20 weeks of gestation, and intrauterine growth restriction (IUGR), a condition where foetal weight at birth falls below the 10th percentile for comparable gestational age [5,6]. Evidence suggests that defective placental implantation causes reduced remodelling of maternal spiral arteries, maintaining high resistance and a contractile phenotype, resulting in reduced blood flow to the placenta and the foetus. The placenta therefore remains abnormally susceptible to fluctuations in blood flow and pressure, leading to ischemic reperfusion injury, with excessive production of RONS and antioxidant imbalance. Toxic by-products are released into the maternal circulation and are detectable biomarkers of OS, which have an impact on the maternal vasculature, as seen in PE through endothelial dysfunction (ED) [7,8]. Predisposition to PE has been linked to the same risk factors for CVD, suggesting an inter-play between the placenta and the cardiovascular system. This is supported by evidence that cardiovascular injury can occur before the development of PE. The inability of the cardiovascular system to sustain the challenge of pregnancy may therefore be the cause of reduced blood flow to the placenta, resulting in pregnancy pathologies [9].

In recent years, experimental data collected from redox studies in a wide variety of model organisms such as bacteria, yeast, plants, and mice have been used to develop computational models and to make inferences on redox signalling in the human system. These models allow us to investigate how changes in stimuli such as growth factors, oxygen tension, RONS and antioxidant levels can impact the fine balance between redox homeostasis and damage, culminating in pathological outcomes [10].

The scope of this review is to summarise the processes involved in redox-signalling and oxidative damage, in the context of pregnancy and cardiovascular regulation, while presenting state-of-the-art redox-specific computational modelling, which could prove fundamental in advancing our understanding of OS in pregnancy and cardio-obstetrics.

1.1. Redox Signalling

Redox signalling cascades are based on processes of electron-transfer and involve RS and antioxidant cellular systems, as well as redox-sensitive effector proteins. Downstream of stimuli such as OS, metabolic changes, or inflammation, the controlled and spatially confined production of RS is an important cellular mechanism to generate key second messengers (i.e., H_2O_2, NO) that reduce the risk of cellular damage [11,12]. These pathways regulate cell proliferation, autophagy, inflammation, apoptosis, cardiovascular tone regulation and hormone production [13–17].

Effector proteins including kinases, phosphatases, transcription factors, chaperones, and enzymes, partake in reversible redox reactions in the presence of key cysteine residues and respective sulfhydryl groups (-SH), as well as transition metal groups (i.e., selenium, iron, manganese) [18–20]. Oxidation or reduction of these functional groups is considered as a post-translational modification (PTM), usually resulting in a conformational change of the effector protein, influencing dimerization and altering its biological activity, specificity and/or stability.

1.2. Reactive Species

Mitochondria are the primary source of intracellular reactive oxygen species (ROS). During ATP production by the mitochondria via the electron transport chain (ECT), electron leakage can occur which react with oxygen, generating free radicals' superoxide $\bullet O_2^-$, hydroxyl HO•, peroxyl radicals ROO•, and non-radical hydrogen peroxide H_2O_2 [21,22]. Membrane-embedded NADPH oxidase enzymes (Nox) are the second main source of ROS, generating superoxide from NADPH and oxygen [23]. Dual oxidases (DUOX), DUOX1 and DUOX2, are the sole members of the Nox family to contain an additional, extracellular,

peroxidase-like domain that catalyses the extracellular synthesis of H_2O_2 [24]. Apart from the mitochondria, ROS production also occurs in peroxisomes, lysosomes, Golgi, and endoplasmic reticulum membranes, by xanthine oxidases during purine degradation, cytochrome P450 is involved in biosynthesis of fatty acids and clearance of xenobiotics [25–28].

The main reactive nitrogen species (RNS), nitric oxide (NO), is an important signalling molecule involved in PTM, endothelium-mediated vasodilation, angiogenesis, neural development, and immune responses [29,30]. In the presence of ROS, more destructive RNS such as nitrogen dioxide ($\bullet NO_2$), dinitrogen trioxide (N_2O_3), dinitrogen tetroxide (N_2O_4), and peroxynitrite ($ONOO^-$) are generated. In the presence of CO_2, $ONOO^-$ generates $\bullet NO_2$ and $\bullet HCO_3$, which are highly reactive carbonate radicals and have a strong tendency to interact with proteins and lipids, resulting in damaging nitrosylation and carbonylation [31]. The oxidative modification of cysteine residues by NO to form S-nitrosothiols is called S-nitrosylation, which triggers a change in protein structure, alters protein–protein interactions and enables further PTMs such as phosphorylation, acetylation, ubiquitination, and disulphide bond formation. S-nitrosylation is a tightly regulated, key mechanism through which NO signalling is propagated within the cell, tissue, and microenvironment [31].

NOS are cytoplasmic enzymes that catalyse NO generation from L-arginine, NADPH, and oxygen, when binding to specific cofactors calcium-calmodulin, NADPH, Flavin adenine dinucleotide (FAD), flavin mononucleotide (FMN), heme and tetrahydrobiopterin (BH4). Endothelial (eNOS), neuronal (nNOS) and inducible NOS (iNOS) have been identified as three isoforms of NOS expressed by immune cells [32,33]. When NOS becomes uncoupled from its substrate or cofactors, it generates superoxide [34]. Reactive Sulfur Species (RSS) go beyond the scope of the current review [35].

1.3. Antioxidant Cellular Systems

Antioxidant molecules maintain the cell in a reducing environment and are responsible for detoxification of RONS, by partaking in redox reactions, undergoing reversible oxidation, usually at the expense of NADPH [36]. Antioxidant enzymes are found abundantly in the molecular environment. Superoxide dismutase (SOD) catalyses the conversion of superoxide to H_2O_2 through a metal group in the active site. Copper and zinc-SOD are found both in the cytosol and extracellularly, whereas manganese-SOD is mitochondrial [37–39]. Catalase (CAT) converts H_2O_2 into water and oxygen by reduction of the iron atom, at the centre of the heme group in the active site [40,41]. Thioredoxins are small enzymes characterised by two proximal cysteine residues in the active site (CXXC motif). The free sulfhydryl groups (-SH) are oxidised to a disulphide bond (-SS-), and the electrons are transferred to acceptor molecules in the cells, RS, oxidised proteins and lipids, redox-signalling effector proteins, in a process of reversible oxidation. Reduction of thioredoxin is mediated by thioredoxin reductase (ThxRed), using NADPH as substrate [42,43]. Glutathione (GSH) is the primary antioxidant involved in redox state homeostasis and drug detoxification, serving as electron-donor in redox reactions. The two free sulfhydryl groups of two reduced GSH molecules are oxidised to form a disulphide bond, in the dimeric glutathione disulphide (GSSG). Through GSH oxidation to GSSG, Glutathione S-transferases mediate detoxification of cytotoxic substances and xenobiotics, while Glutathione Peroxidase (GPx) converts hydrogen superoxide to water and oxygen [44]. Glutathione reductase reconverts GSSG to GSH, using NADPH [45]; the GSH/GSSG ratio is a key biomarker of the cellular oxidative state.

2. Redox Signalling in Pregnancy

Pregnant women are exposed to increased levels of Reactive Oxygen and Nitrogen species (RONS) throughout pregnancy. Elevated levels of free radicals are crucial for the development of a successful foetal–maternal interface within the placenta making them indispensable for signalling transduction, activating proangiogenic genes, promoting vasodilation, and anti-inflammatory processes as well as activation of redox-sensitive

transcription factors and protein kinases [46–48]. Activation of redox-sensitive transcription factors such as activator protein 1(AP-1), p53 and nuclear factor kappa-light-chain-enhancer of activated B cells (NF-κB) are essential for regulation of pro-inflammatory cytokines, cell differentiation, and apoptosis. Activation of protein kinases regulates the cell cycle and signalling pathways through regulation of mitogen activated protein kinase (MAPK).

RONS production occurs mainly in the placental mitochondria [48,49] During the early stages of pregnancy, low oxygen tension (2.5% O_2) is a key activator and regulator of hypoxia-inducible factors (HIF-1α and HIF-2α) within the placenta, increasing the level of eNOS in extravillous trophoblasts and also modulation of the angiogenic mediator, vascular endothelial growth factor (VEGF). Increased levels of eNOS and VEGF stimulate invasion, angiogenesis, proliferation, and migration of trophoblasts into the maternal decidua [50–52]. Figure 1 recapitulates HIF-1α signalling in the trophoblast during the first trimester.

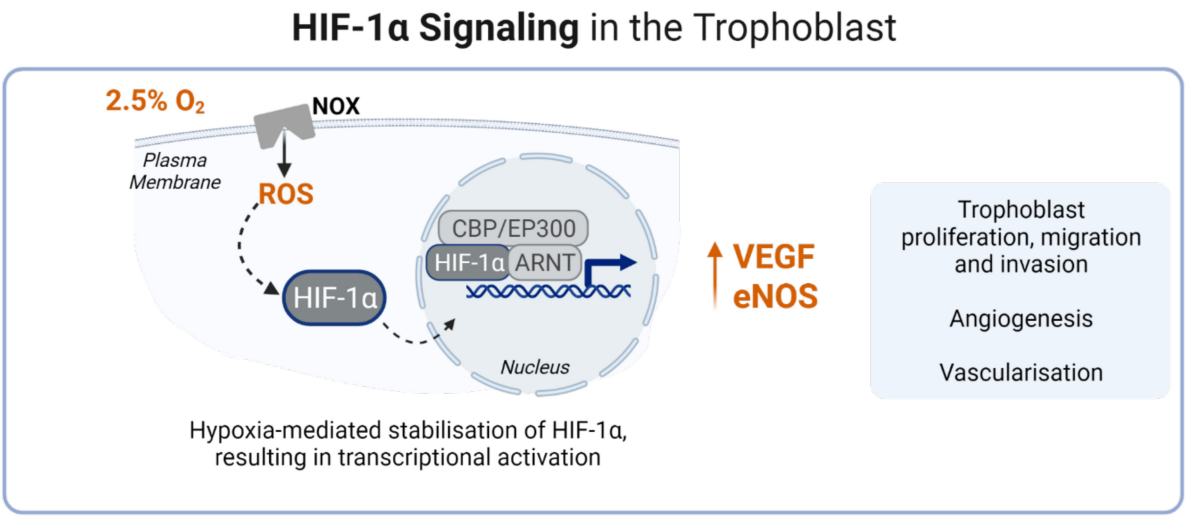


Figure 1. HIF-1α signalling in the trophoblast, during the first trimester. Dashed arrows indicate activation, upright arrow indicates increase, blue arrow indicates transcription, black arrow indicates generation.

At the end of the first trimester, trophoblasts have invaded the maternal spiral arteries reaching the myometrium, which allows adequate blood flow from the mother to the placenta. Blood availability increases oxygen tension to 8.5% which promotes trophoblast differentiation and maturation. In syncytiotrophoblasts, increased oxygen levels coupled with demanding nutritional requirements stimulate mitochondrial metabolic activity leading to a switch in steroidogenic state, generating elevated concentrations of ROS [49,52,53]. In order to inactivate these free radicals, the placenta produces numerous antioxidant enzymes including CAT, SOD and GPx [52]. In addition, low-molecular-weight compounds, such as vitamin C, β-carotene, ascorbic acid, and glutathione, are produced by the placenta to combat rising OS [47,52].

Disruption of the delicate balance between antioxidants and oxidants increases free radicals in the maternal circulation and causes lipid peroxidation, protein degradation and ultimately cell death and ED [47]. Deficiency in the antioxidant defence, abnormal phosphorylation of the aforementioned transcription factors and protein kinases, results in an increase in soluble fms-like tyrosine kinase-1 (sFlt-1) levels and subsequent placental malperfusion [47,48]. Within the placenta, inefficient invasion of trophoblasts into maternal spiral arteries results in deficient blood flow, hypoxia, and ischemia, exacerbating free radicals release in the maternal circulation. Trophoblast damage results in the secretion of molecules implicated in ED, such as metalloproteases (MMPs), sFLT1 and soluble endoglin (sEng), inflammatory cytokines (TNF-α, IL-6), intracellular adhesion molecules (ICAM-1) and vascular cell adhesion molecules (VCAM-1) responsible for vascular remodelling, smooth muscle hypertrophy and cellular apoptosis [47,54].

The placenta, being a highly metabolic organ, requires a substantial amount of energy to maintain physiological and morphological functions and to support the growth and development of the foetus. Hence, the placenta has significant oxygen requirements throughout pregnancy [53]. Dysregulation of ROS signalling during pregnancy is linked to several pregnancy pathologies such as recurrent miscarriage, PE, IUGR, Gestational Diabetes Mellitus (GDM) and preterm birth [47,49,50,52]. The pathophysiological mechanisms involved in redox regulation during pregnancy are summarised in Figure 2.

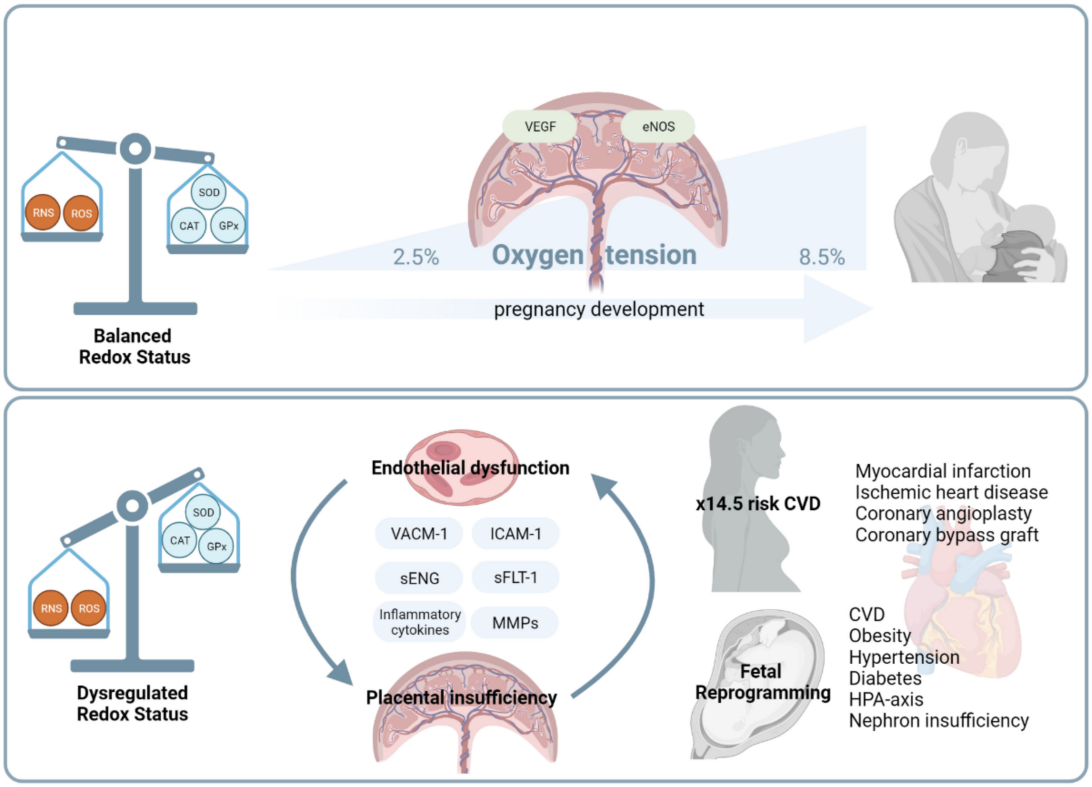


Figure 2. Role of Oxidative Stress in Pregnancy Pathologies.

2.1. Role of Oxidative Stress in Adverese Pregnancy Outcomes

Despite extensive investigation, a defined pathological relationship between OS and adverse pregnancy outcomes is yet to be fully elucidated. During GDM, the mother develops glucose intolerance in the second part of pregnancy. ROS associated with GDM is mainly produced by prolonged exposure to hyperglycemia. Glucose auto-oxidation increases the concentration of free radicals overwhelming the antioxidant response and resulting in increased protein carbonylation in the placental cell membranes [55]. Additionally, oxidative and nitrosative stress can exert synergistic effects. S-nitrosylation-mediated modifications result in structural alterations in term GDM placentas that show increased villous immaturity, increased angiogenesis and altered trophoblast proliferation and differentiation [56,57].

IUGR is characterized by the inability of the foetus to meet a standard growth curve. It has been hypothesized that the development of this pathology is due to first-trimester insufficient placentation and incomplete invasion of the maternal arteries leading to placental ischaemia [58]. Lipid peroxidation, DNA damage and ROS biomarkers (malondialdehyde, xanthine oxidase, glutathione peroxidase, superoxide dismutase and catalases) are elevated in pregnancies affected by IUGR [55].

Although there are several hypotheses on the aetiology of PE, the most common event is an injury to the vascular endothelium [58]. Increased vascular resistance reduces trophoblastic invasion of the maternal spiral arteries, leading to intermittent placental perfusion which increases ROS within the trophoblast and endothelial cells [55,58]. Other

studies suggest the inability of the syncytiotrophoblasts to sense and generate ROS, possibly due to the abnormal regulation of NADPH in this cellular layer [55]. PE shows an extensive disturbance level of the maternal vasculature, which is not observed in IUGR pregnancies, but is present when PE and IUGR occur simultaneously. A recent theory for the development of PE has been attributed to poor maternal cardiovascular health failing to compensate for haemodynamic and metabolic requirement during pregnancy, a result of genetic or environmental risk factors [9,59].

In all the mentioned pregnancy pathologies, the placenta is in an environment of elevated concentrations of RONS, which may lead to the shortening of the telomeres and cellular metabolic arrest and induce cell senescence or promote placental apoptosis [55]. Thus, premature placental ageing of the foetal–maternal interface is exacerbated in the high oxidative environment and is commonly observed in adverse pregnancy outcomes.

2.2. Effects on Oxidative Damage to Foetal Health

Pathological pregnancies compromise the intrauterine environment, which may lead to foetal cells reprogramming to overcome the stressors. Foetal programming implicates alterations of physiologic systems of cardiovascular control, ultimately increasing the risk of future susceptibility to cardiometabolic diseases. This phenomenon is denominated the Developmental Origins of Health and Diseases (DOHaD), stated by Dr Barker after studying the association of maternal undernutrition with the increased incidence of coronary heart disease, hypertension, and obesity in adult life [60,61].

The most studied reprogramming association is the link between foetal undernutrition and the development of cardiovascular diseases and associated risk factors such as hypertension, cardiac hypertrophy, and obesity. However, other less studied associations have been observed. Increased levels of maternal cortisol are associated with behavioural problems during childhood. Excessive concentrations of glucocorticoids in GDM or obese mothers are associated with the reprogramming of the foetal hypothalamus-pituitary-adrenal (HPA)-axis at both the basal and the stress-induced level. OS is associated with the development of autism spectrum disorders, hypertension, heart diseases, a decreased number of nephrons and kidney dysfunction through the dysregulation of the Renin-Angiotensin system. In animal studies, intrauterine hypoxia induces foetal growth restriction, cardiovascular dysfunction, multiorgan morbidities associated with brain, heart, liver, and kidney [62–65]. Animal models have observed that hypoxia during intrauterine life induces left ventricular hypertrophy, susceptibility to develop arrhythmias and ischemia-perfusion injury. Undernutrition during the foetal life in sheep is linked to cardiac hypertrophy with the increased NADPH oxidase in the heart prior to the observation of hypertension [60].

Interestingly, foetal outcomes after intrauterine ROS imbalance have a sexual–dimorphic response. The female foetus seems to have a certain degree of protection, leading to reduced hypertension or a milder hypertensive form. Antioxidant deficiency equally seems to show the same sexual-dimorphism pattern, where female offspring express much higher amounts of renal antioxidants than male foetuses. This sexual dimorphic response can be explained by the prospective role of oestrogen's ability to overcome and adapt to suboptimal intrauterine conditions in female foetuses [60,66–68].

2.3. Effects on Oxidative Damage in Pregnancy on Future Maternal Health

In healthy pregnant women there is systemic maternal vasodilation with a decrease in peripheral vascular resistance, increase in cardiac output, and thickness of the left ventricular wall. In pathological pregnancies, oxidative dysregulation and high concentrations of inflammatory cytokines increase ED, arterial stiffness, vascular resistance and impairs myocardial contractility, leading to left ventricular hypertrophy in the mothers. Persistent ED increases to a 14.5-fold risk of developing a poor cardiometabolic after delivery and years after delivery. PE is associated with a 2- to 7-fold increase in the risk of CV diseases later in life; 3% of PE women develop cardiopulmonary complications and 70% of these

occur after delivery [69]. Women suffering from PE show subclinical atherosclerosis and are more likely to be treated for primary hypertension within 10 years after delivery. These associations are still significant after adjusting for confounding conditions before pregnancy, making PE a risk factor for the development of CVD and not only a cause of previous CVD [70,71]. It has been well studied that even 15 years after a pathological pregnancy, women still show changes in the microvascular function (cerebral microvascular bed), at the macrovascular level (increased arterial stiffness) and the structural vessel level (thicker carotid intima-media) [70,72,73]. Women suffering from PE have an increased risk of developing ischemic heart disease, myocardial infarction, coronary angioplasty, and coronary bypass graft [70].

Additionally, comorbidities such as insulin resistance, visceral obesity, increased high-density lipoprotein (HDL) cholesterol concentrations, and increased triglyceride concentrations accompanied by hypertension can lead to more deleterious effects on ED, leading to severe clinical outcomes such as CVDs and type II diabetes [54].

2.4. Oxidative Stress and Endothelial Dysfunction

The endothelium is a highly active monolayer of endothelial cells that line the interior surface of blood and lymphatic vessels and plays an important role in homeostasis and modulating immune inflammatory reactions. Endothelial cells regulate vascular tone by secreting vasoactive molecules responsible for relaxation or vessel constriction. This directly affects tissue oxygen supply, long-term organ perfusion and vascular structure remodelling [74,75].

Under physiological conditions, endothelial cells generate vasoprotective NO to maintain the balance between ROS and antioxidants. NO signalling depends on eNOS cellular localisation. eNOS-mediated NO synthesis at the Golgi membrane causes S-nitrosylation of newly synthesised proteins, affecting cellular trafficking, protein–protein interaction and other PTMs processes (Figure 3a) [76,77]. At the plasma membrane, eNOS modulates vasodilation through NO synthesis. In resting endothelial cells, eNOS activity is reversible and is negatively regulated by NO itself through S-nitrosylation. Upon receptor-mediated activation of eNOS, such as downstream of VEGF signalling, eNOS is phosphorylated and S-nitrosylation levels decrease, resulting in strong activation of eNOS and dramatic increase in NO levels (Figure 3b) [78].

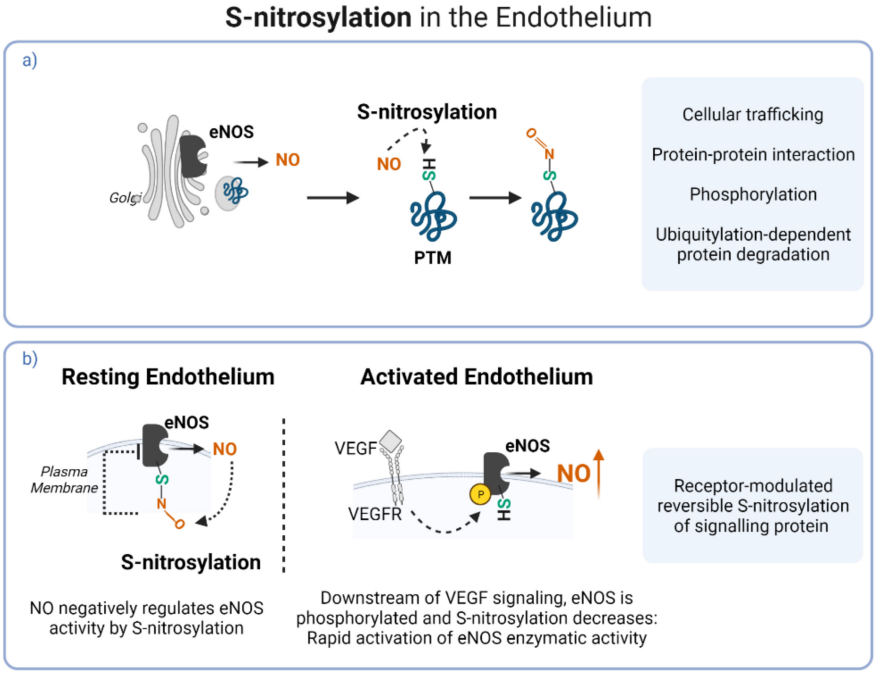


Figure 3. S-nitrosylation mechanisms in the endothelium. (**a**) eNOS-mediated S-nitrosylation of proteins as PTM. (**b**) S-nitrosylation negative, reversible, regulation of eNOS activity.

ED is defined by a decrease in the production of protective NO driven by elevated superoxide anion levels [79] and is one of the main risk factors for stroke and heart failure, while being a signature of PE. In general, ED is a state caused by an imbalance of vasodilation and vasoconstriction molecules [80], causing a disruption in the NO signalling pathway and leading to NO synthase uncoupling. eNOS and iNOS are constitutively expressed in the heart. In addition to superoxide anions, uncoupled NOS activity leads to peroxynitrite, which has been associated with aging in mice [81]. Likewise, several oxidative enzymes are involved in this process, and it has been shown that the inhibition of the NADPH oxidase normalizes ED in mice [82].

2.5. Oxidative Stress, NOX, and Cardiovascular Disease

The main sources of ROS in the context of CVD include NOX, xanthine oxidase, NO synthases, cytochrome P450, and mitochondrial respiration [83–85]. In the cardiovascular system, NOX1, 2, 4 and 5 are mainly expressed in certain cell types. For instance, NOX2 and 4 are expressed in cardiomyocytes, fibroblasts, endothelial cells, or smooth muscle cells, while NOX1, 4 and 5 are predominantly expressed in smooth muscle cells. NOX are generally regulated by Angiotensin II, which has both pro-hypertrophic and pro-fibrotic mediated effects in cardiac cells, notably via the endothelin-1 release [86].

Serpillon et al. (2009) showed elevated levels of superoxide in a rat model of type 2 diabetes was associated with endothelial but not cardiac dysfunction [87]. Additional studies have demonstrated that overexpression of NOX2 and 4 is associated with OS in CVD. In NOX4 knockout mice, decreased levels of superoxide were observed, while opposingly overexpression of NOX4 worsened cardiac function and induced apoptosis and fibrosis in response to pressure overload [88]. Both studies suggest NOX to be a potent source of superoxide in cardiac cells. Furthermore, patients with metabolic syndrome have increased NOX activity as well as elevated plasma levels of oxidized low-density lipoprotein and nitrotyrosine [89]. Another study in 2002 showed a correlation between NOX mRNA expression and the severity of atherosclerotic lesions in human coronary arteries [90]. Through these studies, the importance of NOX in CVD has been well established.

2.6. Therapeutic Interventions Targeting Oxidative Stress during Pregnancy

In addition to the physiological mechanisms previously mentioned, to prevent and repair damage from OS, other key regulatory molecules have been identified with clinical potential: enzymes such as ceruloplasmin, heme proteins, paraoxonase (PON1) or nonenzymatic albumin, bilirubin, uric acid, creatinine, cysteine, carotenoids, flavonoids, coenzyme Q (reduced), metal ion binding proteins (ferritin, transferrin, metallothioneins) [49].

Additionally, genetic, and environmental factors such as maternal obesity and poor nutrition may lead to increased OS during pregnancy. In this section, we describe the range of micronutrients, experimentally and/or clinically evaluated, as possible antioxidant therapies due to their ability to inhibit ROS production, scavenge existing ROS, regulate NO synthesis or release and modify antioxidant enzymes [91].

An overview is given in Figure 4.

2.6.1. Vitamins

Vitamin C and E are known exogenous antioxidants that regulate ROS through down-regulation of NADPH and upregulation of eNOS. Vitamin E protects cells against lipid peroxidation [92]. Additionally, Vitamin D supplements given in the early stage of pregnancy have been shown effective against PE through mediating immune modulation and vascular functioning [93]. However, most large-scale clinical trials with thousands of study participants have been inconclusive, rendering vitamins an ineffective treatment to reduce OS [92,94].

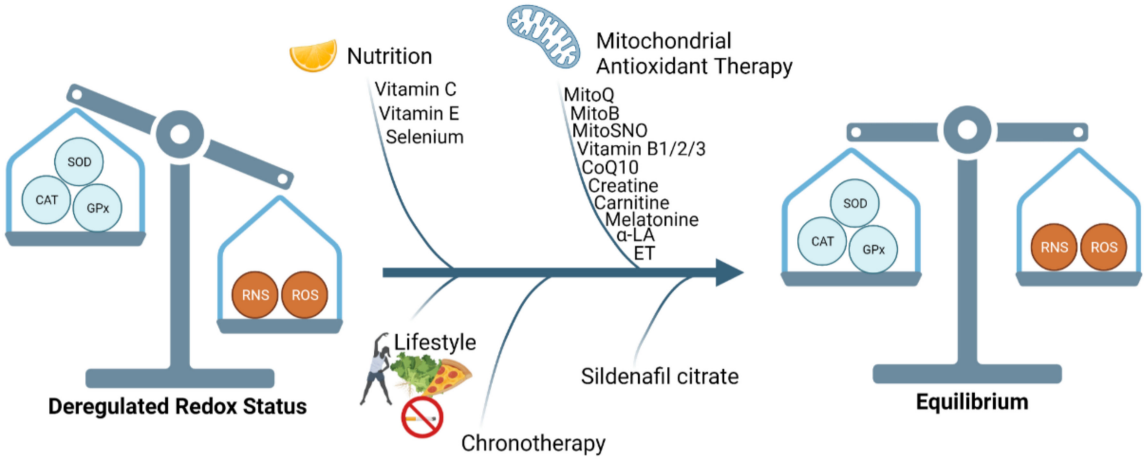


Figure 4. Interventions for Redox imbalance. Nutrition, lifestyle changes, chronotherapy, mitochondrial antioxidant therapy and sildenafil citrate interventions have been proven beneficial or are under investigation. alpha-LA = α-Lipoic Acid; ET = L-Ergothioneine.

2.6.2. Selenium

Selenium (Se), a trace element of amino acid selenocysteine, is mainly obtained from dietary components and is a vital element for GPx and ThxRed enzymatic function. Se deficiency during pregnancy can result in maternal and foetal morbidity and pregnancy complications such as intrauterine growth restriction (IUGR), gestational hypertension, and preterm birth. Various studies with Se dosage ranging from 60 to 200 µg/day intake between 12–24 weeks of pregnancy have been documented. However, recommendations for Se supplementation are currently not possible due to limited accuracy for Se homeostasis measurements and the poor understanding of complex interactions between micronutrients to different doses of Se [95,96].

2.6.3. Lifestyle Intervention

Lifestyle modifications including regular exercise, weight loss, dietary changes, reducing toxic substances such as tobacco, alcohol and pollutants can help reduce OS and increase physiological antioxidant defence. Systematic reviews analysing the impact of physical exercise during pregnancy have concluded that exercise has a protective effect against PE [97]. Whereas other studies have contradictory advice on aerobic exercise, especially during early pregnancy [94]. Due to the heterogeneity in study results, and the lack of consensus on the optimal intensity of physical activity, its protective effects against OS in pregnancy pathologies cannot be satisfactorily assessed. Larger studies with well-defined methodological designs are required to strengthen the evidence that physical activity helps scavenge ROS and reduce OS.

2.6.4. Sildenafil Citrate

NO has become a potential therapeutic approach for vasodilation of the fetoplacental circulation, embryo development and foetus growth [98]. NO activates soluble guanylyl cyclase to convert guanosine triphosphate (GTP) to cyclic guanosine monophosphate (cGMP), which is then degraded by phosphodiesterase 5 (PDE5) to guanosine monophosphate (GMP). Sildenafil citrate is a selective inhibitor of PDE5 and enhances the relaxation and cGMP accumulation. In a rat model, Sildenafil was shown to restore normal values of blood pressure, reduce proteinuria and plasma levels of sFlt-1 and sEng in preeclamptic rats. However, clinical trials showed no significant difference between control and preeclamptic women, while the Dutch arm of the multicentre STRIDER trial for the treatment of severe IUGR was halted due to detrimental effects of Sildenafil citrate on newborn survival [98–100].

2.6.5. Chronotherapy

Circadian rhythms have a profound effect on human physiology and healthy cellular function. At a molecular level, the circadian clock is comprised of core transcription factors: CLOCK, BMAL1, Period (Per), and Cryptochrome (Cry), that act in a Transcription Translation Oscillating (TTO) loop [101]. Recent studies have shown that these factors play a role in the maintenance of blood pressure and metabolism. In an in vivo experimental model, BMAL1 knockout mice exhibited elevated endothelial damage, disrupted NO signalling and high ROS production, resulting in elevated oxidative damage [101,102]. In a 2013 randomised control trial in pregnant women, the group receiving chronotherapy in addition to low-dose acetylsalicylic acid (ASA) (100 mg/d) at 16 weeks, resulted in lower ROS-induced molecular damage, along with improved antioxidant enzymatic activity [103].

Melatonin, an antioxidant secreted by the pineal gland, is responsible for the maintenance of circadian rhythm and seasonal timing cues. In uncomplicated pregnancies, melatonin levels remain elevated during pregnancy and are responsible for growth and development of the foetal brain. However, in pregnancy complications such as PE, maternal circulating melatonin levels remain significantly low [104]. An in vitro and open label clinical trial study by Hobson et al. (2018), have shown that melatonin did not reduce OS or the production of the anti-angiogenic factors sFlt1, sEng, and activin A in preeclamptic placental explants. They concluded that while melatonin can be used as an adjunct therapy, it is not an efficient preventive therapy for ROS-induced pregnancy disorders [105].

2.6.6. Mitochondrial Antioxidant Therapy

Mitochondrial therapy in the form of naturally occurring antioxidants and commercial drugs has been considered as a potential intervention for pregnancy disorders resulting from elevated OS.

Mitochondrial-targeted antioxidants include MitoQ [106], MitoB [107,108], MitoPerox, MitoSNO [109], and MitoTempo [110], which have been shown to decrease oxidative damage and ameliorating effects in ischemia-reperfusion injury [106] and cardiac hypertrophy [111].

Primary mitochondrial disorders in which oxidative phosphorylation is disrupted can further be treated with antioxidant nutritional interventions [112,113]. Vitamin B1 supplementation is commonly used to enhance oxidative phosphorylation system (OXPHOS) and pyruvate dehydrogenase complex flux. In patients with defects in riboflavin transport and processing, as well as electron transport chain (ETC) complex deficiencies, vitamin B2 supplementation has also shown similar positive effects [114–116]. Increased amounts of vitamin B3, a precursor of NAD^+ and $NADP^+$, can cause lactic acidosis, which can be mitigated by exercise and fasting [117].

Mitochondrial activity and biogenesis can be further modified by metabolic agents, such as coenzyme Q10 (CoQ10), creatine, α-Lipoic Acid (α-LA), and L-carnitine. CoQ10 acts as a diffusible electron carrier, transferring electrons from complex I and II to complex III of the ETC. CoQ10 further inhibits the propagation of lipid peroxidation and is a potent ROS scavenger [118]. Creatine supplementation has been shown to prevent both structural and functional damage to mitochondria of cells under OS [119,120]. The potent antioxidant α-LA has been shown to improve mitochondrial performance and epigenetically affect IL-1B and IL-6 gene expression, which are associated with OS and inflammation. However, its therapeutic benefit has yet to be supported by clinical trials [121,122].

L-carnitine is involved in long-chain fatty acid transport from the cytosol to the mitochondrial matrix and is important for β-oxidation, modulation of acyl-CoA/CoA ratio, excretion of toxic acyl groups, muscle storage of energy as acetyl-carnitine and additionally functions as a free radical scavenger [123].

Finally, L-Ergothioneine (ET) is a histidine derived dietary amino acid and known for its radical scavenging properties, demonstrating reduction in markers of OS in serologic samples taken from healthy human subjects, who were administered ET (5 or 25 mg) once a day for 7 days [124,125]. Using the reduced uterine placental perfusion (RUPP) rat model, Williamson et al. (2020) [126] showed that ET treatment significantly ameliorated

hypertension, increasing pup weight, decreasing circulating levels of antiangiogenic sFlt-1 and significantly reducing mitochondria-specific H_2O_2 in vivo. ET has a favourable safety profile, long half-life, cytoprotective properties, and has the ability to regulate mitochondrial function; hence, ET could become a potential therapy for ROS-induced pregnancy disorders such as PE and IUGR [126].

Nevertheless, a considerable amount of research is still needed to accurately understand the exact processes involved in the metabolism of these therapeutic interventions.

The mechanisms by which hypoxia can lead to a higher incidence of cardiovascular dysfunction in the offspring are not fully understood; however, evidence suggests that prenatal hypoxia is linked to abnormal development of the foetus including the cardiovascular system. A study in a rat model of maternal malnourishment showed that early postnatal supplementation with Coenzyme Q10 had beneficial effects on the developmental origins of CVD, reducing signs of cardiac aging, telomere shortening and cellular senescence [127]. Another study in a mice model demonstrated that prenatal hypoxia leads to sex- and age-dependent effects on offspring cardiac and vascular function later in life. MitoQ may have potential benefits in offsetting the cardiovascular pathologies by increasing sensitivity to vasorelaxation in aged male and female offspring, preventing pulmonary artery dysfunction in prenatally hypoxic young male offspring and improving systolic function in aged prenatally hypoxic female offspring [128].

While limited to in vivo models, these potential therapeutic benefits are encouraging and warrant further exploration of mitochondrial antioxidants as an intervention to prevent long-term negative cardiovascular outcomes of a suboptimal in-utero environment.

2.7. Detection and Assessment of Oxidative Stress

Biomarkers for OS and oxidative damage are exploited as tools to assess both the status of a human disease and health enhancing effects of antioxidants.

2.7.1. Measurement of RONS

ROS and RNS are the key molecules of OS [129]. Direct measurements of their cellular distribution are a common approach to determine OS severity. Most common methods consist of colorimetric and fluorometric assays. Cellular RONS levels can be estimated using fluorogenic probes, such as Dichlordihydrofluorescein-diacetate, which is reduced to dichlorofluorescein by ROS, changing its fluorescent properties [130]. Similarly, 4,5-diaminofluorescein (DAF-2) is subject to nitrosation in the presence of RNS, forming the highly fluorescent triazole DAF-2 T [131]. Dihydroethidium is a viable cell permeable probe, which produces fluorescence upon oxidation by RONS and thus a measure for RONS activity [132]. These probes lack specificity and better approximations can be achieved by combining these measurements with specific inhibitors of RONS synthases as well as scavengers [133].

Colorimetric assays apply to a wide range of RONS. Most H_2O_2 specific dyes, such as Amplex® Red [134], homovanillic acid [135], and tetramethylbenzidine [136], function in combination with Horseradish peroxidase (HRP). A general limitation is due to HRP reacting with other thiols, possibly skewing the result; therefore, it is suggested for H_2O_2 detection in cultured cells, organ cultures, and isolated buffer perfused tissues [137]. To distinguish cellular from mitochondrial ROS, additional mitochondria specific dyes, such as MitoSOX™ and CellROX ® can be applied [138,139]. Another approach is the measurement of ROS derivatives. Transition metal ions (Fe^{2+}, Fe^{3+}) form radicals by reacting with hydroperoxides; these radicals can be measured colorimetric and are proposed to be proportional to the amount of peroxides present in the sample [140].

A historical colorimetric assay for RNS detection is the Griess reaction (1879) based on the interaction of nitrite, under acidic conditions, with a series of organic compounds (i.e., sulfanilic acid, 1-naphthylamine) to produce a red-violet dye. This is measured by spectrophotometry with a limited sensitivity (500 nmol/L), improved by fluorometric detection [133,140].

NO concentrations can further be assessed based on their effects on vasodilation. In this bioassay, endothelial cells are grown on carrier beads that fill a capillary column linked to a fluidic system. In the downstream chambers, the tension of smooth muscle cells from aortic vessels, stripped from the endothelium, is assessed by isometric transducers. Muscle relaxation is proportional to NO levels synthesised by the endothelium [29,141]. This method has been extensively used to characterise NO-mediated regulation of vascular function in response to hormones and bioactive molecules, and have been further developed to allow for modulation of oxygen tension [142].

2.7.2. Assessment of Oxidative Damage

Despite the variety of fluorescent probes described above, ROS assessments remain challenging. These species are by definition highly reactive and possess a short lifespan. Examining the damage caused by OS to proteins, lipids, and nucleic acids is an alternative approach.

Protein Damage: ROS oxidizes amino acid residues and protein backbones, increasing protein carbonylation and nitrosylation levels, serving as a marker of OS. The global extent of these modifications on the proteome can be measured using 2,4-dinitrophenylhydrazine, 2D gel electrophoresis, Western blot, and OxyBlot [143,144].

Lipid Damage: Lipid peroxidation is widely used as an indicator of free radical formation. Membrane unsaturated fatty acids are targeted by free radicals, creating peroxy radicals. Traditionally, lipid peroxidation is measured by thiobarbituric reactive compound detection, which is generated from the reduction of lipid peroxidation products. Although this method is highly sensitive, it lacks specificity.

High specificity and direct quantitative measurement of lipid peroxidation products can be achieved with chromatography techniques, including High-Performance Liquid Chromatography (HPLC) and Gas Chromatography-Mass Spectrometry (GC-MS) [145,146].

Compared to other liquid chromatography techniques, in HPLC, the high-pressure pump supplying the solvent and the small column calibre grant faster separation of lipid species at a higher resolution [147]. HPLC alone is the gold standard for quantification of known biomarkers such as Malondialdehyde (MDA) and 4-hydroxy-2-nonenal (4-HNE), commonly used in clinical and functional studies [148,149].

In GC-MS, GC is used to separate small volatile or semi-volatile compounds that can withstand high-temperatures without degradation, such as fatty acids [150]. Then, MS allows the precise identification of peroxidation products, establishing the position of hydroxyl groups along the lipid chain. Although it is expensive and time-consuming, MS is the technique of choice for untargeted lipidomics [151,152].

DNA Damage: The most prominent oxidative modifications of nucleic acids are hydrogylation of deoxyguanosine residues, thymidine glycol, single and double-stranded breaks, and levels of DNA repair enzymes. Specifically, 8-Hydroxy-2′-deoxyguanosine is extracted by the DNA repair system and then circulates in both the blood and urine. Common methods for quantitative analysis are HPLC, GC-MS, tandem HPLC and Elisa [153,154]. HPLC and immunohistochemistry (IHC) can also be used to assess DNA repair enzyme levels.

To assess DNA strand breaks, polymerase chain reaction and agarose gel electrophoresis exploit the fact that cleaved DNA fragments can migrate out of the nucleus and migrate faster than undamaged DNA when exposed to an electric field. Single-cell gel electrophoresis, also known as a comet assay, is considered the gold standard [155].

In vivo measurements remain challenging. The analysis of oxidized lipids in vivo is limited by their low abundance and the diversity of previously described physicochemical properties.

However, most experimentally identified therapeutic targets do not pass clinical trials. This can be due to a negative outcome of a clinical trial, due to safety or efficacy issues and clinical trial failure due to expertise-based, execution based, or knowledge-based failure [156]. Hwang et al. reported that 54% of therapeutics failed during clinical development, of which 57% failed due to inadequate efficacy, 17 due to safety concerns and 22% due to commercial reasons [157]. The investigation of therapeutics for pregnancy complications

is particularly challenged by the fact that pregnant women are often excluded from clinical trials. Trials that are based on a different population can lead to approval of therapeutics that behave unexpectedly, even negatively, in the actual target population [158].

A detailed collection of OS assessment methods can be found in Supplementary Materials S1.

3. Current Computational Models—Enhanced Interpretation of Complexities of Oxidative Stress

Complex interactions and high throughput data integration are often modelled computationally to simulate and study mechanisms leading to a certain phenotype. This allows the performance of thousands of in silico experiments that have to be validated by only a limited amount of laboratory experiments. Both predictive and quantitative computational models of redox reactions have been created to enlighten the mechanistic features of redox-sensitive proteins [159].

Computational models are usually based on experimental data and high-throughput methods and represent the current state of knowledge. However, the modelling process and in silico experiments can further be used to test hypotheses, interpret the results of in vitro and in vivo experiments, refine experimental designs, and lead to new insights [160].

Static models are used to describe the relationships between model components, while dynamic models are primarily used to describe changes over time. Protein–protein interaction networks are a popular example of static models. However, components, such as proteins, can also be described in dynamic models, using, i.e., ordinary differential equations (ODE) describing how components interact with each other, and how interactions are changed in response to stimuli. ODEs are used in deterministic models that, by definition, give the same output every time.

Notwithstanding, biological systems contain a certain amount of uncertainty. Stochastic simulations allow the modelling of systems containing rare, random, and uncertain reactions. As these simulations vary between runs, they must be repeated until a conclusive result is reached. Stochastic models include algorithms, such as Monte Carlo, Markov chain, Random walk [161]. Random protein damage via ROS modelling benefits from stochastic algorithm use [162]. The following paragraphs discuss the latest redox specific models, grouped by model type (Figure 5).

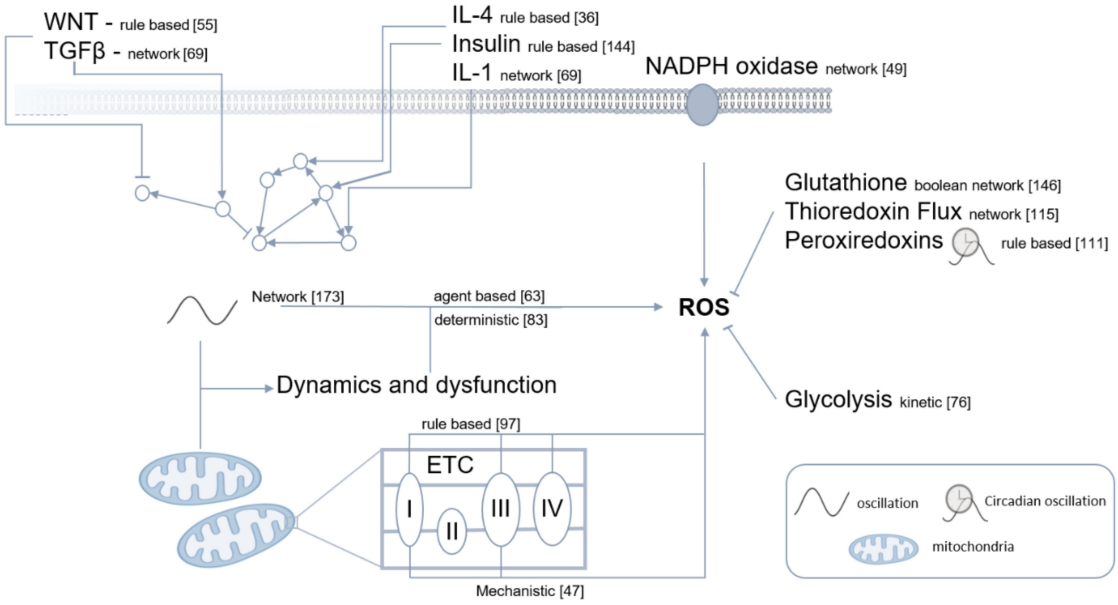


Figure 5. Interacting redox-sensitive pathways with existing computational models. The generalized model type is named, including a model reference. Detailed information can be found in Supplementary Material S2.

Computational models are usually created based on a specific hypothesis. Although the idea of a comprehensive model is appealing, the computational cost under current conditions would be too high and thus difficult to realize. Models are usually used to describe behaviour and mechanisms resulting in a specific behaviour. As mitochondria are the main producers of ROS, most redox-specific models focus on mitochondrial function. The model by Gauthier et al. (2013) revealed how ROS levels are controlled by the redox balance in mitochondria, which was later extended to show mitochondrial complex 1 as the main ROS producing site. This information is beneficial in drug development and treatment decision making [163,164]. Other models revealed the specific interplay of redox-sensitive proteins [165]. The inclusion of competing redox mechanisms revealed reversible protein tyrosine phosphatase oxygenation via ROS as the primary regulator in IL-4 signalling. This result has implications in therapeutic methods for ROS-related immune response deregulations [166].

More complex approaches, such as multimethod multicell simulations, including stochastic damage-dependent frequencies, illuminated mitochondrial dynamics and dysfunction specific to ageing [167]. Even models of the oscillatory relationship between ROS and ROS scavengers [168], and the role of peroxiredoxins (Prxs) and silfiredoxin for cellular circadian redox oscillation [169], have been created.

The diversity of redox regulated processes and tissues in which they occur indicates that special effects may have to be considered. This increases the complexity of a model and changes its construction. To support more integrative approaches, instead of ODE, partial differential equations and agent-based models, in which different compartments can be considered, are applied. System biology approaches focus on network modelling, which is characterized by viewing cells and molecular processes within them on different levels. This approach consists of two methodologies: static large-scale biological network modelling focusing on omics data integration, visualization, and topological analysis; and dynamic quantitative modelling.

Network-Based Redox Models

Mitochondrial function has also been described in network-based models, supporting the function of oscillating mitochondria in cardiomyocyte cell death [170]. Boolean network modelling of OS, set out to pinpoint dysfunctional components in OS responses using temporal variations, described the role of GSH in the cellular redox state and its role in ROS reduction and apoptosis inhibition [171]. Even the redox concentration dependency of insulin signalling has been studied using ODEs, which has implications for insulin-related disorders [172].

Computational models can not only describe existing mechanisms. An ideal example of how experimental and computer science benefit from one another is the Padayachee et al. (2020) thioredoxin model. The Thioredoxin system flux is an important indicator of the function and efficiency of the thioredoxin system within a biological sample. Flux has traditionally been measured in vitro by NADPH oxidation, while the thioredoxin redox state has been used as a proxy for the activity of the system. In vivo measurement of the flux, however, has remained challenging. This model suggested that in vivo thioredoxin oxidation measures can be used as surrogate indicators for flux, thus opening up new methods to experimental approaches that can lead to more accurate results [173]. Thiol state prediction models have yet to be adapted to animal systems [174]. Other computational redox models related to ageing have been extensively reviewed elsewhere [162,175].

Large networks can be turned into molecular interaction maps (MIM) as part of disease maps (DMs), allowing omics integration [176,177]. MIMs describe molecular interactions in a machine and human readable fashion and are frequently used for advanced network analyses [176,178]. DMs are a specialized approach for complex modelling, which supports the inclusion of compartments. Systems Biology Markup Language (SBML) is a machine-readable format that can be intuitively interpreted by users. SBML models consist of species, such as genes, miRNA, proteins, and other molecules, and biochemical reactions.

Most system biology tools, such as CellDesigner, Newt, Copasi, and Cytoscape, are freely available and give introductions to biologists unfamiliar with computational modelling. The research area includes the objective to increase the reproducibility and reusability of models [179].

These techniques have not been fully exploited in the context of maternal and fetal health and there is currently no comprehensive redox-signalling model resource, which is not surprising considering the number of different processes and tissues redox signalling is involved in. However, there are a number of models related to specific redox-signalling pathways. Mitochondria-specific models have recently been reviewed [180]. Other resources include the PantherDB "oxidative stress response" pathway. Reactome further provides ROS specific pathways "oxidative stress induced senescence" (R-HSA-2559580), "cell redox homeostasis" (R-HSA-1222541), "detoxification of reactive oxygen species" (R-HSA-3299685), and "ROS and RNS production in phagocytes" (R-HSA-1222556), and the CardioGlyco model [181].

Other models worth mentioning in this review are biophysics quantum and atom level models of electron transfer. This enabled the accurate estimation of biological macromolecule redox potentials and stressed the importance of long-range electrostatic interactions [159], with the outlook to study the role of redox potentials on DNA [182]. Of particular interest were the electronic properties of the transition metals iron and zinc in proteins, as it has an effect on structure, function, and stability of the metalloproteins [183,184]. These models, however, cannot currently be integrated into more complex system models due to technical limitations. A detailed table of redox-related models can be viewed in Supplementary Materials S2.

4. Future Perspectives

Pregnancy-related research entails challenges. The inherent vulnerability of the patient groups, as well as common comorbidities in pregnancy complications, increase the required number of biological samples for statistical analysis significantly. The use of cell lines, explant cultures, animal models, and computational modelling are useful circumventions [160].

Redox signalling plays a major role in both successful and complicated pregnancies. We have shown the plethora of processes falling under the term "redox signalling" and associated maternal and foetal outcomes. The complexity of redox signalling requires consideration of more than one biomarker to obtain meaningful results. On the experimental side, this calls for more integrative approaches considering both pro- and antioxidant reactions with a higher sensitivity to physiological variation.

Although computational modelling of redox-related processes is often utilized in health sciences, these models have not been exploited in the context of feto-maternal health research, notwithstanding that computational modelling reduces the need for experimental replicates by identifying biomarker candidates [160].

The combination of existing models to a larger network, including other redox-signalling pathways, may lead to deeper insights to provide the opportunity to explore interventions and their effects on complex biological processes [185]. To this end, we created a redox signalling SBML model (Figure 6) available in Supplementary Materials S3, which will be integrated into the placenta-specific disease map currently under development.

This map includes proteins, chemical entities, receptors, and phenotypes involved in ROS, RSS, and RNS pathways and previously described redox-sensitive protein signalling. Notably, mitochondrial ROS production is not integrated here, as it has been previously created [180] and can be extended using the presented map. Both activity flow and progress description are included, increasing human interpretability. Activity flow describes the general flow of information between elements, while process descriptions include detailed mechanistic descriptions of molecular interactions [186]. The redox signalling map contains 224 unique proteins, 58 simple molecules, 238 interactions, and 5 compartments (general cell, nucleus, mitochondrion, endoplasmic reticulum, and peroxisome) making spatial considerations possible. The redox map was created in CellDesigner and is SBML compliant.

Each species is annotated to enable database linkage. Proteins are named according to gene name conventions, simple molecules contain ChEBI naming conventions; all reactions are annotated with the respective publication they were extracted from.

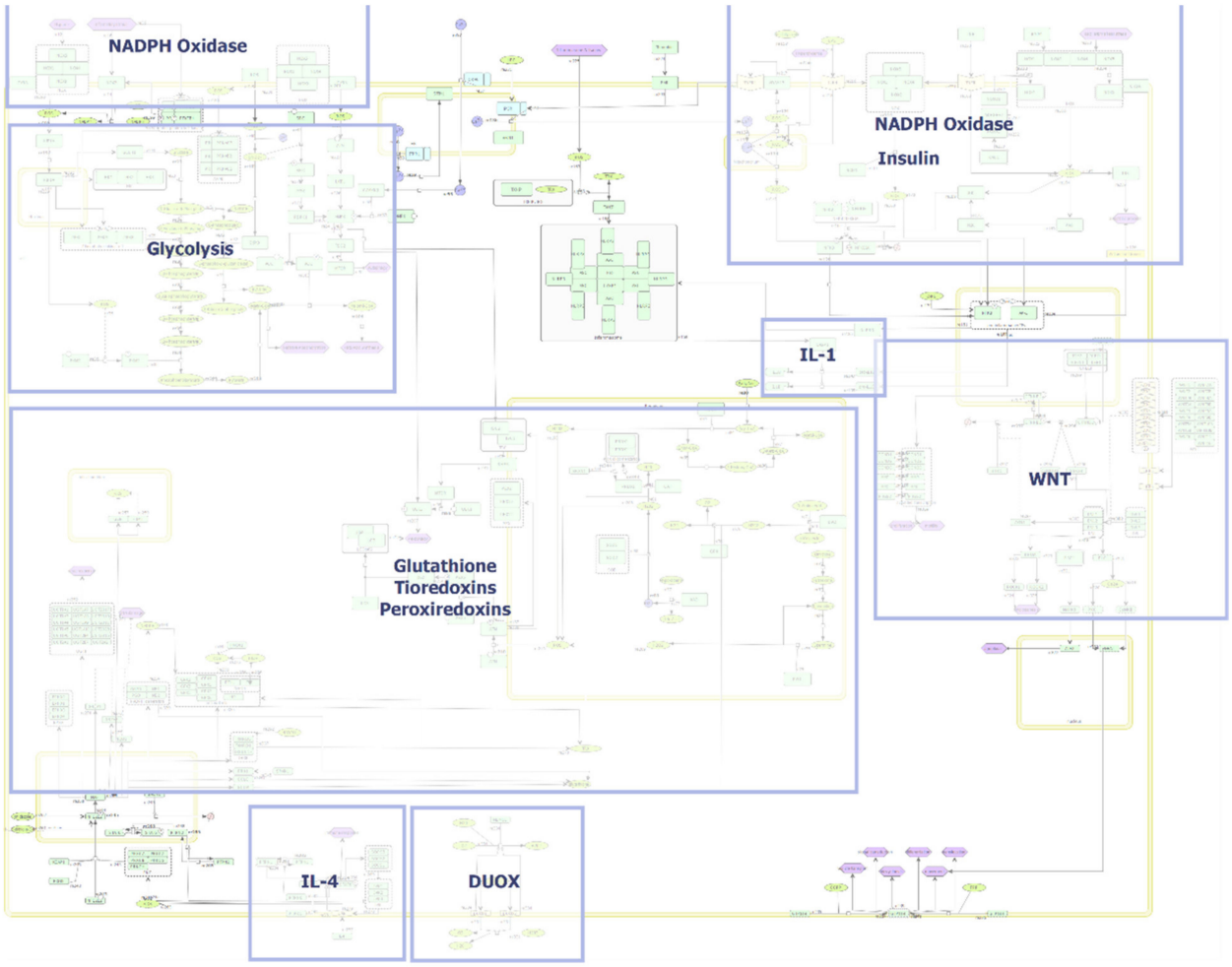


Figure 6. Redox signalling map grouped according to signalling process. Interacting species are indicated as nodes and their interactions as lines. Interactions can be "inhibition", "positive influence", "modulation", "state transition", and "transport". Unclear interactions are visualized as dashed lines. (Green = proteins; bright green = simple molecules; purple = phenotypes; blue = ions).

5. Conclusions

In this review, we aimed to summarize the mechanism of redox signalling, briefly discussing the different reactive species affecting pregnancies and maternal health at molecular and physiological levels. We also discussed various therapeutic interventions investigated through multiple models and their potential benefits.

Despite ample evidence of the importance of the redox status in pregnancy pathologies, the exact molecular mechanism remains to be elucidated and determination of oxidative damage remains challenging, even with advanced research methodologies. A closer collaboration between experimental and computational scientists yields opportunities to alleviate both experimental challenges and the general challenge of recruiting samples from the vulnerable patient groups. The computational models described in this review can be used to unravel complex signalling pathways. With the combination of knowledge held within these models, we created a molecular interaction map of redox signalling processes. This model can be used in combination with pregnancy pathology specific data to elucidate the molecular interplay involved in the pathology of interest (Supplementary Materials S4).

Henceforth, as hypothesised by Hoch et al. (2021), this approach enables the identification of signalling regulators and potential therapeutic targets [63].

Supplementary Materials: The following supporting information can be downloaded at: https://www.mdpi.com/article/10.3390/antiox11030585/s1, Supplementary Materials S1: Table of experimental methods to assess redox status, Supplementary Materials S2: Table of computational models of redox sensitive pathways., Supplementary Materials S3: SBML compliant CellDesigner Model in xml format of redox signalling map, Supplementary Materials S4: Brief outlook on redox signalling map application using public data.

Author Contributions: The first draft of this review manuscript has been co-written by S.M., J.S., C.A., J.-C.H. and C.S.M.R. S.M., C.S.M.R. and J.-C.H. contributed equally to this work and are co-first authors. J.S., C.M. (Cathal McCarthy) and C.A. contributed equally to this work and are co-last authors. C.M. (Cathal McCarthy), F.P.M., D.V., S.G., C.M. (Céline Méhats) supervised and made contributions to the manuscript. All authors edited the manuscript. All authors have read and agreed to the published version of the manuscript.

Funding: This research has received funding from European Union's Horizon 2020 research and innovation program under Marie Skłodowska-Curie Actions Innovative Training Network (H2020-MSCA-ITN 2017), Grant No. 765274, acronym iPLACENTA.

Acknowledgments: We thank Matti Hoch and the department of bioinformatics and systems biology (University Rostock, Germany) for allowing the use of Minerva beta version plugins.

Conflicts of Interest: The authors declare no conflict of interest.

References

1. Hayes, J.D.; Dinkova-Kostova, A.T.; Tew, K.D. Oxidative Stress in Cancer. *Cancer Cell* **2020**, *38*, 167–197. [CrossRef] [PubMed]
2. Incalza, M.A.; D'Oria, R.; Natalicchio, A.; Perrini, S.; Laviola, L.; Giorgino, F. Oxidative stress and reactive oxygen species in endothelial dysfunction associated with cardiovascular and metabolic diseases. *Vasc. Pharmacol.* **2018**, *100*, 1–19. [CrossRef] [PubMed]
3. Liguori, I.; Russo, G.; Curcio, F.; Bulli, G.; Aran, L.; Della-Morte, D.; Gargiulo, G.; Testa, G.; Cacciatore, F.; Bonaduce, D.; et al. Oxidative stress, aging, and diseases. *Clin. Interv. Aging* **2018**, *13*, 757–772. [CrossRef] [PubMed]
4. Maritim, A.C.; Sanders, R.A.; Watkins, J.B., 3rd. Diabetes, oxidative stress, and antioxidants: A review. *J. Biochem. Mol. Toxicol.* **2003**, *17*, 24–38. [CrossRef]
5. Mert, I.; Oruc, A.S.; Yuksel, S.; Cakar, E.S.; Buyukkagnıcı, U.; Karaer, A.; Danısman, N. Role of oxidative stress in preeclampsia and intrauterine growth restriction. *J. Obstet. Gynaecol. Res.* **2012**, *38*, 658–664. [CrossRef] [PubMed]
6. Rashid, C.; Bansal, A.; Simmons, R.A. Oxidative Stress, Intrauterine Growth Restriction, and Developmental Programming of Type 2 Diabetes. *Physiology* **2018**, *33*, 348–359. [CrossRef] [PubMed]
7. Lyall, F.; Robson, S.C.; Bulmer, J.N. Spiral Artery Remodeling and Trophoblast Invasion in Preeclampsia and Fetal Growth Restriction: Relationship to Clinical Outcome. *Hypertension* **2013**, *62*, 1046–1054. [CrossRef] [PubMed]
8. Ness, R.B.; Sibai, B.M. Shared and disparate components of the pathophysiologies of fetal growth restriction and preeclampsia. *Am. J. Obstet. Gynecol.* **2006**, *195*, 40–49. [CrossRef]
9. Melchiorre, K.; Giorgione, V.; Thilaganathan, B. The placenta and preeclampsia: Villain or victim? *Am. J. Obstet. Gynecol.* **2022**, *226*, S954–S962. [CrossRef]
10. Pillay, C.S.; Eagling, B.D.; Driscoll, S.R.; Rohwer, J. Quantitative measures for redox signaling. *Free Radic. Biol. Med.* **2016**, *96*, 290–303. [CrossRef]
11. Forman, H.J.; Ursini, F.; Maiorino, M. An overview of mechanisms of redox signaling. *J. Mol. Cell. Cardiol.* **2014**, *73*, 2–9. [CrossRef] [PubMed]
12. Genestra, M. Oxyl radicals, redox-sensitive signalling cascades and antioxidants. *Cell. Signal.* **2007**, *19*, 1807–1819. [CrossRef] [PubMed]
13. Bartoli, C.G.; Casalongué, C.A.; Simontacchi, M.; Garcia, B.M.; Foyer, C.H. Interactions between hormone and redox signalling pathways in the control of growth and cross tolerance to stress. *Environ. Exp. Bot.* **2013**, *94*, 73–88. [CrossRef]
14. Brüne, B.; Dehne, N.; Grossmann, N.; Jung, M.; Namgaladze, D.; Schmid, T.; Von Knethen, A.; Weigert, A. Redox Control of Inflammation in Macrophages. *Antioxid. Redox Signal.* **2013**, *19*, 595–637. [CrossRef] [PubMed]
15. Chiarugi, P. From anchorage dependent proliferation to survival: Lessons from redox signalling. *IUBMB Life* **2008**, *60*, 301–307. [CrossRef] [PubMed]
16. Lee, J.; Giordano, S.; Zhang, J. Autophagy, mitochondria and oxidative stress: Cross-talk and redox signalling. *Biochem. J.* **2012**, *441*, 523–540. [CrossRef]

17. Touyz, R.M.; Tabet, F.; Schiffrin, E.L. Redox-dependent signalling by angiotensin II and vascular remodelling in hypertension. *Clin. Exp. Pharmacol. Physiol.* **2003**, *30*, 860–866. [CrossRef]
18. McMahon, M.; Thomas, N.; Itoh, K.; Yamamoto, M.; Hayes, J.D. Redox-regulated Turnover of Nrf2 Is Determined by at Least Two Separate Protein Domains, the Redox-sensitive Neh2 Degron and the Redox-insensitive Neh6 Degron. *J. Biol. Chem.* **2004**, *279*, 31556–31567. [CrossRef]
19. Haddad, J.J. Antioxidant and prooxidant mechanisms in the regulation of redox(y)-sensitive transcription factors. *Cell. Signal.* **2002**, *14*, 879–897. [CrossRef]
20. Corcoran, A.; Cotter, T.G. Redox regulation of protein kinases. *FEBS J.* **2013**, *280*, 1944–1965. [CrossRef]
21. Zhao, R.-Z.; Jiang, S.; Zhang, L.; Yu, Z.-B. Mitochondrial electron transport chain, ROS generation and uncoupling (Review). *Int. J. Mol. Med.* **2019**, *44*, 3–15. [CrossRef] [PubMed]
22. Kühlbrandt, W. Structure and function of mitochondrial membrane protein complexes. *BMC Biol.* **2015**, *13*, 89. [CrossRef] [PubMed]
23. Dworakowski, R.; Anilkumar, N.; Zhang, M.; Shah, A. Redox signalling involving NADPH oxidase-derived reactive oxygen species. *Biochem. Soc. Trans.* **2006**, *34*, 960–964. [CrossRef] [PubMed]
24. De Deken, X.; Wang, D.; Many, M.-C.; Costagliola, S.; Libert, F.; Vassart, G.; Dumont, J.E.; Miot, F. Cloning of Two Human Thyroid cDNAs Encoding New Members of the NADPH Oxidase Family. *J. Biol. Chem.* **2000**, *275*, 23227–23233. [CrossRef] [PubMed]
25. Kelley, E.E.; Khoo, N.K.; Hundley, N.J.; Malik, U.Z.; Freeman, B.A.; Tarpey, M.M. Hydrogen peroxide is the major oxidant product of xanthine oxidase. *Free Radic. Biol. Med.* **2010**, *48*, 493–498. [CrossRef] [PubMed]
26. Heinzel, B.; John, M.; Klatt, P.; Böhme, E.; Mayer, B. Ca^{2+}/calmodulin-dependent formation of hydrogen peroxide by brain nitric oxide synthase. *Biochem. J.* **1992**, *281*, 627–630. [CrossRef] [PubMed]
27. Beauchamp, C.; Fridovich, I. A mechanism for the production of ethylene from methional. The generation of the hydroxyl radical by xanthine oxidase. *J. Biol. Chem.* **1970**, *245*, 4641–4646. [CrossRef]
28. Albertolle, M.E.; Guengerich, F.P. The relationships between cytochromes P450 and H_2O_2: Production, reaction, and inhibition. *J. Inorg. Biochem.* **2018**, *186*, 228–234. [CrossRef]
29. Palmer, R.M.J.; Ferrige, A.G.; Moncada, S. Nitric oxide release accounts for the biological activity of endothelium-derived relaxing factor. *Nature* **1987**, *327*, 524–526. [CrossRef]
30. Ignarro, L.J.; Buga, G.M.; Wood, K.S.; Byrns, R.E.; Chaudhuri, G. Endothelium-derived relaxing factor produced and released from artery and vein is nitric oxide. *Proc. Natl. Acad. Sci. USA* **1987**, *84*, 9265–9269. [CrossRef]
31. Radi, R. Oxygen radicals, nitric oxide, and peroxynitrite: Redox pathways in molecular medicine. *Proc. Natl. Acad. Sci. USA* **2018**, *115*, 5839–5848. [CrossRef] [PubMed]
32. Nussler, A.K.; Billiar, T.R. Inflammation, immunoregulation, and inducible nitric oxide synthase. *J. Leukoc. Biol.* **1993**, *54*, 171–178. [CrossRef]
33. Bredt, D.S.; Hwang, P.M.; Snyder, S.H. Localization of nitric oxide synthase indicating a neural role for nitric oxide. *Nature* **1990**, *347*, 768–770. [CrossRef] [PubMed]
34. Luo, S.; Lei, H.; Qin, H.; Xia, Y. Molecular Mechanisms of Endothelial NO Synthase Uncoupling. *Curr. Pharm. Des.* **2014**, *20*, 3548–3553. [CrossRef] [PubMed]
35. Olson, K.R. Are Reactive Sulfur Species the New Reactive Oxygen Species? *Antioxid. Redox Signal.* **2020**, *33*, 1125–1142. [CrossRef]
36. Espinosa-Diez, C.; Miguel, V.; Mennerich, D.; Kietzmann, T.; Pérez, P.S.; Cadenas, S.; Lamas, S. Antioxidant responses and cellular adjustments to oxidative stress. *Redox Biol.* **2015**, *6*, 183–197. [CrossRef] [PubMed]
37. Wan, X.S.; Devalaraja, M.N.; Clair, D.K.S. Molecular Structure and Organization of the Human Manganese Superoxide Dismutase Gene. *DNA Cell Biol.* **1994**, *13*, 1127–1136. [CrossRef] [PubMed]
38. Barra, D.; Schinina, M.E.; Simmaco, M.; Bannister, J.V.; Bannister, W.H.; Rotilio, G.; Bossa, F. The primary structure of human liver manganese superoxide dismutase. *J. Biol. Chem.* **1984**, *259*, 12595–12601. [CrossRef]
39. Tainer, J.; Getzoff, E.D.; Richardson, J.; Richardson, D.C. Structure and mechanism of copper, zinc superoxide dismutase. *Nature* **1983**, *306*, 284–287. [CrossRef]
40. Reid, T.J.; Murthy, M.R.; Sicignano, A.; Tanaka, N.; Musick, W.D.; Rossmann, M.G. Structure and heme environment of beef liver catalase at 2.5 A resolution. *Proc. Natl. Acad. Sci. USA* **1981**, *78*, 4767–4771. [CrossRef]
41. Goyal, M.M.; Basak, A. Human catalase: Looking for complete identity. *Protein Cell* **2010**, *1*, 888–897. [CrossRef] [PubMed]
42. Holmgren, A. Thioredoxin structure and mechanism: Conformational changes on oxidation of the active-site sulfhydryls to a disulfide. *Structure* **1995**, *3*, 239–243. [CrossRef]
43. Arnér, E.S.J.; Holmgren, A. Physiological functions of thioredoxin and thioredoxin reductase. *Eur. J. BioChem.* **2000**, *267*, 6102–6109. [CrossRef] [PubMed]
44. Lubos, E.; Loscalzo, J.; Handy, D.E. Glutathione Peroxidase-1 in Health and Disease: From Molecular Mechanisms to Therapeutic Opportunities. *Antioxid. Redox Signal.* **2011**, *15*, 1957–1997. [CrossRef] [PubMed]
45. Staal, G.; Helleman, P.; De Wael, J.; Veeger, C. Purification and properties of an abrnomal glutathione reductace from human erythrocytes. *Biochim. Biophys. Acta Enzym.* **1969**, *185*, 63–69. [CrossRef]
46. Schoots, M.H.; Gordijn, S.J.; Scherjon, S.A.; Van Goor, H.; Hillebrands, J.-L. Oxidative stress in placental pathology. *Placenta* **2018**, *69*, 153–161. [CrossRef] [PubMed]
47. Burton, G.J.; Jauniaux, E. Oxidative stress. *Best Pract. Res. Clin. Obstet. Gynaecol.* **2011**, *25*, 287–299. [CrossRef] [PubMed]

48. Mannaerts, D.; Faes, E.; Cos, P.; Briedé, J.J.; Gyselaers, W.; Cornette, J.; Gorbanev, Y.; Bogaerts, A.; Spaanderman, M.; Van Craenenbroeck, E.; et al. Oxidative stress in healthy pregnancy and preeclampsia is linked to chronic inflammation, iron status and vascular function. *PLoS ONE* **2018**, *13*, e0202919. [CrossRef]
49. Toboła-Wróbel, K.; Pietryga, M.; Dydowicz, P.; Napierała, M.; Brązert, J.; Florek, E. Association of Oxidative Stress on Pregnancy. *Oxidative Med. Cell. Longev.* **2020**, *2020*, 6398520. [CrossRef]
50. Bolat, F.; Haberal, N.; Tunali, N.; Aslan, E.; Bal, N.; Tuncer, I. Expression of vascular endothelial growth factor (VEGF), hypoxia inducible factor 1 alpha (HIF-1α), and transforming growth factors β1 (TGFβ1) and β3 (TGFβ;3) in gestational trophoblastic disease. *Pathol. Res. Pract.* **2010**, *206*, 19–23. [CrossRef]
51. Nanduri, J.; Vaddi, D.R.; Khan, S.A.; Wang, N.; Makarenko, V.; Semenza, G.L.; Prabhakar, N.R. HIF-1α Activation by Intermittent Hypoxia Requires NADPH Oxidase Stimulation by Xanthine Oxidase. *PLoS ONE* **2015**, *10*, e0119762. [CrossRef] [PubMed]
52. Chiarello, D.I.; Abad, C.L.; Rojas, D.; Toledo, F.; Vazquez, C.; Mate, A.; Sobrevia, L.; Marín, R. Oxidative stress: Normal pregnancy versus preeclampsia. *Biochim. Biophys. Acta Mol. Basis Dis.* **2020**, *1866*, 165354. [CrossRef] [PubMed]
53. Sferruzzi-Perri, A.N.; Higgins, J.S.; Vaughan, O.R.; Murray, A.J.; Fowden, A.L. Placental mitochondria adapt developmentally and in response to hypoxia to support fetal growth. *Proc. Natl. Acad. Sci. USA* **2019**, *116*, 1621–1626. [CrossRef] [PubMed]
54. McElwain, C.; Tuboly, E.; McCarthy, F.P.; McCarthy, C.M. Mechanisms of Endothelial Dysfunction in Pre-eclampsia and Gestational Diabetes Mellitus: Windows into Future Cardiometabolic Health? *Front. Endocrinol.* **2020**, *11*, 655. [CrossRef] [PubMed]
55. Duhig, K.; Chappell, L.C.; Shennan, A.H. Oxidative stress in pregnancy and reproduction. *Obstet. Med.* **2016**, *9*, 113–116. [CrossRef] [PubMed]
56. Sobrevia, L.; Ooi, L.; Ryan, S.; Steinert, J.R. Nitric Oxide: A Regulator of Cellular Function in Health and Disease. *Oxidative Med. Cell. Longev.* **2015**, *2016*, 9782346. [CrossRef] [PubMed]
57. Visiedo, F.; Santos-Rosendo, C.; Mateos-Bernal, R.M.; Gil-Sánchez, M.D.M.; Bugatto, F.; Diosdado, M.A.; Segundo, C.; López-Tinoco, C. Characterization of NO-Induced Nitrosative Status in Human Placenta from Pregnant Women with Gestational Diabetes Mellitus. *Oxidative Med. Cell. Longev.* **2017**, *2017*, 5629341. [CrossRef] [PubMed]
58. Sultana, Z.; Maiti, K.; Aitken, R.J.; Morris, J.; Dedman, L.; Smith, R. Oxidative stress, placental ageing-related pathologies and adverse pregnancy outcomes. *Am. J. Reprod. Immunol.* **2017**, *77*, e12653. [CrossRef] [PubMed]
59. Manna, S.; McCarthy, C.; McCarthy, F. Placental Ageing in Adverse Pregnancy Outcomes: Telomere Shortening, Cell Senescence, and Mitochondrial Dysfunction. *Oxidative Med. Cell. Longev.* **2019**, *2019*, 3095383. [CrossRef] [PubMed]
60. Rodríguez-Rodríguez, P.; Cortijo, D.R.; Reyes-Hernández, C.G.; De Pablo, A.L.L.; González, M.C.; Arribas, S.M. Implication of Oxidative Stress in Fetal Programming of Cardiovascular Disease. *Front. Physiol.* **2018**, *9*, 602. [CrossRef] [PubMed]
61. Barker, D.J.P. Fetal origins of coronary heart disease. *BMJ* **1995**, *311*, 171–174. [CrossRef]
62. Helle, E.; Priest, J.R. Maternal Obesity and Diabetes Mellitus as Risk Factors for Congenital Heart Disease in the Offspring. *J. Am. Heart Assoc.* **2020**, *9*, e011541. [CrossRef] [PubMed]
63. Mirabelli, M.; Chiefari, E.; Tocci, V.; Greco, E.; Foti, D.; Brunetti, A. Gestational diabetes: Implications for fetal growth, intervention timing, and treatment options. *Curr. Opin. Pharmacol.* **2021**, *60*, 1–10. [CrossRef] [PubMed]
64. Palinski, W. Effect of Maternal Cardiovascular Conditions and Risk Factors on Offspring Cardiovascular Disease. *Circulation* **2014**, *129*, 2066–2077. [CrossRef] [PubMed]
65. Fall, C.H.D. Fetal Malnutrition and Long-Term Outcomes. In *Nestlé Nutrition Workshop Series: Pediatric Program*; S. Karger AG: Basel, Switzerland, 2013; Volume 74, pp. 11–25. [CrossRef]
66. Evans, L.; Myatt, L. Sexual dimorphism in the effect of maternal obesity on antioxidant defense mechanisms in the human placenta. *Placenta* **2017**, *51*, 64–69. [CrossRef] [PubMed]
67. Wang, L.; Ahn, Y.J.; Asmis, R. Sexual dimorphism in glutathione metabolism and glutathione-dependent responses. *Redox Biol.* **2020**, *31*, 101410. [CrossRef] [PubMed]
68. Muralimanoharan, S.; Guo, C.; Myatt, L.; Maloyan, A. Sexual dimorphism in miR-210 expression and mitochondrial dysfunction in the placenta with maternal obesity. *Int. J. Obes.* **2015**, *39*, 1274–1281. [CrossRef] [PubMed]
69. Orabona, R.; Sciatti, E.; Prefumo, F.; Vizzardi, E.; Bonadei, I.; Valcamonico, A.; Metra, M.; Frusca, T. Pre-eclampsia and heart failure: A close relationship. *Ultrasound Obstet. Gynecol.* **2018**, *52*, 297–301. [CrossRef] [PubMed]
70. Turbeville, H.R.; Sasser, J.M. Preeclampsia beyond pregnancy: Long-term consequences for mother and child. *Am. J. Physiol. Physiol.* **2020**, *318*, F1315–F1326. [CrossRef] [PubMed]
71. Herrera-Garcia, G.; Contag, S. Maternal Preeclampsia and Risk for Cardiovascular Disease in Offspring. *Curr. Hypertens. Rep.* **2014**, *16*, 475. [CrossRef]
72. Ramsay, E.J.; Stewart, F.; Greer, I.A.; Sattar, N. Microvascular dysfunction: A link between pre-eclampsia and maternal coronary heart disease. *BJOG* **2003**, *110*, 1029–1031. [CrossRef] [PubMed]
73. Tihtonen, K.M.; Kööbi, T.; Uotila, J.T. Arterial stiffness in preeclamptic and chronic hypertensive pregnancies. *Eur. J. Obstet. Gynecol. Reprod. Biol.* **2006**, *128*, 180–186. [CrossRef] [PubMed]
74. Deanfield, J.E.; Halcox, J.P.; Rabelink, T.J. Endothelial function and dysfunction: Testing and clinical relevance. *Circulation* **2007**, *115*, 1285–1295. [CrossRef] [PubMed]
75. Godo, S.; Shimokawa, H. Divergent roles of endothelial nitric oxide synthases system in maintaining cardiovascular homeostasis. *Free Radic. Biol. Med.* **2017**, *109*, 4–10. [CrossRef] [PubMed]

76. Iwakiri, Y.; Satoh, A.; Chatterjee, S.; Toomre, D.K.; Chalouni, C.M.; Fulton, D.; Groszmann, R.J.; Shah, V.H.; Sessa, W.C. Nitric oxide synthase generates nitric oxide locally to regulate compartmentalized protein S-nitrosylation and protein trafficking. *Proc. Natl. Acad. Sci. USA* **2006**, *103*, 19777–19782. [CrossRef] [PubMed]
77. Hess, D.T.; Matsumoto, A.; Kim, S.-O.; Marshall, H.E.; Stamler, J.S. Protein S-nitrosylation: Purview and parameters. *Nat. Rev. Mol. Cell Biol.* **2005**, *6*, 150–166. [CrossRef] [PubMed]
78. Erwin, P.A.; Lin, A.J.; Golan, D.E.; Michel, T. Receptor-regulated Dynamic S-Nitrosylation of Endothelial Nitric-oxide Synthase in Vascular Endothelial Cells. *J. Biol. Chem.* **2005**, *280*, 19888–19894. [CrossRef] [PubMed]
79. Ghosh, A.; Gao, L.; Thakur, A.; Siu, P.M.; Lai, C.W.K. Role of free fatty acids in endothelial dysfunction. *J. Biomed. Sci.* **2017**, *24*, 50. [CrossRef]
80. Endemann, D.H. Endothelial Dysfunction. *J. Am. Soc. Nephrol.* **2004**, *15*, 1983–1992. [CrossRef]
81. Ma, S.; Ma, C.C.-H. Recent developments in the effects of nitric oxide-donating statins on cardiovascular disease through regulation of tetrahydrobiopterin and nitric oxide. *Vasc. Pharmacol.* **2014**, *63*, 63–70. [CrossRef]
82. Durrant, J.R.; Seals, D.R.; Connell, M.L.; Russell, M.J.; Lawson, B.R.; Folian, B.J.; Donato, A.J.; Lesniewski, L.A. Voluntary wheel running restores endothelial function in conduit arteries of old mice: Direct evidence for reduced oxidative stress, increased superoxide dismutase activity and down regulation of NADPH oxidase. *J. Physiol.* **2009**, *587*, 3271–3285. [CrossRef] [PubMed]
83. Coyle, C.H.; Kader, K.N. Mechanisms of H_2O_2-Induced Oxidative Stress in Endothelial Cells Exposed to Physiologic Shear Stress. *ASAIO J.* **2007**, *53*, 17–22. [CrossRef] [PubMed]
84. Scherz-Shouval, R.; Elazar, Z. ROS, mitochondria and the regulation of autophagy. *Trends Cell Biol.* **2007**, *17*, 422–427. [CrossRef] [PubMed]
85. Paravicini, T.M.; Touyz, R.M. NADPH Oxidases, Reactive Oxygen Species, and Hypertension: Clinical implications and therapeutic possibilities. *Diabetes Care* **2008**, *31* (Suppl. S2), S170–S180. [CrossRef] [PubMed]
86. Weng, X.; Yu, L.; Liang, P.; Li, L.; Dai, X.; Zhou, B.; Wu, X.; Xu, H.; Fang, M.; Chen, Q.; et al. A crosstalk between chromatin remodeling and histone H3K4 methyltransferase complexes in endothelial cells regulates angiotensin II-induced cardiac hypertrophy. *J. Mol. Cell. Cardiol.* **2015**, *82*, 48–58. [CrossRef] [PubMed]
87. Serpillon, S.; Floyd, B.C.; Gupte, R.S.; George, S.; Kozicky, M.; Neito, V.; Recchia, F.; Stanley, W.; Wolin, M.S.; Gupte, S.A. Superoxide production by NAD(P)H oxidase and mitochondria is increased in genetically obese and hyperglycemic rat heart and aorta before the development of cardiac dysfunction. The role of glucose-6-phosphate dehydrogenase-derived NADPH. *Am. J. Physiol. Circ. Physiol.* **2009**, *297*, H153–H162. [CrossRef] [PubMed]
88. Kuroda, J.; Ago, T.; Matsushima, S.; Zhai, P.; Schneider, M.D.; Sadoshima, J. NADPH oxidase 4 (Nox4) is a major source of oxidative stress in the failing heart. *Proc. Natl. Acad. Sci. USA* **2010**, *107*, 15565–15570. [CrossRef] [PubMed]
89. Fortuño, A.; José, G.S.; Moreno, M.U.; Beloqui, O.; Díez, J.; Zalba, G. Phagocytic NADPH Oxidase Overactivity Underlies Oxidative Stress in Metabolic Syndrome. *Diabetes* **2006**, *55*, 209–215. [CrossRef] [PubMed]
90. Sorescu, D.; Weiss, D.; Lassègue, B.; Clempus, R.E.; Szöcs, K.; Sorescu, G.P.; Valppu, L.; Quinn, M.; Lambeth, J.D.; Vega, J.D.; et al. Superoxide Production and Expression of Nox Family Proteins in Human Atherosclerosis. *Circulation* **2002**, *105*, 1429–1435. [CrossRef]
91. Sen, S.; Iyer, C.; Meydani, S.N. Obesity during pregnancy alters maternal oxidant balance and micronutrient status. *J. Perinatol.* **2013**, *34*, 105–111. [CrossRef]
92. Chappell, L.C.; Seed, P.T.; Briley, A.L.; Kelly, F.J.; Lee, R.; Hunt, B.J.; Parmar, K.; Bewley, S.; Shennan, A.H.; Steer, P.J.; et al. Effect of antioxidants on the occurrence of pre-eclampsia in women at increased risk: A randomised trial. *Lancet* **1999**, *354*, 810–816. [CrossRef]
93. Hyppönen, E.; Cavadino, A.; Williams, D.; Fraser, A.; Vereczkey, A.; Fraser, W.D.; Bánhidy, F.; Lawlor, D.; Czeizel, A.E. Vitamin D and Pre-Eclampsia: Original Data, Systematic Review and Meta-Analysis. *Ann. Nutr. Metab.* **2013**, *63*, 331–340. [CrossRef] [PubMed]
94. Williamson, R.D.; McCarthy, C.; McCarthy, F.; Kenny, L.C. Oxidative stress in pre-eclampsia; have we been looking in the wrong place? Pregnancy Hypertens. *Int. J. Women Cardiovasc. Health* **2017**, *8*, 1–5. [CrossRef]
95. Duntas, L.H. Selenium and at-risk pregnancy: Challenges and controversies. *Thyroid Res.* **2020**, *13*, 16. [CrossRef]
96. Hubalewska-Dydejczyk, A.; Duntas, L.; Gilis-Januszewska, A. Pregnancy, thyroid, and the potential use of selenium. *Hormones* **2019**, *19*, 47–53. [CrossRef] [PubMed]
97. Kasawara, K.T.; Nascimento, S.L.D.; Costa, M.L.; Surita, F.G.; Silva, J.L.P.E. Exercise and physical activity in the prevention of pre-eclampsia: Systematic review. *Acta Obstet. Gynecol. Scand.* **2012**, *91*, 1147–1157. [CrossRef]
98. Dastjerdi, M.V.; Hosseini, S.; Bayani, L. Sildenafil citrate and uteroplacental perfusion in fetal growth restriction. *J. Res. Med. Sci.* **2012**, *17*, 632–636.
99. Ferreira, R.D.D.S.; Negrini, R.; Bernardo, W.M.; Simões, R.; Piato, S. The effects of sildenafil in maternal and fetal outcomes in pregnancy: A systematic review and meta-analysis. *PLoS ONE* **2019**, *14*, e0219732. [CrossRef]
100. Sharp, A.; Cornforth, C.; Jackson, R.; Harrold, J.; Turner, M.A.; Kenny, L.C.; Baker, P.N.; Johnstone, E.D.; Khalil, A.; Von Dadelszen, P.; et al. Maternal sildenafil for severe fetal growth restriction (STRIDER): A multicentre, randomised, placebo-controlled, double-blind trial. *Lancet Child Adolesc. Health* **2018**, *2*, 93–102. [CrossRef]
101. Gekakis, N.; Staknis, D.; Nguyen, H.B.; Davis, F.C.; Wilsbacher, L.D.; King, D.P.; Takahashi, J.S.; Weitz, C.J. Role of the CLOCK protein in the mammalian circadian mechanism. *Science* **1998**, *280*, 1564–1569. [CrossRef]

102. Richards, J.; Diaz, A.N.; Gumz, M.L. Clock genes in hypertension. *Blood Press. Monit.* **2014**, *19*, 249–254. [CrossRef] [PubMed]
103. Ayala, D.E.; Ucieda, R.; Hermida, R.C. Chronotherapy with Low-Dose Aspirin for Prevention of Complications in Pregnancy. *Chronobiol. Int.* **2012**, *30*, 260–279. [CrossRef] [PubMed]
104. Marseglia, L.; D'Angelo, G.; Manti, S.; Reiter, R.J.; Gitto, E. Potential Utility of Melatonin in Preeclampsia, Intrauterine Fetal Growth Retardation, and Perinatal Asphyxia. *Reprod. Sci.* **2016**, *23*, 970–977. [CrossRef]
105. Hobson, S.; Gurusinghe, S.; Lim, R.; Alers, N.O.; Miller, S.L.; Kingdom, J.C.; Wallace, E.M. Melatonin improves endothelial function in vitro and prolongs pregnancy in women with early-onset preeclampsia. *J. Pineal Res.* **2018**, *65*, e12508. [CrossRef] [PubMed]
106. Adlam, V.J.; Harrison, J.; Porteous, C.M.; James, A.M.; Smith, R.A.J.; Murphy, M.; Sammut, I. Targeting an antioxidant to mitochondria decreases cardiac ischemia-reperfusion injury. *FASEB J.* **2005**, *19*, 1088–1095. [CrossRef] [PubMed]
107. Cochemé, H.M.; Logan, A.; Prime, T.A.; Abakumova, I.; Quin, C.; McQuaker, S.J.; Patel, J.V.; Fearnley, I.M.; James, A.M.; Porteous, C.M.; et al. Using the mitochondria-targeted ratiometric mass spectrometry probe MitoB to measure H_2O_2 in living *Drosophila*. *Nat. Protoc.* **2012**, *7*, 946–958. [CrossRef] [PubMed]
108. Salin, K.; Auer, S.K.; Villasevil, E.M.; Anderson, G.J.; Cairns, A.; Mullen, W.; Hartley, R.; Metcalfe, N. Using the MitoB method to assess levels of reactive oxygen species in ecological studies of oxidative stress. *Sci. Rep.* **2017**, *7*, 41228. [CrossRef] [PubMed]
109. Prime, T.A.; Forkink, M.; Logan, A.; Finichiu, P.G.; McLachlan, J.; Pun, P.B.L.; Koopman, W.J.; Larsen, L.; Latter, M.J.; Smith, R.A.; et al. A ratiometric fluorescent probe for assessing mitochondrial phospholipid peroxidation within living cells. *Free Radic. Biol. Med.* **2012**, *53*, 544–553. [CrossRef] [PubMed]
110. McCarthy, C.M.; Kenny, L.C. Therapeutically targeting mitochondrial redox signalling alleviates endothelial dysfunction in preeclampsia. *Sci. Rep.* **2016**, *6*, 32683. [CrossRef] [PubMed]
111. Graham, D.; Huynh, N.N.; Hamilton, C.A.; Beattie, E.; Smith, R.A.; Cochemé, H.M.; Murphy, M.P.; Dominiczak, A.F. Mitochondria-Targeted Antioxidant $MitoQ_{10}$ Improves Endothelial Function and Attenuates Cardiac Hypertrophy. *Hypertension* **2009**, *54*, 322–328. [CrossRef]
112. Kerr, D.S. Treatment of mitochondrial electron transport chain disorders: A review of clinical trials over the past decade. *Mol. Genet. Metab.* **2010**, *99*, 246–255. [CrossRef] [PubMed]
113. Ronco, P.; Debiec, H. Molecular Pathogenesis of Membranous Nephropathy. *Annu. Rev. Pathol. Mech. Dis.* **2020**, *15*, 287–313. [CrossRef] [PubMed]
114. Balasubramaniam, S.; Yaplito-Lee, J. Riboflavin metabolism: Role in mitochondrial function. *J. Transl. Genet. Genom.* **2020**, *4*, 285–306. [CrossRef]
115. Penn, A.; Lee, J.W.; Thuillier, P.; Wagner, M.; Maclure, K.M.; Menard, M.R.; Hall, L.D.; Kennaway, N.G. MELAS syndrome with mitochondrial tRNA Leu [UUR] mutation: Correlation of clinical state, nerve conduction, and muscle 31P magnetic resonance spectroscopy during treatment with nicotinamide and riboflavin. *Neurology* **1992**, *42*, 2147–2152. [CrossRef] [PubMed]
116. Bosch, A.M.; Abeling, N.G.G.M.; Ijlst, L.; Knoester, H.; Van Der Pol, W.L.; Stroomer, A.E.M.; Wanders, R.J.; Visser, G.; Wijburg, F.A.; Duran, M.; et al. Brown-Vialetto-Van Laere and Fazio Londe syndrome is associated with a riboflavin transporter defect mimicking mild MADD: A new inborn error of metabolism with potential treatment. *J. Inherit. Metab. Dis.* **2010**, *34*, 159–164. [CrossRef] [PubMed]
117. Tischner, C.; Wenz, T. Keep the fire burning: Current avenues in the quest of treating mitochondrial disorders. *Mitochondrion* **2015**, *24*, 32–49. [CrossRef]
118. Luo, K.; Yu, J.H.; Quan, Y.; Shin, Y.J.; Lee, K.E.; Kim, H.L.; Ko, E.J.; Chung, B.H.; Lim, S.W.; Yang, C.W. Therapeutic potential of coenzyme Q10 in mitochondrial dysfunction during tacrolimus-induced beta cell injury. *Sci. Rep.* **2019**, *9*, 7995. [CrossRef]
119. Ostojic, S.M. Plasma creatine as a marker of mitochondrial dysfunction. *Med. Hypotheses* **2018**, *113*, 52–53. [CrossRef]
120. Kazak, L.; Cohen, P. Creatine metabolism: Energy homeostasis, immunity and cancer biology. *Nat. Rev. Endocrinol.* **2020**, *16*, 421–436. [CrossRef]
121. Dos Santos, S.M.; Romeiro, C.F.R.; Rodrigues, C.A.; Cerqueira, A.R.L.; Monteiro, M.C. Mitochondrial Dysfunction and Alpha-Lipoic Acid: Beneficial or Harmful in Alzheimer's Disease? *Oxidative Med. Cell. Longev.* **2019**, *2019*, 8409329. [CrossRef]
122. Di Nicola, S.; Proietti, S.; Cucina, A.; Bizzarri, M.; Fuso, A. Alpha-Lipoic Acid Downregulates IL-1β and IL-6 by DNA Hypermethylation in SK-N-BE Neuroblastoma Cells. *Antioxidants* **2017**, *6*, 74. [CrossRef] [PubMed]
123. Longo, N.; Frigeni, M.; Pasquali, M. Carnitine transport and fatty acid oxidation. *Biochim. Biophys. Acta* **2016**, *1863*, 2422–2435. [CrossRef] [PubMed]
124. Morillon, A.-C.; Williamson, R.D.; Baker, P.N.; Kell, D.B.; Kenny, L.C.; English, J.A.; McCarthy, F.P.; McCarthy, C. Effect of L-Ergothioneine on the metabolic plasma profile of the RUPP rat model of pre-eclampsia. *PLoS ONE* **2020**, *15*, e0230977. [CrossRef] [PubMed]
125. Smith, E.; Ottosson, F.; Hellstrand, S.; Ericson, U.; Orho-Melander, M.; Fernandez, C.; Melander, O. Ergothioneine is associated with reduced mortality and decreased risk of cardiovascular disease. *Heart* **2019**, *106*, 691. [CrossRef] [PubMed]
126. Williamson, R.D.; McCarthy, F.P.; Manna, S.; Groarke, E.; Kell, D.B.; Kenny, L.C.; McCarthy, C.M. L-(+)-Ergothioneine Significantly Improves the Clinical Characteristics of Preeclampsia in the Reduced Uterine Perfusion Pressure Rat Model. *Hypertension* **2020**, *75*, 561–568. [CrossRef] [PubMed]

127. Nuzzo, A.M.; Camm, E.J.; Sferruzzi-Perri, A.; Ashmore, T.J.; Yung, H.-W.; Cindrova-Davies, T.; Spiroski, A.-M.; Sutherland, M.; Logan, A.; Austin-Williams, S.; et al. Placental Adaptation to Early-Onset Hypoxic Pregnancy and Mitochondria-Targeted Antioxidant Therapy in a Rodent Model. *Am. J. Pathol.* **2018**, *188*, 2704–2716. [CrossRef] [PubMed]
128. Aljunaidy, M.M.; Morton, J.S.; Kirschenman, R.; Phillips, T.; Case, C.P.; Cooke, C.-L.M.; Davidge, S.T. Maternal treatment with a placental-targeted antioxidant (MitoQ) impacts offspring cardiovascular function in a rat model of prenatal hypoxia. *Pharmacol. Res.* **2018**, *134*, 332–342. [CrossRef] [PubMed]
129. Di Meo, S.; Reed, T.T.; Venditti, P.; Victor, V.M. Role of ROS and RNS Sources in Physiological and Pathological Conditions. *Oxid. Med. Cell. Longev.* **2016**, *2016*, 1245049. [CrossRef]
130. Miller, E.W.; Tulyanthan, O.; Isacoff, E.; Chang, C.J. Molecular imaging of hydrogen peroxide produced for cell signaling. *Nat. Chem. Biol.* **2007**, *3*, 263–267. [CrossRef]
131. Itoh, Y.; Ma, F.H.; Hoshia, H.; Okaa, M.; Nodaa, K.; Ukaia, Y.; Kojimab, H.; Naganob, T.; Todaa, N. Determination and Bioimaging Method for Nitric Oxide in Biological Specimens by Diaminofluorescein Fluorometry. *Anal. Biochem.* **2000**, *287*, 203–209. [CrossRef] [PubMed]
132. Zielonka, J.; Vasquez-Vivar, J.; Kalyanaraman, B. Detection of 2-hydroxyethidium in cellular systems: A unique marker product of superoxide and hydroethidine. *Nat. Protoc.* **2007**, *3*, 8–21. [CrossRef] [PubMed]
133. Griendling, K.; Touyz, R.M.; Zweier, J.L.; Dikalov, S.; Chilian, W.; Chen, Y.-R.; Harrison, D.G.; Bhatnagar, A. Measurement of Reactive Oxygen Species, Reactive Nitrogen Species, and Redox-Dependent Signaling in the Cardiovascular System. *Circ. Res.* **2016**, *119*, e39–e75. [CrossRef] [PubMed]
134. Zhao, B.; Summers, F.A.; Mason, R.P. Photooxidation of Amplex red to resorufin: Implications of exposing the Amplex red assay to light. *Free Radic. Biol. Med.* **2012**, *53*, 1080–1087. [CrossRef] [PubMed]
135. Paital, B. A Modified Fluorimetric Method for Determination of Hydrogen Peroxide Using Homovanillic Acid Oxidation Principle. *BioMed Res. Int.* **2014**, *2014*, 342958. [CrossRef]
136. Chen, Y.; Zhong, Q.; Wang, Y.; Yuan, C.; Qin, X.; Xu, Y. Colorimetric detection of hydrogen peroxide and glucose by exploiting the peroxidase-like activity of papain. *RSC Adv.* **2019**, *9*, 16566–16570. [CrossRef]
137. Tarpey, M.M.; Wink, D.A.; Grisham, M.B. Methods for detection of reactive metabolites of oxygen and nitrogen: In vitro and in vivo considerations. *Am. J. Physiol. Integr. Comp. Physiol.* **2004**, *286*, R431–R444. [CrossRef] [PubMed]
138. Yokoyama, C.; Sueyoshi, Y.; Ema, M.; Mori, Y.; Takaishi, K.; Hisatomi, H. Induction of oxidative stress by anticancer drugs in the presence and absence of cells. *Oncol. Lett.* **2017**, *14*, 6066–6070. [CrossRef]
139. Kauffman, M.E.; Kauffman, M.K.; Traore, K.; Zhu, H.; Trush, M.A.; Jia, Z.; Li, Y.R. MitoSOX-Based Flow Cytometry for Detecting Mitochondrial ROS. *React. Oxyg. Species* **2016**, *2*, 361–370. [CrossRef] [PubMed]
140. Katerji, M.; Filippova, M.; Duerksen-Hughes, P. Approaches and Methods to Measure Oxidative Stress in Clinical Samples: Research Applications in the Cancer Field. *Oxidative Med. Cell. Longev.* **2019**, *2019*, 1279250. [CrossRef]
141. Gryglewski, R.; Moncada, S.; Palmer, R. Bioassay of prostacyclin and endothelium-derived relaxing factor (EDRF) from porcine aortic endothelial cells. *J. Cereb. Blood Flow Metab.* **1986**, *87*, 685–694. [CrossRef] [PubMed]
142. Isbell, T.S.; Koenitzer, J.R.; Crawford, J.H.; White, C.; Kraus, D.W.; Patel, R.P. Assessing NO-Dependent Vasodilatation Using Vessel Bioassays at Defined Oxygen Tensions. *Methods Enzymol.* **2005**, *396*, 553–568. [CrossRef] [PubMed]
143. Weber, D.; Davies, M.J.; Grune, T. Determination of protein carbonyls in plasma, cell extracts, tissue homogenates, isolated proteins: Focus on sample preparation and derivatization conditions. *Redox Biol.* **2015**, *5*, 367–380. [CrossRef] [PubMed]
144. Zhang, Y.; Deng, Y.; Yang, X.; Xue, H.; Lang, Y. The Relationship Between Protein S-Nitrosylation and Human Diseases: A Review. *Neurochem. Res.* **2020**, *45*, 2815–2827. [CrossRef]
145. Ichihara, K.; Fukubayashi, Y. Preparation of fatty acid methyl esters for gas-liquid chromatography. *J. Lipid Res.* **2010**, *51*, 635–640. [CrossRef] [PubMed]
146. Hughes, H.; Smith, C.; Horning, E.; Mitchell, J. High-performance liquid chromatography and gas chromatography-mass spectrometry determination of specific lipid peroxidation products in vivo. *Anal. Biochem.* **1983**, *130*, 431–436. [CrossRef]
147. Patton, G.M.; Fasulo, J.M.; Robins, S.J. Analysis of lipids by high performance liquid chromatography: Part I. *J. Nutr. Biochem.* **1990**, *1*, 493–500. [CrossRef]
148. Ferreira, R.C.; Fragoso, M.B.T.; Tenório, M.C.D.S.; Martins, A.S.D.P.; Borbely, A.U.; Moura, F.A.; Goulart, M.O.F.; De Oliveira, A.C.M. Biomarkers of placental redox imbalance in pregnancies with preeclampsia and consequent perinatal outcomes. *Arch. Biochem. Biophys.* **2020**, *691*, 108464. [CrossRef] [PubMed]
149. Karatas, F.; Karatepe, M.; Baysar, A. Determination of free malondialdehyde in human serum by high-performance liquid chromatography. *Anal. Biochem.* **2002**, *311*, 76–79. [CrossRef]
150. Fisk, H.L.; West, A.L.; Childs, C.E.; Burdge, G.C.; Calder, P.C. The Use of Gas Chromatography to Analyze Compositional Changes of Fatty Acids in Rat Liver Tissue during Pregnancy. *J. Vis. Exp.* **2014**, *85*, e51445. [CrossRef]
151. Enoiu, M.; Wellman, M.; Leroy, P.; Ziegler, J.-M.; Mitrea, N.; Siest, G. Gas and liquid chromatography-mass spectrometry of aldehydic products from lipid peroxidation. *Analusis* **2000**, *28*, 285–290. [CrossRef]
152. Cháfer-Pericás, C.; Rahkonen, L.; Sánchez-Illana, A.; Kuligowski, J.; Torres-Cuevas, I.; Cernada, M.; Cubells, E.; Nuñez-Ramiro, A.; Andersson, S.; Vento, M.; et al. Ultra high performance liquid chromatography coupled to tandem mass spectrometry determination of lipid peroxidation biomarkers in newborn serum samples. *Anal. Chim. Acta* **2015**, *886*, 214–220. [CrossRef] [PubMed]

153. Bhattacharyya, A.; Chattopadhyay, R.; Mitra, S.; Crowe, S.E. Oxidative Stress: An Essential Factor in the Pathogenesis of Gastrointestinal Mucosal Diseases. *Physiol. Rev.* **2014**, *94*, 329–354. [CrossRef] [PubMed]
154. Awooda, H.A. Pathophysiology of Cerebral Ischemia: Role of Oxidative/Nitrosative Stress. *J. Biosci. Med.* **2019**, *7*, 20–28. [CrossRef]
155. Figueroa-González, G.; Pérez-Plasencia, C. Strategies for the evaluation of DNA damage and repair mechanisms in cancer. *Oncol. Lett.* **2017**, *13*, 3982–3988. [CrossRef] [PubMed]
156. Galson, S.; Austin, C.P.; Khandekar, E.; Hudson, L.D.; Di Masi, J.A.; Califf, R.; Wagner, J.A. The failure to fail smartly. *Nat. Rev. Drug Discov.* **2021**, *20*, 259–260. [CrossRef] [PubMed]
157. Hwang, T.J.; Carpenter, D.; Lauffenburger, J.; Wang, B.; Franklin, J.M.; Kesselheim, A. Failure of Investigational Drugs in Late-Stage Clinical Development and Publication of Trial Results. *JAMA Intern. Med.* **2016**, *176*, 1826–1833. [CrossRef] [PubMed]
158. Kaye, D.K. The moral imperative to approve pregnant women's participation in randomized clinical trials for pregnancy and newborn complications. *Philos. Ethic Humanit. Med.* **2019**, *14*, 11. [CrossRef]
159. Tazhigulov, R.N.; Gurunathan, P.; Kim, Y.; Slipchenko, L.V.; Bravaya, K.B. Polarizable embedding for simulating redox potentials of biomolecules. *Phys. Chem. Chem. Phys.* **2019**, *21*, 11642–11650. [CrossRef]
160. Brodland, G.W. How computational models can help unlock biological systems. *Semin. Cell Dev. Biol.* **2015**, *47–48*, 62–73. [CrossRef] [PubMed]
161. Leemis, L.M. Computational probability applications. In Proceedings of the 2014 Winter Simulation Conference, Savannah, GA, USA, 7–10 December 2014; pp. 51–65.
162. Guimera, A.M.; Shanley, D.P.; Proctor, C.J. Modelling the role of redox-related mechanisms in musculoskeletal ageing. *Free Radic. Biol. Med.* **2019**, *132*, 11–18. [CrossRef]
163. Markevich, N.I.; Hoek, J.B. Computational modeling analysis of mitochondrial superoxide production under varying substrate conditions and upon inhibition of different segments of the electron transport chain. *Biochim. Biophys. Acta Bioenerg.* **2015**, *1847*, 656–679. [CrossRef] [PubMed]
164. Gauthier, L.D.; Greenstein, J.L.; Cortassa, S.; O'Rourke, B.; Winslow, R.L. A Computational Model of Reactive Oxygen Species and Redox Balance in Cardiac Mitochondria. *Biophys. J.* **2013**, *105*, 1045–1056. [CrossRef] [PubMed]
165. Haack, F.; Lemcke, H.; Ewald, R.; Rharass, T.; Uhrmacher, A.M. Spatio-temporal Model of Endogenous ROS and Raft-Dependent WNT/Beta-Catenin Signaling Driving Cell Fate Commitment in Human Neural Progenitor Cells. *PLoS Comput. Biol.* **2015**, *11*, e1004106. [CrossRef] [PubMed]
166. Dwivedi, G.; Gran, M.A.; Bagchi, P.; Kemp, M.L. Dynamic Redox Regulation of IL-4 Signaling. *PLoS Comput. Biol.* **2015**, *11*, e1004582. [CrossRef]
167. Hoffman, T.E.; Barnett, K.J.; Wallis, L.; Hanneman, W.H. A multimethod computational simulation approach for investigating mitochondrial dynamics and dysfunction in degenerative aging. *Aging Cell* **2017**, *16*, 1244–1255. [CrossRef] [PubMed]
168. Kembro, J.M.; Cortassa, S.; Lloyd, D.; Sollott, S.J.; Aon, M.A. Mitochondrial chaotic dynamics: Redox-energetic behavior at the edge of stability. *Sci. Rep.* **2018**, *8*, 15422. [CrossRef] [PubMed]
169. Del Olmo, M.; Kramer, A.; Herzel, H. A Robust Model for Circadian Redox Oscillations. *Int. J. Mol. Sci.* **2019**, *20*, 2368. [CrossRef] [PubMed]
170. Zhou, L.; Aon, M.A.; Almas, T.; Cortassa, S.; Winslow, R.L.; O'Rourke, B. A Reaction-Diffusion Model of ROS-Induced ROS Release in a Mitochondrial Network. *PLoS Comput. Biol.* **2010**, *6*, e1000657. [CrossRef]
171. Sridharan, S.; Layek, R.; Datta, A.; Venkatraj, J. Boolean modeling and fault diagnosis in oxidative stress response. *BMC Genom.* **2012**, *13* (Suppl. S6), S4. [CrossRef]
172. Smith, G.R.; Shanley, D.P. Computational modelling of the regulation of Insulin signalling by oxidative stress. *BMC Syst. Biol.* **2013**, *7*, 41. [CrossRef] [PubMed]
173. Padayachee, L.; Rohwer, J.M.; Pillay, C.S. The thioredoxin redox potential and redox charge are surrogate measures for flux in the thioredoxin system. *Arch. Biochem. Biophys.* **2020**, *680*, 108231. [CrossRef] [PubMed]
174. Gerken, M.; Kakorin, S.; Chibani, K.; Dietz, K.-J. Computational simulation of the reactive oxygen species and redox network in the regulation of chloroplast metabolism. *PLoS Comput. Biol.* **2020**, *16*, e1007102. [CrossRef] [PubMed]
175. Hui, W.; Young, D.A.; Rowan, A.D.; Xu, X.; Cawston, T.E.; Proctor, C.J. Oxidative changes and signalling pathways are pivotal in initiating age-related changes in articular cartilage. *Ann. Rheum. Dis.* **2016**, *75*, 449–458. [CrossRef] [PubMed]
176. Mazein, A.; Ostaszewski, M.; Kuperstein, I.; Watterson, S.; Le Novère, N.; Lefaudeux, D.; De Meulder, B.; Pellet, J.; Balaur, I.; Saqi, M.; et al. Systems medicine disease maps: Community-driven comprehensive representation of disease mechanisms. *NPJ Syst. Biol. Appl.* **2018**, *4*, 21. [CrossRef] [PubMed]
177. Barabási, A.-L.; Gulbahce, N.; Loscalzo, J. Network medicine: A network-based approach to human disease. *Nat. Rev. Genet.* **2010**, *12*, 56–68. [CrossRef] [PubMed]
178. Serhan, C.N.; Gupta, S.K.; Perretti, M.; Godson, C.; Brennan, E.; Li, Y.; Soehnlein, O.; Shimizu, T.; Werz, O.; Chiurchiù, V.; et al. The Atlas of Inflammation Resolution (AIR). *Mol. Asp. Med.* **2020**, *74*, 100894. [CrossRef] [PubMed]
179. Hucka, M.; Finney, A.; Sauro, H.M.; Bolouri, H.; Doyle, J.C.; Kitano, H.; Arkin, A.P.; Bornstein, B.J.; Bray, D.; Cornish-Bowden, A. The systems biology markup language (SBML): A medium for representation and exchange of biochemical network models. *Bioinformatics* **2003**, *19*, 524–531. [CrossRef] [PubMed]

180. Correia, Y.; Scheel, J.; Gupta, S.; Wang, K. Placental mitochondrial function as a driver of angiogenesis and placental dysfunction. *Biol. Chem.* **2021**, *402*, 887–909. [CrossRef]
181. Karlstaedt, A.; Khanna, R.; Thangam, M.; Taegtmeyer, H. Glucose 6-Phosphate Accumulates via Phosphoglucose Isomerase Inhibition in Heart Muscle. *Circ. Res.* **2020**, *126*, 60–74. [CrossRef] [PubMed]
182. D'Annibale, V.; Nardi, A.N.; Amadei, A.; D'Abramo, M. Theoretical Characterization of the Reduction Potentials of Nucleic Acids in Solution. *J. Chem. Theory Comput.* **2021**, *17*, 1301–1307. [CrossRef]
183. Yu, J.; Horsley, J.R.; Abell, A.D. Unravelling electron transfer in peptide-cation complexes: A model for mimicking redox centres in proteins. *Phys. Chem. Chem. Phys.* **2020**, *22*, 8409–8417. [CrossRef] [PubMed]
184. Coimbra, J.; Bras, N.; Fernandes, P.; Rangel, M.; Ramos, M.J. A computational study on the redox properties and binding affinities of iron complexes of hydroxypyridinones. *J. Mol. Model.* **2019**, *25*, 172. [CrossRef] [PubMed]
185. Pereira, E.J.; Smolko, C.M.; Janes, K.A. Computational Models of Reactive Oxygen Species as Metabolic Byproducts and Signal-Transduction Modulators. *Front. Pharmacol.* **2016**, *7*, 457. [CrossRef] [PubMed]
186. Touré, V.; Zobolas, J.; Kuiper, M.; Vercruysse, S. Causal Builder: Bringing the MI2CAST causal interaction annotation standard to the curator. *Database* **2021**, *2021*, baaa107. [CrossRef] [PubMed]

International Journal of
Molecular Sciences

MDPI

Article

Heterogenous Differences in Cellular Senescent Phenotypes in Pre-Eclampsia and IUGR following Quantitative Assessment of Multiple Biomarkers of Senescence

Samprikta Manna [1,2], Colm J. Mc Elwain [3], Gillian M. Maher [2,4], Marta Giralt Martín [3], Andrea Musumeci [3], Fergus P. McCarthy [1,2,*] and Cathal McCarthy [3]

1 Department of Obstetrics and Gynaecology, Cork University Maternity Hospital, University College Cork, T12 YE02 Cork, Ireland
2 INFANT Research Centre, University College Cork, T12 K8AF Cork, Ireland
3 Department of Pharmacology and Therapeutics, Western Gateway Building, University College Cork, T12 XF62 Cork, Ireland
4 School of Public Health, Western Gateway Building, University College Cork, T12 XF62 Cork, Ireland
* Correspondence: fergus.mccarthy@ucc.ie

Abstract: Premature ageing of the placenta in pregnancy outcomes is associated with the persistent presence of oxidative stress and placental insufficiency reducing its functional capacity. In this study, we investigated cellular senescence phenotypes of pre-eclampsia and IUGR pregnancies by simultaneously measuring several biomarkers of senescence. Maternal plasma and placental samples were collected at term gestation from nulliparous women undergoing pre-labour elective caesarean section with pre-eclampsia without intrauterine growth restriction (PE; n = 5), pre-eclampsia associated with intrauterine growth restriction (n = 8), intrauterine growth restriction (IUGR < 10th centile; n = 6), and age-matched controls (n = 20). Placental absolute telomere length and senescence gene analysis was performed by RTqPCR. The expression of cyclin-dependent kinase inhibitors (p21 and p16) was determined by Western blot. Senescence-associated secretory phenotypes (SASPs) were evaluated in maternal plasma by multiplex ELISA assay. Placental expression of senescence-associated genes showed significant increases in CHEK1, PCNA, PTEN, CDKN2A, and CCNB-1 ($p < 0.05$) in pre-eclampsia, while TBX-2, PCNA, ATM, and CCNB-1 expression were evident ($p < 0.05$) and were significantly decreased in IUGR compared with controls. Placental p16 protein expression was significantly decreased in pre-eclampsia only compared with controls ($p = 0.028$). IL-6 was significantly increased in pre-eclampsia (0.54 pg/mL ± 0.271 vs. 0.3 pg/mL ± 0.102; $p = 0.017$) while IFN-γ was significantly increased in IUGR (4.6 pg/mL ± 2.2 vs. 2.17 pg/mL ± 0.8; $p = 0.002$) compared with controls. These results provide evidence of premature senescence in IUGR pregnancies, and while cell cycle checkpoint regulators are activated in pre-eclampsia, the cellular phenotype is one of cell repair and subsequent proliferation rather than progression to senescence. The heterogeneity of these cellular phenotypes highlights the complexity of characterising cellular senescence and may equally be indicative of the differing pathophysiological insults unique to each obstetric complication.

Keywords: placental ageing; pre-eclampsia; intrauterine growth restriction; cellular senescence

check for updates

Citation: Manna, S.; Mc Elwain, C.J.; Maher, G.M.; Giralt Martín, M.; Musumeci, A.; McCarthy, F.P.; McCarthy, C. Heterogenous Differences in Cellular Senescent Phenotypes in Pre-Eclampsia and IUGR following Quantitative Assessment of Multiple Biomarkers of Senescence. *Int. J. Mol. Sci.* **2023**, *24*, 3101. https://doi.org/10.3390/ijms24043101

Academic Editor: Hiten D. Mistry

Received: 15 November 2022
Revised: 20 December 2022
Accepted: 18 January 2023
Published: 4 February 2023

Copyright: © 2023 by the authors. Licensee MDPI, Basel, Switzerland. This article is an open access article distributed under the terms and conditions of the Creative Commons Attribution (CC BY) license (https://creativecommons.org/licenses/by/4.0/).

1. Introduction

Pre-eclampsia (PE) is a gestational hypertensive disorder which affects 3–5% of pregnancies worldwide and clinically manifests as maternal de-novo hypertension and associated maternal organ dysfunction including uteroplacental dysfunction [1]. Intrauterine growth restriction (IUGR) can be defined as a rate of foetal growth which is below the normal growth potential, i.e., between the 10th and 90th percentile as per the gestational age [2,3]. IUGR affects 13.7 million babies born yearly with low birth weight [2]. Pre-eclampsia is associated with impaired spiral artery modelling and poor placental perfusion

resulting in aberrant redox signalling and an induction of oxidative stress [4]. Additionally, systemic inflammation and endothelial dysfunction are pathogenic mediators of pre-eclampsia which account for a myriad of maternal multi-organ damage and poor long-term maternal cardiovascular outcomes [4].

Senescence can be defined as a cellular defensive mechanism triggered in response to multiple external or internal stressors resulting in irreversible cell cycle arrest [5]. In conditions of exaggerated oxidative stress, persistent impairment of redox balance and subsequent DNA damage result in the initiation of a premature senescence phenotype [6]. Additionally, telomere shortening can trigger cellular senescence, but senescence is equally evident independent of telomere shortening [7,8]. Premature cellular senescence can be classified by activation of a DNA damage response pathway and its associated signaling kinases which culminate in the stimulation of cell cycle inhibitors, such as p16INK4a, p21/p53, and p27, reduction in cellular proliferation, and loss of Lamin-B activity, which is a marker of the altered enlarged and flattened morphology of senescent cells [9]. Moreover, the accumulation of mitochondrial DNA (mtDNA), as a result of ROS inducing damage and strand breaks, has been associated with premature onset of ageing in both in vivo and in vitro models, with higher susceptibility to mtDNA mutagenesis [10,11]. Activation of a senescence-associated secretory phenotype (SASP) incorporating a core set of cytokines, such as IL-6, IL-8, IL-13, IGFBPs, and MMPs, results in accumulated senile cells creating a pro-inflammatory microenvironment that indicates establishment of senescence [12]. The phenotypes of premature cellular senescence are highly heterogeneous and often differ depending on the initial stressor [13]. Senescence-specific gene expression has been extensively studied. Genes such as PTEN and CDKN2A regulate cellular senescence by acting through the p16/p19^{Arf} pathway, whereas CHEK-1, PCNA, and CCNB-1 are modulated by DNA damage response and halt in cell cycle progression [14–16]. Additionally, there is no single universal biomarker that specifically identifies senescence, hence a combination of multiple markers when simultaneously present are used to confirm senescence [17].

The placenta along with maternal decidua normally exhibits progressive senescence closer to term parturition [18]. A recent review by Cox and Redman, which explored evidence of placental ageing through cellular senescence accompanied by morphological changes including modulation of pro-inflammatory phenotypes, highlighted excessive oxidative stress as a driver of premature placental ageing in adverse pregnancy conditions including pre-eclampsia [19]. This stress-induced senescence is proposed to result from poor placental perfusion, resulting in increased ROS generation that subsequently engages biochemical pathways which disrupt cell cycle progression in addition to accelerating the activation of pro-inflammatory cytokines and chemokines, which form part of the senescence-associated secretory phenotype (SASP) [13,19].

In adverse pregnancy outcomes, such as pre-eclampsia and IUGR, impaired placentation and the subsequent burden of placental oxidative stress may trigger a premature senescence phenotype leading to early parturition and pre-term delivery of the foetus [13]. Syncytiotrophoblasts show features characteristic of senescent cells, including the biomarker senescence-associated β-galactosidase (SA-β-gal), together with increased expression of the cyclin kinases inhibitors p16 and p21, and p53 [20]. To date, the association between altered telomere length and placental pathogenesis of both pre-eclampsia and IUGR has been somewhat contradictory, with some publications reporting no significant difference in placental telomere length between pre-eclampsia and healthy uncomplicated pregnancies [21,22]. Contrarily, IUGR has consistently been reported to have lower placental telomerase activity and shorter telomere length when compared with healthy uncomplicated pregnancies [23–26]. In this study, we examined multiple biomarkers of senescence in pre-eclampsia and IUGR and investigated if premature senescence phenotypes were congruent across both placental pathologies.

2. Results

2.1. Study Demographics

Thirty-nine participants all delivered by pre-labour caesarean section were recruited in Cork University Maternity Hospital between 2019 and 2021. These were grouped as: pre-eclampsia (n = 5), pre-eclampsia associated with intrauterine growth restriction (n = 8), IUGR (<10th centile) (n = 6), and maternal age-matched controls (n = 20) as shown in Table 1. There were no significant differences in maternal age, maternal BMI, or gestational age for all groups when compared with controls. While there was no significant difference in maternal mean arterial blood pressure (MAP) during the first trimester (~11 weeks) across study groups, MAP at 20–24 weeks was significantly elevated in both pre-eclampsia (96.4 ± 6.8 vs. 83.2 ± 8.4; $p = 0.04$) and pre-eclampsia associated with IUGR (97.2 ± 12.7 vs. 83.2 ± 8.4; $p = 0.027$) compared with controls. Foetal birthweight in pre-eclampsia associated with IUGR (1926 g ± 527.7 g vs. 3218 g ± 359.6 g, $p < 0.0001$) and IUGR (2585 g ± 401.8 g vs. 3218 g ± 359.6 g, $p = 0.035$) were significantly reduced when compared with controls. Similarly, foetal individualised customised centile (ICC) was significantly reduced in pre-eclampsia associated with IUGR (2.1 ± 2.5, $p = 0.0001$) and IUGR (8.11 ± 1.9, $p = 0.0034$) pregnancies compared with controls.

Table 1. Patient characteristics in study cohort. Data are represented as mean ± SD. Mean arterial pressure has been calculated as MAP = [Systolic BP + (2 × Diastolic BP)]/3.

	Pre-Eclampsia	Pre-Eclampsia Associated with IUGR	IUGR (>10th Centile)	Term Controls
	(n = 5)	(n = 8)	(n = 6)	(n = 20)
Maternal				
Mean Age (years ± SD)	38.6 ± 5.2	33.35 ± 3.1	33.67 ± 3.1	33.7 ± 4.40
Mean BMI (kg/m^2 ± SD)	29.9 ± 9.6	27.7 ± 3.7	25.31 ± 3.5	24.4 ± 5.4
Mean Arterial Blood Pressure (mmHg) ± SD (10–12 weeks)	92 ± 10.4	77.08 ± 32.4	84.61 ± 5.2	86.3 ± 8.9
Mean Arterial Blood Pressure (mmHG) ± SD (20–24 weeks)	96.4 ± 6.8 *	97.2 ± 12.7 *	83.1 ± 7.2	83.2 ± 8.4
Foetal				
Mean Gestational Age at delivery (weeks ± SD)	36 ± 1.9	34.6 ± 2.7	32.43 ± 13.1	38 ± 0.7
Mean birth weight (grams ± SD)	2878 ± 788.5	1926 ± 572.7 *	2585 ± 401.8 *	3218 ± 359.6
Foetal Sex (M = Male; F = Female)	F = 3 M = 2	F = 3 M = 5	F = 4 M = 2	F = 10 M = 10
Foetal Individualised Customised Centile (±SD)	46.8 ± 39.3	2.15 ± 2.5 *	8.11 ± 1.9 *	40.4 ± 21.9

* Statistically significant compared with controls with $p < 0.05$.

2.2. Senescence Associated Gene Expression Showed Substantial Differences in the Placental Tissue between Pre-Eclampsia and IUGR

Initially, using a Human Cellular Senescence Profiler Array with subsequent real-time PCR validation, multiple senescence-associated genes including cell cycle regulatory and DNA damage response (DDR) genes CHEK-1, CCNB-1, CDKN2A, ATM, GLB-1, ID-1, IGFBP-5, PCNA, PTEN, SOD-2, and TBX2 were examined in placental tissue samples. Of the panel of senescent-associated genes examined, there was a significant increase in placental expression of checkpoint kinase 1 (CHEK-1) (4.9-fold ± 0.94, $p = 0.008$; Figure 1A), Cyclin B (CCNB-1) (3-fold ± 1.4, $p = 0.036$; Figure 1B), prolifer-

ating cell nuclear antigen (PCNA) (6.9-fold ± 1.3, p = 0.013; Figure 1C), cyclin kinase CDKN2A (3.5-fold ± 0.9, p = 0.007; Figure 1D), and phosphatase-tensin homolog PTEN (12.8-fold ± 1, p = 0,003; Figure 1E) levels in pre-eclampsia. The expression of transcription factor TBX2 (0.3-fold ± 0.9, p = 0.016; Figure 1F), ataxia kinase ATM (0.7 ± 1.26, p = 0.02; Figure 1G), cyclin B CCNB-1 (0.3-fold ± 1.7, p = 0.028; Figure 1B), and DNA repair gene PCNA (0.2-fold ± 0.9, p = 0.046; Figure 1C) were significantly decreased in this IUGR, when compared with controls. There was no significant difference amongst the other senescence-associated genes between study groups (Supplementary Figure S1).

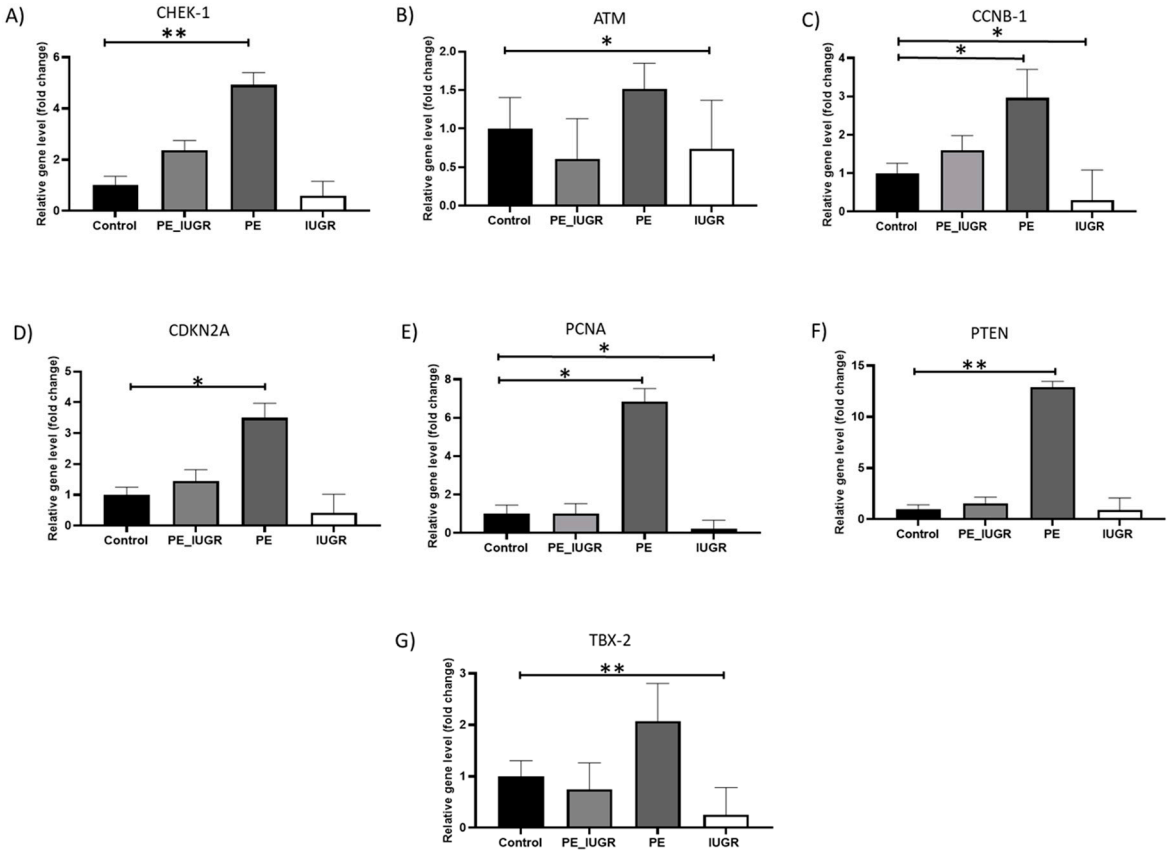


Figure 1. Senescence-associated gene expression in placental tissue in pre-eclampsia and IUGR. (**A**) CHEK-1 expression in pre-eclampsia only was significantly elevated (p = 0.006); (**B**) ATM was significantly decreased in IUGR (p = 0.02); (**C**) CCNB-1 was significantly elevated in pre-eclampsia only (p = 0.028), whereas it was significantly reduced in IUGR (p = 0.036); (**D**) CDKN2A was significantly elevated in pre-eclampsia only (p = 0.012); (**E**) PCNA was significantly elevated in pre-eclampsia only (p = 0.014), whereas it was significantly decreased in IUGR (p = 0.04); (**F**) PTEN was significantly elevated in pre-eclampsia only (p = 0.005); (**G**) TBX-2 was significantly reduced in IUGR only (p = 0.005). All measurements were relative gene expression compared with controls. Data are mean fold change compared with controls at level 1 ± SD, $p < 0.05$; p-value < 0.05, it is flagged with one star (*) and p-value < 0.01, it is flagged with two stars (**).

2.3. Absolute Telomere Length in Placental Tissue Revealed No Significant Changes across All Subgroups

While placental absolute telomere length (aTL) was longer in pre-eclampsia (9.05 kbp ± 5.7 vs. 5.9 kbp ± 4.5) and pre-eclampsia associated with IUGR (6.84 kbp ± 3.2 vs. 5.9 kbp ± 4.5) compared with controls, this increase was not statistically significant (Figure 2). Adjusting for the variables maternal age, maternal BMI, gestational age, foetal individualised customised centile (ICC), and foetal sex, pre-eclampsia had a 4.88 kbp (95% CI: −0.391, 10.15) longer telomere length; additionally, pre-eclampsia associated with IUGR had a 1.65 kbp (95% CI: −3.53, 6.88) increase in telomere length compared with controls (Table 2).

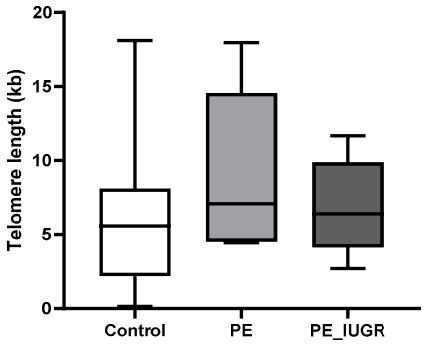


Figure 2. Absolute telomere length in pre-eclampsia. aTL in placental tissue was not significantly altered in pre-eclampsia or pre-eclampsia associated with IUGR compared with controls. Data are represented as mean aTL ± SD, $p < 0.05$.

Table 2. Crude and adjusted association between placental absolute telomere length (aTL) in kbp for pre-eclampsia and pre-eclampsia associated with IUGR, compared with controls. [a] Adjusted for maternal age, BMI, gestational age, ICC, and foetal sex. Abbreviations: 95% CI = 95% confidence interval, BMI = body mass index, ICC = individualised customised centile, aTL = absolute telomere length.

Exposure Groups	Crude Estimate (95% CI)	Adjusted Estimate [a] (95% CI)
Pre-eclampsia only (N = 5)	3.191 (−1.288, 7.671)	4.882 (−0.391, 10.155)
Pre-eclampsia with IUGR (N = 8)	0.986 (−2.761, 4.734)	1.675 (−3.527, 6.878)

When absolute telomere length was examined in IUGR (4.96 kbp ± 3.5 vs. 5.9 kbp ± 4.5), there was no significant change compared with controls (Figure 3). Adjusting for the variables maternal age, maternal BMI, gestational age, foetal individualised customised centile (ICC), and foetal sex, placental aTL was shorter in IUGR compared with controls but this reduction in aTL was not statistically significant (−1.5 kbp 95% CI: −6.852, 3.807) (Table 3).

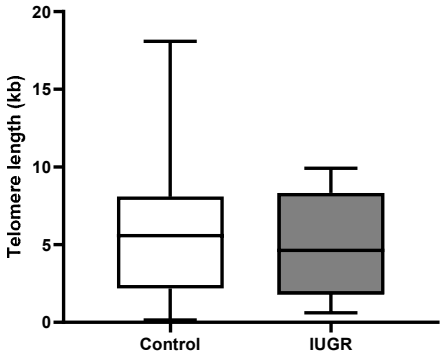


Figure 3. Absolute telomere length in IUGR. ATL in placental tissue showed no significant changes in IUGR compared with controls. Data are represented as mean aTL ± SD, $p < 0.05$.

Table 3. The Crude and adjusted association between placental absolute telomere length (aTL) in kbp for IUGR placentas compared with controls. [a] Adjusted for maternal age, BMI, gestational age, ICC, and foetal sex. Abbreviations: 95% CI = 95% confidence interval, BMI = body mass index, ICC = individualised customised centile, aTL = absolute telomere length.

Exposure Groups	Crude Estimate (95% CI)	Adjusted Estimate [a] (95% CI)
IUGR < 10th centile (N = 6)	−0.895 (−5.214, 3.423)	−1.522 (−6.852, 3.807)

2.4. Placental Expression of Cyclin-Dependent Kinase Inhibitor p16 Is Decreased in Pre-Eclampsia Only

Cell cycle arrest resulting from upregulation of cyclin-dependent kinase inhibitors, p21 and p16, is a classical feature of senescence. p16 protein expression was significantly decreased in pre-eclampsia placentas when compared with controls (p = 0.031) (Figure 4A), while this reduction in p16 expression was not evident in placental tissue from pre-eclampsia associated with IUGR compared with controls (Figure 4B). Additionally, there was no significant difference in p16 protein expression in IUGR (Figure 4C) when compared with controls.

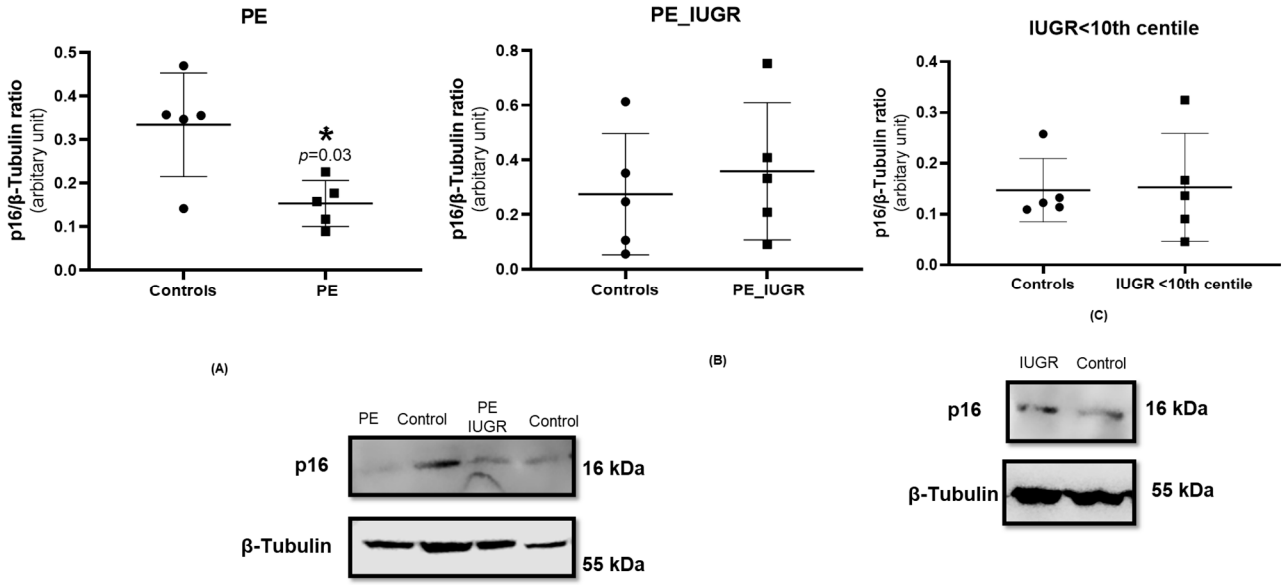


Figure 4. Western blot for placental p16 protein expression performed using the standard SDS-page gel method for (**A**) pre-eclampsia only, n = 5, (**B**) pre-eclampsia associated with IUGR, n = 5, and (**C**) IUGR, n = 5. Statistical analysis with Wilcoxon matched-pairs signed rank test with two-tailed test, * $p < 0.05$ vs. control placenta. p-value < 0.05, it is flagged with one star (*). Protein expression of p16 was normalised to the expression of the housekeeping reference protein β-tubulin.

There was no significant difference in p21 protein expression in pre-eclampsia (Figure 5A) and pre-eclampsia associated with IUGR (Figure 5B) when compared with controls. Similarly, there was no significant difference in p21 protein expression in IUGR (Figure 5C) when compared with controls.

A reduction in Lamin B1 protein expression has been detected in senescent cells and is induced by various triggers including cell replication and oncogene activation. Lamin B1 has roles in DNA replication and cell cycle progression in addition to maintaining nuclear envelope integrity. Expression of Lamin B1 was not significantly different in pre-eclampsia groups (Supplementary Figure S2a,b) or IUGR (Figure S2c), respectively, when compared with controls. We compared absolute mtDNA copy numbers in placental tissue for pre-eclampsia subgroups and IUGR, comparing them to controls (Supplementary Figure S3). Even though all groups showed increases in placental mtDNA copy numbers, both pre-eclampsia subgroups and IUGR failed to reach statistical significance compared with controls.

2.5. Senescence Associated Secretory Phenotypes in Maternal Plasma Reveal Different Cytokine Profiles in Pre-Eclampsia and IUGR

Senescence-associated secretory phenotypes (SASP) consist of a core panel of inflammatory cytokines and mediators including, interferon-γ (INF-γ), interleukins (IL-13, IL-6, IL-8), monocyte chemoattractant protein-1 (MCP-1) and macrophage inflammatory protein 1 alpha (MIP-1α), and matrix metalloproteinase-3 (MMP-3) [27–29]. Of the original panel of

seven SASP markers, IL-6 was significantly increased in pre-eclampsia only when compared with controls (0.59 pg/mL ± 0.2 vs. 0.29 pg/mL ± 0.1; $p = 0.017$) (Figure 6A). Expression of the remaining six SASP markers did not differ significantly between pre-eclampsia and controls (Figure 6B–G). There was no significant difference in the expression of any SASP marker between PE/IUGR when compared with pre-eclampsia or when compared with controls. Interferon-γ expression was significantly increased (4.6 pg/mL ± 2.2 vs. 2.17 pg/mL ± 0.8; $p = 0.002$) (Figure 7E) in IUGR when compared with controls. There were no other significant changes observed in SASP markers compared with controls (Figure 7B–G).

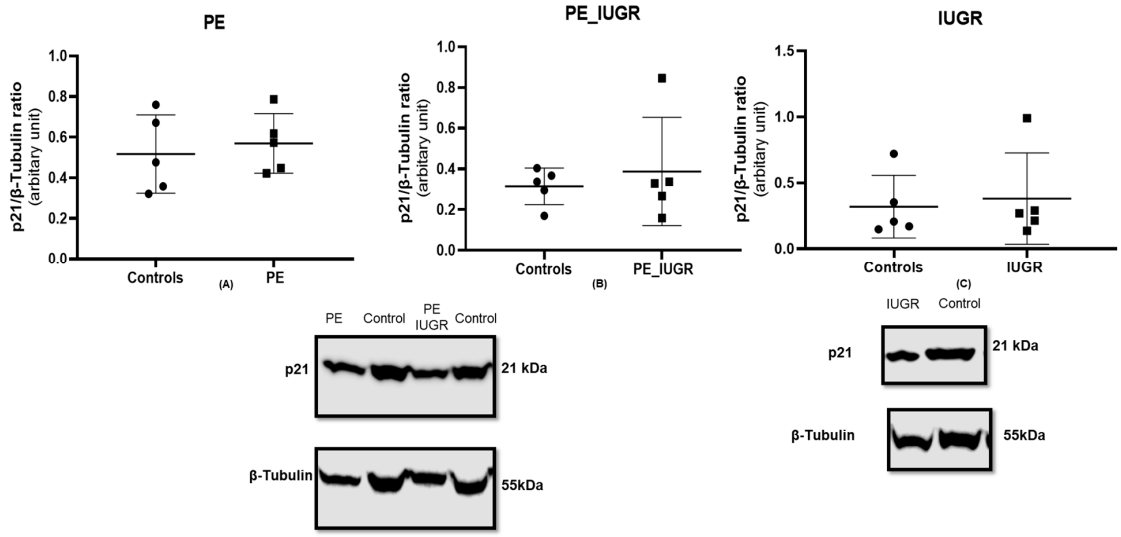


Figure 5. p21 expression in placental tissue using the standard SDS-page gel method; (**A**) pre-eclampsia, n = 5, (**B**) pre-eclampsia associated with IUGR, n = 5, and (**C**) IUGR >10th centile, n = 5. Statistical analysis with Wilcoxon matched-pairs signed rank test with two-tailed test. Protein expression of p21 was normalised to the expression of the housekeeping reference protein B-tubulin.

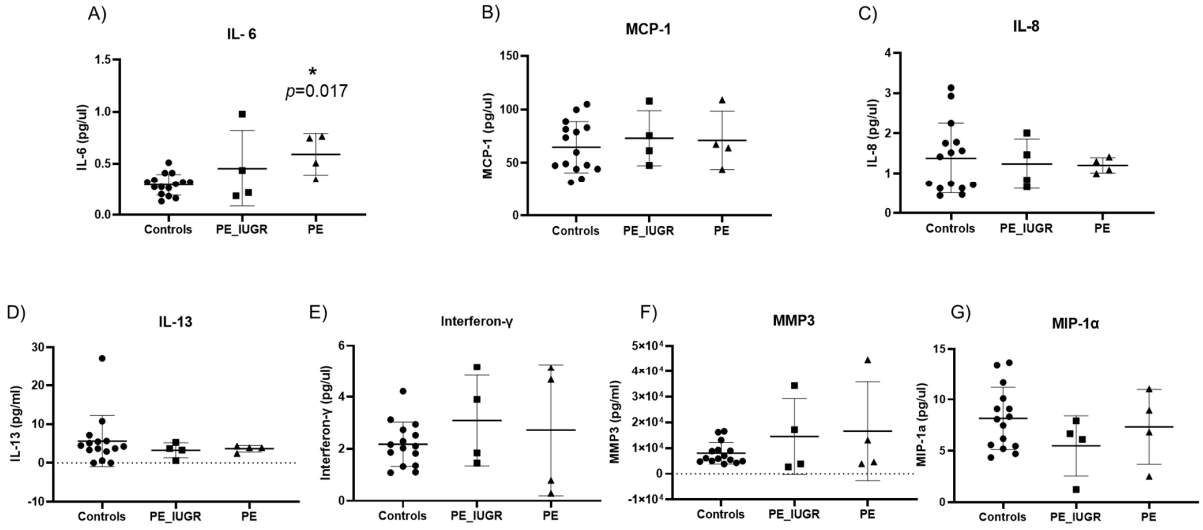


Figure 6. Senescence-associated secretory phenotypes (SASP) in pre-eclampsia with or without intrauterine growth restriction. (**A**) IL-6 was significantly increased in maternal plasma of pre-eclampsia only pregnancies ($p = 0.017$) when compared with controls. All other cytokines: (**B**) MCP-1, (**C**) IL-8, (**D**) IL-13, (**E**) Interferon-γ, (**F**) MMP-3, and (**G**) MIP-1α showed no significant differences between pre-eclampsia subgroups compared with controls. Data are represented as mean ± SD, $p < 0.05$; p-value < 0.05, it is flagged with one star (*).

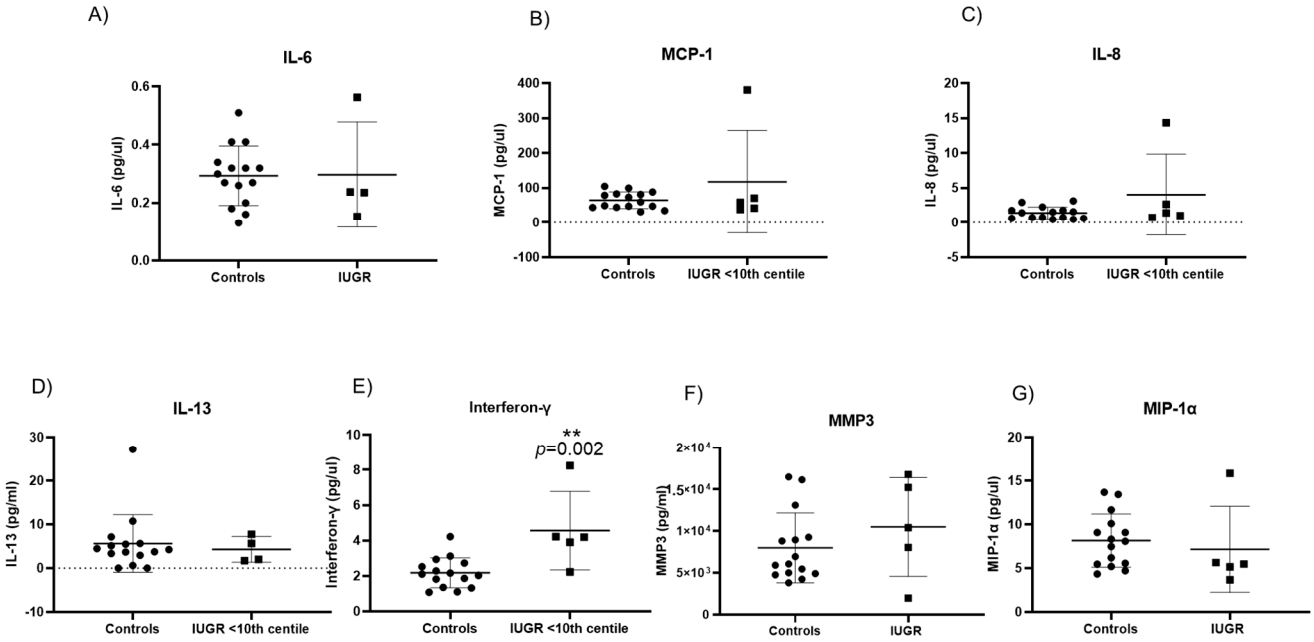


Figure 7. Senescence-associated secretory phenotypes (SASP) evident in intrauterine growth restriction IUGR: (**E**) Interferon-γ ($p = 0.002$) of IUGR pregnancies were significantly increased in maternal plasma when compared with controls. All other cytokines: (**A**) IL-6, (**B**) MCP-1, (**C**) IL-8, (**D**) IL-13, (**F**) MMP-3, and (**G**) MIP-1α showed no significant difference when compared with controls. Data are represented as mean ± SD, $p < 0.05$; $p = 0.002$ flagged as two stars (**).

3. Discussion

Premature placental ageing has been associated with adverse pregnancy outcomes such as pre-eclampsia, intrauterine growth restriction, and stillbirth. High oxidative stress and an inadequate antioxidant defense lends to impaired redox signalling and oxidative damage [30]. While the physiological triggers of senescence in vivo are not fully understood, evidence of hypoperfusion coupled with high oxidative stress and placental insufficiency may orchestrate a multistep cellular senescence response. This study sought to assess the evidence of placental ageing resulting from cellular senescence in both pre-eclampsia and IUGR by evaluating multiple biomarkers of senescence. Cellular senescence is defined as a state of terminal proliferation, accompanied by characteristic metabolic and pro-inflammatory changes. Our results showed a significant decrease in senescence-associated genes ATM, CCNB-1, PCNA, and TBX2 in IUGR placentas, and a significant increase in maternal circulating interferon-γ levels when compared with controls. On the other hand, in pre-eclampsia, we showed a significant increase in placental expression of CHEK-1, CCNB-1, PCNA, CDKN2A, and PTEN accompanied with a significant reduction in p16 placental protein levels, and a significant increase in maternal circulating IL-6 levels when compared with controls. There was no significant difference in absolute placental telomere length between any study groups, when compared with controls. The graphical abstract portrays the molecular individualities observed in PE and IUGR cohorts.

Initially, the expression of senescent-associated genes was characterised in placental tissue in pre-eclampsia, pre-eclampsia associated with IUGR, and IUGR. There was a significant increase in key regulators of DNA repair and checkpoint surveillance, namely CHEK-1 and PTEN in pre-eclampsia only, with an additional increase in expression of markers promoting proliferation (PCNA and CCNB1). Proliferating cell nuclear antigen (PCNA) is a proliferation marker, which regulates the replication complex formation and has a role in DNA metabolism, affecting DNA damage repair (DDR) pathways [31]. CHEK-1 is a DDR signalling kinase which arrests cell cycle to allow DNA repair, while the phosphatase and tensin homolog (PTEN), which had the largest increase in expression, equally controls DNA repair and regulates G1/S and G2/M checkpoints in the cell cycle

to ensure appropriate cell survival. Cells experiencing DNA damage due to external or internal stressors act through the ATM/ATR pathway; CCNB-1 is downregulated leading to DNA damage-induced cellular senescence via G2 cell cycle arrest [32]. Despite the induction of the DDR, potentially facilitating DNA repair due to exaggerated oxidative stress in pre-eclampsia, the significant increase in CCNB1, a marker of G2 phase in the cell cycle, and PCNA suggest that placental cells respond to oxidative damage by promoting necessary DNA repair and re-enter the cell cycle rather than inducing senescence.

Conversely, in IUGR, there was a significant reduction in ataxia telangiectasia mutated (ATM), cell proliferation markers CCNB1, and PCNA gene expression in placental tissue compared with controls. ATM is activated by double strand break (DSB) in an attempt to repair the damage incurred [33]. TBX-2, a transcription repressor of senescence which plays an important role in the regulation of cellular fate, maintaining cellular proliferation [34–37], was also significantly reduced in IUGR only. The deficiency in the capacity to mount an appropriate DNA damage response, aligned with a significant reduction in cell proliferation, may be indicative of premature terminal differentiation of trophoblasts at a mean GA of <33 weeks, signifying a premature cellular senescence phenotype in this subgroup. While there was no significant difference in placental expression of senescence-associated genes in the pre-eclampsia associated with IUGR group, there was an obvious heterogeneity in expression of all genes, which was reflective of the individual signature profiles of pre-eclampsia and IUGR.

Lysosomal-β-galactosidase (GLB-1) has been associated as a source of senescence-associated β galactosidase (SA- β-gal) activity, a marker of cellular senescence [38]. ID-1 has been shown to act through the p16ink4a/retinoblastoma (pRb) tumour-suppressor pathway, affecting telomerase activity [39]. Insulin-like growth factor binding protein (IGBP-5) has been shown to regulate apoptosis through DDR and upregulation of the p53 pathway [40]. Superoxide dismutase 2 (SOD-2) is an antioxidant enzyme providing defense against oxidative stress [41]. There were no significant differences seen for genes GLB-1, ID-1, IGFBP-5, and SOD-2 (Supplementary Material).

Increased oxidative stress and accumulation of double-stranded DNA damage foci located at telomeres, irrespective of telomerase activity, may simulate premature senescence [42]. In this study, we evaluated absolute telomere length (aTL) in our study groups controlling for maternal age, BMI, gestational age, foetal sex, and foetal ICC. There was no significant difference in absolute telomere length across the three groups compared with controls. However, we showed notable variances in telomere length: pre-eclampsia with/without IUGR had longer placental aTL, whereas IUGR had a much shorter aTL. Multiple studies have failed to show any association between pre-eclampsia and placental telomere length [19,20,37]; however, IUGR has been associated with decreased placental telomerase activity and shorter telomere length when compared with healthy uncomplicated pregnancies [23–26]. Biron-Shental et al. reported shorter telomere length for pre-eclampsia and IUGR placentas compared with controls [23]. Despite the lack of evidence of significant telomere shortening in this study, it is worth noting that premature senescence can be induced independently of telomere length.

Activation of cyclin-dependent kinase (CDK) inhibitors including p16 and p21 are critical mediators of cell cycle progression and hence have important regulatory roles in promoting premature senescence. Both p21 and p16 are negative modulators of cell proliferation in part due to their control of cyclin-CDK activity in response to extracellular and intracellular signals. In this study, placental expression of p21 was not significantly different in any of the study groups compared with controls. However, placental expression of p16 was significantly reduced in pre-eclampsia only, with no change evident in pre-eclampsia associated with IUGR or IUGR alone. Conversely, placental CDKN2A gene expression was significantly increased in pre-eclampsia in our study. The CDKN2A gene locus is responsible for production of p16INK4a and p19Arf, which act as cell cycle inhibitors and are expressed at higher levels in senescent cells [15,43]; however, despite the increase in gene expression, a subsequent increase in p16 activity was not evident in pre-eclampsia. Previ-

ous studies have reported higher p16 expression in term placental syncytiotrophoblasts, equally evident in pre-eclampsia and IUGR [20,44–46]. The reduction of p16 expression in pre-eclampsia in this study suggests that although the evident DDR response mediated via upregulation of CHEK-1 may trigger activation of G2 checkpoint with resultant arrest of cell cycle, entry towards a senescent phenotype is not fully stabilised, which may allow cells to re-enter the cell cycle and maintain cellular mitotic property, which is supported by increase in PCNA and CCNB1 expression in pre-eclampsia [47]. As there was no change in either p21 or p16 expression in pre-eclampsia associated with IUGR or IUGR, it would suggest that growth restriction may induce the alternative senescent phenotype.

Nuclear lamins are structural proteins lining the lamina or inner nuclear envelope surface [48], which provide structural integrity. Senescent cells display enlarged flattened profiles with a distorted nuclear envelope resulting from a reduction in Lamin B1 expression. Loss of Lamin B1 has been reported as a robust marker of cellular senescence but the exact pathway initiating Lamin B1 reduction remains unclear; furthermore, loss of Lamin B1 precedes activation of the SA-β-Gal pathway and the accumulation of SASPs [49]. In this study, there was no significant difference in the placental expression of Lamin B1 in any of the study groups, which suggests that there is no overt disruption to the nuclear structure in response to DDR. Exaggerated oxidative stress in senescent cells has been associated with the accumulation of dysfunctional mitochondria. We subsequently looked for evidence of mitochondrial dysfunction by measuring mtDNA in placental tissue and reported no significant changes across the three study groups. Mitochondrial dysfunction has been associated with disease severity and complexity. Mitochondrial DNA (mtDNA) copy numbers is a measure of mtDNA levels per cell and is associated with mitochondrial enzyme activity and adenosine triphosphate (ATP) production. Mitochondria, as the source of ROS production, plays a pivotal role in the pathophysiology of placental hypoperfusion diseases as well as cellular dysfunction and ageing. Multiple publications have shown increased mtDNA in maternal circulation and cord blood in pregnancies affected by PE, PE/IUGR, and IUGR [50,51]. Contrarily, the quality of mitochondrial quality and mtDNA copy number is significantly reduced in ageing cells [52–54]. This study did not provide evidence of increased mtDNA copy numbers in PE, PE associated with IUGR, and IUGR, and based on this surrogate marker of mitochondrial dysfunction, we propose that mitochondrial dysfunction is not a significant contributor to the heterogeneity evident in our study.

One of the hallmarks of senescence is the ability of growth-arrested cells to remain metabolically active and secrete SASPs, which affects events within the cell and causes senile modulation of the extra-cellular environment as well as neighbouring cells [55]. Our results showed significant increase in IL-6 levels in maternal plasma in women with pre-eclampsia only. Multiple reports have shown that increased IL-6 levels are associated with both severity and onset of pre-eclampsia [56,57]. Despite its well-defined role as an inflammatory mediator, IL-6 also has a major role in cell cycle regulation through activation of the janus kinase-signal transducer and activator of transcription (JAK/STAT) and mitogen-activated protein kinase (MAPK) signal transduction pathways [34,58]. The classical MAPK/ERK family is an intercellular checkpoint for cellular mitogenesis, controlling cell cycle progression (34). In this study, the increase in IL-6 may be more indicative of systemic maternal inflammation in pre-eclampsia rather than a consequence of a senescent phenotype in pre-eclampsia. Interferon gamma (IFN-γ), a pro-inflammatory cytokine, has been reported to induce cellular senescence through the p53-dependent DNA damage signaling pathway [48,59,60]. Our results show significant elevation of circulating IFN-γ in IUGR pregnancies, which may be indicative of premature cellular senescence. Similar to all other senescent biomarkers, there was no significant difference in circulating cytokines in the pre-eclampsia associated with IUGR study group.

The approach of measuring multiple senescence markers in pre-eclampsia, pre-eclampsia associated with IUGR, and IUGR (<10th centile) is a significant strength of this study as it facilitated a complete investigation of premature senescence phenotypes in these

obstetric complications. To date, identifying the physiological stressors of senescence in vivo are not fully elucidated. Despite the limitation of small sample numbers in this study, it is evident that there are significant differences in cell proliferation/senescence phenotypes in pre-eclampsia and IUGR. The heterogeneity of these phenotypes in pre-eclampsia and IUGR alone are equally different in pre-eclampsia associated with IUGR, where an altered molecular profile was evident with no obvious evidence of cellular senescence or altered proliferation.

4. Materials and Methods

4.1. Study Design

Subjects were recruited as part of the COMRADES study, a non-interventional cohort study of nulliparous singleton pregnancies with the aim of characterising placental premature senescence in pre-eclampsia (PE) and intrauterine growth restriction (IUGR). Patients were recruited from Cork University Maternity Hospital, Ireland, between 2019 and 2021. The COMRADES study was conducted according to the guidelines laid down in the Declaration of Helsinki, and all the procedures were approved by the Clinical Research Ethics Committee of the Cork Teaching (ECM4 (ff) 04/12/18), and all women provided written informed consent. After receiving consent from participants, samples were collected from nulliparous, singleton pregnancies undergoing pre-labour caesarean section. Pre-eclampsia was defined according to the ISSHP 2018 guidelines: BP $\geq$ 140 mm Hg systolic or $\geq$90 mm Hg diastolic measured on at least 2 occasions at least 4 h, associated with proteinuria (>300 mg protein on 24-h collection, urine protein creatinine > 30 mg/mmol or +3 dipstick) [1]. Pre-eclampsia participants were subdivided into two groups: associated with growth restriction (n = 8) and no growth restriction (n = 5). IUGR was defined according to RCOG as estimated foetal weight less than 10th centile for gestational age [61]. IUGR-recruited pregnancies were classified as <10th centile (n = 6). Matched selected controls (n = 20) were collected from healthy pregnant women who had uncomplicated pregnancies, which were defined as pregnancies not affected by pre-eclampsia or IUGR and delivered at >37 weeks. Controls were matched with the pre-eclampsia and IUGR cases for maternal age.

4.2. Sample Collection

Maternal term plasma was collected in EDTA vacutainers (BD, Ireland) and centrifuged at 2400$\times$ *g* for 10 min at 4 °C. Placental tissue was sectioned within 20 min of delivery, with 5 tissue sections (2–4 cm diameter each) taken from identified regions across the placenta. All samples were snap frozen in liquid nitrogen and stored at −80 °C [62].

4.3. Placental DNA Extraction and Absolute Telomere Length Quantification

Genomic DNA was extracted from 10 mg of placental tissue using the DNeasy Blood and Tissue kit (Qiagen, Dublin, Ireland) in accordance with the manufacturer's instructions. Absolute quantification of telomere was determined using the ScienCell qPCR Kit (#8918). The telomere primer set recognizes and amplifies telomere sequences, while the single copy reference (SCR) primer set recognizes and amplifies a 100 bp-long region on human chromosome 17 and serves as a reference for data normalisation. All reactions with genomic DNA sample (5 µg/µL) sample were performed in duplicate, and template controls were included in each run. Reference genomic DNA was used as an internal control. Comparative ΔΔCq (Quantification Cycle Value) method was used with manufacturer made standard curve for quantification using Cq (Quantification Cycle) values of telomere qPCR (TEL) and single copy reference qPCR (SCR) obtained for the genomic DNA samples as per the manufacturer's instructions.

4.4. Absolute Quantification of Placental mtDNA

Mitochondrial DNA (mtDNA) extraction was done following the methodology described by Williamson et al. (2018) [50]. Real-time PCR was used for mtDNA assessment

through StepOne Plus Detection system (Applied Biosciences, Waltham, MA, USA) using Taqman probes for mtDNA hMitoF5, hMitoR5 [50,63]. A standard curve was used to determine the absolute quantification of mtDNA and represented as copies/mL [63,64].

4.5. Isolation of RNA and Real-Time PCR Analysis

Placental tissue was mechanically homogenised in Trizol Reagent (Invitrogen™ Thermo Fisher Scientific, Dublin, Ireland) using TissueLyser II (Qiagen, Manchester, UK) and RNA was isolated which was subsequently purified using the Qiagen RNeasy® Plus Mini (#74134) clean-up protocol according to the manufacturer's instructions. cDNA synthesis was performed using the Superscript IV Double-Stranded cDNA Synthesis Kit (Invitrogen™ Thermo Fisher Scientific, Ireland). Initial assessment for senescence-associated genes were performed using the RT2 Profiler PCR Array Gene Expression for senescence-associated genes in 96-well plates (Cat no. PAHS-050Z, Qiagen, Ireland). The samples from each group were pooled into and loaded on each 96-well plate. In total, there were 4 groups: PE, PE associated with IUGR, IUGR, and controls, and 4 plates were subjected to Real Time qPCR on the Applied Biosciences StepOne Plus Detection System. The qPCR Assays used in PCR Arrays enables 96 genes in a 96-well plate to be simultaneously analysed using the RT^2 SYBR Green q PCR Array System protocol. Relative quantification was performed using data analysis web portal (GeneGlobe, Germantown, MD, USA, https://geneglobe.qiagen.com/us/ (accessed on 17 January 2023)) to calculate the fold change using $2^{-\Delta\Delta CT}$ formula, where ΔCT is calculated between gene of interest (GOI) and an average of reference genes (HKG), followed by ΔΔCT calculations. Five HKG genes, namely ACTB, B2M, GAPDH, RPLP0, and HPRT1 were included in each PCR plate as internal controls. Eleven genes were selected for validation based on the significant differences between groups when compared with controls, obtained from the RT2 profiler PCR Array: CHEK1, CCNB1, PCNA, PTEN, CDKN2A, ATM, TBX2, GLB1, ID1, IGFBP5, and SOD2. Taqman probes were used for genes of interest (Applied Biosciences, Westmeath, Ireland). The Tata box protein (TBP) gene was used as an internal control with SYBR green primers (Supplementary Table S1). Standard relative PCR quantification was performed to validate the fold change using $2^{-\Delta\Delta CT}$) formula. Taqman probes were used for genes of interest (Applied Biosciences, Ireland). The Tata box protein (TBP) gene was used as an internal control (Eurofins, Dublin, Ireland; Supplementary Table S1). TBP has been shown to be most stable in placental tissue, ensuring sensitivity and specificity of gene expression profile [65]. Real-time PCR was performed on the Applied Biosciences StepOne Plus Detection System. Standard relative PCR quantification was performed using the manufacturer's instruction, and fold change was calculated based on relative change between GOI and the internal standard.

4.6. Protein Isolation and Western Blot

Placental tissue (50 mg) was homogenized using TissueLyser II (Qiagen, Hilden, Germany) and protein was isolated using tetraethylammonium bicarbonate buffer (Sigma-Aldrich, Co., Wicklow, Ireland) supplemented with a phosphatase inhibitor (PhosSTOP™, Roche, Dublin, Ireland) and protease inhibitor (Roche, Ireland). PE, PE associated with IUGR, and IUGR cases were age-matched with controls. We separated 35 µg of protein by SDS-PAGE on a 10% TRIS polyacrylamide-glycine gel (Bio-Rad Laboratories, Kildare, Ireland) and transferred it to a methanol-activated PVDF membrane (Amersham™ Hybond® Sigma-Aldrich, Wicklow, Ireland). Membranes were blocked in 5% BSA for 1 h at room temperature and incubated overnight at 4 °C with primary antibodies; anti-p21 (1:1000 Abcam; ab109520, Cambridge, UK), anti-Lamin B1 (1:1000 Cell Signaling; E6M5T, Cork, Ireland), anti-p16 (1:500 Abcam; ab108349, Cambridge, UK), or anti-GAPDH (1:3000 Cell Signaling #2118, Brennan and company, Dublin, Ireland), and anti- β-Tubulin (1:2000 Cell Signaling, #2146, Brenan and company, Dublin, Ireland), secondary anti-rabbit IgG, HRP-linked antibody (1:2000 Cell Signaling Technology, #7074 Brenan and company, Dublin, Ireland). GAPDH and β-Tubulin were selected as internal reference control proteins for western blots because of their stability and expression within placental cells [66–68].

After overnight incubation membranes were washed and incubated at room temperature for 1 h with anti-HRP secondary antibody, membranes were washed in TBS-T and developed using Pierce™ ECL Western Blotting Substrate, Thermo Fischer Scientific, Biosciences, Dublin, Ireland) and LICOR Odyssey image analyzer. Densitometry was performed using LICOR Image Studio Lite Version 5.2. After the protein of interest was developed, membranes were stripped of residual primary and secondary antibodies using a Western Blot Stripping Buffer (Thermo Fischer, Dublin, Ireland) for 30 min with gentle shaking and re-probed with a suitable housekeeper protein.

4.7. Senescence Associated Secretory Phenotypes (SASP) Analysis

Maternal plasma samples were analysed for SASP using the Human U-Plex kit IL-6, IL-8, IL-13, IL-1α, IFN-γ, MCP-1, and MIP-1α (MesoScale Discovery, Rockville, MD, USA; K15067L) and the Human MMP3 Ultra-sensitive kit (MesoScale Discovery, Rockville, MD, USA; K15034CL). All samples were prepared using the manufacturer's instructions and plates analysed on the Meso QuickPlex SQ 120 platform. Results were generated as calculated concentration means on the Mesoscale (MSD) Discovery Workbench 4.0 assay analysis software. The MSD analysis software determines individual cytokine concentrations from electro chemiluminescent signals via backfitting to the calibration curve.

4.8. Statistical Analysis

All data are expressed as mean $\pm$ SD, or fold change relative to control. Analysis was performed using GraphPad Prism 8.3. Comparisons of data between cases and controls were performed using a one-way ANOVA. The two-tailed Wilcoxon matched-pairs signed rank test was used for statistical analysis of Figures 4 and 5. p values < 0.05 were considered as statistically significant. Linear regression analysis, comparing absolute telomere length in cases and controls, was done using STATA 14.2.

5. Conclusions

In the study we showed that despite activation of DNA damage response, in part as a result of oxidative damage, the cellular phenotype signified a re-entry into the cell cycle and continued cell proliferation rather than progressing towards senescence in pre-eclampsia. IUGR presented a completely different phenotype, which was representative of significantly reduced cell proliferation and premature terminal differentiation which may progress towards senescence. Despite the assessment of multiple biomarkers of senescence in this study, it highlights the complexity in distinguishing between cellular subtypes at a single cell level as well as between cell types, which may be reflective of the differing orchestrators of placental pathogenesis of these pathologies.

Limitations

This study has a limited sample size which might influence the overall conclusions drawn in this study. The limited sample number was due to a stringent study design of recruiting nulliparous women with PE, PE associated with IUGR, and IUGR cohorts. Only term pregnancies were included in the study to overcome the effect of premature births. Women with IUGR pregnancies that were complicated by any foetal abnormalities were excluded.

Supplementary Materials: The supporting information can be downloaded at: https://www.mdpi.com/article/10.3390/ijms24043101/s1.

Author Contributions: S.M. performed all experiments and data analysis described above and wrote the first draft of the manuscript. S.M., C.J.M.E. and A.M. carried out patient recruitment, and sample collection and preparation. G.M.M. performed statistical analysis for absolute Telomere length using software STATA version14.2. M.G.M. assisted with laboratory experiments. C.M. and F.P.M. supervised and designed the study and made significant contributions to the manuscript. All authors edited the manuscript. All authors have read and agreed to the published version of the manuscript.

Funding: This project is funded by the European Union's Horizon 2020 research and innovation program under Marie Skłodowska-Curie Actions Innovative Training Network (H2020-MSCA-ITN 2017), Grant No. 765274, acronym iPLACENTA (http://www.iplacenta.eu, accessed on 17 January 2023).

Institutional Review Board Statement: All procedures performed in studies involving human participants were in accordance with the ethical standards of the institutional and/or national research committee and with the 1964 Helsinki Declaration and its later amendments or comparable ethical standards. All the procedures were approved by the Clinical Research Ethics Committee of the Cork Teaching Hospitals (ECM4 (ff) 04/12/18), and all women provided written informed consent.

Informed Consent Statement: Informed consent was obtained from all individual participants included in the study.

Data Availability Statement: Anonymised data that support the findings of this study are available from the corresponding author, upon reasonable request. Anonymised data will be made available in a suitable open access repository in the future.

Conflicts of Interest: The authors declare no conflict of interest.

References

1. Brown, M.A.; Magee, L.A.; Kenny, L.C.; Karumanchi, S.A.; McCarthy, F.P.; Saito, S.; Hall, D.R.; Warren, C.E.; Adoyi, G.; Ishaku, S. The hypertensive disorders of pregnancy: ISSHP classification, diagnosis & management recommendations for international practice. *Pregnancy Hypertens.* **2018**, *13*, 291–310. [CrossRef]
2. Sharma, D.; Shastri, S.; Farahbakhsh, N.; Sharma, P. Intrauterine growth restriction—Part 1. *J. Matern.-Fetal Neonatal Med.* **2016**, *29*, 3977–3987. [CrossRef] [PubMed]
3. Sharma, D.; Shastri, S.; Sharma, P. Intrauterine Growth Restriction: Antenatal and Postnatal Aspects. *Clin. Med. Insights Pediatr.* **2016**, *10*, 67–83. [CrossRef] [PubMed]
4. Paauw, N.D.; Lely, A.T. Cardiovascular Sequels During and After Preeclampsia. *Adv. Exp. Med. Biol.* **2018**, *1065*, 455–470. [CrossRef]
5. Calcinotto, A.; Kohli, J.; Zagato, E.; Pellegrini, L.; Demaria, M.; Alimonti, A. Cellular Senescence: Aging, Cancer, and Injury. *Physiol. Rev.* **2019**, *99*, 1047–1078. [CrossRef] [PubMed]
6. Sultana, Z.; Maiti, K.; Dedman, L.; Smith, R. Is there a role for placental senescence in the genesis of obstetric complications and fetal growth restriction? *Am. J. Obstet. Gynecol.* **2018**, *218*, S762–S773. [CrossRef]
7. Ho, J.H.; Chen, Y.-F.; Ma, W.-H.; Tseng, T.-C.; Chen, M.-H.; Lee, O.K. Cell Contact Accelerates Replicative Senescence of Human Mesenchymal Stem Cells Independent of Telomere Shortening and p53 Activation: Roles of Ras and Oxidative Stress. *Cell Transplant.* **2011**, *20*, 1209–1220. [CrossRef]
8. Morgan, R.G.; Ives, S.J.; Walker, A.E.; Cawthon, R.M.; Andtbacka, R.H.I.; Noyes, D.; Lesniewski, L.A.; Richardson, R.S.; Donato, A.J. Role of arterial telomere dysfunction in hypertension: Relative contributions of telomere shortening and telomere uncapping. *J. Hypertens.* **2014**, *32*, 1293–1299. [CrossRef]
9. Farr, J.N.; Khosla, S. Cellular senescence in bone. *Bone* **2019**, *121*, 121–133. [CrossRef]
10. Chocron, E.S.; Munkácsy, E.; Pickering, A.M. Cause or casualty: The role of mitochondrial DNA in aging and age-associated disease. *Biochim. Biophys. Acta (BBA)-Mol. Basis Dis.* **2019**, *1865*, 285–297. [CrossRef]
11. Sanchez-Contreras, M.; Kennedy, S.R. The Complicated Nature of Somatic mtDNA Mutations in Aging. *Front. Aging* **2022**, *2*, 805126. [CrossRef] [PubMed]
12. Birch, J.; Gil, J. Senescence and the SASP: Many therapeutic avenues. *Genes Dev.* **2020**, *34*, 1565–1576. [CrossRef] [PubMed]
13. Manna, S.; McCarthy, C.; McCarthy, F.P. Placental Ageing in Adverse Pregnancy Outcomes: Telomere Shortening, Cell Senescence, and Mitochondrial Dysfunction. *Oxidative Med. Cell. Longev.* **2019**, *2019*, 3095383. [CrossRef] [PubMed]
14. Feringa, F.M.; Raaijmakers, J.A.; Hadders, M.A.; Vaarting, C.; Macurek, L.; Heitink, L.; Krenning, L.; Medema, R.H. Persistent repair intermediates induce senescence. *Nat. Commun.* **2018**, *9*, 3923. [CrossRef]
15. Baker, D.J.; Jin, F.; van Deursen, J.M. The yin and yang of the Cdkn2a locus in senescence and aging. *Cell Cycle* **2008**, *7*, 2795–2802. [CrossRef]
16. Poehlmann, A.; Habold, C.; Walluscheck, D.; Reissig, K.; Bajbouj, K.; Ullrich, O.; Hartig, R.; Gali-Muhtasib, H.; Diestel, A.; Roessner, A.; et al. Cutting edge: Chk1 directs senescence and mitotic catastrophe in recovery from G_2 checkpoint arrest. *J. Cell. Mol. Med.* **2011**, *15*, 1528–1541. [CrossRef]
17. González-Gualda, E.; Baker, A.G.; Fruk, L.; Muñoz-Espín, D. A guide to assessing cellular senescence in vitro and in vivo. *FEBS J.* **2021**, *288*, 56–80. [CrossRef]
18. Wijaya, J.C.; Khanabdali, R.; Georgiou, H.M.; Kalionis, B. Ageing in human parturition: Impetus of the gestation clock in the decidua†. *Biol. Reprod.* **2020**, *103*, 695–710. [CrossRef]
19. Cox, L.S.; Redman, C. The role of cellular senescence in ageing of the placenta. *Placenta* **2017**, *52*, 139–145. [CrossRef]
20. Chuprin, A.; Gal, H.; Biron-Shental, T.; Biran, A.; Amiel, A.; Rozenblatt, S.; Krizhanovsky, V. Cell fusion induced by ERVWE1 or measles virus causes cellular senescence. *Genes Dev.* **2013**, *27*, 2356–2366. [CrossRef]

21. Harville, E.W.; Williams, M.A.; Qiu, C.-F.; Mejia, J.; Risques, R.A. Telomere length, pre-eclampsia, and gestational diabetes. *BMC Res. Notes* **2010**, *3*, 113. [CrossRef] [PubMed]
22. Broady, A.J.; Loichinger, M.H.; Ahn, H.J.; Davy, P.M.C.; Allsopp, R.C.; Bryant-Greenwood, G.D. Protective proteins and telomere length in placentas from patients with pre-eclampsia in the last trimester of gestation. *Placenta* **2017**, *50*, 44–52. [CrossRef] [PubMed]
23. Biron-Shental, T.; Sukenik Halevy, R.; Goldberg-Bittman, L.; Kidron, D.; Fejgin, M.D.; Amiel, A. Telomeres are shorter in placental trophoblasts of pregnancies complicated with intrauterine growth restriction (IUGR). *Early Hum. Dev.* **2010**, *86*, 451–456. [CrossRef] [PubMed]
24. Biron-Shental, T.; Sukenik-Halevy, R.; Sharon, Y.; Goldberg-Bittman, L.; Kidron, D.; Fejgin, M.D.; Amiel, A. Short telomeres may play a role in placental dysfunction in preeclampsia and intrauterine growth restriction. *Am. J. Obstet. Gynecol.* **2010**, *202*, 381.e1–381.e7. [CrossRef]
25. Biron-Shental, T.; Sadeh-Mestechkin, D.; Amiel, A. Telomere homeostasis in IUGR placentas—A review. *Placenta* **2016**, *39*, 21–23. [CrossRef]
26. Toutain, J.; Prochazkova-Carlotti, M.; Cappellen, D.; Jarne, A.; Chevret, E.; Ferrer, J.; Idrissi, Y.; Pelluard, F.; Carles, D.; Maugey-Laulon, B.; et al. Reduced Placental Telomere Length during Pregnancies Complicated by Intrauterine Growth Restriction. *PLoS ONE* **2013**, *8*, e54013. [CrossRef]
27. Alimbetov, D.; Davis, T.; Brook, A.J.; Cox, L.S.; Faragher, R.G.; Nurgozhin, T.; Zhumadilov, Z.; Kipling, D. Suppression of the senescence-associated secretory phenotype (SASP) in human fibroblasts using small molecule inhibitors of p38 MAP kinase and MK2. *Biogerontology* **2016**, *17*, 305–315. [CrossRef]
28. Hudgins, A.D.; Tazearslan, C.; Tare, A.; Zhu, Y.; Huffman, D.; Suh, Y. Age- and Tissue-Specific Expression of Senescence Biomarkers in Mice. *Front. Genet.* **2018**, *9*, 59. [CrossRef]
29. Coppé, J.P.; Desprez, P.Y.; Krtolica, A.; Campisi, J. The senescence-associated secretory phenotype: The dark side of tumor suppression. *Annu. Rev. Pathol.* **2010**, *5*, 99–118. [CrossRef]
30. Raijmakers, M.T.M.; Dechend, R.; Poston, L. Oxidative Stress and Preeclampsia. *Hypertension* **2004**, *44*, 374–380. [CrossRef]
31. Tanase, D.M.; Gosav, E.M.; Radu, S.; Ouatu, A.; Rezus, C.; Ciocoiu, M.; Costea, C.F.; Floria, M. Arterial Hypertension and Interleukins: Potential Therapeutic Target or Future Diagnostic Marker? *Int. J. Hypertens.* **2019**, *2019*, 3159283. [CrossRef] [PubMed]
32. Nakayama, Y.; Yamaguchi, N. Chapter Seven—Role of Cyclin B1 Levels in DNA Damage and DNA Damage-Induced Senescence. In *International Review of Cell and Molecular Biology*; Jeon, K.W., Ed.; Academic Press: Cambridge, MA, USA, 2013; Volume 305, pp. 303–337.
33. Maréchal, A.; Zou, L. DNA damage sensing by the ATM and ATR kinases. *Cold Spring Harb. Perspect. Biol.* **2013**, *5*, a012716. [CrossRef] [PubMed]
34. Moran, D.M.; Mattocks, M.A.; Cahill, P.A.; Koniaris, L.G.; McKillop, I.H. Interleukin-6 mediates G(0)/G(1) growth arrest in hepatocellular carcinoma through a STAT 3-dependent pathway. *J. Surg. Res.* **2008**, *147*, 23–33. [CrossRef] [PubMed]
35. Zhang, W.; Liu, H.T. MAPK signal pathways in the regulation of cell proliferation in mammalian cells. *Cell Res.* **2002**, *12*, 9–18. [CrossRef] [PubMed]
36. Freeman, D.J.; McManus, F.; Brown, E.A.; Cherry, L.; Norrie, J.; Ramsay, J.E.; Clark, P.; Walker, I.D.; Sattar, N.; Greer, I.A. Short-and long-term changes in plasma inflammatory markers associated with preeclampsia. *Hypertension* **2004**, *44*, 708–714. [CrossRef] [PubMed]
37. Seif, F.; Khoshmirsafa, M.; Aazami, H.; Mohsenzadegan, M.; Sedighi, G.; Bahar, M. The role of JAK-STAT signaling pathway and its regulators in the fate of T helper cells. *Cell Commun. Signal.* **2017**, *15*, 23. [CrossRef]
38. Wagner, J.; Damaschke, N.; Yang, B.; Truong, M.; Guenther, C.; McCormick, J.; Huang, W.; Jarrard, D. Overexpression of the novel senescence marker β-galactosidase (GLB1) in prostate cancer predicts reduced PSA recurrence. *PLoS ONE* **2015**, *10*, e0124366. [CrossRef]
39. Alani, R.M.; Young, A.Z.; Shifflett, C.B. Id1 regulation of cellular senescence through transcriptional repression of p16/Ink4a. *Proc. Natl. Acad. Sci. USA* **2001**, *98*, 7812–7816. [CrossRef]
40. Sanada, F.; Taniyama, Y.; Muratsu, J.; Otsu, R.; Shimizu, H.; Rakugi, H.; Morishita, R. IGF Binding Protein-5 Induces Cell Senescence. *Front. Endocrinol.* **2018**, *9*, 53. [CrossRef] [PubMed]
41. Velarde, M.C.; Flynn, J.M.; Day, N.U.; Melov, S.; Campisi, J. Mitochondrial oxidative stress caused by Sod2 deficiency promotes cellular senescence and aging phenotypes in the skin. *Aging* **2012**, *4*, 3–12. [CrossRef]
42. Hewitt, G.; Jurk, D.; Marques, F.D.M.; Correia-Melo, C.; Hardy, T.; Gackowska, A.; Anderson, R.; Taschuk, M.; Mann, J.; Passos, J.F. Telomeres are favoured targets of a persistent DNA damage response in ageing and stress-induced senescence. *Nat. Commun.* **2012**, *3*, 708. [CrossRef] [PubMed]
43. He, S.; Sharpless, N.E. Senescence in Health and Disease. *Cell* **2017**, *169*, 1000–1011. [CrossRef] [PubMed]
44. Davy, P.; Nagata, M.; Bullard, P.; Fogelson, N.; Allsopp, R. Fetal growth restriction is associated with accelerated telomere shortening and increased expression of cell senescence markers in the placenta. *Placenta* **2009**, *30*, 539–542. [CrossRef] [PubMed]
45. Nuzzo, A.M.; Giuffrida, D.; Masturzo, B.; Mele, P.; Piccoli, E.; Eva, C.; Todros, T.; Rolfo, A. Altered expression of G1/S phase cell cycle regulators in placental mesenchymal stromal cells derived from preeclamptic pregnancies with fetal-placental compromise. *Cell Cycle* **2017**, *16*, 200–212. [CrossRef]

46. Gao, Q.; Zhu, X.; Chen, J.; Mao, C.; Zhang, L.; Xu, Z. Upregulation of P53 promoted G1arrest and apoptosis in human umbilical cord vein endothelial cells from preeclampsia. *J. Hypertens.* **2016**, *34*, 1380. [CrossRef]
47. Müllers, E.; Silva Cascales, H.; Burdova, K.; Macurek, L.; Lindqvist, A. Residual Cdk1/2 activity after DNA damage promotes senescence. *Aging Cell* **2017**, *16*, 575–584. [CrossRef]
48. Wang, S.; Zhou, M.; Lin, F.; Liu, D.; Hong, W.; Lu, L.; Zhu, Y.; Xu, A. Interferon-γ Induces Senescence in Normal Human Melanocytes. *PLoS ONE* **2014**, *9*, e93232. [CrossRef]
49. Freund, A.; Laberge, R.-M.; Demaria, M.; Campisi, J. Lamin B1 loss is a senescence-associated biomarker. *Mol. Biol. Cell* **2012**, *23*, 2066–2075. [CrossRef]
50. Williamson, R.D.; McCarthy, F.P.; Khashan, A.S.; Totorika, A.; Kenny, L.C.; McCarthy, C. Exploring the role of mitochondrial dysfunction in the pathophysiology of pre-eclampsia. *Pregnancy Hypertens* **2018**, *13*, 248–253. [CrossRef]
51. Novielli, C.; Mandò, C.; Tabano, S.; Anelli, G.M.; Fontana, L.; Antonazzo, P.; Miozzo, M.; Cetin, I. Mitochondrial DNA content and methylation in fetal cord blood of pregnancies with placental insufficiency. *Placenta* **2017**, *55*, 63–70. [CrossRef]
52. Foote, K.; Reinhold, J.; Yu, E.P.K.; Figg, N.L.; Finigan, A.; Murphy, M.P.; Bennett, M.R. Restoring mitochondrial DNA copy number preserves mitochondrial function and delays vascular aging in mice. *Aging Cell* **2018**, *17*, e12773. [CrossRef] [PubMed]
53. Spano, L.; Etain, B.; Meyrel, M.; Hennion, V.; Gross, G.; Laplanche, J.L.; Bellivier, F.; Marie-Claire, C. Telomere length and mitochondrial DNA copy number in bipolar disorder: Identification of a subgroup of young individuals with accelerated cellular aging. *Transl. Psychiatry* **2022**, *12*, 135. [CrossRef] [PubMed]
54. Castellani, C.A.; Longchamps, R.J.; Sumpter, J.A.; Newcomb, C.E.; Lane, J.A.; Grove, M.L.; Bressler, J.; Brody, J.A.; Floyd, J.S.; Bartz, T.M.; et al. Mitochondrial DNA copy number can influence mortality and cardiovascular disease via methylation of nuclear DNA CpGs. *Genome Med.* **2020**, *12*, 84. [CrossRef] [PubMed]
55. Kumari, R.; Jat, P. Mechanisms of Cellular Senescence: Cell Cycle Arrest and Senescence Associated Secretory Phenotype. *Front. Cell Dev. Biol.* **2021**, *9*, 645593. [CrossRef] [PubMed]
56. Xiao, J.P.; Yin, Y.X.; Gao, Y.F.; Lau, S.; Shen, F.; Zhao, M.; Chen, Q. The increased maternal serum levels of IL-6 are associated with the severity and onset of preeclampsia. *Cytokine* **2012**, *60*, 856–860. [CrossRef] [PubMed]
57. Udenze, I.; Amadi, C.; Awolola, N.; Makwe, C.C. The role of cytokines as inflammatory mediators in preeclampsia. *Pan Afr. Med. J.* **2015**, *20*, 219. [CrossRef]
58. Kojima, H.; Kunimoto, H.; Inoue, T.; Nakajima, K. The STAT3-IGFBP5 axis is critical for IL-6/gp130-induced premature senescence in human fibroblasts. *Cell Cycle* **2012**, *11*, 730–739. [CrossRef]
59. Kim, K.S.; Kang, K.W.; Seu, Y.B.; Baek, S.-H.; Kim, J.-R. Interferon-γ induces cellular senescence through p53-dependent DNA damage signaling in human endothelial cells. *Mech. Ageing Dev.* **2009**, *130*, 179–188. [CrossRef]
60. Hubackova, S.; Kucerova, A.; Michlits, G.; Kyjacova, L.; Reinis, M.; Korolov, O.; Bartek, J.; Hodny, Z. IFNγ induces oxidative stress, DNA damage and tumor cell senescence via TGFβ/SMAD signaling-dependent induction of Nox4 and suppression of ANT2. *Oncogene* **2016**, *35*, 1236–1249. [CrossRef]
61. Suhag, A.; Berghella, V. Intrauterine Growth Restriction (IUGR): Etiology and Diagnosis. *Curr. Obstet. Gynecol. Rep.* **2013**, *2*, 102–111. [CrossRef]
62. Burton, G.J.; Sebire, N.J.; Myatt, L.; Tannetta, D.; Wang, Y.L.; Sadovsky, Y.; Staff, A.C.; Redman, C.W. Optimising sample collection for placental research. *Placenta* **2014**, *35*, 9–22. [CrossRef] [PubMed]
63. Ajaz, S.; Czajka, A.; Malik, A. Accurate measurement of circulating mitochondrial DNA content from human blood samples using real-time quantitative PCR. *Methods Mol. Biol.* **2015**, *1264*, 117–131. [CrossRef] [PubMed]
64. Li, B.; Kalinowski, P.; Kim, B.; Pauls, A.D.; Poburko, D. Emerging methods for and novel insights gained by absolute quantification of mitochondrial DNA copy number and its clinical applications. *Pharmacol. Ther.* **2022**, *232*, 107995. [CrossRef] [PubMed]
65. Meller, M.; Vadachkoria, S.; Luthy, D.A.; Williams, M.A. Evaluation of housekeeping genes in placental comparative expression studies. *Placenta* **2005**, *26*, 601–607. [CrossRef] [PubMed]
66. Lanoix, D.; St-Pierre, J.; Lacasse, A.A.; Viau, M.; Lafond, J.; Vaillancourt, C. Stability of reference proteins in human placenta: General protein stains are the benchmark. *Placenta* **2012**, *33*, 151–156. [CrossRef] [PubMed]
67. Li, S.-C.; Lan, K.-C.; Hung, H.-N.; Huang, W.-T.; Lai, Y.-J.; Cheng, H.-H.; Tsai, C.-C.; Huang, K.-L.; You, H.-L.; Hsu, T.-Y. HSPA4 Is a Biomarker of Placenta Accreta and Enhances the Angiogenesis Ability of Vessel Endothelial Cells. *Int. J. Mol. Sci.* **2022**, *23*, 5682. [CrossRef]
68. McIntyre, K.R.; Vincent, K.M.M.; Hayward, C.E.; Li, X.; Sibley, C.P.; Desforges, M.; Greenwood, S.L.; Dilworth, M.R. Human placental uptake of glutamine and glutamate is reduced in fetal growth restriction. *Sci. Rep.* **2020**, *10*, 16197. [CrossRef]

Disclaimer/Publisher's Note: The statements, opinions and data contained in all publications are solely those of the individual author(s) and contributor(s) and not of MDPI and/or the editor(s). MDPI and/or the editor(s) disclaim responsibility for any injury to people or property resulting from any ideas, methods, instructions or products referred to in the content.

Clinical Proteomics

RESEARCH

Open Access

A proteomic profile of the healthy human placenta

Samprikta Manna[1*†], Julia Scheel[5†], Aisling Noone[4], Colm J. McElwain[2], Caitriona Scaife[6], Shailendra Gupta[5], Jane English[3,4†], Cathal McCarthy[2†] and Fergus P. McCarthy[1,3†]

Abstract

Background: The placenta remains one of the least studied organs within the human body. Yet, placental dysfunction has been associated with various pregnancy complications leading to both maternal and fetal death and long-term health consequences. The aim of this study was to characterise the protein networks of healthy term placental sub-anatomical regions using label free quantification mass spectrometry.

Methods: Three healthy placentae were sampled at five sample sites and each biopsy was dissected into maternal-, middle-, and fetal- sub-anatomical regions. Quadrupole-orbitrap mass spectrometer was used in data dependant analysis mode to identify 1859 unique proteins before detailed differential expression between regions.

Results: Protein profiling identified 1081, 1086, and 1101 proteins in maternal, middle, and fetal sub-anatomical regions respectively. Differentially expressed proteins were identified considering the effect between sample site location and sub-anatomical region on protein expression. Of these, 374 differentially expressed proteins (Two-way ANOVA adjusted p-value < 0.05, HSD Tukey adjusted p-value 0.05) were identified between sample site locations and sub-anatomical regions. The placenta specific disease map NaviCenta (https://www.sbi.uni-rostock.de/minerva/index.xhtml?id=NaviCenta) was used to focus functional analysis results to the placenta specific context. Subsequently, functional analysis with a focus on senescence, and mitochondrial function were performed. Significant differences were observed between sub-anatomical regions in protein intensity and composition. A decrease in anti-senescent proteins within the maternal sub-anatomical region, and an increase in proteins associated with a switch from ATP to fatty acid consumption as a source of energy between middle and fetal sub-anatomical regions were observed.

Conclusion: These results suggest that normal proteomic variations exist within the anatomical structure of the placenta, thus recommending serial sectioning methodology for consistent placental research.

Keywords: Placenta, Proteomics, Bioinformatics, Network analysis, Disease map, Systems biology

Background

The placenta is a complex organ playing a critical role in the development and preservation of a healthy pregnancy. It is appropriately defined by Harland Mossman as "The normal mammalian placenta is an apposition or fusion of the fetal membranes to the uterine mucosa for physiological exchange" [1, 2]. The placenta is a dynamic organ undergoing rapid growth, and dramatic molecular and histological rearrangements along gestational stages, in order to adapt to fetal requirements [3].

†Samprikta Manna and Julia Scheel are contributed equally as first authors

†Jane English, Cathal McCarthy and Fergus P. McCarthy contributed equally as last authors

*Correspondence: Samprikta.manna@ucc.ie; 117220575@umail.ucc.ie

[1] Department of Obstetrics and Gynaecology, Cork University Maternity Hospital, University College Cork, Cork, Ireland
Full list of author information is available at the end of the article

© The Author(s) 2023. **Open Access** This article is licensed under a Creative Commons Attribution 4.0 International License, which permits use, sharing, adaptation, distribution and reproduction in any medium or format, as long as you give appropriate credit to the original author(s) and the source, provide a link to the Creative Commons licence, and indicate if changes were made. The images or other third party material in this article are included in the article's Creative Commons licence, unless indicated otherwise in a credit line to the material. If material is not included in the article's Creative Commons licence and your intended use is not permitted by statutory regulation or exceeds the permitted use, you will need to obtain permission directly from the copyright holder. To view a copy of this licence, visit http://creativecommons.org/licenses/by/4.0/. The Creative Commons Public Domain Dedication waiver (http://creativecommons.org/publicdomain/zero/1.0/) applies to the data made available in this article, unless otherwise stated in a credit line to the data.

Nevertheless, the placenta remains the least studied organ in the human body, whose structural and functional composition have possible implications for long term maternal and child health outcomes [4, 5]. A healthy placenta at term is a disc shaped organ around 22 cm in diameter and weighing approximately 500 g [2]. Although the placental is a fetal organ, its anatomical regions can be loosely termed as: Maternal and Fetal, based on its proximity to foetus [6, 7]. This multifaceted transient organ is characterised by different anatomical structures; the chorionic plate with umbilical cord attached, at the fetal side (fetal sub-anatomical region), the basal plate which borders the maternal endometrium (maternal sub-anatomical region) and the intermediate region connecting the basal plate and chorionic plate (middle sub-anatomical region) [8, 9]. Placental villi, the core structural unit are classified as stem villi which connect to the chorionic plate with limited exchange functionality; intermediate villi classified as mature or immature consisting of cytotrophoblast subtypes with differing functional roles and the syncytiotrophoblasts layer which acts as principal transfer site especially in first and second trimester. As pregnancy progresses the terminal villi which are completely formed at 20 weeks' gestation, are the dominant morphological feature with syncytiotrophoblasts being immersed in maternal blood facilitating its functional role in nutrient and gaseous exchange [6, 10]. The placenta ages gradually as the pregnancy proceeds. At 40 weeks of gestation, the placenta is at its verge of decline, exhibiting morphological and physiological senescence [11]. However, in presence of undesirable oxidative stress, placental aging may be accelerated in certain pregnancy conditions such as preeclampsia (PE), intrauterine growth restriction (IUGR) and stillbirth, characterized by both mitochondrial dysfunction and premature cellular senescence [12, 13].

The placental proteome has been used to further our understanding of the molecular mechanisms involved in development of the placenta and in the pathophysiology of placental disorders [3]. Furthermore, this technology has been used in clinical research to aid in the discovery of protein or metabolite biomarkers to incorporate as a diagnostic tool for clinical utility [14]. Proteomics has been widely used in pregnancy complication such as PE and IUGR, by using novel methods in specific trimester of pregnancies, for diagnosis, and understanding pathophysiological mechanism to improve maternal and neonatal health outcomes [15].

Uniformity of placental sampling has been lacking in research with some studies focusing on single placental sampling sites which may not always be representative of the global signature of this large heterogenous metabolic organ. Standardization of placental tissue sampling can improve the quality of placental research, and facilitate sharing of samples between groups, allowing larger datasets to be generated [16]. Burton et al., summarized the factors such as methodological flaws including sampling and processing samples that might be limiting placental research [17]. The aim of this research was to determine the proteomic signature of a healthy term placenta, while investigating proteomic composition and molecular pathways enriched across the placental sub-anatomical regions.

Methods

Patient recruitment and sample collection

Subjects were recruited as part of the COMRADES Study, a non-interventional cohort study of nulliparous singleton pregnancies with the aim of characterizing placental premature senescence in preeclampsia (PE) and Intra-uterine growth restriction (IUGR). The COMRADES study was conducted according to the guidelines laid down in the Declaration of Helsinki, and all the procedures were approved by the Clinical Research Ethics Committee of the Cork Teaching (ECM4 (ff) 04/12/18). All women provided written informed consent to take part in the study. Three normotensive, healthy pregnant participants with no obstetric complications were recruited as a part of the COMRADES Study between February and July 2020. Placental samples were collected from nulliparous, singleton pregnancies undergoing Caesarean section for non- obstetric indications such as breech presentation with consent from the participants. Placental sampling was completed within 20 min of delivery, snap frozen in liquid nitrogen and stored at -80 °C for long term storage. Placental sectioning was performed in accordance with the standard protocol described by Burton et al. [16].

Tissue samples [2–4 cm in diameter] were isolated from 5 different sample sites across the placenta. We defined the sub-anatomical regions of the placenta as: maternal, middle, and fetal to evaluate the basal plate, chorionic plate and the middle part connecting the two surfaces of the placenta. Sectioning was performed by keeping close to the fetal membrane from the chorionic plate, the maternal part was sectioned closer to the basal membrane and the middle region was selected from between maternal and fetal sections (Additional file 1: Figure S1). Fetal membranes were not included in the sectioning [16].

Protein extraction and quantification

Processing of placental tissue for proteomics analysis was based on previously established laboratory protocols [18]. Placental tissue (50 mg) was homogenized using TissueLyser II (Qiagen, Germany) and protein isolated)

using Tetraethylammonium bicarbonate (TEAB) buffer (Sigma-Aldrich, Ireland) in presence of Phosphatase inhibitor (PhosSTOP™, Roche, Ireland) and Protease Inhibitor (Roche, Ireland) Mechanical tissue homogenization. Protein quantification was assessed with BCA Assay (Pierce™ Thermo Fisher Scientific, USA) and protein volume adjusted to 50 µg/50 µl concentration with MS grade dH_2O (Additional file 2).

Protein solubilisation and desalination

Protein solubilisation and desalination process has been previously described [18]. Protein enzymatic digestion was performed using Trypsin (Promega, MyBio, Ireland) with the aid of Rapigest (1%) solution (Waters, Ireland). To aid with Trypsin (Promega – details) 50 mM Tris(2-carboxyethyl) phosphine hydrochloride (TCEP) (Sigma-Aldrich, Ireland) solution was added to the denatured proteins and samples reduced for 60 min at 60 °C, followed by addition of 200 mM Indole-3-acetic acid (IAA) solution (Sigma-Aldrich, Ireland) to alkylate proteins, which were incubated overnight at 37 °C with 1:100 sequential grade trypsin according to manufacturer's instruction followed by addition of 1% Formic acid was used to stop digestion. Precipitation of Rapigest was done by centrifuging samples at 13,000 rpm for 10 min and supernatants collected and air dried on MiVac Quattro sample concentrator (Fisher Scientific, Sweden) followed by resuspension in 0.5% Formic Acid (FA) (Sigma-Aldrich, Ireland). Desalting and sample clean-up was performed using Zip-Tip columns with 0.6 µl binding volume C18 resin (Sigma-Aldrich, Ireland). For maximum binding of protein to resin present on zip-tip column, the tips are equilibrated using 0.1% Trifluoroacetic acid (TFA) in H2O; followed by washing and binding of protein, and finally the protein are eluted into 10 µl elution solution composed of 50% ACN in 0.1% TFA. The process was repeated to achieve 1 µg/µl concentration. The samples are then re-dried on MiVac Quattro sample concentrator (Fisher Scientific, Sweden) and all samples were resuspended in 0.1% FA to 1 µg/µl volume for LC–MS/MS analysis. Equal aliquots of digested protein in the experiment were pooled into one sample for internal quality control (QC) standard which was injected three times at the beginning of the MS study and throughout the experiment every 10 to condition the column and monitor the MS performance. LC–MS/MS analysis was performed in the Proteomics Core in the Conway Institute of Biomolecular and Biomedical Research, UCD, Dublin.

Mass spectrometry (MS) sample preparation

Proteomics samples were enzymatically digested with Trypsin (Promega sequencing grade) according to manufacturer's instruction and in the presence of Rapigest SF (Waters). Briefly, samples were first reduced with Tris(2-carboxyethyl) phosphine hydrochloride (TCEP) at 60 °C for 60 min, and alkylated with Iodoacetamide (IAA, final concentration y mM) for 30 min in the dark, prior to the addition of trypsin in a ratio of enzyme to protein of 1:100 (w/w). The samples were incubated overnight at 37 °C followed by addition of 1% Formic acid the next morning to stop digestion and precipitate the Rapigest. Removal of Rapigest by-products was performed by centrifugation of samples at 13000 rpm for 10 min and supernatants collected and dried under vacuum with a MiVac Quattro sample concentrator (Fisher Scientific, Sweden). The dried digests were resuspended in 0.5% Formic Acid (FA) (Sigma-Aldrich, Ireland) prior to de-salting with C18 ZipTips (Millipore). Finally, the desalted digests were resuspended in 0.1% FA for LC–MS/MS analysis. Equal aliquots of digested protein from each sample in the experiment were pooled into a single sample for an internal quality control (QC) standard which was injected three times at the beginning of the MS study and throughout the experiment every 10 samples, and to condition the column and monitor the MS performance. LC–MS/MS analysis was performed in the Proteomics Core in the Conway Institute of Biomolecular and Biomedical Research, UCD, Dublin.

Mass spectrometry

All samples were injected in a randomized sequence combining Internal standards and samples for discovery of sub anatomical region proteomic profiles. 5 µl of each sample was injected in duplicate onto the Thermo Scientific Q-Exactive® connected to a Dionex Ultimate 3000 High-performance Liquid Chromatography (HPLC) system. The digests were loaded onto a fused silica emitter (75 µm ID), pulled using a laser puller (Sutter Instruments P2000) and packed with UChrom C18 (1.8um) reverse phase media (nanoLCMS Solutions LCC). Peptides were separated using an increasing acetonitrile gradient (250nL/min) for 60 min [18]. The mass spectrometer was operated in data dependent analysis (DDA) mode on a TopN 12 mode with setting: mass range 300-1600Th; resolution for MS1 scan 70,000; AGC target 3e6; resolution for MS2 scan 17,500; AGC target 2e4; charge exclusion unassigned, 1; dynamic exclusion 40 s.

Bioinformatics and data pre-processing

Raw data obtained from LC–MS/MS runs were searched against the Uniprot Human reference proteome UP000005640 (downloaded 24–05-2021) with MaxQuant (version 1.6.17) using default settings and additionally including the 'Match Between Runs' and 'Label free quantification (LFQ)' options. The ProteinGroups.

txt output file obtained from the MaxQuant analysis was processed in Perseus (version 1.6.15.0). Data was filtered to remove possible contaminants. Samples were categorised by sub-anatomical region. LFQ intensity data was log2 transformed, and proteins not identified in all biological replicates were removed. After rigorous filtering to assure reproducibility, including filtering for valid values in at least 100% of biological replicates, 70% valid values of samples per sample site, and 70% valid values of samples per sub-anatomical region, these proteomic differences did not persist. Furthermore, proteins absent in 70% of samples in at least one sub-anatomical region/sample site were removed. Missing values were replaced by values from the normal distribution.

Statistical analysis

Statistical analysis was conducted using the built-in statistical tests in Perseus. To analyse the effect of sub-anatomical region and sample site on protein expression a two-way ANOVA was performed. Two-way ANOVA models allow accounting for more than one known source of variation. In this study "sub-anatomical region" and "sample site" were considered independent variables and LFQ protein intensity was the dependent variable (https://www.ncbi.nlm.nih.gov/pmc/articles/PMC2528956/pdf/nihms60473.pdf). Simple main effects were analysed using simple ANOVA and Tukey's HSD tests. The results were corrected for false discovery ($p < 0.05$) within Perseus [19].

Pathway analysis

Functional analysis of differentially overrepresented gene ontology (GO) terms and pathways associated with differentially expressed proteins, was performed using Cytoscape v 3.9.1 ClueGO plugin [20]. GO and pathway term overrepresentation results were corrected for false discovery using Bonferroni step down correction ($p < 0.05$) and considered significantly overrepresented with an adjusted p value < 0.5.

Placenta specific characteristics

The term disease map was defined as "a comprehensive, knowledge-based representation of disease mechanisms" [21, 22]. The NaviCenta consists of human and machine-readable representations of processes involved in healthy and dysfunctional placentae in SBGN process description and activity flow (https://www.sbi.uni-rostock.de/minerva/index.xhtml?id=NaviCenta). Phenotype predictions based on user defined data uploaded onto the NaviCenta were performed with plugins [23]. The uploaded information consisted of HGNC identifiers for the genes of all identified proteins, their difference score as calculated in Perseus, and adjusted p values.

Mitochondria and senescence specific function analysis

Identified proteins that map to mitochondrial function were filtered using or the products of genes associated with mitochondrial functions incorporating information from the Human Protein Atlas mitochondrial sub-cellular location (www.proteinatlas.org) [24], MitoXplorer human interactome [25], and MitoCarta3.0 [26]. The overlap between mitochondrial protein and gene databases, proteins identified in maternal, middle, and fetal regions were visualized using InteractiVenn [27]. Separately, DEPs were filtered to exclusively contain proteins that map to senescence associated molecular process. Senescence associated proteins and genes were identified from the Human Ageing Genomic Resource College Build 20 [28], Cell Senescence Gene Database CSGene [29], and the NCBI gene database with search key "senescence" (https://www.ncbi.nlm.nih.gov/gene/?term=senescence, accessed October 2021). GO biological process terms were visualized using the R Version 4.0.5 and R package GOPlot [30].

Results

Study demographics

Patient demographic and clinical information can be found in Table 1. Each placenta had five sample sites (A-E) taken across the placenta. These samples were then separated into three sub-anatomical regions: fetal, middle, and maternal (Additional file 1: Figure S1; resulting in a total number of 45 samples. Sub-anatomical regions were confirmed histologically (Additional file 1: Figure S1).

Proteome profile shows variation across placental regions and sample sites

In total 1081, 1086, and 1101 proteins were identified in maternal, middle, and fetal sub-anatomical regions, respectively. We identified 14, 8, and 21 proteins as

Table 1 Patient demographics and clinical parameters of recruited women

Characteristics	Mean ± SD
Maternal age (years)	34.6 ± 2.5
BMI (kg/m^2)	23.6 ± 4.1
Parity	0
Gestational age (days)	270.7 ± 5.5
Systolic BP (mm Hg)	122.0 ± 7.5
Diastolic BP (mm Hg)	74.7 ± 5.5
Fetal weight (kg)	3.3 ± 0.2
Fetal individualized customised centile	52.9 ± 5.4
Maternal smoking/tobacco habit	no

exclusive to the maternal, middle, or fetal sub-anatomical regions, respectively (Fig. 1).

We analyzed fifteen individual samples were available. Contaminants were removed from further analysis.

EnrichR Cell Marker Database [31] cell type prediction identified only minor differences between sub-anatomical regions (Additional file 1: Figure S2). Although placental tissues were not specifically implicated based on cell markers, most enriched cell types indicate fetal tissues, such as monocytes from fetal kidney, natural killer T (NKT) cells from fetal kidney, mitotic fetal germ cells and other phenotypically similar cell types, which is in line with the placenta being a fetal organ.

Proteomic differences were also found between sample sites, with 520 unique proteins identified in sample site E (Additional file 1: Figure S3). ClueGO functional analysis showed that in particular proteins aligning with GO terms of membrane organization, protein-containing complex and subunit organization, vesicle-mediated transport, organo-nitrogen compound biosynthetic process, and translation initiation factor activity are over-represented (Additional file 1: Figure S4). All unique proteins to sample site E but SNRPD2, SPP2, EPS8-l1, and ACAA2 were filtered out for the analysis of both sub-anatomical region and sample site considering biological replicates.

The placental proteome varies with sub-anatomical region

Two-way ANOVA considering both sub-anatomical region and sample site revealed 374 out of 1038 DEPs (adjusted p-value < 0.05) between sub-anatomical regions. Strong interaction between the effect of sample site and sub-anatomical region on LFQ protein intensity was indicated (p-value interaction < 0.05) for some proteins. The intensity of biological replicates of four proteins (CBR1, HBG2, ANXA4, and FHL1) which demonstrates the highest interaction between sub-anatomical region and sample site on protein intensity are shown in Fig. 2. No pattern was apparent, allowing the separate analysis of DEPs between sub-anatomical regions and sample sites.

Simple ANOVAs revealed no significant DEPs between sample sites. Sub-anatomical region comparison maintained the previously identified 374

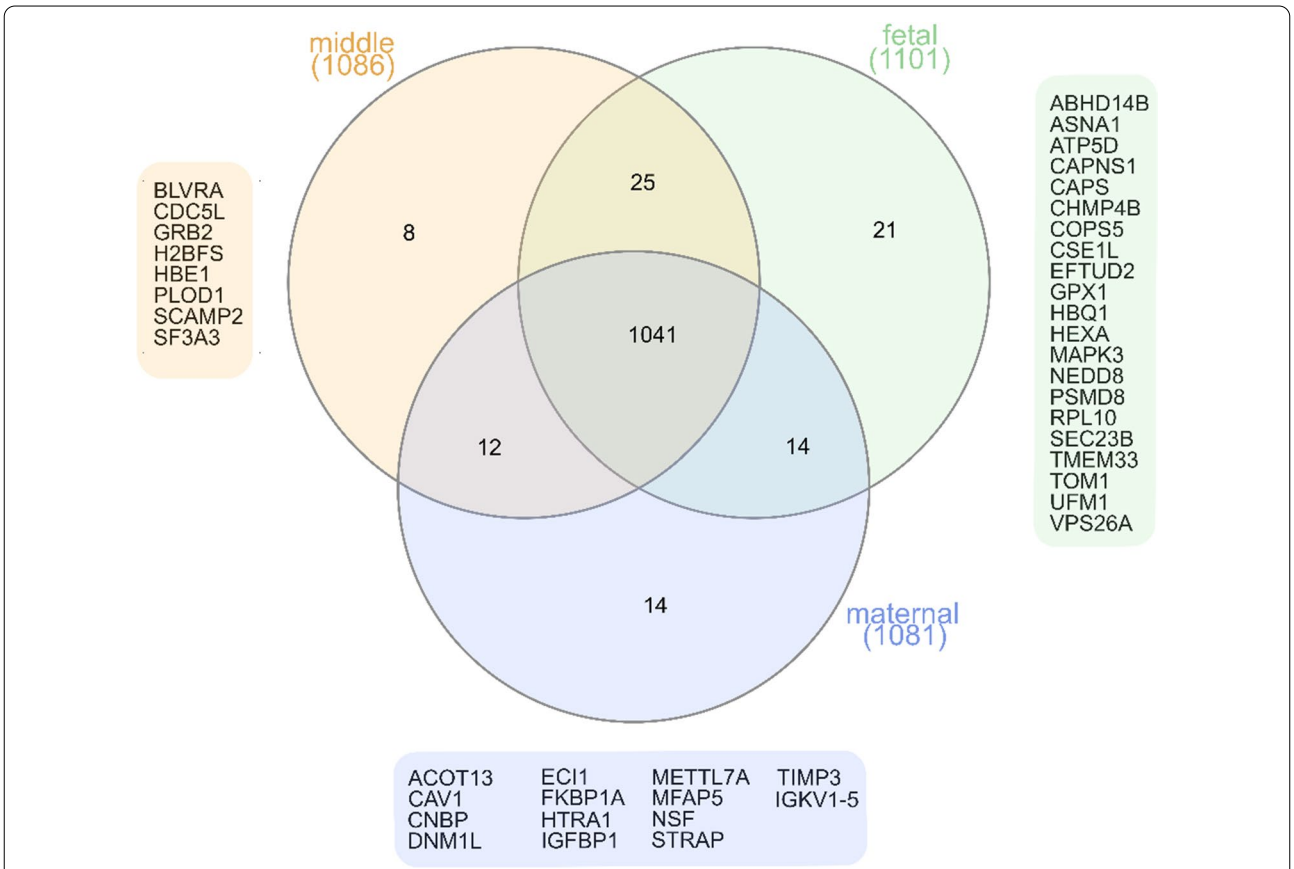


Fig. 1 Venn diagram of identified proteins in middle, fetal, and maternal regions. Proteins identified in exclusively one sub-anatomical region are listed next their respective sub-anatomical region

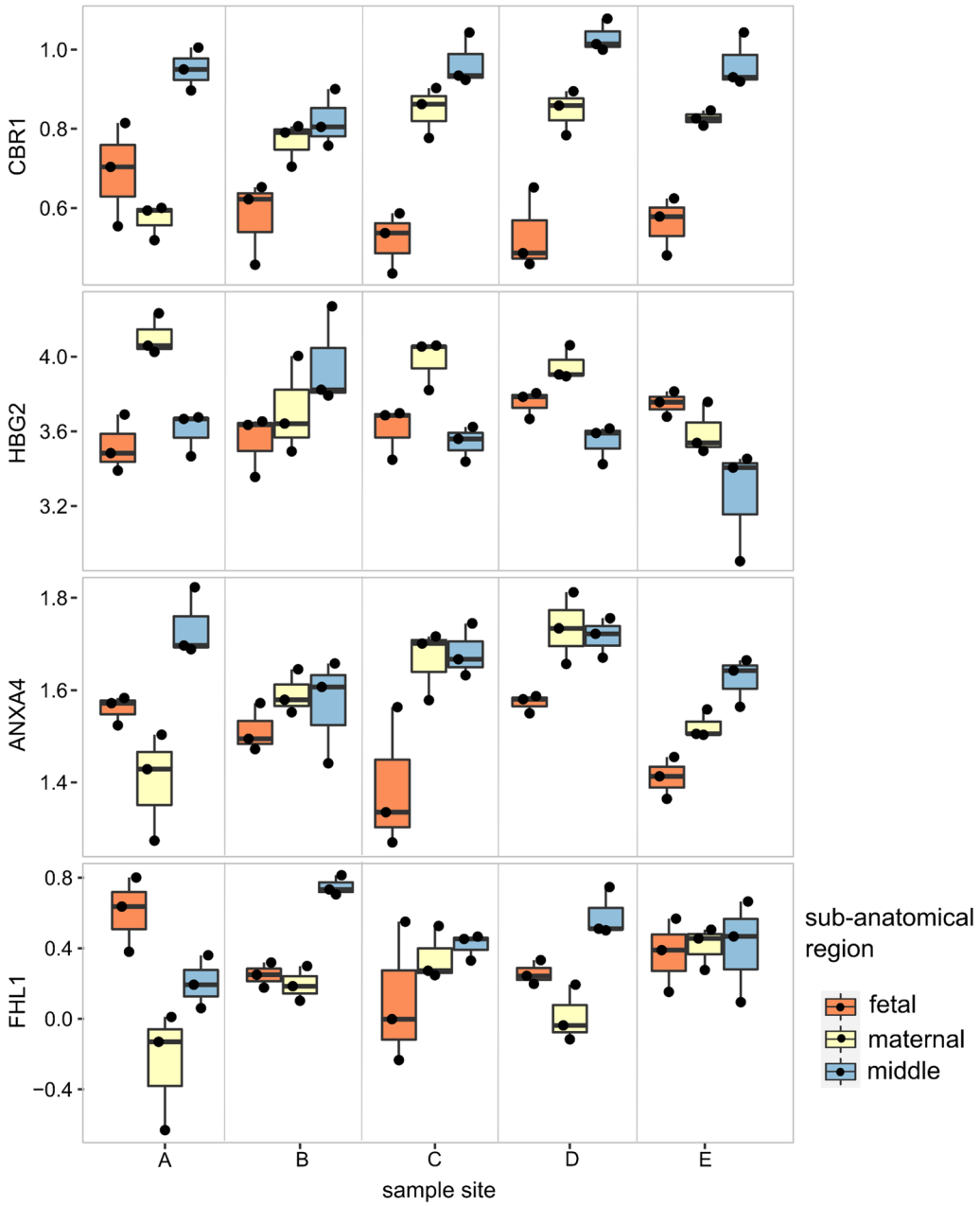


Fig. 2 The top four proteins FHL1, ANXA4, HBG2, CBR1 show the strongest interaction between protein content in sub-anatomic regions and sample sites. Interaction was defined as two-way ANOVA adj p val < 0.05. Samples were sorted according to sample site and colour coded according to sub-anatomical region

DEPs. Maternal vs middle sub-anatomical region comparison revealed 128 upregulated, and 152 downregulated DEPs on the maternal side. Maternal vs fetal comparison revealed 115 upregulated, and 123 downregulated DEPs, respectively. Middle vs fetal sub-anatomical region comparison revealed 64 upregulated, and 41 downregulated DEPs in the middle sub-anatomical region (Table 2, Additional file 1: Figure 3).

The top three up and downregulated DEP are detailed in Table 2. These proteins are associated with an array of molecular functions such as actin binding, protein binding, DNA binding, heparin binding, lipid binding and collagen binding.

Table 2 Summary of differentially expressed proteins (HGNC identifier) between maternal, middle, and fetal sub-anatomical regions

	Up DEP	Top 3 DEP	FC	Down DEP	Top 3 DEP	FC
Maternal vs middle sub-anatomical region	128	MYH11***	1.48	152	PZP***	− 1.41
		NUTF2*	1.01		SCIN***	− 1.15
		CFHR1***	0.80		KDELC2***	− 0.79
Maternal vs fetal sub-anatomical region	115	MYH11***	1.24	123	KRT19***	− 0.71
		COL14A1***	1.16		SNRPD2**	− 0.69
		NUTF2**	1.00		CAPS*	− 0.52
Middle vs fetal	64	PZP***	2.29	41	DES***	− 0.74
		SCIN***	0.80		SNRPD2**	− 0.66
		LTF***	0.70		ERAP1***	− 0.46

Top three DEPs MYH11, NUTF2, CFHr1, COL14A1, NUTF2, PZP, SCIN, LFT based on highest fold change (FC). Adjusted p val < 0.05, up = upregulated, down = downregulated. *** = adjusted p val < 0.001, ** = adjusted p val < 0.01, * = adjusted p val < 0.05. p values adjusted for FDR

Functional analysis of placenta regions and sample site proteome

To further our understanding of functional differences between sub-anatomical regions based on associated DEP, functional analysis was conducted. DEP of maternal vs fetal, maternal vs middle, middle vs fetal sub-anatomical regions were directly compared within ClueGO regarding biological process gene ontology (GO), molecular function GO, and cellular component GO overrepresentation. As there was overlap between up and downregulated DEPs (Additional file 1: Figure S4), functional comparisons were separated to consider upregulated DEPs and downregulated DEPs [20].

GO overrepresentation analysis indicated a number of biological processes and molecular functions to be enriched (Fig. 3). Processes and functions important in inflammation, humoral and stress responses were overrepresented in both up and down regulated proteins. Processes associated with transcription and translation, such as regulation of RNA, RNA catabolic processes, and

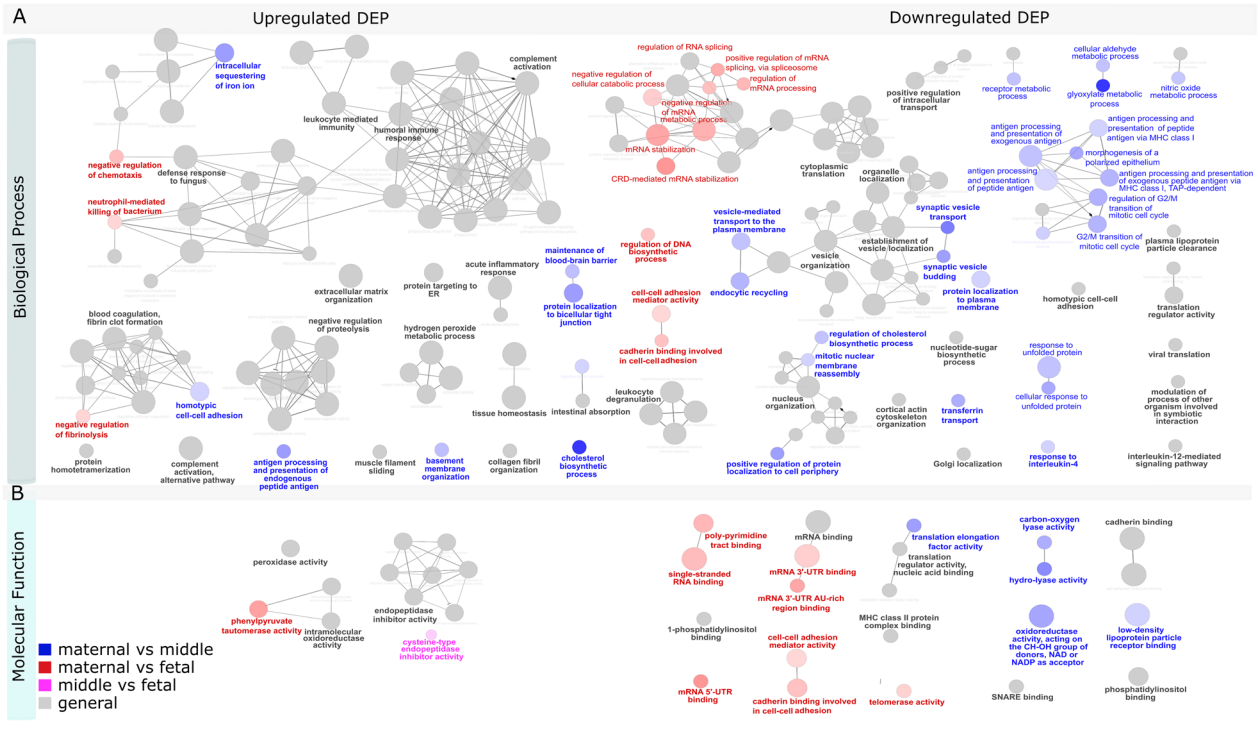


Fig. 3 ClueGO functional analysis of differentially expressed proteins (DEP) between maternal, middle, and fetal sub-anatomical regions. Significantly (adj. p < 0.05) overrepresented biological process (**A**) and molecular function (**B**). GO terms can be grouped by similarity, in which case only the group GO term is legible. The size of nodes indicates the number of proteins encoding genes falling into each term. Similarity or hierarchic relationship between GO terms is indicated by edges

regulation of DNA biosynthetic process were primarily overrepresented in downregulated DEPs in the maternal compared to the fetal sub-anatomical region. Processes associated with intracellular transport were primarily enriched in downregulated DEPs in the maternal compared to the middle sub-anatomical region (Table 3).

Mitochondria and senescence associated processes and functions such as, regulation of G2/M transition mitotic cell cycle, nitric oxide metabolism, oxidoreductase activity, and telomerase activity were overrepresented in downregulated DEPs between maternal and middle sub-anatomical regions. Proteins associated with glyoxylate metabolic processes were overrepresented in downregulated DEPs between maternal and middle or fetal sub-anatomical regions.

Terms that are overrepresented in general but not significant to one specific comparison group are visualized in grey. Upside arrows indicate upregulation, and downside arrows downregulation. Simplified results are summarized, including adj. p value (significance) indicator and associated proteins.

GO overrepresentation analysis revealed a myriad of differentially regulated processes and functions. In order to focus results further, and make them placenta specific, we used the NaviCenta, a placenta specific disease map. In contrast to traditional methods to characterize the function of deregulated genes or proteins the NaviCenta allows for consideration of DEPs including their respective fold change.

Placenta specific functional analysis

Placenta specific phenotype prediction showed the proteins found in the maternal sub-anatomical region indicate increased endothelial cell (EC) migration, EC apoptosis, and EC proliferation in comparison to both middle and fetal sub-anatomical regions. The phenotypes

Table 3 Summary table of GO terms overrepresented in DEPs between maternal and middle sub-anatomical region (blue), maternal and fetal sub-anatomical region (red), middle and fetal sub-anatomical region (pink), compared to each other

	GO term		Proteins	Significance [*]
transcription and translation	regulation of DNA biosynthetic process	↓	DDX39B,HNRNPA1,HNRNPD,HNRNPU,HSP90AA1,HSP90AB1,NIBAN2	*
	regulation of mRNA processing	↓	CIRBP, DDX17, DHX9, HNRNPA1, HNRNPU, HSPA8, PRDX6, PTBP1, SNRNP70	**
	regulation of mRNA splicing	↓	CIRBP, HSPA8, PRDX6, SNRNP70	*
	positive regulation of mRNA splicing via spliceosome	↓	CIRBP, HSPA8, PRDX6, SNRNP70	*
	negative regulation of cellular catabolic process	↓	CIRBP, DHX9, ELAVL1, HNRNPA0, HNRNPD, HNRNPU, HP, HSP90AB1, PABPC1, SCFD1, SEC22B, SNRNP70, SYNCRIP, USP14	***
	negative regulation of mRNA metabolic process	↓	CIRBP, DHX9, ELAVL1, HNRNPA0, HNRNPD, HNRNPU, PABPC1, PTBP1, SYNCRIP	***
	(CRD-mediated) mRNA stabilization	↓	DHX9, HNRNPU, SYNCRIP	**
	translation regulator activity	↓	CIRBP, EEF1B2, EEF2, EIF3B, EIF4A1, EIF4H, IGF2BP3, PABPC1, RPS9, TUFM	**
	mRNA binding	↓	ACO1, CARHSP1, CIRBP, DHX9, EIF4A1, ELAVL1, HNRNPA0, HNRNPD, HNRNPM, HNRNPU, IGF2BP3, PABPC1, PCBP1, PCBP2, PTBP1, PURB, RPS3A, RPS5, SERBP1, SNRNP70, SYNCRIP, TPR	***
	single-stranded RNA binding	↓	ANXA1, DHX9, EIF4H, HNRNPA1, HNRNPH1, HNRNPU, PABPC1, PTBP1	***
	mRNA 3'-UTR AU rich region binding	↓	ELAVL1, HNRNPA0, HNRNPD	*
	mRNA 5'-UTR binding	↓	IGF2BP3, RPS3A, SYNCRIP	*
	poly-pyrimidine tract binding	↓	HNRNPH1, HNRNPU, PABPC1, PTBP1	**
	translation elongation factor activity	↓	EEF1B2, EEF2, TUFM	*
cholesterol	cholesterol biosynthetic process	↑		
	regulation of cholesterol biosynthetic process	↓	APOB, KPNB1, RAN, VDAC2	*
	low-density lipoprotein particle receptor binding	↓	AP2A1, AP2M1, APOB, CSRP1, LRPAP1, PICALM	***
mitochondria and senescence	glyoxylate metabolic process	↓	ALDH4A1, IDH1, IDH2	*
	regulation of G2/M transition of mitotic cell cycle	↓	DYNC1H1, DYNC1I2, FHL1, HSP90AA1, PPP2R1A, PSMC2, PSMC3, PSMD13, PSMD2, TUBA1A, TUBB, TUBB4B	**
	nitric oxide metabolic process	↓	ASS1, CYB5R3, DDAH2, DNM2, HSP90AA1, HSP90AB1, VDAC2	***
	G2/M transition of mitotic cell cycle	↓	DNM2, DYNC1H1, DYNC1I2, FHL1, HSP90AA1, PPP1CB, PPP2R1A, PSMC2, PSMC3, PSMD13, PSMD2, TUBA1A, TUBB, TUBB4B	***
	carbon-oxygen lyase activity	↓	ACO1, FASN, HADHA, HADHB, TPI1, XRCC6	**
	oxidoreductase activity, acting on the CH-OH group of donors, NAD or NADP as acceptor	↓	AKR1B1, AKR7A2, CBR1, FASN, HADHA, HADHB, HSD17B1, IDH1, IDH2, LDHB, MDH1, PGD, TSTA3	***
	telomerase activity	↓	HNRNPD, HSP90AA1, HSP90AB1	*
	cysteine-type endopeptidase inhibitor activity	↑	LTF, PRDX5, SERPINB9	*
transport	transferrin transport	↓	CIRBP, HSPA8, PRDX6, SNRNP70	**
	endocytic recycling	↓	ARHGAP1, EHD1, EHD2, RAB11B, RAB14, RAB7A, SNX3	**
	receptor metabolic process	↓	AP2A1, AP2M1, CAPN1, DNM2, EZR, LRPAP1, PICALM, RAB11B, TFRC, VAMP3	**
	positive regulation of intracellular transport	↓	DHX9, DYNC1H1, EHD1, EHD2, EZR, FLNA, HSP90AB1, KIF5B, NUMA1, RAN, TPR, YWHAZ	**
	vesicle-mediated transport to the plasma membrane	↓	ARHGAP1, DNM2, EHD1, EHD2, KRT18, RAB11B, RAB14, RAB7A, SNX3, VAMP3	***
	protein localization to plasma membrane	↓	AKR1B1, AP2M1, EHD1, EHD2, EPB41L3, EZR, FLNA, KIF5B, KRT18, LRPAP1, PICALM, RAB7A, SLC9A3R1, VAMP3	**
stress and immune response	antigen processing and presentation of endogenous peptide antigen	↓	AP2A1, AP2M1, DNM2, DYNC1H1, DYNC1I2, ERAP1, PDIA3, PSMC2, PSMC3, PSMD13, PSMD2, RAB7A, SEC22B, VAMP3	***
	antigen processing and presentation of exogenous antigen	↓	AP2A1, AP2M1, AP3B1, DNM2, DYNC1H1, DYNC1I2, PDIA3, PSMC2, PSMC3, PSMD13, PSMD2, RAB7A, SEC22B, VAMP3	***
	antigen processing and presentation of peptide antigen via MHC class I	↓	ERAP1, PDIA3, PSMC2, PSMC3, PSMD13, PSMD2, SEC22B, VAMP3	**
	negative regulation of chemotaxis	↑	C5, DDT, DPP4, ELANE, S100A8, S100A9	**
	neutrophil-mediated killing of bacterium	↑	CTSG, ELANE, F2	**
	leukocyte mediated immunity	↑	A1BG, ACLY, ALAD, B2M, C1QB, C3, C4A, C4BPA, C5, C8G, CD14, CORO1A, COTL1, CPNE1, CPNE3, CTSD, CTSG, ELANE [57]	***
	humoral imune response	↑	A2M, C1QB, C3, C4A, C4BPA, C5, C8G, CFB, CFH, CFHR1, CPNE1, CTSG, DEFA3, ELANE, F2, FGA, FGB, GPI, IGHA1[38]	***
	acute inflammatory response	↑	APOA2, ASS1, C3, ELANE, F2, ITIH4, ORM1, S100A8, SERPINA3, SERPINC1	***
	IL-23 mediated signaling pathway	↓	LMNB1, PDCD4, RPLP0, SERPINB2, TALDO1	*
	response to IL-4	↓	FASN, HSP90AB1, HSPA5, RPLP0, STAT5B	**
	phenylpyruvate tautomerase activity	↑	DDT, S100A8, S100A9	***

adj. p value	
*	< 0.05
**	< 0.01
***	< 0.001

contraction is higher in the maternal sub-anatomical region compared to both fetal and middle sub-anatomical regions, but lower in the middle sub-anatomical region compared to the fetal sub-anatomical region. Complement cascade and chemotaxis are lower in maternal and middle sub-anatomical regions compared to the fetal sub-anatomical region. Ferritinophagy is lower in the maternal than the middle sub-anatomical region, while mRNA splicing is higher in the maternal than the middle sub-anatomical region (Table 4).

Placental sub-anatomical regions present differing mitochondrial status

The list of all identified proteins was filtered to only include proteins (HGNC IDs) included in the mitochondrial gene and proteome databases Human Protein Atlas mitochondrial sub-cellular location(www.proteinatlas.org), MitoXplorer human interactome [25], and human MitoCarta3.0 [26] (Fig. 4). HPA contains 1139 proteins associated with mitochondrial function, MitoCarta 3.0 1136, and MitoXplorer 1229, respectively (Fig. 4A). These databases showed overlapping content proteins both with each other and with the DEPs identified between sub-anatomical placenta regions. Ensuing functional analysis was conducted using the intersection of any mitochondrial database with placental proteins. Of all identified proteins 147 out of 1081 in the maternal sub-anatomical region, 144 out of 1086 in the middle sub-anatomical region, and 148 out of 1101 in the fetal sub-anatomical region are associated with mitochondrial function and processes. 53 DEPs out of the previous 374 DEPs are associated with mitochondrial function and processes.

The tricarboxylic acid cycle is indicated in all three conditional comparisons. Downregulated proteins are more evident on the maternal side compared with middle and fetal regions, and exclusively upregulated proteins comparing middle with fetal sub-anatomical region. Protein homotetramerization is indicated by upregulated proteins in the maternal region compared to both the fetal and the middle regions. Proteins associated with negative regulation of oxidative stress-induced cell death are upregulated in the maternal region compared with both middle and fetal regions. Summarizing the results, a general switch from glucose to lipid consumption appears to be initiated in the maternal and middle compared to the fetal sub-anatomical region. Terms indicating glycolysis, tricarboxylic acid cycle, and lipid consumption as an energy source are gluconeogenesis, glucose 6-phosphate metabolic process, fatty acid transmembrane transport, acetyl-CoA biosynthetic process from pyruvate, NADH regeneration, and fatty acid beta oxidation.

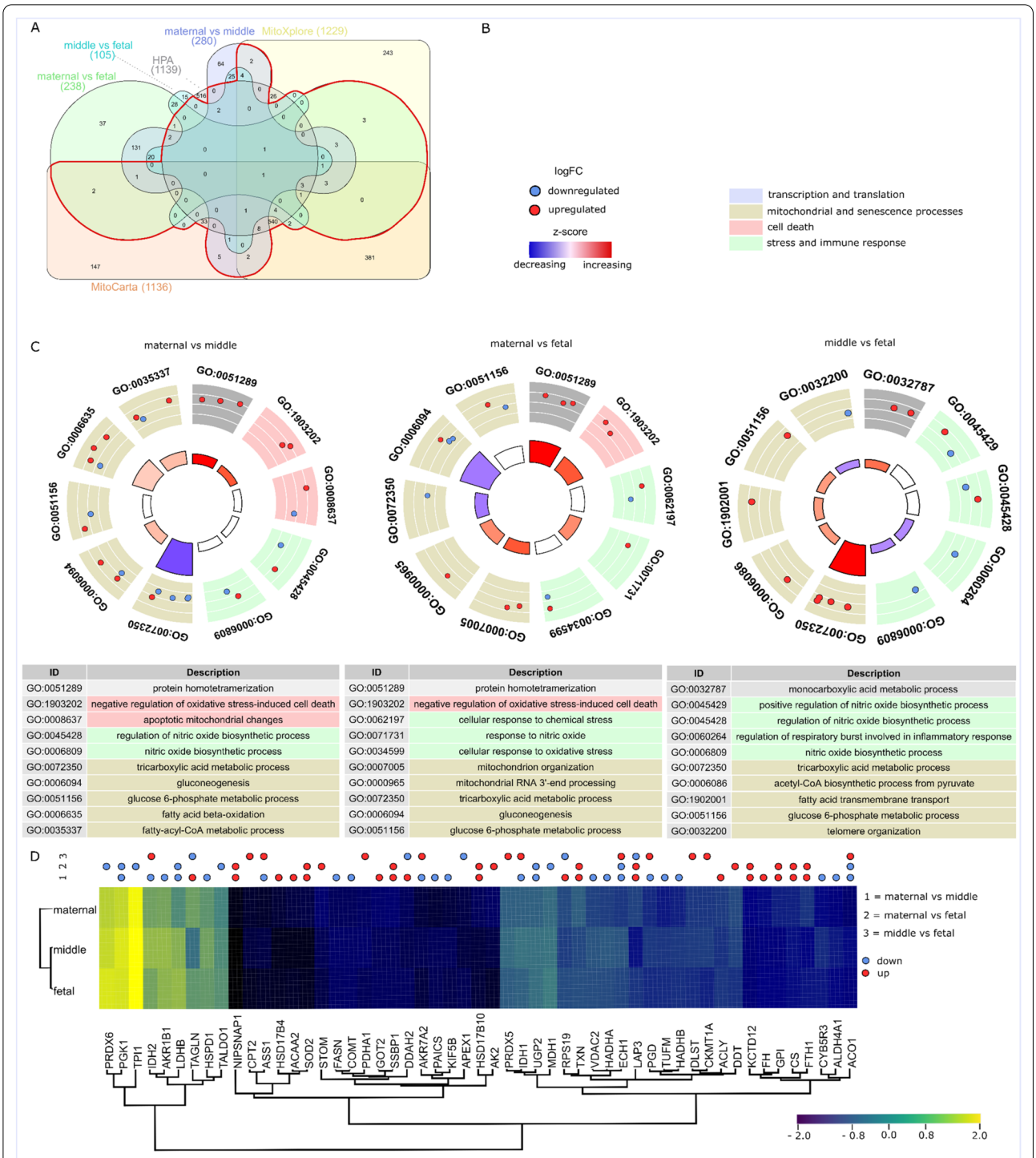
Comparing maternal and fetal sub-anatomical region, mitochondria associated terms such as mitochondrion organization and mitochondrial RNA 3'-end processing are upregulated in the maternal sub-anatomical region, while APEX1 associated with telomere organization is downregulated in the middle sub-anatomical region compared to the fetal sub-anatomical region.

Placental sub-anatomical regions offer divergent senescence status

The difference in senescence state between the three sub-anatomical regions was analysed using three senescence specific databases. Human Ageing Genomic Resource (HAGR) CellAge Build 20, consisting of 307 genes (Avelar

Table 4 NaviCenta differential phenotype prediction based on DEP (Benjamini – Hochberg FDR correction) p-value including adj. Pval < 0.01 between maternal, middle, and fetal sub-anatomical regions and the proteins leading to each phenotype prediction

Phenotype	Mat-fet log2FC	pval	Gene Name	Mat-mid log2FC	pval		Mid-fet log2FC	pval	Gene Names
EC migration	0.28	$5.94\ e^{-24}$	PLG	0.18	$3.76\ e^{-28}$	PLG	0	1	
Inflammatory response	−0.26	$5.91\ e^{-21}$	IGHG4	0	1		−0.31	$2.30\ e^{-35}$	IGHG4
contraction	1	$1.51\ e^{-13}$	MYH11	1	$5.41\ e^{-35}$	MYH11, TAGLN	−0.33	$3.13\ e^{-22}$	TAGLN
EC apoptosis	0.2	$1.84\ e^{-11}$	BLVRB	0.15	$2.39\ e^{-13}$	BLVRB	0	1	
EC proliferation	0.2	$5.12\ e^{-11}$	BLVRB	0.15	$5.83\ e^{-13}$	BLVRB	0	1	
Complement cascade	−0.27	$1.03\ e^{-08}$	IGHG4	0	1		−0.31	$3.94\ e^{-19}$	IGHG4
chemotaxis	−0.27	$3.91\ e^{-08}$	IGHG4	0	1		−0.31	$5.30\ e^{-18}$	IGHG4
Antigen clearance	0.41	0.003	IGHA1, IGLC3	−0.05	0.070		0.63	$2.22\ e^{-11}$	IGHA1
Destruction of pathogens	0.15	0.008	MPO	0.07	0.048		0	1	
Ferritinophagy	0.2	0.453		−0.14	0.001	FTL, FTH1	0	1	
mRNA splicing	0	1		0.12	0.003	ACIN1	0	1	



ID	Description
GO:0051289	protein homotetramerization
GO:1903202	negative regulation of oxidative stress-induced cell death
GO:0008637	apoptotic mitochondrial changes
GO:0045428	regulation of nitric oxide biosynthetic process
GO:0006809	nitric oxide biosynthetic process
GO:0072350	tricarboxylic acid metabolic process
GO:0006094	gluconeogenesis
GO:0051156	glucose 6-phosphate metabolic process
GO:0006635	fatty acid beta-oxidation
GO:0035337	fatty-acyl-CoA metabolic process

ID	Description
GO:0051289	protein homotetramerization
GO:1903202	negative regulation of oxidative stress-induced cell death
GO:0062197	cellular response to chemical stress
GO:0071731	response to nitric oxide
GO:0034599	cellular response to oxidative stress
GO:0007005	mitochondrion organization
GO:0000965	mitochondrial RNA 3'-end processing
GO:0072350	tricarboxylic acid metabolic process
GO:0006094	gluconeogenesis
GO:0051156	glucose 6-phosphate metabolic process

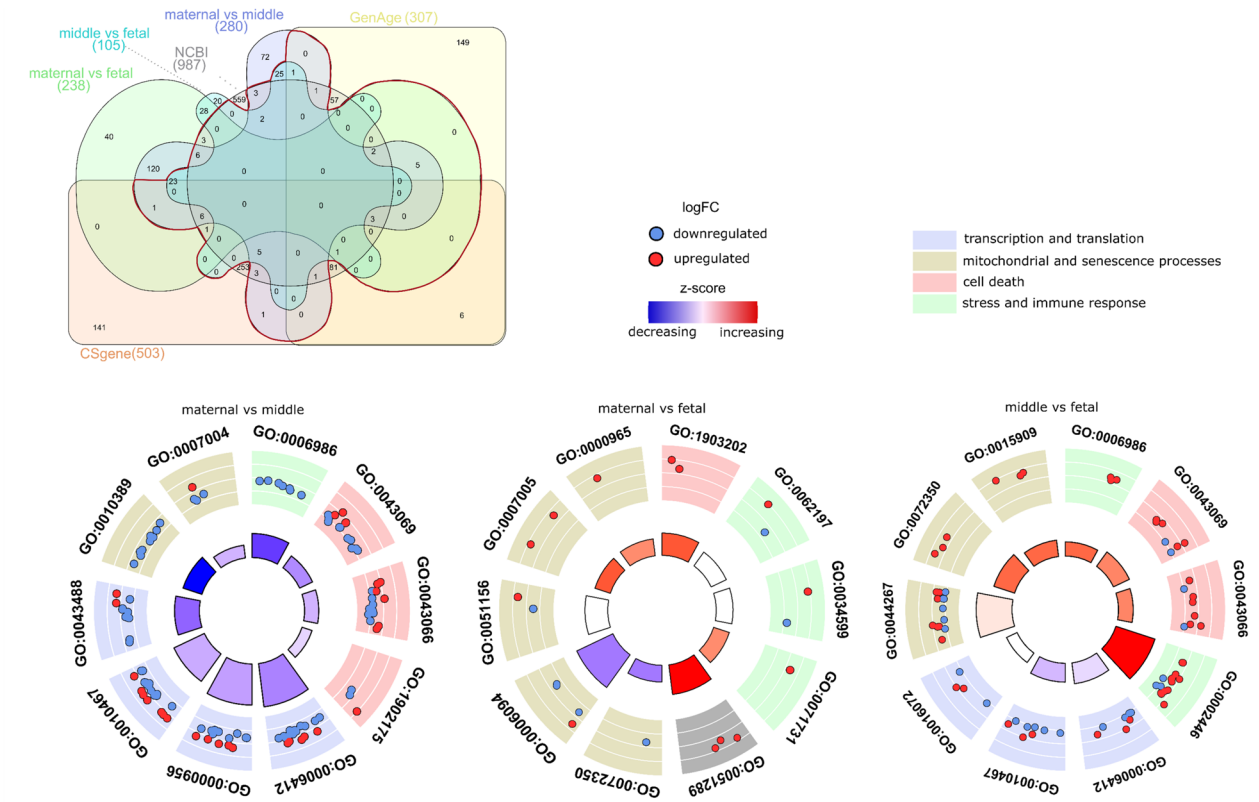
ID	Description
GO:0032787	monocarboxylic acid metabolic process
GO:0045429	positive regulation of nitric oxide biosynthetic process
GO:0045428	regulation of nitric oxide biosynthetic process
GO:0060264	regulation of respiratory burst involved in inflammatory response
GO:0006809	nitric oxide biosynthetic process
GO:0072350	tricarboxylic acid metabolic process
GO:0006086	acetyl-CoA biosynthetic process from pyruvate
GO:1902001	fatty acid transmembrane transport
GO:0051156	glucose 6-phosphate metabolic process
GO:0032200	telomere organization

Fig. 4 Mitochondria associated DEPs and their functional analysis. **A** Venn diagram of DEPs of maternal vs fetal, maternal vs middle, middle vs fetal, and proteins and genes associated with mitochondrial functions and processes from the databases MitoXplorer, human protein atlas (HPA)—mitochondria specific, and MitoCarta V3.0. The section of proteins used for further analysis is within the red border. **B** GO biological processes included and figure legend to **C**. GOCircle plots of the 10 most significantly overrepresented mitochondria associated with GO biological process terms, including DEPs falling into each term. Regulation direction is colour coded: upregulated (red), downregulated (blue). Size of the inner segments is indicative of the number of proteins falling into each term. The colour of each inner segment indicates the z-score—general up or downregulation of the GO term considering the number up- and downregulated proteins. **D** Clustered heatmap of average normalized LFQ intensities of mitochondria associated DEPs. Proteins are grouped into samples from maternal, middle, fetal sub-anatomical regions

et al. 2020), Cell Senescence Gene Database (CSGene) consisting of 503 genes, and the National Centre for Biotechnology Information Search database (NCBI) specifically genes associated with senescence in homo sapiens consisting of 988 genes. Of all identified proteins 790 out of 1081 in the maternal sub-anatomical region, 794 out of 1086 in the middle sub-anatomical region, and 804 out of 1101 in the fetal sub-anatomical region were associated with senescence.

In total, 290 of the previously 374 DEPs were associated with senescence (Fig. 5). Both transcription and translational processes (translation, nuclear-transcribed mRNA catabolic process, gene expression, regulation of mRNA stability) were differentially regulated between maternal and middle sub-anatomical region, with primarily downregulated proteins on the maternal side, most of which were also downregulated in the middle compared to the fetal sub-anatomical region. Interestingly, proteins associated with negative regulation of, or regulation of cell death and apoptotic processes were primarily downregulated in the maternal compared to the middle sub-anatomical region and upregulated in the middle compared with the fetal sub-anatomical region.

Proteins associated with stress responses were downregulated in the maternal compared to the middle sub-anatomical region and primarily upregulated in the



ID	Description
GO:0006986	response to unfolded protein
GO:0043069	negative regulation of programmed cell death
GO:0043066	negative regulation of apoptotic process
GO:1902175	regulation of oxidative stress-induced intrinsic apoptotic signaling pathway
GO:0006412	translation
GO:0000956	nuclear-transcribed mRNA catabolic process
GO:0010467	gene expression
GO:0043488	regulation of mRNA stability
GO:0010389	regulation of G2/M transition of mitotic cell cycle
GO:0007004	telomere maintenance via telomerase

ID	Description
GO:1903202	negative regulation of oxidative stress-induced cell death
GO:0062197	cellular response to chemical stress
GO:0034599	cellular response to oxidative stress
GO:0071731	response to nitric oxide
GO:0051289	protein homotetramerization
GO:0072350	tricarboxylic acid metabolic process
GO:0006094	gluconeogenesis
GO:0051156	glucose 6-phosphate metabolic process
GO:0007005	mitochondrion organization
GO:0000965	mitochondrial RNA 3'-end processing

ID	Description
GO:0006986	response to unfolded protein
GO:0043069	negative regulation of programmed cell death
GO:0043066	negative regulation of apoptotic process
GO:0002446	neutrophil mediated immunity
GO:0006412	translation
GO:0010467	gene expression
GO:0016072	rRNA metabolic process
GO:0044267	cellular protein metabolic process
GO:0072350	tricarboxylic acid metabolic process
GO:0015909	long-chain fatty acid transport

Fig. 5 Senescence associated DEPs and their functional analysis. **A** Venn diagram of DEPs of maternal vs fetal, maternal vs middle, middle vs fetal, and proteins and genes associated with mitochondrial functions and processes from the databases CellAge, CSGene, and NCBI database results for the keyword senescence. The section of proteins used for further analysis is within the red border. **B** GOCircle plots of the 10 most significantly overrepresented GO biological process terms, including senescence associated DEPs falling into each term. Regulation direction is colour coded: upregulated (red), downregulated (blue). Size of the inner segments is indicative of the number of proteins falling into each term. The colour of each inner segment indicates the z-score—general up or downregulation of the GO term considering the number up- and downregulated proteins

middle compared to the fetal sub-anatomical region. Other senescence associated proteins (regulation of G2/M transition of mitotic cell cycle, telomere maintenance) were primarily downregulated in the maternal compared to the middle sub-anatomical region.

Discussion

The placenta is a highly complex organ and crucial for embryo development, however molecular interactions and their association with pregnancy complications remain poorly understood [32, 33].

In this study, for the first time, the proteomics structure of healthy placentae was investigated. Three placentae from healthy uncomplicated pregnancies were sampled at five sample sites, and further categorised into three sub-anatomical regions. We ensured reproducibility by ensuring that the 5 identical cross sections collected from the placenta which were further divided into three sub-anatomical regions, represented approximate sub-anatomical regions, i.e., maternal, mid and fetal through histopathological confirmation. Subsequent LFQ mass spectrometry analysis revealed distinct protein signatures of placental sub-anatomical regions. Resulting functional differences were characterized using functional analysis.

Placental sub-anatomical regions differ in senescence states switch from glucose to fatty acids as a source for energy

Mitochondria and senescence associated processes and functions such as, regulation of G2/M transition mitotic cell cycle, nitric oxide metabolism, and telomere maintenance are overrepresented in downregulated DEPs between maternal and middle sub-anatomical regions, indicating increased cell-cycle arrest of cells in the maternal sub-anatomical region compared with the middle sub-anatomical region. Additionally, proteins associated with glyoxylate metabolic processes were overrepresented in upregulated DEPs between middle and fetal sub-anatomical regions, suggesting an age induced switch from glucose to fatty acids via the activation of glyoxylate cycle, as a source of energy [34]. A high number of DEPs were associated with senescence, some of which overlap with mitochondria associated proteins. Interestingly both maternal versus fetal and maternal versus middle sub-anatomical region comparison indicate a decrease in senescence associated protein levels. When inspected more closely these DEPs, such as DEAD-Box Helicase 17 (DDX17), and heterogeneous nuclear ribonucleoprotein A1 (HNRNPA1), between maternal and fetal sub-anatomical regions do not possess pro-senescent qualities but protective functions against senescence [35, 36].

Similarly, the DEPs trifunctional enzyme subunit alpha and beta (HADHA) and (HADHB), 3-hydroxyacyl-CoA dehydrogenase type-2 (HSD17B10), and L-lactate dehydrogenase B chain (LHDB) are associated with senescence, mitochondrial dysfunction, and the beta-oxidation pathway [37, 38]. Downregulation of HADHA, HADHB, and HSD17B10 have been shown to induce mitochondrial dysfunction and senescence [39]. LHDB is involved in the conversion of pyruvate to (S)-lactate; its downregulation causes downregulation of mitochondrial function. Whereas the induction of LDHB expression causes enhanced mitochondrial function- including positive changes in mitochondrial respiratory subunits, mitochondrial membrane potential, ATP, NAD + /NADH ratio [40]. This indicates that the more senescent phenotype within the maternal sub-anatomical region is caused by the downregulation of mitochondrial proteins with anti-senescent properties.

The placentas collected are from term gestation (> 37 weeks of gestation), hence the ageing changes seen in the maternal sub-anatomical region is more physiologically rather than pathological. This hypothesis is also supplemented by lower ferritinophagy in the maternal sub-anatomical region. Ferritinophagy is a ferroptosis regulator and associated with iron-dependent regulated necrosis usually caused by massive lipid peroxidation-mediated membrane damage [41]. Moreover, we also report mitochondrial dysfunction in the form of glucose to lipid oxidation shift for energy production within the maternal sub-anatomical region compared to middle, or fetal sub-anatomical regions. This change can be indicative of change in trophoblastic microenvironment as a consequence of higher oxidative stress within this region [42].

Mitochondrial activity is higher in the middle sub-anatomical region compared to maternal and fetal sub-anatomical regions

Mitochondrial-related DEPs were predominantly downregulated on the maternal side compared with the middle sub-anatomical regions, and predominantly upregulated proteins comparing the middle with the fetal sub-anatomical region.

The upregulated proteins in the middle versus fetal sub-anatomical region, included IDH1, IDH2, ALDH4A1 and PDHA1. Isocitrate dehydrogenases (IDH) protein 1 found in the cytosol, while IDH2 is found in mitochondria and converts isocitrate to alpha-ketoglutarate (α-KG) in the TCA cycle and production of NADPH [43]. Upregulated protein expression of IDH1 and IDH2 levels in the middle region compared to maternal or fetal regions, suggests a higher production of NADPH and higher mitochondrial activity in this sub-anatomical region. In fact, studies have shown that IDH2 in pregnancy is inversely related to pregnancy conditions such as IUGR

and high maternal BMI [44, 45]. Superoxide dismutase 2 (SOD2), which is upregulated in the middle sub-anatomical region compared to the fetal sub-anatomical region, is an enzymatic antioxidant that regulates oxidative stress, lack of antioxidant defence can lead to increased oxidative stress which in turn can damage cells, proteins, as well as DNA and accelerate aging. In pregnancy, this may lead to placental insufficiency linked to preeclampsia and IUGR [46, 47]. The increased expression of SOD2 along with IDH1, IDH2 indicate high energy homeostasis and metabolism, along with antioxidant defence in the middle sub-anatomical region [48, 49].

Apurinic/apyrimidinic endodeoxyribonuclease 1 or APEX-1 are multifunctional protein usually associated to DNA Damage Repair (DDR) functionality in cells experiencing oxidative insults [50]. Our results indicate that APEX-1 is downregulated in the middle sub-anatomical region compared to the fetal region. This might be indicative of higher oxidative stress experienced by this sub-anatomical region, causing telomere damage. The lack of indicators of oxidative stress within the fetal sub-anatomical region may be due to the presence of anti-senescent proteins, providing protection to the placental cells of this region. Moreover, upregulation of mitochondrial organization of genome and mitochondrial RNA 3'-end processing might be also indicative of mitochondrial stress response experience by the maternal sub-anatomical compared to fetal. However, the mechanism by which mitochondrial organization works is not completely understood [51].

The effect of sub-anatomical region on protein intensity is not equal across sample sites

Independent analysis of unique proteins identified in placental sample sites revealed a myriad of proteins solely identified in one sample site E (Fig. 1) before normalisation. These were filtered out when adjusted for consideration of sub-anatomical regions. Additionally, strong interaction between the effect of sample site and sub-anatomical region on LFQ protein intensity was shown. This suggests that the effect between sub-anatomical region on LFQ proteins intensity is not the same for all sample sites. This may have been caused by individual variations and the placenta not being geometrically oval and stresses the importance of sampling several placenta sites from the same patient and recruiting an increased study number to compensate for the extremely high individual variability of placental shapes, size, and structure [16, 52]. Our sample collection protocol has been based on recommendation detailed by Burton et al., 2014 where we selected five different sites across the placenta [16]. As our results show, there is minute variations across the different sampling sites, with one site in particular showcasing unique proteins. We, therefore, concur with published recommendation for proteomic analysis by including at least five sites while sampling for both qualitative and quantitative validity [16]. We also identified proteomic differences between sub-anatomical regions, which we recommend considering in future studies. However, we did not include fetal and maternal membranes for sub-anatomical proteomic analysis. Through our results, we demonstrate a variable protein composition between sub-anatomical regions, with higher senescence associated protein and upregulated translation and transcription proteins in maternal and middle compared to fetal sub-anatomical region, hence we conclude separating these regions for a robust placental analysis.

NaviCenta provides additional information to placental data analysis

Traditional functional analysis techniques such as GO terms are not tissue specific but consider all biological processes and molecular functions present within the human body. Even using the manually curated CellMarker database, the different placental cells could not be identified. Traditional functional analysis is unbiased. Although this is an advantage, in the context of placenta research, a more placenta focused approach is useful. The NaviCenta exclusively contains placenta tissue specific cells and phenotypes and enables network based in silico perturbations and the integration of log2FC, and p-value information. The NaviCenta indicated deregulated apoptosis, non-apoptotic cell death, and cell proliferation associated phenotypes of endothelial cells in particular [22]. These have been shown to be governed by mitochondrial function [53] and are associated with a more senescent state [54].

Conclusion

This study provides a comprehensive proteomic assessment of separate sub-anatomical regions of the placenta reporting proteomic signature of healthy placentae, providing an insight into mitochondrial functioning and placental ageing. The proteome differences between placental sub-anatomical regions, referred to as maternal, middle, and fetal side, indicating cell senescence, mitochondrial dysfunction, and specifically activities of endothelial cells. Our results indicate a pronounced increase in senescence in both the maternal and middle sub-anatomical regions by downregulation of proteins protective against senescence. DEPs indicate additionally a senescence associated switch from ATP to fatty acids as a source of energy.

Novelty and limitation

Availability of official annotation for sub-anatomical regions

The sub-anatomical regions in this study are referred to as maternal, middle, and fetal sub-anatomical regions. In fact, the placenta is essentially a fetal organ and a selective barrier between maternal and fetal circulations [6]. The chosen nomenclature solely describes the location in reference to the foetus as described in Fig. 1 and was not intended to insinuate that there was transfer between maternal and fetal sub-anatomical region instead of the capillaries of the terminal villi.

Individual variability of placental shape and structure

We observed that although there were no DEPs between the five placenta sample sites, some proteins showed increased interaction between sample site and sub-anatomical regions. This may have been caused by individual variations in placental morphology not being a geometrically perfect oval. This stresses the importance of extracting several placenta samples from the same patient and recruiting an increased number of participants to compensate for the extremely high individual variability of placental shapes, size, and structure [16, 52].

Label free quantification

LC–MS techniques largely fall into two categories (i) relative quantification; and (ii) using a stable isotope-labelled standard to determine peptide abundance. Most research questions are addressed using relative quantification. Relative quantification can be further grouped into (i) labelled; and (ii) label-free. Samples can be labelled in vitro in the form of stable isotope labelling with amino acids in cell culture (SILAC) or modified using *i.e.,* tandem mass tag (TMT). These techniques diminish variability caused by sample preparation and make protein quantitation more exact [55, 56]. LFQ is a cost- and labour-effective alternative to both SILAC and TMT. The advantage here is that protein abundance alterations can be measured across samples independently of isotopic labelling. A disadvantage, however, is the acquisition time, as each sample must be run consecutively [57]. In this study, samples were minimally manipulated after extraction. No additional experimental conditions, but the proteomic differences between sub-anatomical regions were studied, making LFQ the preferred technique.

NaviCenta—the placenta specific disease map

When it comes to disease or even tissue specific functional analysis and systemic data interpretation, computational and mathematical tools are not widely available, yet. The NaviCenta is a human and machine readable multiscale computational model. The NaviCenta consists of information regarding processes and cell interactions within the placenta, and of relevance to healthy placentation, including molecular interactions between proteins, RNA, and DNA, enriched with regulatory factors, such as transcription factors, miRNA, and lncRNA, which can be used for network-based analyses [21]. In this study, the NaviCenta was used to perform placenta specific phenotype prediction, also considering protein fold change, which the general functional analysis was integrated into, enabling a more meaningful interpretation of results.

Supplementary Information

The online version contains supplementary material available at https://doi.org/10.1186/s12014-022-09388-4.

Additional file 1. Supplementary figures and functional analysis of DEPs between placental sub-anatomical regions.

Additional file 2. Table of DEPs between sub-anatomical regions.

Acknowledgements

We would like to acknowledge Dr. Caitriona Scaife in The UCD Conway Mass Spectrometry Core facility for running the samples at their facility. In addition, we would like to thank Dr. Jane English for designing the proteomic workflow. We would also like to thank Dr. Andrea Musumeci and Dr. Kirsten Dowling for their knowledge, expertise, and constant support. Lastly, we would like to acknowledge iPLACENTA (https://www.iplacenta.eu/) for supporting our research.

Author contributions

SM and AN performed all experiments. JS performed all data, functional and statistical analysis described above. SM and JS wrote the first draft of the manuscript. SM and CJME carried out patient recruitment, and sample collection and preparation. CMC, JE, and FPMC supervised and designed the study, and SG supervised and provided feedback on the manuscript. SM, JS CMC, JE, and FPMC made significant contributions to the manuscript. CS was responsible for running the samples on mass-spectrometer and primary data analysis. All authors read and approved the final manuscript.

Funding

This project is funded by the European Union's Horizon 2020 research and innovation programme under Marie Skłodowska-Curie Actions Innovative Training Network (H2020-MSCA-ITN 2017), Grant No. 765274, acronym iPLACENTA (http://www.iplacenta.eu).

Data availability

Functional analysis of proteins identified in placental sub-anatomical regions: Original EnrichR results are available under.
Maternal: https://maayanlab.cloud/Enrichr/enrich?dataset=9c376a64adf43c8c8c1782694549483e, accessed 29 December 2021.
Middle: https://maayanlab.cloud/Enrichr/enrich?dataset=27fb12bd286394d15787f76f1e9dc3d4, accessed 29 December 2021.
Fetal: https://maayanlab.cloud/Enrichr/enrich?dataset=60a1314c656e72744ea87b28d82c475a, accessed 30 December 2021.
The raw mass spectrometry data is privately available on Fairdom hub upon request.
Mitochondrial proteins and genes: Human protein atlas information specific to the mitochondrial subcellular location was downloaded from https://www.proteinatlas.org/search/subcell_location:Mitochondria. The mitochondrial interactome from MitoXplorer was downloaded from http://mitoxplorer.ibdm.univ-mrs.fr/interactome.php. Human MitoCarta 3.0 was downloaded

from https://www.broadinstitute.org/mitocarta/mitocarta30-inventory-mammalian-mitochondrial-proteins-and-pathways.
NaviCenta: The placenta specific disease map is available under https://www.sbi.uni-rostock.de/minerva/index.xhtml?id=NaviCenta. Plugins used for phenotype prediction are available upon request.
Mitochondrial and Senescence Data:
Mat-fet: https://maayanlab.cloud/Enrichr/enrich?dataset=23a1f5d1e2214762a57c6e9d41a4b006.
Mito mat-mid: https://maayanlab.cloud/Enrichr/enrich?dataset=a0339b7b961cadf671ad33f94a050c5c.
Mito mid-fet: https://maayanlab.cloud/Enrichr/enrich?dataset=b6eaac4d63fa78e94acac4c9cf4506da.
Enrichr bp:
Mat-fet: https://maayanlab.cloud/Enrichr/enrich?dataset=d2f9dc83798e33f0159517ba9df04fba.
mat-mid: https://maayanlab.cloud/Enrichr/enrich?dataset=ac55a8568727078143b9bace07f1b013.
mid-fet: https://maayanlab.cloud/Enrichr/enrich?dataset=6b734e65e15f5aeb003e23e4c574ea50.

Declarations

Ethics approval and consent to participate

All procedures performed in studies involving human participants were in accordance with the ethical standards of the institutional and/or national research committee and with the 1964 Helsinki Declaration and its later amendments or comparable ethical standards. All the procedures were approved by the Clinical Research Ethics Committee of the Cork Teaching Hospitals (ECM4 (ff) 04/12/18), and all women provided written informed consent. Informed consent was obtained from all individual participants included in the study.

Consent for publication

The authors affirm that human research participants provided informed consent for publication.

Competing interests

Authors report no conflict of Interest.

Author details

[1]Department of Obstetrics and Gynaecology, Cork University Maternity Hospital, University College Cork, Cork, Ireland. [2]Department of Pharmacology and Therapeutics, Western Gateway Building, University College Cork, Cork, Ireland. [3]INFANT Research Centre, Cork, Ireland. [4]Department of Anatomy and Neuroscience, Western Gateway Building, University College Cork, Cork, Ireland. [5]Dept. of Systems Biology and Bioinformatics, University of Rostock, 18057 Rostock, Germany. [6]UCD Conway Institute for Biomolecular and Biomedical Research, University College Dublin, Dublin, Ireland.

Received: 1 August 2022 Accepted: 9 December 2022
Published: 2 January 2023

References

1. Mossman HW. Comparative morphogenesis of the fetal membranes and accessory uterine structures. Placenta. 1991;12(1):1–5.
2. Burton GJ, Fowden AL. The placenta: a multifaceted, transient organ. Philos Trans R Soc Biol Sci. 2015;370(1663):20140066.
3. Khorami Sarvestani S, Shojaeian S, Vanaki N, Ghresi-Fard B, Amini M, Gilany K, et al. Proteome profiling of human placenta reveals developmental stage-dependent alterations in protein signature. Clin Proteomics. 2021;18(1):18.
4. Woods L, Perez-Garcia V, Hemberger M. Regulation of Placental Development and Its Impact on Fetal Growth—New Insights From Mouse Models. Front Endocrinol. 2018;9:570.
5. Maltepe E, Penn AA. Development, Function, and Pathology of the Placenta. In: Gleason CA, Juul SE, editors. Avery's Diseases of the Newborn. 10th ed. Philadelphia: Elsevier; 2018. p. 40- 60.e8.
6. Holder B, Aplin JD, Gomez-Lopez N, Heazell AEP, James JL, Jones CJP, et al. 'Fetal side' of the placenta: anatomical mis-annotation of carbon particle 'transfer' across the human placenta. Nat Commun. 2021;12(1):7049.
7. Bové H, Bongaerts E, Slenders E, Bijnens EM, Saenen ND, Gyselaers W, et al. Ambient black carbon particles reach the fetal side of human placenta. Nat Commun. 2019;10(1):3866.
8. Burton GJ, Jauniaux E. What is the placenta? American journal of obstetrics and gynecology. 2015;213(4):S6. e1-S6. e4.
9. Roberts RM, Green JA, Schulz LC. The evolution of the placenta. Reproduction (Cambridge, England). 2016;152(5):R179–89.
10. Wang Y, Zhao S. Integrated Systems Physiology: from Molecules to Function to Disease. Vascular Biology of the Placenta. San Rafael (CA): Morgan & Claypool Life Sciences. Copyright © 2010 by Morgan & Claypool Life Sciences.; 2010
11. Fox H. Aging of the placenta. Arch Dis Child Fetal Neonatal Ed. 1997;77(3):F171–5.
12. Manna S, McCarthy C, McCarthy FP. Placental Ageing in Adverse Pregnancy Outcomes: Telomere Shortening, Cell Senescence, and Mitochondrial Dysfunction. Oxid Med Cell Longev. 2019;2019:3095383.
13. Sultana Z, Maiti K, Aitken J, Morris J, Dedman L, Smith R. Oxidative stress, placental ageing-related pathologies and adverse pregnancy outcomes. Am J Reprod Immunol. 2017;77(5): e12653.
14. Law KP, Han TL, Tong C, Baker PN. Mass spectrometry-based proteomics for pre-eclampsia and preterm birth. Int J Mol Sci. 2015;16(5):10952–85.
15. Nguyen TPH, Patrick CJ, Parry LJ, Familari M. Using proteomics to advance the search for potential biomarkers for preeclampsia: A systematic review and meta-analysis. PLoS ONE. 2019;14(4):e0214671.
16. Burton GJ, Sebire NJ, Myatt L, Tannetta D, Wang YL, Sadovsky Y, et al. Optimising sample collection for placental research. Placenta. 2014;35(1):9–22.
17. Burton DGA, Krizhanovsky V. Physiological and pathological consequences of cellular senescence. Cell Mol Life Sci. 2014;71(22):4373–86.
18. English JA, Lopez LM, O'Gorman A, Föcking M, Hryniewiecka M, Scaife C, et al. Blood-based protein changes in childhood are associated with increased risk for later psychotic disorder: evidence from a nested case-control study of the ALSPAC Longitudinal Birth Cohort. Schizophr Bull. 2018;44(2):297–306.
19. Tyanova S, Temu T, Sinitcyn P, Carlson A, Hein MY, Geiger T, et al. The Perseus computational platform for comprehensive analysis of (prote)omics data. Nat Methods. 2016;13(9):731–40.
20. Bindea G, Mlecnik B, Hackl H, Charoentong P, Tosolini M, Kirilovsky A, et al. ClueGO: a Cytoscape plug-in to decipher functionally grouped gene ontology and pathway annotation networks. Bioinformatics (Oxford, England). 2009;25(8):1091–3.
21. Mazein A, Ostaszewski M, Kuperstein I, Watterson S, Le Novère N, Lefaudeux D, et al. Systems medicine disease maps: community-driven comprehensive representation of disease mechanisms. Syst Biol Appl. 2018;4(1):21.
22. Scheel J, Gupta S, Wolkenhauer O. NaviCenta: Navigate the placenta. Placenta. 2021;112: e35.
23. Hoch M, Smita S, Cesnulevicius K, Lescheid D, Schultz M, Wolkenhauer O, et al. Network- and enrichment-based inference of phenotypes and targets from large-scale disease maps. Syst Biol Appl. 2022;8(1):13.
24. Uhlén M, Fagerberg L, Hallström BM, Lindskog C, Oksvold P, Mardinoglu A, et al. Proteomics. Tissue-based map of the human proteome. Science. 2015;347(6220):1260419.
25. Yim A, Koti P, Bonnard A, Marchiano F, Dürrbaum M, Garcia-Perez C, et al. mitoXplorer, a visual data mining platform to systematically analyze and visualize mitochondrial expression dynamics and mutations. Nucleic Acids Res. 2020;48(2):605–32.
26. Rath S, Sharma R, Gupta R, Ast T, Chan C, Durham TJ, et al. MitoCarta3.0: an updated mitochondrial proteome now with sub-organelle localization and pathway annotations. Nucleic Acids Res. 2021;49(D1):D1541.
27. Heberle H, Meirelles GV, da Silva FR, Telles GP, Minghim R. InteractiVenn: a web-based tool for the analysis of sets through Venn diagrams. BMC Bioinformatics. 2015;16(1):169.
28. Avelar RA, Ortega JG, Tacutu R, Tyler EJ, Bennett D, Binetti P, et al. A multidimensional systems biology analysis of cellular senescence in aging and disease. Genome Biol. 2020;21(1):91.

29. Zhao M, Chen L, Qu H. CSGene: a literature-based database for cell senescence genes and its application to identify critical cell aging pathways and associated diseases. Cell Death Dis. 2016;7(1):e2053.
30. Walter W, Sánchez-Cabo F, Ricote M. GOplot: an R package for visually combining expression data with functional analysis. Bioinformatics. 2015;31(17):2912–4.
31. Zhang X, Lan Y, Xu J, Quan F, Zhao E, Deng C, et al. Cell Marker: a manually curated resource of cell markers in human and mouse. Nucleic Acids Res. 2018;47(D1):D721–8.
32. Burton GJ, Jauniaux E. Oxidative stress. Best Pract Res Clin Obstet Gynaecol. 2011;25(3):287–99.
33. Burton GJ, Fowden AL. Review: The placenta and developmental programming: balancing fetal nutrient demands with maternal resource allocation. Placenta. 2012;33(Suppl):S23–7.
34. Samokhvalov V, Ignatov V, Kondrashova M. Inhibition of Krebs cycle and activation of glyoxylate cycle in the course of chronological aging of Saccharomyces cerevisiae. Compensatory role of succinate oxidation Biochimie. 2004;86(1):39–46.
35. Wang H, Han L, Zhao G, Shen H, Wang P, Sun Z, et al. hnRNP A1 antagonizes cellular senescence and senescence-associated secretory phenotype via regulation of SIRT1 mRNA stability. Aging Cell. 2016;15(6):1063–73.
36. Jia Q, Nie H, Yu P, Xie B, Wang C, Yang F, et al. HNRNPA1-mediated 3′ UTR length changes of HN1 contributes to cancer- and senescence-associated phenotypes. Aging (Albany NY). 2019;11(13):4407–37.
37. Djouadi F, Bastin J. Mitochondrial Genetic Disorders: Cell Signaling and Pharmacological Therapies. Cells. 2019;8:4.
38. Li S, Zhan J-K, Wang Y-J, Lin X, Zhong J-Y, Wang Y, et al. Exosomes from hyperglycemia-stimulated vascular endothelial cells contain versican that regulate calcification/senescence in vascular smooth muscle cells. Cell Biosci. 2019;9(1):1.
39. Dahl ES, Buj R, Leon KE, Newell JM, Imamura Y, Bitler BG, et al. Targeting IDH1 as a Prosenescent Therapy in High-grade Serous Ovarian Cancer. Mol Cancer Res. 2019;17(8):1710–20.
40. Tian C, Kim YJ, Hali S, Choo O-S, Lee J-S, Jung S-K, et al. Suppressed expression of LDHB promotes age-related hearing loss via aerobic glycolysis. Cell Death Dis. 2020;11(5):375.
41. Mazhar M, Din AU, Ali H, Yang G, Ren W, Wang L, et al. Implication of ferroptosis in aging. Cell Death Discovery. 2021;7(1):149.
42. Munir R, Lisec J, Swinnen JV, Zaidi N. Lipid metabolism in cancer cells under metabolic stress. Br J Cancer. 2019;120(12):1090–8.
43. Charitou P, Rodriguez-Colman M, Gerrits J, van Triest M, Groot Koerkamp M, Hornsveld M, et al. FOXOs support the metabolic requirements of normal and tumor cells by promoting IDH1 expression. EMBO Rep. 2015;16(4):456–66.
44. Chen F, Wang T, Feng C, Lin G, Zhu Y, Wu G, et al. Proteome Differences in placenta and endometrium between normal and intrauterine growth restricted pig fetuses. PLoS ONE. 2015;10(11): e0142396.
45. Mitsuya K, Parker AN, Liu L, Ruan J, Vissers MCM, Myatt L. Alterations in the placental methylome with maternal obesity and evidence for metabolic regulation. PLoS ONE. 2017;12(10): e0186115.
46. Roland L, Beauchemin D, Acteau G, Fradette C, St-Pierre I, Bilodeau JF. Effects of labor on placental expression of superoxide dismutases in preeclampsia. Placenta. 2010;31(5):392–400.
47. Williamson RD, McCarthy FP, Manna S, Groarke E, Kell DB, Kenny LC, et al. L-(+)-ergothioneine significantly improves the clinical characteristics of preeclampsia in the reduced uterine perfusion pressure rat model. Hypertension. 2020;75(2):561–8.
48. Mondesir J, Willekens C, Touat M, de Botton S. IDH1 and IDH2 mutations as novel therapeutic targets: current perspectives. J Blood Med. 2016;7:171–80.
49. DeBerardinis RJ, Thompson CB. Cellular metabolism and disease: what do metabolic outliers teach us? Cell. 2012;148(6):1132–44.
50. Tummanatsakun D, Proungvitaya T, Roytrakul S, Limpaiboon T, Wongkham S, Wongkham C, et al. Serum Apurinic/Apyrimidinic Endodeoxyribonuclease 1 (APEX1) Level as a Potential Biomarker of Cholangiocarcinoma. Biomolecules. 2019;9:9.
51. Rackham O, Filipovska A. Organization and expression of the mammalian mitochondrial genome. Nat Rev Genet. 2022;23(10):606–23.
52. Yampolsky M, Salafia CM, Shlakhter O, Haas D, Eucker B, Thorp J. Modeling the variability of shapes of a human placenta. Placenta. 2008;29(9):790–7.
53. Antico Arciuch VG, Elguero ME, Poderoso JJ, Carreras MC. Mitochondrial regulation of cell cycle and proliferation. Antioxid Redox Signal. 2012;16(10):1150–80.
54. Sabbatinelli J, Prattichizzo F, Olivieri F, Procopio AD, Rippo MR, Giuliani A. Where metabolism meets senescence: focus on endothelial cells. Front Physiol. 2019;10:1523.
55. Ong SE, Blagoev B, Kratchmarova I, Kristensen DB, Steen H, Pandey A, et al. Stable isotope labeling by amino acids in cell culture, SILAC, as a simple and accurate approach to expression proteomics. Mol Cell Proteomics. 2002;1(5):376–86.
56. Thompson A, Schäfer J, Kuhn K, Kienle S, Schwarz J, Schmidt G, et al. Tandem mass tags: a novel quantification strategy for comparative analysis of complex protein mixtures by MS/MS. Anal Chem. 2003;75(8):1895–904.
57. Bantscheff M, Schirle M, Sweetman G, Rick J, Kuster B. Quantitative mass spectrometry in proteomics: a critical review. Anal Bioanal Chem. 2007;389(4):1017–31.

Publisher's Note

Springer Nature remains neutral with regard to jurisdictional claims in published maps and institutional affiliations.

Ready to submit your research? Choose BMC and benefit from:

- fast, convenient online submission
- thorough peer review by experienced researchers in your field
- rapid publication on acceptance
- support for research data, including large and complex data types
- gold Open Access which fosters wider collaboration and increased citations
- maximum visibility for your research: over 100M website views per year

At BMC, research is always in progress.

Learn more biomedcentral.com/submissions

BMC